ANNALS of PHYSICS

Editor
Herman Feshbach

Assistant Editors
Henry Ehrenreich
Roman W. Jackiw
Arthur M. Jaffe
William H. Press

Editorial Council
J. D. Bjorken
D. Brink
P. G. De Gennes
J. Eisenberg
G. Field
S. Hanna
V. Hughes
L. Kadanoff
B. Mottleson
L. Okun
J. Peoples, Jr.
E. Picasso
D. Scalapino
I. I. Shapiro
K. Wilson

Founding Editors
Philip M. Morse
Bernard T. Feld   Herman Feshbach   Richard Wilson

VOLUME 201 • 1990

ACADEMIC PRESS, INC.
Harcourt Brace Jovanovich, Publishers
San Diego New York Boston
London Sydney Tokyo Toronto

Annals of Physics
Volume 201, Number 1, July 1990

CONTENTS

B. Chakraborty, M. R. Khan, Susmita Sarkar, V. Krishan, and B. Bhattacharyya. Induced Magnetization of Alfven Waves 1

Amiram Leviatan and Michael W. Kirson. Normal Modes of the Neutron–Proton Interacting-Boson Model of Nuclei 13

E. J. Ferrer, V. de la Incera, and A. E. Shabad. Photon Magnetic Mass and Meissner Effect in the Bose–Einstein Condensate of W-Mesons 51

R. Jackiw. Dynamical Symmetry of the Magnetic Vortex 83

Guy Battle. Ondelettes: The Spinor QED_3 Connection. 117

Henning Esbensen and Peter Sigmund. Barkas Effect in a Dense Medium: Stopping Power and Wake Field 152

G. Feldman and T. Fulton. Log Terms for Leading Radiative Corrections in Atoms in the Dirac–Fock Approximation. 193

Abstracts of Papers to Appear in Future Issues 221

ANNALS OF PHYSICS
(ISSN 0003-4916)

Published monthly (except semimonthly in February, May, August, and November) at 41 Tempelhof, B-8000 Brugge, Belgium by Academic Press, Inc., 1 East First Street, Duluth, MN 55802

1990: Volumes 197–204. Price: $1016.00 U.S.A. and Canada; $1179.00 all other countries
All prices include postage and handling.

Information concerning personal subscription rates may be obtained by writing to the Publishers. All correspondence and subscription orders should be addressed to the office of the Publishers at 1 East First Street, Duluth, MN 55802. Send notices of change of address to the office of the Publishers at least 6 to 8 weeks in advance. Please include both old and new addresses. POSTMASTER: Send changes of address to *Annals of Physics*, 1 East First Street, Duluth, MN 55802.

Second class postage paid at Jamaica, NY 11431. Air freight and mailing in the U.S.A. by Publications Expediting, Inc., 200 Meacham Avenue, Elmont, NY 11003.

Copyright © 1990 by Academic Press, Inc.

Printed in Brugge, Belgium by Catherine Press, Ltd.

STATEMENT OF PURPOSE

The *Annals of Physics* is intended to provide a medium for original work of broad significance in which the author will be able to give attention to clarity and intelligibility, so that his paper may be read by the widest possible audience. It is, of course, impossible to require that papers in the *Annals* be readily understandable by all. However, a reasonable criterion might be that sufficient detail and background should be given so that a reader who had worked in the field within the last few years would be able to follow the arguments and understand their significance without undue hardship. In this way we hope the *Annals* can encourage those who have interests in several fields of physics and who like to think of physics as a unified structure of high aesthetic appeal.

ANNALS OF PHYSICS

Volume 201, Number 1, July 1990

Copyright © 1990 by Academic Press, Inc.
All Rights Reserved

No part of this publication may be reproduced or transmitted in any form or by any means, electronic or mechanical, including photocopy, recording, or any information storage and retrieval system, without permission in writing from the copyright owner.

The appearance of the code at the bottom of the first page of an article in this journal indicates the copyright owner's consent that copies of the article may be made for personal or internal use, or for the personal or internal use of specific clients. This consent is given on the condition, however, that the copier pay the stated per copy fee through the Copyright Clearance Center, Inc. (27 Congress Street, Salem, Massachusetts 01970), for copying beyond that permitted by Sections 107 or 108 of the U.S. Copyright Law. This consent does not extend to other kinds of copying, such as copying for general distribution, for advertising or promotional purposes, for creating new collective works, or for resale. Copy fees for pre-1990 articles are as shown on the article title pages; if no fee code appears on the title page, the copy fee is the same as for current articles.

0003-4916/90 $7.50

This journal is printed on acid-free paper.

♾

ANNALS OF PHYSICS **201**, 1–12 (1990)

Induced Magnetization of Alfven Waves

B. CHAKRABORTY,* M. R. KHAN,* AND SUSMITA SARKAR*

Plasma Physics Group, Mathematics Department, Jadavpur University,
Calcutta 700 032, India

V. KRISHAN

Indian Institute of Astrophysics,
Bangalore 560034, India

AND

B. BHATTACHARYYA

Mathematics Department, North Bengal University,
Siliguri 734430, India

Received April 5, 1989

The induced magnetization of propagating and standing Alfven waves (IMPAW and IMSAW, respectively) in plasmas, due to the inverse Faraday effect, is investigated here. This effect follows from the magnetic moment per unit volume of the ordered motion of charges of both sign, in presence of an electromagnetic wave propagating parallel to an ambient magnetic field in the low frequency limit. Both IMPAW and IMSAW are found to be inversely proportional to the cube of the ambient field. These are expected to be significant in the study of physics of the sun and other stars, including pulsars, and in the programmes of RF heating of plasmas of tokamaks and other laboratory devices. © 1990 Academic Press, Inc.

I. INTRODUCTION

Spontaneous generation of magnetic fields is possible in plasmas under the influence of electromagnetic (EM) waves. Some work has been done on induced magnetization along the direction of wave propagation in the megagauss range with high power lasers [1–4]. A large amplitude magnetic field has been detected from estimation of the Faraday rotation effect of back scattered radiation in laser induced plasmas [2].

One of the sources of this generation of induced magnetization is the inverse Faraday effect (IFE). It refers to the magnetization in a material medium by a circularly polarized EM wave along its direction of propagation. In IFE the kinetic

---

* Work supported by the BRNS, Department of Atomic Energy, Government of India.

0003-4916/90 $7.50

Copyright © 1990 by Academic Press, Inc.
All rights of reproduction in any form reserved.

energy of ordered motion of particles in presence of an EM wave is transformed into the energy of the induced magnetic field. At high frequencies the IFE is relevant over time scales shorter than twice the oscillation period of the driving wave field beyond which the wave becomes unstable, and parametric instability develops [5, 6].

The IFE is somewhat known for high frequency waves in solids and in analysis of laser plasma interaction. Specifically, this effect is theoretically formulated and experimentally demonstrated both in solids [7, 8] and in plasmas (see [9, 10, 1, 11] and others).

At high frequencies the induced magnetization of IFE is formed mainly from the electron current because the ion current is not a dominating factor for fields of moderate or weak intensity, and is not significantly affected by the background ambient magnetic field. But, for Alfven waves the situation is just the reverse.

The magnetic field generated from IFE of Alfven waves may in short be called the induced magnetization of Alfven waves or IMAW. To our knowledge, IMAW has not been investigated earlier. It is expected to be of some significance in the study of the physics of the sun and other stars, including the pulsars. For the sun and stars it can be called IMAWS.

The IMAW, denoted here as H_i, is inversely proportional to the cube of the ambient magnetic field H_0, and of negative sign both for propagating and standing patterns of Alfven waves in plasmas. Hence, when H_0 is small H_i is large. Being oppositely directed, when relatively large, H_i changes the polarity of the static magnetic field. When H_0 is large, obviously H_i is weak and cannot change the polarity, only the magnitude of the observed static field is reduced by H_i.

The emergence of the pulsar magnetic field to the extent of 10^{12} G from about 10^2 G in the collapse to the neutron star of a pulsar and the geometry of the static magnetic field of the rotating plasma of its magnetosphere offer an interesting scope of the study of the role of IMAWS in this process. Applications of IMAW are also envisaged in the programme of RF heating of tokamaks and some other laboratory plasmas. Moreover, theoretical extension seems possible to other complicated geometries, like those of cylindrical geometries involving additional complications due to inhomogeneities. For instance, the IMAW can be the source of poloidal magnetic fields guided along megnetic fields of different shapes. We intend to focus on both applications and these theoretical aspects of IMAW in our subsequent programme of work. Here we deal with some of the basic physics of IMAW, concentrate on the IMAW for rectilinear propagation both for propagating and standing waves, and briefly touch upon its relevance to some types of problems of solar physics.

For simplicity the magnetized plasma is regarded as a fully ionized, cold, homogeneous, and collision free mixture of mobile fluids of negative and positive charges. In this approximation the particle dynamical apporach is useful for the study of dynamical behaviour of both the species of charges.

Alfven waves are considered to be the low frequency limit of waves propagating parallel to a static applied magnetic field H_0 in such a two component plasma. The source of the generated static magnetic field H_i is the static part of the magnetic moment of charges per unit volume due to their ordered gyratory motion under the influence of the right and left circular polarization components (RCP and LCP components, respectively). This motion of the charges of both electrons and ions couples with both the LCP and RCP parts of the wave in the Alfven wave limit to generate the magnetic moment.

The Alfven wave dispersion relation $KC_A = \omega$, when derived from the general dispersion relation for an EM wave in plasmas (Appendix B), shows that the vacuum light velocity C cancels out in the limit of low frequencies and infinitesimally small amplitude. For this reason and since EM wave features depend on the dispersive magnetic field, which is basically relativistic in nature, the link of Alfven waves in plasmas with the relativistic mass effect remains to an extent in the computations involving the nonlinear impact of finiteness of amplitudes on these. Evaluation of the nonlinear effects of EM waves in plasmas, in the limit of low frequency Alfven waves, shows that a significant part, thought not always the dominant part, of these follow from this nonlinear source. But this link with relativistic effects is completely lost and also other consequences like the generation of the IMAW do not follow directly, when Alfven waves, including their nonlinear modifications, are evaluated with the help of the field equations of the MHD aproximation. So, for some useful purposes, the Alfven wave characteristics should be evaluated from wave characteristics in a two component magnetized cold plasma, in the low frequency limit.

Alfven waves have been proposed as one of the main heating agencies of the solar corona. The solar corona is in the form of magnetic bipolar structures called coronal loops, the two ends of which are embedded in the convection zone. The convective motions kick, rotate, and twist the foot points of a coronal loop, as a result of which Alfven waves are excited in the loop magnetoplasma. The surface Alfven waves deposit energy in a thin resonance region and several such regions together provide the heat required to raise the temperature of the solar corona to a million degrees. The IMAW can considerably lower the effective value of ambient magnetic field. The standing wave patterns are formed when the Alfven waves propagating along the two legs of a coronal loop interfere at the top of the loop. Since the observed magnetic field should be a sum of the ambient and the induced fields, it is possible to put a limit on the maximum amplitude of Alfven waves that can be excited in the coronal loops.

II. INDUCED MAGNETIZATION

(a) *Induced Magnetization Due to Particle Motion in Fields of Unmagnetized Plasmas*

The magnetic moment $\boldsymbol{\mu}$ of a charge q, moving with velocity $\mathbf{u}$, is defined as

$$\boldsymbol{\mu} = \frac{1}{2c}(\mathbf{r} \times \mathbf{j}), \tag{1}$$

where $\mathbf{r}$ is the position vector and $\mathbf{j}\ (=q\mathbf{u})$ is its current. For an electron $q=-e$ and for an ion in a fully ionized plasma $q=e$. For simplicity we assume the plasma here to be fully ionized.

The induced magnetization $\mathbf{H}_i$, generated by motion of a species of charges, is defined by

$$\mathbf{H}_i = 4\pi N \boldsymbol{\mu}, \tag{2}$$

where N is the number density of charges of that species. The simplest quantity proportional to this $\boldsymbol{\mu}$ is the angular momentum per unit mass,

$$\mathbf{L} = (\mathbf{r} \times \boldsymbol{\mu}). \tag{2a}$$

For several species of charges, the induced magnetization is simply the sum given by

$$\mathbf{H}_i = 4\pi \sum_j N_j \boldsymbol{\mu}_j, \tag{3}$$

where N_j, $\mathbf{u}_j$, and $\boldsymbol{\mu}_j$ are respectively the number density, particle velocity and magnetic moment of the jth species.

The left elliptically polarized (LEP) part of the electric field of an EM wave, propagating along the positive direction of the Z-axis, can be written as

$$(\mathbf{E})_{\mathrm{L}} = (p_0 \cos\theta,\ q_0 \sin\theta,\ 0) \tag{4}$$

and the same of the right elliptically polarized (REP) part as

$$(\mathbf{E})_{\mathrm{R}} = (p_0 \cos\theta,\ -q_0 \sin\theta,\ 0), \tag{5}$$

where

$$\theta = KZ - \omega t. \tag{6}$$

Since only the Z component of $\mathbf{L}$, $\boldsymbol{\mu}$, $\mathbf{H}_i$ is nonzero, let L, μ, H_i denote this component of the corresponding vectors. Also, by $\langle x \rangle$ we denote the average of x over the time period $2\pi/\omega$. So

$$\langle L \rangle = \langle x\dot{y} - \dot{x}y \rangle. \tag{7}$$

Evidently L is the Z component of the angular momentum vector $\mathbf{L}$ of (2a), and x and y are the components of the position vector $\mathbf{r}$ along $0X$ and $0Y$, respectively. In terms of the complex combinations

$$x \pm iy = R_{\pm}, \qquad u_x \pm iu_y = \dot{R}_{\pm}, \tag{8}$$

which are convenient to adopt for computation of results, we find that

$$L=\frac{1}{2i}(\dot{R}_{+}R_{-}-R_{+}\dot{R}_{-}), \tag{9}$$

where $i=\sqrt{-1}$.

The relevant equation of motion for an electron being $\dot{\mathbf{u}}=-e\mathbf{E}/m$, through integration of this relation we find that

$$(L)_{\mathrm{L}}=(x\dot{y}-\dot{x}y)_{\mathrm{L}}=\frac{e^2p_0q_0}{m^2\omega^3}, \qquad (L)_{\mathrm{R}}=-\frac{e^2p_0q_0}{m^2\omega^3}. \tag{10}$$

Hence,

$$(L)_{\mathrm{L}}+(L)_{\mathrm{R}}=0, \qquad (\mu)_{\mathrm{L}}+(\mu)_{\mathrm{R}}=0, \qquad (H_i)_{\mathrm{L}}+(Hi)_{\mathrm{R}}=0, \tag{11}$$

showing that the angular momentum, the magnetic moment, and the net induced magnetization vanish for a single species of charges in presence of two waves of the same frequency, one of which is LEP and the other REP.

When both electrons and ions are mobile, in presence of an LEP electric field,

$$(L)_e+(L)_i=\frac{e^2p_0q_0}{m^2\omega^3}+\frac{e^2p_0q_0}{M^2\omega^3} \tag{12}$$

$$(\mu)_e+(\mu)_i=-\frac{e}{2c}\frac{e^2p_0q_0}{m^2\omega^3}+\frac{e}{2c}\cdot\frac{e^2p_0q_0}{M^2\omega^3}. \tag{13}$$

So, the net angular momentum is the sum of these for the electrons and ions, and the net magnetic moment (and consequently the induced magnetization) is their difference for the two species.

(b) *Induced Magnetization Due to Fields in Magnetized Plasmas*

The first harmonic electric field solution is sought in the form

$$E_{1\pm}=ae^{\mp i\theta_{\mathrm{R}}}+be^{\pm i\theta_{\mathrm{L}}}, \tag{14}$$

where

$$\theta_{\mathrm{R}}=K_{\mathrm{R}}Z-\omega_{\mathrm{R}}t, \qquad \theta_{\mathrm{L}}=K_{\mathrm{L}}Z-\omega_{\mathrm{L}}t \tag{15}$$

$$E_{1\pm}=E_{1x}\pm iE_{1y}. \tag{16}$$

Then obviously,

$$E_x=a\cos\theta_{\mathrm{R}}+b\cos\theta_{\mathrm{L}}; \qquad E_y=-a\sin\theta_{\mathrm{R}}+b\sin\theta_{\mathrm{L}}, \tag{17}$$

so that

$$b=0, \qquad \mathbf{E}=(\mathbf{E})_{\mathrm{R}}=(a\cos\theta_{\mathrm{R}}, -a\sin\theta_{\mathrm{R}}, 0), \tag{18}$$

$$a=0, \qquad \mathbf{E}=(\mathbf{E})_{\mathrm{L}}=(b\cos\theta_{\mathrm{L}}, b\sin\theta_{\mathrm{L}}, 0). \tag{19}$$

For the simultaneous action of a purely LCP and a purely RCP of the same amplitude, "a" say, we put $b=a$ in Eq. (19) and use the resulting pair, Eqs. (18) and (19), for further computation. For $\theta_{\mathrm{R}}=\theta_{\mathrm{L}}=\theta$, Eqs. (17) give an elliptically polarized wave which for $b>a$ is REP and for $b<a$ is LEP. Expressions for magnetic moments of electrons and ions in presence of RCP and LCP waves are obtained in Appendix A.

Relations (1) and (3) show that

$$\begin{aligned} H_i &= 4\pi N(\mu_e+\mu_i) \\ &= -\frac{m\omega_{pe}^2 C}{2e\omega}\left[\frac{\alpha^2(1+2Y_i)}{(1+Y_i)^2(1-Y_e)^2}-\frac{\beta^2(1-2Y_i)}{(1-Y_i)^2(1+U_e)^2}\right], \end{aligned} \tag{20}$$

where

$$(\alpha, \beta)=\frac{e(a, b)}{m\omega C}, \qquad M \gg m, \tag{21}$$

and the expressions for Y_e, Y_i, ω_{pe} are defined in (B.5). This formula for induced magnetization holds good at frequencies high as well as low, and is obtained by applying the relation (A.18), for the magnetic moment, on a system of two waves, one of which is LCP and the other of which is RCP.

(c) *Induced Magnetization from Propagating Alfven Waves* (IMPAW)

In the low frequency Alfven wave limit, ions no longer remain the nonparticipating background members for charge neutralization, and those terms of the dispersion relation and expressions for other physical quantities become dominant which are small in the high frequency limit. This shift of importance of factors following the transition of wave frequency from high to low does not become evident in the study of Alfven waves in the MHD approximation, in which the existence of a single electrically conducting fluid is assumed.

In the dispersion relation for Alfven waves, obtained from the dispersion relations (B.3) and (B.4) (Appendix B), respectively, of the RCP and LCP parts of an EM wave, the value of the right hand member changes from a quantity whose magnitude is less than unity for high frequencies to $4\pi\rho c^2/H_0^2$ which is a large number. This is due to the collapse of the denominator there from the value $(1 \pm Y_i)(1 \mp Y_e)$ (which is of order unity for high frequencies) to the quantity $-Y_i Y_e$ which is numerically a large number for low frequencies. Due to this shift in the importance of some terms, the influence of the dispersive magnetic field becomes more evident in this derivation of the dispersion characteristics of Alfven waves than in the standard derivation from the single fluid approximation of the MHD theory.

Equation (20) now reduces to the IMPAW,

$$H_i = -\frac{(a^2+h^2)\,c^2}{H_0 c_A^2}, \tag{22}$$

where

$$C_A^2 = \frac{\mu H_0^2}{4\pi\rho}.$$

In the case of a single wave of RCP only, we put $b=0$ and obtain

$$H_i = -\frac{4\pi\rho a^2 c^2}{H_0^3}. \tag{23}$$

The observed static magnetic field is therefore

$$H_{ob} = H_0 + H_i = H_0 - \frac{a^2 c^2}{H_0 C_A^2}. \tag{24}$$

This formula shows that the magnitude of the observed field is reduced by the induced magnetic field. So the induced magnetization is diamagnetic in nature. When the ambient magnetic field is small, the polarity of the static field is also changed by the induced field. The formula [12; p. 17, (1.49)],

$$\frac{E^2}{8\pi} : \frac{(\delta H)^2}{8\pi} : \frac{1}{2}\rho u^2 = \frac{C_A^2}{c^2} : 1 : 1, \tag{25}$$

is employed to find the amplitude "a" of the electric field of an Alfven wave. In solar corona [13, p. 4], we have

$$\rho = 10^{-16}\,\text{gm/cm}^3 \qquad \text{and} \qquad H_0 = 10^{-2}\,\text{gauss}. \tag{26}$$

And, following Levine and Withbroe [14], we put $u = 30$ km/sec in Eq. (25), then $a = 10^{-6}$ esu, and using (B.1), $C_A = 2.75 \times 10^5$ cm/sec and Eq. (23) we obtain $H_i = 1.18$ gauss.

(d) *Induced Magnetization from Standing Alfven Waves* (IMSAW)

We start with the electric field in the form

$$E_{1\pm} = a(e^{\mp i\theta_{1R}} + e^{\mp i\theta_{2R}}) + b(e^{\pm i\theta_{1L}} + e^{\pm i\theta_{2L}}), \tag{27}$$

where

$$\theta_{1R} = K_{1R} Z - \omega_{1R} t, \text{ etc.} \tag{28}$$

Then Eqs. (A.22) and (A.23) give

$$H_i = 4\pi N \frac{e}{2c} (\langle L_i \rangle - \langle L_e \rangle)$$

$$= -\frac{2c^2}{H_0 C_A^2} [a^2(1+\cos 2K_R Z) + b^2(1+\cos 2K_L Z)]. \tag{29}$$

Since a wave of RCP to an observer appears as a wave of LCP to another observer if he looks antiparallel to the first observer, the RCP and LCP characteristics of waves depend on his frame of reference. So, for the formation of a perfect standing wave pattern by a forward going wave of RCP, in Eq. (27) we put

$$b=0 \qquad \text{and} \qquad K_{2R} = -K_{1R}, \qquad \omega_{2R} = \omega_{1R}. \tag{30}$$

Then, for the observed induced magnetization, H_{ob}, Eq. (29) gives

$$H_{ob} = -\frac{4c^2a^2}{H_0 C_A^2} \cos^2 K_R Z + H_0 \tag{31}$$

so that the IMSAW is $-4c^2a^2 \cos^2(K_R Z)/H_0 C_A^2$.

The extreme values of this H_{ob} are

$$H_0, \qquad H_0 - \frac{4c^2a^2}{H_0 C_A^2}. \tag{32}$$

When H_0 is numerically small,

$$|H_{ob}|_{max} = \frac{4c^2a^2}{H_0 C_A^2}, \qquad |H_{ob}|_{min} = H_0, \tag{33}$$

so that the polarity of the static magnetic field is changed by the standing wave when H_0 is small.

If the wave vector of the Alfven wave is such that $K_R = 2\pi/L$ where L is the length of the loop, then the induced field H_i vanishes at $Z = L/4$ and $3L/4$ and these are the sites of the maximum field. This consequence has implications for microwave emission which is interpreted to be cyclotron emission from coronal loops. The determination of variation of cyclotron frequency along the length of the loop could tell us about the amplitude of Alfven waves in the coronal loops.

APPENDIX A: EM WAVES IN A TWO-COMPONENT, MAGNETIZED, COLLISIONLESS COLD PLASMA

(a) *The Linearized Field Equations and Their Solution*

We assume perturbation by a transverse wave of the type given in Eq. (4) or Eq. (14). So, in the first order approximation, for convenience, we start with the conditions

$$N_{e_1}=0, N_{i_1}=0, \nabla \cdot \mathbf{E}_1 = 0, E_{1Z}=0, u_{i_1 Z}=0, u_{e_1 Z}=0, \tag{A.1}$$

where the subscript 1 is used to denote the field variables of the first harmonic wave, N_e and $\mathbf{u}_e$ (N_i and $\mathbf{u}_i$) are the number density and particle velocity for electrons (ions). The plasma equations of the first approximation are

$$\dot{\mathbf{u}}_{e_1} = -\frac{e}{m}\mathbf{E}_1 - (\mathbf{u}_{e_1} \times \boldsymbol{\Omega}_e), \tag{A.2}$$

$$\dot{\mathbf{u}}_{i_1} = \frac{e}{M}\mathbf{E}_1 + (\mathbf{u}_{i_1} \times \boldsymbol{\Omega}_i), \tag{A.3}$$

$$\nabla \times \mathbf{H}_1 = \frac{1}{C}\frac{\partial \mathbf{E}_1}{\partial t} + \frac{4\pi e N_0}{C}(\mathbf{u}_{i_1} - \mathbf{u}_{e_1}), \tag{A.4}$$

$$\nabla \times \mathbf{E}_1 = -\frac{1}{C}\frac{\partial \mathbf{H}_1}{\partial t}, \qquad \nabla \cdot \mathbf{H}_1 = 0, \tag{A.5}$$

where $\boldsymbol{\Omega}_e$ and $\boldsymbol{\Omega}_i$ are defined in Eqs. (B.5) of Appendix B.

Complex combination of the type (16) transforms the relevant part of these field equations to

$$\dot{u}_{e_{1\pm}} = -\frac{e}{m}E_{1\pm} \pm i\Omega_e u_{e_{1\pm}}, \tag{A.6}$$

$$\dot{u}_{i_{1\pm}} = \frac{e}{M}E_{1\pm} \mp i\Omega_i u_{i_{1\pm}}, \tag{A.7}$$

$$\frac{\partial E_{1\pm}}{\partial Z} = \pm\frac{i}{C}\frac{\partial H_{1\pm}}{\partial t}, \tag{A.8}$$

$$\pm i\frac{\partial H_{1\pm}}{\partial Z} = \frac{1}{C}\frac{\partial E_{1\pm}}{\partial t} + \frac{4\pi N_0 e}{C}(u_{i_1\pm} - u_{e_1\pm}). \tag{A.9}$$

The wave solution given in Eq. (14), with the help of these relations, shows that

$$H_{1\pm} = \pm i(n_{\mathrm{R}} a e^{\mp i\theta_{\mathrm{R}}} + n_{\mathrm{L}} b r^{\pm i\theta_{\mathrm{L}}}) \tag{A.10}$$

$$u_{i_{1\pm}} - u_{e_{1\pm}} = \frac{\pm i\omega}{4\pi N_0 e}[(n_{\mathrm{R}}^2 - 1)\, a e^{\mp i\theta_{\mathrm{R}}} - (n_{\mathrm{L}}^2 - 1)\, b e^{\pm i\theta_{\mathrm{L}}}] \tag{A.11}$$

$$u_{e_{1\pm}} = \pm\frac{ie}{m\omega}\left[\frac{a e^{\mp i\theta_{\mathrm{R}}}}{1 - Y_e} - \frac{b e^{\pm i\theta_{\mathrm{L}}}}{1 + Y_e}\right] \tag{A.12}$$

$$u_{i_{1\pm}} = \mp\frac{ie}{M\omega}\left[\frac{a e^{\mp i\theta_{\mathrm{R}}}}{1 + Y_i} - \frac{b e^{\pm i\theta_{\mathrm{L}}}}{1 - Y_i}\right], \tag{A.13}$$

where

$$n_{\mathrm{R}} = \frac{K_{\mathrm{R}} C}{\omega}, \qquad n_{\mathrm{L}} = \frac{K_{\mathrm{L}} C}{\omega}, \tag{A.14}$$

n_R and n_L being the refractive indices of the RCP and LCP components of the wave. *Eliminating* $H_{1\pm}$ between (A.8) and (A.9), and using in the resulting relation the Eqs. (A.11) and (14) we equate the co-efficients of $e^{\mp i\theta_R}$ from both sides and obtain the dispersion relation (B.3); similarly, from the co-efficients of $e^{\pm i\theta_L}$ the dispersion relation (B.4) is obtained.

(b) *Evaluation of the Magnetic Moment*

In (A.13) and (A.14) we put

$$\dot{R}_{e_\pm}=u_{e_{1\pm}}, \qquad \dot{R}_{i_\pm}=u_{i_{1\pm}} \tag{A.15}$$

and integrate with respect to time to evaluate $R_{e_\pm}$ and $R_{i_\pm}$. Then L is evaluated with the help of the relation (9), giving

$$\langle L_e\rangle=\frac{e^2}{m^2\omega^3}\left[\frac{a^2}{(1-Y_e)^2}-\frac{b^2}{(1+Y_e)^2}\right] \tag{A.16}$$

$$\langle L_i\rangle=\frac{e^2}{M^2\omega^3}\left[\frac{a^2}{(1+Y_i)^2}-\frac{b^2}{(1-Y_i)^2}\right] \tag{A.17}$$

$$\begin{aligned}\mu_e+\mu_i&=\frac{e}{2C}[\langle L_i\rangle-\langle L_e\rangle]\\ &=\frac{e^3a^2}{2C\omega^3}\left[\frac{(m^2-M^2)-2(m^2Y_e+M^2Y_i)}{M^2m^2(1+Y_i)^2\,(1-Y_e)^2}\right]\\ &\quad-\frac{e^3b^2}{2C\omega^3}\left[\frac{(m^2-M^2)+2(m^2Y_e+M^2Y_i)}{M^2m^2(1-Y_i)^2\,(1+Y_e)^2}\right].\end{aligned} \tag{A.18}$$

(c) *Angular Momentum Due to Two Waves of RCP Forming a Standing Wave*

We assume the electric field solution given by Eq. (27) and obtain

$$u_{e_\pm}=\pm\frac{ie}{m\omega}\left[\frac{a}{1-Y_e}(e^{\mp i\theta_{1R}}+e^{\mp i\theta_{2R}})-\frac{b}{1+Y_e}(e^{\pm i\theta_{1L}}+e^{\pm i\theta_{2L}})\right] \tag{A.19}$$

$$u_{i_\pm}=\mp\frac{ie}{M\omega}\left[\frac{a}{1+Y_i}(e^{\mp i\theta_{1R}}+e^{\mp i\theta_{2R}})-\frac{b}{1-Y_i}(e^{\pm i\theta_{1L}}+e^{\pm i\theta_{2L}})\right]. \tag{A.20}$$

Then we find that

$$\begin{aligned}L_e=\frac{e^2}{2m^2\omega^3}&\left[\frac{a^2}{(1-Y_e)^2}-\frac{b^2}{(1+Y_e)^2}+\frac{a^2}{(1-Y_e)^2}(e^{-2iK_RZ}+e^{2iK_RZ})\right.\\ &\left.-\frac{b^2}{(1+Y_e)^2}(e^{2iK_LZ}+e^{-2iK_LZ})\right]+\frac{e^2}{2m^2\omega^3}\left[\frac{a^2}{(1-Y_e)^2}-\frac{b^2}{(1+Y_e)^2}\right.\\ &\left.+\frac{a^2}{(1-Y_e)^2}(e^{-2iK_RZ}+e^{2iK_RZ})-\frac{b^2}{(1+Y_e)^2}(e^{2iK_LZ}+e^{-2iK_LZ})\right].\end{aligned} \tag{A.21}$$

Taking an average over the time period $2\pi/\omega$, the oscillating terms, not shown here, would vanish, leaving

$$\langle L_e \rangle = \frac{e^2}{m^2\omega^3}\left[\frac{a^2(1+\cos 2K_{\mathrm{R}}Z)}{(1-Y_e)} - \frac{b^2(1+\cos 2K_{\mathrm{L}}Z)}{(1+Y_e)^2}\right]. \tag{A.22}$$

Similarly for the ions we obtain

$$\langle L_i \rangle = \frac{e^2}{M^2\omega^3}\left[\frac{a^2(1+\cos 2K_{\mathrm{R}}Z)}{(1+Y_i)^2} - \frac{b^2(1+\cos 2K_{\mathrm{L}}Z)}{(1-Y_i)^2}\right]. \tag{A.23}$$

The net magnetic moment is then evaluated with the help of (A.18).

APPENDIX B: ALFVEN WAVES IN PLASMAS

Alfven waves are the infinitesimally small amplitude dispersive wave solutions of MHD field equations for electrically conducting incompressible media in presence of strong static magnetic field along the direction of propagation. The mechanical effect of magnetic field is partly equivalent to a hydrostatic pressure of amount $H_0^2/8\pi$, which can be balanced by the fluid pressure. The other part is the tension of amount $H_0^2 4\pi$, which acts like a dense bundle of stretched strings. This tension generates Alfven waves, propagating along the magnetic lines of force. These travel with the phase velocity C_{A} (the Alfven velocity), given by

$$C_{\mathrm{A}}^2 = \frac{H_0^2}{4\pi\rho}, \tag{B.1}$$

where ρ is the mass density. The Alfven waves being transverse EM waves of low frequency (frequencies of these waves are smaller than the ion cyclotron frequency) and high magnetic field, these have very high refractive index n, as may be seen from the expression

$$n = \frac{KC}{\omega} = \frac{C}{C_{\mathrm{A}}} \tag{B.2}$$

for n; moreover, the ion mobility is most dominant in the physics of these waves.

One can start with the dispersion relations of RCP and LCP components of an EM wave:

$$\frac{K_{\mathrm{R}}^2 C^2}{\omega_{\mathrm{R}}^2} - 1 = -\frac{X_e + X_i}{(1+Y_i)(1-Y_e)} \tag{B.3}$$

$$\frac{K_{\mathrm{L}}^2 C^2}{\omega_{\mathrm{L}}^2} - 1 = -\frac{X_e + X_i}{(1-Y_i)(1+Y_e)}, \tag{B.4}$$

where

$$X_e = \frac{\omega_{p_e}^2}{\omega^2}; \qquad X_i = \frac{\omega_{p_i}^2}{\omega^2}; \qquad Y_e = \frac{\Omega_e}{\omega}$$

$$Y_i = \frac{\Omega_i}{\omega}; \qquad \Omega_e = \frac{eH_0}{mC}; \qquad \Omega_i = \frac{eH_0}{MC} \tag{B.5}$$

$$\omega_{p_e}^2 = \frac{4\pi Ne^2}{m}; \qquad \omega_{p_i}^2 = \frac{4\pi Ne^2}{M}.$$

Here the subscripts R and L stand for the RCP and LCP waves, respectively; K is the wave number, ω is the wave frequency; for electrons $-e$ is the charge, m is the mass, Ω_e is the gyration frequency, ω_{p_e} is the electron Langmuir frequency; for ions these are e, M, Ω_i and ω_{p_i} respectively.

In the Alfven wave approximation $|Y_i| \gg 1$, and these relations reduce to

$$\frac{K_R^2 C^2}{\omega_R^2} - 1 = \frac{K_L^2 C^2}{\omega_L^2} - 1 = \frac{4\pi\rho C^2}{H_0^2} \tag{B.6}$$

with $\rho = MN$. Since $C_A \ll C$, these reduce to the dispersion relation

$$KC_A = \omega. \tag{B.7}$$

References

1. A. D. Steiger and C. H. Woods, *Phys. Rev. A* **5** (1972), 1467.
2. J. Briand, V. Adrian, M. E. Tammer, A. Gomes, Y. Quemener, J. P. Dinguirard, and J. C. Kieffer, *Phys. Rev. Lett.* **54** (1985), 38.
3. B. Chakraborty, M. Khan, and B. Bhattacharyya, *J. Appl. Phys.* **59** (1986), 1473.
4. B. Chakraborty, M. Khan, B. Bhattacharryya, S. Deb, and H. C. Pant, *Phys. Fluids* **31** (1988), 1303.
5. C. Max and F. Perkins, *Phys. Rev. Lett.* **29** (1972), 1731.
6. L. Stenflo, *Plasma Phys.* **19** (1977), 1187.
7. P. S. Pershan, *Phys. Rev.* **130** (1963), 919.
8. J. P. Vander Ziel, P. S. Pershan, and L. D. Malmstrong, *Phys. Rev. Lett.* **15** (1965), 190.
9. Y. Pomeau and D. Quemada, *C. R. Acad. Sci B* **264** (1967), 517.
10. J. Deschamps, M. Fitaire, and M. Lagoutte, *Phys. Rev. Lett.* **25** (1970), 1330.
11. A. C. L. Chian, *Phys. Fluids* **24** (1981), 369.
12. R. H. Melrose, "Plasma Astrophysics," Vol. I, Gordon & Breach, New York, 1980.
13. A. Hasegawa and C. Uberoi, "The Alfven Wave," National Technical Information Service, U. S. Department of Commerce, Springfield, VA 1982.
14. R. H. Levine and G. L. Withbroe, *Sol. Phys.* **50** (1977), 83.

ANNALS OF PHYSICS **201**, 13–50 (1990)

Normal Modes of the Neutron–Proton Interacting-Boson Model of Nuclei

AMIRAM LEVIATAN

Theoretical Division, Los Alamos National Laboratory,
Los Alamos, New Mexico 87545

AND

MICHAEL W. KIRSON

Department of Nuclear Physics, Weizmann Institute of Science,
76100 Rehovot, Israel

Received December 5, 1989

A geometrically-oriented framework for studying the general proton–neutron interacting-boson model of nuclei is presented. The Hamiltonian is resolved exactly into intrinsic (bandhead related) and collective (in-band related) parts. Shape parameters are introduced through non-spherical proton–neutron bases. Genuine intrinsic modes of the combined system, as well as decoupled spurious Goldstone modes, are identified by applying the Bogoliubov treatment to the intrinsic part of the Hamiltonian. The normal frequencies provide an approximate expression for bandhead energies in the limit of large boson numbers. In this limit, intrinsic states involving the genuine intrinsic normal modes are constructed and serve to estimate transition matrix elements. The method is demonstrated for the cases of spherical, axially-deformed, and triaxial overall shapes of the valence proton–neutron distributions. © 1990 Academic Press, Inc.

1. INTRODUCTION

The empirical success of the interacting-boson model (IBM) [1 3] in describing phenomenologically a wide range of data on nuclear spectra [4] has led to a number of attempts to extend the model and to understand its relationship to other nuclear models [5]. One increasingly popular trend is to seek ways of visualizing the abstract, algebraic structure of the model in semi-classical or geometric terms [6–20]. A rather satisfying visualization has been provided for the original IBM-1 (which makes no distinction between neutrons and protons) in terms of a framework based on intrinsic states and allowing a separation of the Hamiltonian into intrinsic and collective parts and the subsequent identification of intrinsic normal modes of excitation [21, 22]. The same technique has been successfully applied to an interacting-boson model of rotation–vibration spectra of diatomic and

0003-4916/90 $7.50

Copyright © 1990 by Academic Press, Inc.
All rights of reproduction in any form reserved.

triatomic molecules [23]. In view of the growing interest in the form of the model which distinguishes between proton bosons and neutron bosons, known as IBM-2 [24, 25], it is attractive to apply this general technique to the extraction of normal modes and collective motions of this extended model.

This is by no means the first attempt to confer a simple geometrical interpretation on IBM-2. However, most previous treatments [26–38] have singled out specific, pre-defined, modes of motion or have been limited to truncated subspaces of the multidimensional shape-parameter space. None of them has distinguished intrinsic from collective motions in a general way. The present treatment is entirely general, being applicable to an arbitrary IBM-2 Hamiltonian and to any equilibrium shape configuration. It leads naturally to a separation of collective and intrinsic motions, the former associated with spontaneously broken symmetries of the intrinsic Hamiltonian, and generates automatically all the appropriate normal modes of intrinsic excitation. It is also fully quantal, throughout.

In order to establish notation and define terminology, a brief survey of the algebraic structure of IBM-2 is given in Section 2. This is followed, in Section 3, by the definition of the intrinsic states of IBM-2, the associated energy surface, and the appropriate intrinsic boson basis. Section 4 deals with the resolution of a general IBM-2 Hamiltonian into intrinsic and collective parts, which is illustrated by a few representative cases, while Section 5 describes the use of Bogoliubov's treatment for many-boson systems [39] to extract from the intrinsic Hamiltonian the normal modes of intrinsic excitation. Again, some representative cases are given to illustrate the type of results obtainable. The final section is devoted to a summary and discussion. A brief account of some of the ideas presented here has been reported in [40].

2. IBM-2–Algebraic Preliminaries

The model [41] is based on monopole ($J^\pi = 0^+$) and quadrupole ($J^\pi = 2^+$) bosons of proton type and of neutron type, with associated creation operators $s_\pi^\dagger$, $s_\nu^\dagger$, $d_{\pi\mu}^\dagger$, $d_{\nu\mu}^\dagger$ and destruction operators s_π, s_ν, $d_{\pi\mu}$, $d_{\nu\mu}$ satisfying standard boson commutation relations (bosons of different types commute). The first subscript, π (proton) or ν (neutron), distinguishes the two types of bosons, while the second subscript, $\mu = -2, -1, 0, 1$, or 2, is the projection quantum number of the d-bosons. The symbol ρ will be used to represent π or ν where it is not desired to specify one or the other. The alternative form of the destruction operator $\tilde{d}_{\rho\mu} = (-)^\mu d_{\rho,-\mu}$ has the standard transformation properties of a rank-2 spherical tensor under spatial rotations. The associated number operators are

$$\hat{n}_{s\rho} = s_\rho^\dagger s_\rho \tag{2.1a}$$

$$\hat{n}_{d\rho} = d_\rho^\dagger \cdot \tilde{d}_\rho = \sum_\mu d_{\rho\mu}^\dagger d_{\rho\mu} \tag{2.1b}$$

$$\hat{N}_\rho = \hat{n}_{s\rho} + \hat{n}_{d\rho} \tag{2.1c}$$

and $\hat{N}_\pi$ and $\hat{N}_\nu$ (and hence their sum $\hat{N}=\hat{N}_\pi+\hat{N}_\nu$) are conserved. (The eigenvalue of a number operator $\hat{\mathcal{N}}$ will be denoted $\mathcal{N}$, without caret).

Since the proton and neutron boson numbers are conserved, the appropriate algebraic structure of the model is $U_\pi(6)\times U_\nu(6)$. Subalgebras can be constructed with the aid of the individual subalgebras $O_\rho(6)$, $U_\rho(5)$, $O_\rho(5)$, $SU_\rho(3)$, and $O_\rho(3)$, where the last-named is the usual angular-momentum algebra. For instance, for a given algebra $\mathscr{A}_\rho$, with generators g_ρ, there is a "diagonal" subalgebra $\mathscr{A}$ with generators $g=g_\pi+g_\nu$. The allowed irreducible representations (irreps) are limited by the boson nature of the underlying particle operators.

It is convenient to express the generators of the various algebras of interest in terms of spherical tensors of well-defined ranks. The forms adopted here are

$$\mathcal{M}_\rho=s_\rho^\dagger s_\rho \tag{2.2a}$$

$$\Pi^{(2)}_{\rho\mu}=s_\rho^\dagger\tilde{d}_{\rho\mu}+d^\dagger_{\rho\mu}s_\rho \tag{2.2b}$$

$$\bar{\Pi}^{(2)}_{\rho\mu}=i(s_\rho^\dagger\tilde{d}_{\rho\mu}-d^\dagger_{\rho\mu}s_\rho) \tag{2.2c}$$

$$P^{(L)}_{\rho M}=(d^\dagger_\rho\tilde{d}_\rho)^{(L)}_M,\qquad L=0,1,2,3,4 \tag{2.2d}$$

so $\mathcal{M}_\rho=\hat{n}_{s\rho}$ and $P^{(0)}_\rho=\hat{n}_{d\rho}/\sqrt{5}$, while the angular-momentum generators are $\mathbf{J}_\rho=\sqrt{10}\,P^{(1)}_\rho$. In terms of these tensors, the generators of relevant algebras [42] are as follows:

(i) $O(3)$ has generators $P^{(1)}$, and its Casimir operator is $\mathbf{J}^2=10P^{(1)}\cdot P^{(1)}$, with eigenvalues $J(J+1)$;

(ii) $O(5)$ has generators $P^{(1)}$ and $P^{(3)}$, and its Casimir operator is $C_{O(5)}=2P^{(1)}\cdot P^{(1)}+2P^{(3)}\cdot P^{(3)}=\mathbf{J}^2/5+2P^{(3)}\cdot P^{(3)}$, with eigenvalues $\tau(\tau+3)$;

(iii) $O(6)$ has generators $P^{(1)}$, $\Pi^{(2)}$, and $P^{(3)}$, and its Casimir operator is $C_{O(6)}=C_{O(5)}+\Pi^{(2)}\cdot\Pi^{(2)}$, with eigenvalues $\sigma(\sigma+4)$;

(iv) $\overline{O(6)}$ has generators $P^{(1)}$, $\bar{\Pi}^{(2)}$, and $P^{(3)}$, and its Casimir operator is $C_{\overline{O(6)}}=C_{O(5)}+\bar{\Pi}^{(2)}\cdot\bar{\Pi}^{(2)}$, with eigenvalues $\bar{\sigma}(\bar{\sigma}+4)$;

(v) $SU(3)$ has generators $P^{(1)}$ and $Q=\Pi^{(2)}-\sqrt{7}\,P^{(2)}/2$, and its Casimir operator is $C_{SU(3)}=2Q\cdot Q+3\mathbf{J}^2/4$, with eigenvalues $\lambda^2+\lambda\mu+\mu^2+3(\lambda+\mu)$;

(vi) $\overline{SU(3)}$ has generators $P^{(1)}$ and $\bar{Q}=\Pi^{(2)}+\sqrt{7}\,P^{(2)}/2$, and its Casimir operator is $C_{\overline{SU(3)}}=2\bar{Q}\cdot\bar{Q}+3\mathbf{J}^2/4$, with eigenvalues $\bar{\lambda}^2+\bar{\lambda}\bar{\mu}+\bar{\mu}^2+3(\bar{\lambda}+\bar{\mu})$;

(vii) $U(5)$ has generators $P^{(L)}$, $L=0, 1, 2, 3, 4$, and its Casimir operator is $C_{U(5)}=\Sigma_L P^{(L)}\cdot P^{(L)}=\hat{n}_d(\hat{n}_d+4)$ for the d-boson realization;

(viii) $U(6)$ has generators $\hat{n}_s$, $\Pi^{(2)}$, $\bar{\Pi}^{(2)}$, and $P^{(L)}$, and its Casimir operator is $C_{U(6)}=\hat{n}_s^2+\frac{1}{2}\Pi^{(2)}\cdot\Pi^{(2)}+\frac{1}{2}\bar{\Pi}^{(2)}\cdot\bar{\Pi}^{(2)}+C_{U(5)}=\hat{N}(\hat{N}+5)$ in the s-, d-boson realization.

The above listing applies to individual algebras $\mathscr{A}_\rho$, with the appropriate subscript $\rho=\pi$, ν, and to diagonal algebras $\mathscr{A}$ whose generators are the sum of the corresponding generators of $\mathscr{A}_\pi$ and $\mathscr{A}_\nu$. There also exist other direct products and what may be called skew-diagonal algebras, some of whose generators are antisymmetric combinations of neutron and proton generators. For instance, the generators of $SU(3)^*$ [43] are sums of generators of $SU_\pi(3)$ and $\overline{SU_\nu(3)}$. It is useful to note that

$$C_{U(6)} = \hat{N}(\hat{N}+5) - 2\mathscr{M}_6 \tag{2.3a}$$

$$C_{U(5)} = \hat{n}_d(\hat{n}_d+4) - 2\mathscr{M}_5, \tag{2.3b}$$

where the reference is to diagonal $U(6)$ and $U(5)$ algebras, and $\mathscr{M}_5$ and $\mathscr{M}_6$ are defined as

$$\mathscr{M}_5 = 2 \sum_{L=1,3} (d_\pi^\dagger d_\nu^\dagger)^{(L)} \cdot (\tilde{d}_\nu \tilde{d}_\pi)^{(L)} \tag{2.3c}$$

$$\mathscr{M}_6 = \mathscr{M}_5 + (s_\pi^\dagger d_\nu^\dagger - s_\nu^\dagger d_\pi^\dagger) \cdot (\tilde{d}_\nu s_\pi - \tilde{d}_\pi s_\nu). \tag{2.3d}$$

2.1. *Hamiltonians*

In IBM-2, the Hamiltonian is required to be hermitian, rotationally invariant and time-reversal invariant, to conserve N_π and N_ν and to contain only one- and two-body terms. To impose time-reversal invariance, the phases of the boson creation operators are chosen such that

$$(\mathscr{R}_\pi \mathscr{T}) a^\dagger (\mathscr{R}_\pi \mathscr{T})^{-1} = a^\dagger, \tag{2.4}$$

where $a^\dagger$ is an arbitrary creation operator ($s_\rho^\dagger$ or $d_{\rho\mu}^\dagger$), $\mathscr{T}$ is the time-reversal operator and $\mathscr{R}_\pi$ is the operator of rotation about the y-axis through 180° (with the axis of angular-momentum quantization chosen, as usual, to be the z-axis). For any rotational scalar Hamiltonian, time-reversal invariance is then equivalent to reality of the numerical coefficients. The most general Hamiltonian satisfying all these requirements is

$$H = H_\pi + H_\nu + H_{\pi\nu} \tag{2.5a}$$

$$\begin{aligned} H_\rho = {} & \varepsilon_s^{(\rho)} s_\rho^\dagger s_\rho + \varepsilon_d^{(\rho)} d_\rho^\dagger \cdot \tilde{d}_\rho + u_0^{(\rho)} (s_\rho^\dagger)^2 (s_\rho)^2 + u_2^{(\rho)} s_\rho^\dagger d_\rho^\dagger \cdot \tilde{d}_\rho s_\rho \\ & + v_0^{(\rho)} [d_\rho^\dagger \cdot d_\rho^\dagger (s_\rho)^2 + (s_\rho^\dagger)^2 \tilde{d}_\rho \cdot \tilde{d}_\rho] \\ & + v_2^{(\rho)} [s_\rho^\dagger d_\rho^\dagger \cdot (\tilde{d}_\rho \tilde{d}_\rho)^{(2)} + (d_\rho^\dagger d_\rho^\dagger)^{(2)} \cdot \tilde{d}_\rho s_\rho] \\ & + \sum_{L=0,2,4} c_L^{(\rho)} (d_\rho^\dagger d_\rho^\dagger)^{(L)} \cdot (\tilde{d}_\rho \tilde{d}_\rho)^{(L)} \end{aligned} \tag{2.5b}$$

$$\begin{aligned} H_{\pi\nu} = {} & u_0 s_\pi^\dagger s_\nu^\dagger s_\nu s_\pi + u_2 s_\pi^\dagger d_\nu^\dagger \cdot \tilde{d}_\nu s_\pi + u_2' s_\nu^\dagger d_\pi^\dagger \cdot \tilde{d}_\pi s_\nu \\ & + u_2'' (s_\pi^\dagger d_\nu^\dagger \cdot \tilde{d}_\pi s_\nu + s_\nu^\dagger d_\pi^\dagger \cdot \tilde{d}_\nu s_\pi) + v_0 (s_\pi^\dagger s_\nu^\dagger \tilde{d}_\nu \cdot \tilde{d}_\pi + d_\pi^\dagger \cdot d_\nu^\dagger s_\nu s_\pi) \\ & + v_2 [s_\pi^\dagger d_\nu^\dagger \cdot (\tilde{d}_\nu \tilde{d}_\pi)^{(2)} + (d_\pi^\dagger d_\nu^\dagger)^{(2)} \cdot \tilde{d}_\nu s_\pi] \\ & + v_2' [s_\nu^\dagger d_\pi^\dagger \cdot (\tilde{d}_\pi \tilde{d}_\nu)^{(2)} + (d_\nu^\dagger d_\pi^\dagger)^{(2)} \cdot \tilde{d}_\pi s_\nu] \\ & + \sum_{L=0}^{4} c_L (d_\pi^\dagger d_\nu^\dagger)^{(L)} \cdot (\tilde{d}_\nu \tilde{d}_\pi)^{(L)}, \end{aligned} \tag{2.5c}$$

where the 30 numerical coefficients are real. This will be referred to as the normal-ordered form of H.

There are alternative possible forms of the Hamiltonian. For fixed values of N_π and N_ν (half the number of valence nucleons, either particles or holes, of each kind in the relevant nucleus), the excitation energies are determined by only 21 independent coefficients. In the form of H appropriate for computing a specific spectrum, the $\varepsilon_s^{(\rho)}$, $u_0^{(\rho)}$, $u_2^{(\rho)}$, u_0, u_2, and u_2' terms of Eq. (2.5) may be omitted.

The Hamiltonian can also be expressed in terms of multipole operators, as defined in Eq. (2.2). The multipole form of H involves

$$\begin{aligned} H_{\pi\nu} = {} & a_0 \mathscr{M}_\pi \mathscr{M}_\nu + f_0 \mathscr{M}_\pi P_\nu^{(0)} + f_0' \mathscr{M}_\nu P_\pi^{(0)} \\ & + a_2 \Pi_\pi^{(2)} \cdot \Pi_\nu^{(2)} + a_2' \bar{\Pi}_\pi^{(2)} \cdot \bar{\Pi}_\nu^{(2)} + f_2 \Pi_\pi^{(2)} \cdot P_\nu^{(2)} + f_2' \Pi_\nu^{(2)} \cdot P_\pi^{(2)} \\ & + \sum_{L=0}^{4} b_L P_\pi^{(L)} \cdot P_\nu^{(L)}, \end{aligned} \tag{2.6}$$

where $a_0 = u_0$, $f_0 = \sqrt{5}\, u_2$, $f_0' = \sqrt{5}\, u_2'$, $a_2 = (u_2'' + v_0)/2$, $a_2' = (u_2'' - v_0)/2$, $f_2 = v_2$, $f_2' = v_2'$, $b_0 = (c_0 + 3c_1 + 5c_2 + 7c_3 + 9c_4)/5$, $b_1 = (-2c_0 - 5c_1 - 5c_2 + 12c_4)/10$, $b_2 = (14c_0 + 21c_1 - 15c_2 - 56c_3 + 36c_4)/70$, $b_3 = (-14c_0 + 40c_2 - 35c_3 + 9c_4)/70$, $b_4 = (14c_0 - 28c_1 + 20c_2 - 7c_3 + c_4)/70$. The mutlipole form of H_ρ is not unique, and also not particularly useful here, so will be omitted.

Finally, the Hamiltonian can be expressed in terms of Casimir operators. There is some freedom in the choice of which Casimir operators to use, but the following form has proved to be useful. As before, $C_{\mathscr{A}}$ represents the quadratic Casimir operator of some diagonal algebra $\mathscr{A}$, while $C_{\mathscr{A}}^{(\rho)}$ is the corresponding Casimir operator of $\mathscr{A}_\rho$. Since all Casimir operators here are sums of squares of generators, they all take the form

$$C_{\mathscr{A}} = C_{\mathscr{A}}^{(\pi)} + C_{\mathscr{A}}^{(\nu)} + C_{\mathscr{A}}^{(\pi\nu)} \tag{2.7}$$

where $C_{\mathscr{A}}^{(\pi\nu)}$, which is defined by this equation, is a sum of products of corresponding generators of $\mathscr{A}_\pi$ and $\mathscr{A}_\nu$, and hence belongs exclusively to $H_{\pi\nu}$. The Casimir form of H is

$$\begin{aligned} H_\rho = {} & \xi_1^{(\rho)} \hat{N}_\rho + \xi_2^{(\rho)} \hat{n}_{d\rho} + \xi_3^{(\rho)} \hat{N}_\rho^2 + \xi_4^{(\rho)} \hat{N}_\rho \hat{n}_{d\rho} + \xi_5^{(\rho)} \hat{n}_{d\rho}^2 \\ & + \xi_6^{(\rho)} C_{SU(3)}^{(\rho)} + \xi_7^{(\rho)} C_{O(6)}^{(\rho)} + \xi_8^{(\rho)} C_{O(5)}^{(\rho)} + \xi_9^{(\rho)} \mathbf{J}_\rho^2 \end{aligned} \tag{2.8a}$$

$$\begin{aligned} H_{\pi\nu} = {} & \xi_1 \hat{N}_\pi \hat{N}_\nu + \xi_2 \hat{N}_\pi \hat{n}_{d_\nu} + \xi_3 \hat{n}_{d_\pi} \hat{N}_\nu + \xi_4 \hat{n}_{d_\pi} \hat{n}_{d_\nu} + \xi_5 \mathscr{M}_5 + \xi_6 \mathscr{M}_6 \\ & + \xi_7 C_{SU(3)}^{(\pi\nu)} + \xi_8 C_{\overline{SU(3)}}^{(\pi\nu)} + \xi_9 C_{SU(3)^*}^{(\pi\nu)} \\ & + \xi_{10} C_{O(6)}^{(\pi\nu)} + \xi_{11} C_{O(5)}^{(\pi\nu)} + \xi_{12} \mathbf{J}_\pi \cdot \mathbf{J}_\nu, \end{aligned} \tag{2.8b}$$

where $\xi_1^{(\rho)} = \varepsilon_s^{(\rho)} - u_0^{(\rho)} - 5v_0^{(\rho)}$, $\xi_2^{(\rho)} = \varepsilon_d^{(\rho)} - \varepsilon_s^{(\rho)} + u_0^{(\rho)} + 4v_0^{(\rho)} + 5v_2^{(\rho)}/2\sqrt{7} + (21c_0^{(\rho)} - 20c_2^{(\rho)} - 36c_4^{(\rho)})/35$, $\xi_3^{(\rho)} = u_0^{(\rho)}$, $\xi_4^{(\rho)} = -2u_0^{(\rho)} + u_2^{(\rho)} - 2v_0^{(\rho)}$, $\xi_5^{(\rho)} = u_0^{(\rho)} - u_2^{(\rho)} + 2v_0^{(\rho)} + v_2^{(\rho)}/2\sqrt{7} + (7c_0^{(\rho)} + 10c_2^{(\rho)} + 18c_4^{(\rho)})/35$, $\xi_6^{(\rho)} =$

$-v_2^{(\rho)}/2\sqrt{7}$, $\xi_7^{(\rho)} = v_0^{(\rho)} + v_2^{(\rho)}/\sqrt{7}$, $\xi_8^{(\rho)} = -v_0^{(\rho)} - 3v_2^{(\rho)}/2\sqrt{7} + (-7c_0^{(\rho)} + 10c_2^{(\rho)} - 3c_4^{(\rho)})/35$, $\xi_9^{(\rho)} = v_2^{(\rho)}/2\sqrt{7} + (c_4^{(\rho)} - c_2^{(\rho)})/7$; $\xi_1 = u_0$, $\xi_2 = -u_0 + u_2 + u_2'' - v_0$, $\xi_3 = -u_0 + u_2' + u_2'' - v_0$, $\xi_4 = u_0 - u_2 - u_2' - 2u_2'' + 2v_0 + (7c_0 - 7c_1 + 15c_2 + 7c_3 + 13c_4)/35$, $\xi_5 = u_2'' - v_0 + (-14c_0 + 28c_1 - 20c_2 + 7c_3 - c_4)/70$, $\xi_6 = -u_2'' + v_0$, $\xi_7 = -v_2'/4\sqrt{7} + (c_1 - c_3)/20 + (c_4 - c_2)/28$, $\xi_8 = v_2/4\sqrt{7} + (c_1 - c_3)/20 + (c_4 - c_2)/28$, $\xi_9 = (v_2 - v_2')/4\sqrt{7}$, $\xi_{10} = \frac{1}{2}v_0 + (v_2' - v_2)/\sqrt{7} + (c_3 - c_1)/5 + (c_2 - c_4)/7$, $\xi_{11} = -\frac{1}{2}v_0 + (v_2 - v_2')/\sqrt{7} + (-7c_0 + 21c_1 - 5c_2 - 21c_3 + 12c_4)/70$, $\xi_{12} = 3(v_2' - v_2)/4\sqrt{7} + (c_3 - c_1)/5$. There is also an alternative form, in which $C^{(\rho)}_{\overline{O(6)}}$ and $C^{(\pi\nu)}_{\overline{O(6)}}$ replace $C^{(\rho)}_{O(6)}$ and $C^{(\pi\nu)}_{O(6)}$. Using coefficients $\bar{\xi}$, this alternative form has $\bar{\xi}_1^{(\rho)} = \varepsilon_s^{(\rho)} - u_0^{(\rho)} + 5v_0^{(\rho)} + 10v_2^{(\rho)}/\sqrt{7}$, $\bar{\xi}_2^{(\rho)} = \varepsilon_d^{(\rho)} - \varepsilon_s^{(\rho)} + u_0^{(\rho)} - 4v_0^{(\rho)} - 11v_2^{(\rho)}/2\sqrt{7} + (21c_0^{(\rho)} - 20c_2^{(\rho)} - 36c_4^{(\rho)})/35$, $\bar{\xi}_3^{(\rho)} = u_0^{(\rho)}$, $\bar{\xi}_4^{(\rho)} = -2u_0^{(\rho)} + u_2^{(\rho)} + 2v_0^{(\rho)} + 4v_2^{(\rho)}/\sqrt{7}$, $\bar{\xi}_5^{(\rho)} = u_0^{(\rho)} - u_2^{(\rho)} - 2v_0^{(\rho)} - \sqrt{7}\,v_2^{(\rho)}/2 + (7c_0^{(\rho)} + 10c_2^{(\rho)} + 18c_4^{(\rho)})/35$, $\bar{\xi}_6^{(\rho)} = -v_2^{(\rho)}/2\sqrt{7}$, $\bar{\xi}_7^{(\rho)} = -v_0^{(\rho)} - v_2^{(\rho)}/\sqrt{7}$, $\bar{\xi}_8^{(\rho)} = v_0^{(\rho)} + v_2^{(\rho)}/2\sqrt{7} + (-7c_0^{(\rho)} + 10c_2^{(\rho)} - 3c_4^{(\rho)})/35$, $\bar{\xi}_9^{(\rho)} = v_2^{(\rho)}/2\sqrt{7} + (c_4^{(\rho)} - c_2^{(\rho)})/7$; $\bar{\xi}_1 = u_0$, $\bar{\xi}_2 = -u_0 + u_2 + u_2'' + v_0 + 4(v_2' - v_2)/\sqrt{7} + 4(c_3 - c_1)/5 + 4(c_2 - c_4)/7$, $\bar{\xi}_3 = -u_0 + u_2' + u_2'' + v_0 + 4(v_2' - v_2)/\sqrt{7} + 4(c_3 - c_1)/5 + 4(c_2 - c_4)/7$, $\bar{\xi}_4 = u_0 - u_2 - u_2' - 2u_2'' - 2v_0 + 8(v_2 - v_2')/\sqrt{7} + (7c_0 + 49c_1 - 25c_2 - 49c_3 + 53c_4)/35$, $\bar{\xi}_5 = u_2'' + v_0 + 4(v_2' - v_2)/\sqrt{7} + (-14c_0 - 28c_1 + 20c_2 + 63c_3 - 41c_4)/70$, $\bar{\xi}_6 = -u_2'' - v_0 + 4(v_2 - v_2')/\sqrt{7} + 4(c_1 - c_3)/5 + 4(c_4 - c_2)/7$, $\bar{\xi}_7 = -v_2'/4\sqrt{7} + (c_1 - c_3)/20 + (c_4 - c_2)/28$, $\bar{\xi}_8 = v_2/4\sqrt{7} + (c_1 - c_3)/20 + (c_4 - c_2)/28$, $\bar{\xi}_9 = (v_2 - v_2')/4\sqrt{7}$, $\bar{\xi}_{10} = -\frac{1}{2}v_0 + (v_2 - v_2')/\sqrt{7} + (c_1 - c_3)/5 + (c_4 - c_2)/7$, $\bar{\xi}_{11} = \frac{1}{2}v_0 + (v_2' - v_2)/\sqrt{7} + (-7c_0 - 7c_1 + 15c_2 + 7c_3 - 8c_4)/70$, $\bar{\xi}_{12} = 3(v_2' - v_2)/4\sqrt{7} + (c_3 - c_1)/5$. The Casimir form is particularly ueful for identifying dynamical symmetries [44, 45], which occur when the only Casimir operators appearing in Eq. (2.8) are those belonging to a chain of algebras $\mathscr{A}_1 \supset \mathscr{A}_2 \supset \cdots \supset \mathscr{A}_n \supset O(3)$.

A particularly popular IBM-2 Hamiltonian is the following "standard form" [25]

$$H = \varepsilon_\pi \hat{n}_{d_\pi} + \varepsilon_\nu \hat{n}_{d_\nu} + \kappa Q_\pi \cdot Q_\nu + \kappa' \mathbf{J}_\pi \cdot \mathbf{J}_\nu$$
$$+ \sum_{L=1,3} \alpha_L (d_\pi^\dagger d_\nu^\dagger)^{(L)} \cdot (\tilde{d}_\nu \tilde{d}_\pi)^{(L)} + \alpha_2 (s_\pi^\dagger d_\nu^\dagger - s_\nu^\dagger d_\pi^\dagger) \cdot (\tilde{d}_\nu s_\pi - \tilde{d}_\pi s_\nu) \quad (2.9a)$$

$$Q_\rho = \Pi_\rho^{(2)} + \chi_\rho P_\rho^{(2)}, \quad (2.9b)$$

where $\Pi_\rho^{(2)}$ and $P_\rho^{(2)}$ are given in Eqs. (2.2). Some terms in (2.9a) are occasionally omitted and frequently $\varepsilon_\pi = \varepsilon_\nu$. This corresponds to the normal-order parameters $\varepsilon_d^{(\rho)} = \varepsilon_\rho$, $u_2 = \alpha_2$, $u_2' = \alpha_2$, $u_2'' = \kappa - \alpha_2$, $v_0 = \kappa$, $v_2 = \kappa\chi_\nu$, $v_2' = \kappa\chi_\pi$, $c_0 = \kappa\chi_\pi\chi_\nu - 6\kappa'$, $c_1 = \frac{1}{2}\kappa\chi_\pi\chi_\nu - 5\kappa' + \alpha_1$, $c_2 = -3\kappa\chi_\pi\chi_\nu/14 - 3\kappa'$, $c_3 = -4\kappa\chi_\pi\chi_\nu/7 + \alpha_3$, $c_4 = 2\kappa\chi_\pi\chi_\nu/7 + 4\kappa'$; to the multipole parameters $f_0 = \sqrt{5}\,\alpha_2$, $f_0' = \sqrt{5}\,\alpha_2$, $a_2 = \kappa - \frac{1}{2}\alpha_2$, $a_2' = -\frac{1}{2}\alpha_2$, $f_2 = \kappa\chi_\nu$, $f_2' = \kappa\chi_\pi$, $b_0 = (3\alpha_1 + 7\alpha_3)/5$, $b_1 = 10\kappa' - \frac{1}{2}\alpha_1$, $b_2 = \kappa\chi_\pi\chi_\nu$

$+ (3\alpha_1 - 8\alpha_3)/10$, $b_3 = -\frac{1}{2}\alpha_3$, $b_4 = -(4\alpha_1 + \alpha_3)/10$; and to the Casimir parameters $\xi_2^{(\rho)} = \varepsilon_\rho$, $\xi_4 = (\alpha_3 - \alpha_1)/5$, $\xi_5 = -\alpha_2 + (4\alpha_1 + \alpha_3)/10$, $\xi_6 = \alpha_2$, $\xi_7 = -\kappa\chi_\pi/4\sqrt{7} + \kappa\chi_\pi\chi_\nu/14 + (\alpha_1 - \alpha_3)/20$, $\xi_8 = \kappa\chi_\nu/4\sqrt{7} + \kappa\chi_\pi\chi_\nu/14 + (\alpha_1 - \alpha_3)/20$, $\xi_9 = \kappa(\chi_\nu - \chi_\pi)/4\sqrt{7}$, $\xi_{10} = \frac{1}{2}\kappa + \kappa(\chi_\pi - \chi_\nu)/\sqrt{7} - 2\kappa\chi_\pi\chi_\nu/7 + (\alpha_3 - \alpha_1)/5$, $\xi_{11} = -\frac{1}{2}\kappa + \kappa(\chi_\nu - \chi_\pi)/\sqrt{7} + 2\kappa\chi_\pi\chi_\nu/7 + (3\alpha_1 - \alpha_3)/10$, $\xi_{12} = 3\kappa(\chi_\pi - \chi_\nu)/4\sqrt{7} - 3\kappa\chi_\pi\chi_\nu/14 + \kappa' + (\alpha_3 - \alpha_1)/5$ or $\bar{\xi}_2^{(\rho)} = \varepsilon_\rho$, $\bar{\xi}_2 = 2\kappa - 4\kappa(\chi_\nu - \chi_\pi)/\sqrt{7} - 8\kappa\chi_\pi\chi_\nu/7 + 4(\alpha_3 - \alpha_1)/5$, $\bar{\xi}_3 = 2\kappa + 4\kappa(\chi_\pi - \chi_\nu)/\sqrt{7} - 8\kappa\chi_\pi\chi_\nu/7 + 4(\alpha_3 - \alpha_1)/5$, $\bar{\xi}_4 = -4\kappa + 8\kappa(\chi_\nu - \chi_\pi)/\sqrt{7} + 16\kappa\chi_\pi\chi_\nu/7 + 7(\alpha_1 - \alpha_3)/5$, $\bar{\xi}_5 = 2\kappa + 4\kappa(\chi_\pi - \chi_\nu)/\sqrt{7} - 8\kappa\chi_\pi\chi_\nu/7 - \alpha_2 + (9\alpha_3 - 4\alpha_1)/10$, $\bar{\xi}_6 = -2\kappa + 4\kappa(\chi_\nu - \chi_\pi)/\sqrt{7} + 8\kappa\chi_\pi\chi_\nu/7 + \alpha_2 + 4(\alpha_1 - \alpha_3)/5$, $\bar{\xi}_7 = -\kappa\chi_\pi/4\sqrt{7} + \kappa\chi_\pi\chi_\nu/14 + (\alpha_1 - \alpha_3)/20$, $\bar{\xi}_8 = \kappa\chi_\nu/4\sqrt{7} + \kappa\chi_\pi\chi_\nu/14 + (\alpha_1 - \alpha_3)/20$, $\bar{\xi}_9 = \kappa(\chi_\nu - \chi_\pi)/4\sqrt{7}$, $\bar{\xi}_{10} = -\frac{1}{2}\kappa + \kappa(\chi_\nu - \chi_\pi)/\sqrt{7} + 2\kappa\chi_\pi\chi_\nu/7 + (\alpha_1 - \alpha_3)/5$, $\bar{\xi}_{11} = \frac{1}{2}\kappa + \kappa(\chi_\pi - \chi_\nu)/\sqrt{7} - 2\kappa\chi_\pi\chi_\nu/7 + (\alpha_3 - \alpha_1)/10$, $\bar{\xi}_{12} = 3\kappa(\chi_\pi - \chi_\nu)/4\sqrt{7} - 3\kappa\chi_\pi\chi_\nu/14 + \kappa' + (\alpha_3 - \alpha_1)/5$. (Any omitted parameter is taken to have value zero).

3. IBM-2 ENERGY SURFACE

In the spirit of earlier work on the geometrical representation of IBM-1 [6–9, 22] and of an interacting-boson model for molecular rotation–vibration spectra [23], an intrinsic state for IBM-2 [26, 28, 33] is defined in terms of a double condensate,

$$|C\rangle = (N_\pi!\, N_\nu!)^{-1/2}\, (B_\pi^\dagger)^{N_\pi}\, (B_\nu^\dagger)^{N_\nu}\, |0\rangle, \tag{3.1}$$

where $B_\rho^\dagger$ is a hybrid-boson creation operator (an arbitrary linear combination of $s_\rho^\dagger$ and $d_{\rho\mu}^\dagger$) and $|0\rangle$ is the boson vacuum. The most general form of the hybrid boson operator is

$$B_\rho^\dagger = \left(s_\rho^\dagger + \sum_\mu \alpha_\mu^{(\rho)} d_{\rho\mu}^\dagger\right)\left[1 + \sum_\mu |\alpha_\mu^{(\rho)}|^2\right]^{-1/2} \tag{3.2}$$

in terms of five complex parameters $\alpha_\mu^{(\rho)}$. It turns out to be sufficient to restrict attention to a $\mathscr{T}$-even condensate (see Eq. (2.4)), which imposes $(\alpha_\mu^{(\rho)})^* = (-)^\mu \alpha_{-\mu}^{(\rho)}$. There thus remain five real coefficients, which can always be parametrized in terms of two intrinsic shape variables β_ρ, γ_ρ ($\beta_\rho \geqslant 0$, $0 \leqslant \gamma_\rho \leqslant \pi/3$) and three Euler angles of spatial rotation, Φ_ρ, Θ_ρ and Ψ_ρ (collectively denoted Ω_ρ) [26]. The energy surface associated with a given Hamiltonian H is then the expectation value of H in the double-condensate state $|C\rangle$, and is in principle a function of 10 parameters, the four shape variables β_π, β_ν, γ_π, γ_ν and six Euler angles Ω_π, Ω_ν. In practice H is always a rotational scalar, so its expectation value is independent of the overall orientation of the double condensate. This freedom is used here to select an intrinsic frame in which $\Phi_\pi = \Theta_\pi = \Psi_\pi = 0$, and Φ_ν, Θ_ν, Ψ_ν become the Euler angles of relative orientation of the proton and neutron condensates. The subscript ν will henceforth be omitted from these angles.

The IBM-2 energy surface, a function of the seven intrinsic variables β_ρ, γ_ρ, Ω, is thus given by

$$E(\beta_\rho, \gamma_\rho, \Omega) = \langle C|\, H\,|C\rangle \tag{3.3a}$$

$$|C\rangle = (N_\pi !\, N_\nu !)^{-1/2}\, (b_c^\dagger)^{N_\pi}\, (\hat{b}_c^\dagger)^{N_\nu}\, |0\rangle \tag{3.3b}$$

$$b_c^\dagger = [s_\pi^\dagger + \beta_\pi \cos\gamma_\pi \cdot d_{\pi_0}^\dagger + \beta_\pi \sin\gamma_\pi \cdot (d_{\pi_2}^\dagger + d_{\pi_{-2}}^\dagger)/\sqrt{2}](1+\beta_\pi^2)^{-1/2} \tag{3.3c}$$

$$\begin{aligned}\hat{b}_c^\dagger = \Big\{ s_\nu^\dagger + \beta_\nu \sum_\mu [\cos\gamma_\nu \cdot \mathscr{D}_{\mu 0}^{(2)}(\Omega) \\ + \sin\gamma_\nu \cdot (\mathscr{D}_{\mu 2}^{(2)}(\Omega) + \mathscr{D}_{\mu -2}^{(2)}(\Omega))/\sqrt{2}]\, d_{\nu\mu}^\dagger \Big\}\, (1+\beta_\nu^2)^{-1/2},\end{aligned} \tag{3.3d}$$

where $\mathscr{D}_{\mu\mu'}^{(2)}(\Omega)$ is a Wigner $\mathscr{D}$-function. (To avoid proliferation of subscripts, the boson condensate operator for protons in the intrinsic frame will be denoted $b_c^\dagger$ and that for neutrons $\hat{b}_c^\dagger$. Note that $b_c^\dagger$ is generally a function of β_π, γ_π; $\hat{b}_c^\dagger$ a function of β_ν, γ_ν, Φ, Θ, Ψ obtained from $b_c^\dagger$ by the replacement $\pi \to \nu$ and a rotation through the Euler angles Ω.) The evaluation of the energy surface is straightforward and produces

$$\begin{aligned}E(\beta_\rho, \gamma_\rho, \Omega) = E_0 + N_\pi N_\nu \sum_\rho [p_\rho \beta_\rho^4/(1+\beta_\rho^2)^2 + q_\rho \beta_\rho^2/(1+\beta_\rho^2)] \\ - 2\sqrt{2/7} \sum_\rho N_\rho (N_\rho - 1) v_2^{(\rho)} \beta_\rho^3 \cos 3\gamma_\rho/(1+\beta_\rho^2)^2 \\ + N_\pi N_\nu \Bigg[q\beta_\pi^2 \beta_\nu^2 + \sum_{k,l=1,2} r_{k\ell}\, g_{k\ell}(\beta_\rho, \gamma_\rho, \Omega) \\ + r_5\, g_5(\beta_\rho, \gamma_\rho, \Omega) \Bigg] \Bigg/ (1+\beta_\pi^2)(1+\beta_\nu^2)\end{aligned} \tag{3.4a}$$

$$\begin{aligned}g_{k\ell}(\beta_\rho, \gamma_\rho, \Omega) = \beta_\pi^k \beta_\nu^\ell \{\cos k\gamma_\pi \cos \ell\gamma_\nu (1 + 3\cos 2\Theta) \\ - \sqrt{3}\, [\cos k\gamma_\pi (-)^\ell \sin \ell\gamma_\nu \cos 2\Psi \\ + (-)^k \sin k\gamma_\pi \cos \ell\gamma_\nu \cos 2\Phi](1 - \cos 2\Theta) \\ + (-)^{k+\ell} \sin k\gamma_\pi \sin \ell\gamma_\nu [(3 + \cos 2\Theta) \cos 2\Phi \cos 2\Psi \\ - 4\cos\Theta \sin 2\Phi \sin 2\Psi]\}\end{aligned} \tag{3.4b}$$

$$\begin{aligned}g_5(\beta_\rho, \gamma_\rho, \Omega) = \beta_\pi^2 \beta_\nu^2 \{(7 + 5\cos 2\gamma_\pi)(7 + 5\cos 2\gamma_\nu)(9 + 20\cos 2\Theta + 35\cos 4\Theta)/35 \\ + 4\sqrt{3}\, [\sin 2\gamma_\pi (7 + 5\cos 2\gamma_\nu) \cos 2\Phi \\ + (7 + 5\cos 2\gamma_\pi) \sin 2\gamma_\nu \cos 2\Psi](3 + 4\cos 2\Theta - 7\cos 4\Theta)/7\end{aligned}$$

$$\begin{aligned}
&+48 \sin 2\gamma_\pi \sin 2\gamma_\nu[(5+4\cos 2\Theta \\
&+7\cos 4\Theta)\cos 2\Phi \cos 2\Psi - 2(\cos\Theta + 7\cos 3\Theta)\sin 2\Phi \sin 2\Psi]/7 \\
&+[(1-\cos 2\gamma_\pi)(7+5\cos 2\gamma_\nu)\cos 4\Phi \\
&+(7+5\cos 2\gamma_\pi)(1-\cos 2\gamma_\nu)\cos 4\Psi](3-4\cos 2\Theta+\cos 4\Theta) \\
&+4\sqrt{3}\sin 2\gamma_\pi(1-\cos 2\gamma_\nu)[(5-4\cos 2\Theta-\cos 4\Theta)\cos 2\Phi\cos 4\Psi \\
&-4(\cos\Theta-\cos 3\Theta)\sin 2\Phi \sin 4\Psi] \\
&+4\sqrt{3}(1-\cos 2\gamma_\pi)\sin 2\gamma_\nu[(5-4\cos 2\Theta-\cos 4\Theta)\cos 4\Phi\cos 2\Psi \\
&-4(\cos\Theta-\cos 3\Theta)\sin 4\Phi\sin 2\Psi] \\
&+(1-\cos 2\gamma_\pi)(1-\cos 2\gamma_\nu)[(35+28\cos 2\Theta+\cos 4\Theta)\cos 4\Phi\cos 4\Psi \\
&-8(7\cos\Theta+\cos 3\Theta)\sin 4\Phi\sin 4\Psi]\}
\end{aligned} \tag{3.4c}$$

$$E_0=\sum_\rho [N_\rho e_s^{(\rho)}+N_\rho(N_\rho-1)u_0^{(\rho)}]+u_0 N_\pi N_\nu \tag{3.4d}$$

$$\begin{aligned}
p_\rho=\bar{c}_\rho-\bar{a}_\rho; \qquad \bar{c}_\pi&=(N_\pi-1)c_\pi/N_\nu, \qquad \bar{c}_\nu=(N_\nu-1)c_\nu/N_\pi, \\
\bar{a}_\pi&=(N_\pi-1)a_\pi/N_\nu, \qquad \bar{a}_\nu=(N_\nu-1)a_\nu/N_\pi
\end{aligned} \tag{3.4e}$$

$$a_\rho=(\varepsilon_d^{(\rho)}-\varepsilon_s^{(\rho)})/(N_\rho-1)-2u_0^{(\rho)}+u_2^{(\rho)}+2v_0^{(\rho)} \tag{3.4f}$$

$$c_\rho=(\varepsilon_d^{(\rho)}-\varepsilon_s^{(\rho)})/(N_\rho-1)-u_0^{(\rho)}+(7c_0^{(\rho)}+10c_2^{(\rho)}+18c_4^{(\rho)})/35 \tag{3.4g}$$

$$q_\pi=\bar{a}_\pi+u_2'-u_0, \qquad q_\nu=\bar{a}_\nu+u_2-u_0 \tag{3.4h}$$

$$q=u_0-u_2-u_2'+(c_0+3c_1+5c_2+7c_3+9c_4)/25 \tag{3.4i}$$

$$\begin{aligned}
r_{11}=(u_2''+v_0)/2, \qquad r_{12}&=-v_2/\sqrt{14}, \qquad r_{21}=-v_2'/\sqrt{14}, \\
r_{22}&=(14c_0+21c_1-15c_2-56c_3+36c_4)/980
\end{aligned} \tag{3.4j}$$

$$r_5=(14c_0-28c_1+20c_2-7c_3+c_4)/35840. \tag{3.4k}$$

The multipole terms in Eq. (2.6) with coefficients a_2', b_1, and b_3 do not contribute at all to the energy surface. The Euler-angle dependence arises solely from the quadrupole and hexadecupole terms in Eq. (2.6) (in fact, $r_{11}=a_2$, $r_{12}=-f_2/\sqrt{14}$, $r_{21}=-f_2'/\sqrt{14}$, $r_{22}=b_2/14$, $r_5=b_4/512$), the γ_ρ dependence from these same five terms and the $v_2^{(\rho)}$ terms of H_ρ, Eq. (2.5b). Aside from the constant E_0, the shape of the energy surface is determined by the 12 coefficients p_ρ, q_ρ, $v_2^{(\rho)}$ $(\rho=\pi, \nu)$, q, $r_{k\ell}(k, \ell=1, 2)$, r_5, i.e., 12 combinations of the 30 Hamiltonian parameters.

The function (3.4a) of the seven intrinsic shape parameters β_ρ, γ_ρ, Ω is clearly too complicated for a detailed analysis of its shape and its possible extrema, but some general comments are possible. The two-dimensional symmetric section $(\beta_\pi=\beta_\nu,\ \gamma_\pi=\gamma_\nu,\ \Phi=\Theta=\Psi=0)$ of the seven-dimensional energy surface takes the form $E_0+N_\pi N_\nu\beta^2(A-B\beta\cos 3\gamma+C\beta^2)/(1+\beta^2)^2$, where $A=q_\pi+q_\nu+4r_{11}$, $B=2\sqrt{2/7}\,[v_2^{(\pi)}(N_\pi-1)/N_\nu+v_2^{(\nu)}(N_\nu-1)/N_\pi]-4(r_{12}+r_{21})$, and $C=p_\pi+$

$p_\nu + q_\pi + q_\nu + q + 4r_{22} + 9216r_5/35$ are independent of β and γ. (The contribution of the Majorana terms vanishes identically on this section.) This is precisely the form of the IBM-1 energy surface [7], and has no triaxial minimum, so even the most general IBM-2 Hamiltonian cannot produce identically-triaxial aligned proton and neutron condensates. For aligned condensates, with relative Euler angles $\Phi = \Theta = \Psi = 0$, the functions $g_{\kappa\ell}(\beta_\rho, \gamma_\rho, 0) = 3\beta_\pi^k \beta_\nu^\ell [\cos k(\gamma_\pi - \gamma_\nu) \cdot \delta_{k\ell} + \cos(k\gamma_\pi + \ell\gamma_\nu) \cdot (1 - \delta_{k\ell})]$ and $g_5(\beta_\rho, \gamma_\rho, 0) = 768[7 + 5\cos 2(\gamma_\pi - \gamma_\nu)]/35$, so if $r_{12} = 0 = r_{21}$ and $v_2^{(\pi)} = 0 = v_2^{(\nu)}$ this four-dimensional section of the energy surface is a function only of $\gamma_\pi - \gamma_\nu$, and not of $\gamma_\pi + \gamma_\nu$.

Given appropriate choices of Hamiltonian parameters, many physically-interesting minima of the energy surface can be accommodated. Examples include: (i) $\beta_\pi = 0 = \beta_\nu$, two spherical condensates; (ii) $\beta_\pi > 0$, $\beta_\nu > 0$, $\gamma_\pi = 0 = \gamma_\nu$ (or $\gamma_\pi = \pi/3 = \gamma_\nu$), $\Theta = 0$, parallel prolate (or oblate) condensates; (iii) $\beta_\pi > 0$, $\beta_\nu > 0$, $\gamma_\pi = 0$, $\gamma_\nu = \pi/3$, $\Theta = \pi/2$, $\Psi = \pi/2$, a prolate proton condensate and an oblate neutron condensate, with axes of symetry parallel; (iv) $\beta_\pi > 0$, $\beta_\nu > 0$, $\gamma_\pi = 0$, $\gamma_\nu = \pi/3$, $\Theta = 0$, a prolate proton condensate and an oblate neutron condensate, with axes of symmetry orthogonal; (v) $\beta_\rho > 0$, $0 < \gamma_\rho < \pi/3$, $\Phi = \Theta = \Psi = 0$, $\gamma_\pi \neq \gamma_\nu$, two aligned triaxial condensates. (In cases (iii) and (iv), it would clearly be possible to have oblate protons and prolate neutrons, rather than the choice presented.)

There are many Hamiltonians whose energy surfaces are independent of the relative Euler angles (their parameters are such that the multipole parameters a_2, f_2, f_2', b_2, and b_4 in Eq. (2.6) vanish, and their Casimir forms have vanishing coefficients ξ_i, $i = 5, 6, 7, 8, 9$ in Eq. (2.8)), and many whose energy surfaces are totally γ-unstable (independent of γ_π and γ_ν). The later are necessarily also independent of the relative Euler angles Ω, but also have $v_2^{(\rho)} = 0$. There are even Hamiltonians whose energy surface is completely flat, independent of β_ρ, γ_ρ, and Ω. Since all 12 coefficients defining the shape of the energy surface must then vanish, such Hamiltonians are determined by 12 conditions on their 30 parameters. They can always be transcribed in the form

$$\begin{aligned} H_{\text{flat}} = {} & \sum_\rho [\varepsilon_s^{(\rho)} \hat{N}_\rho + u_0^{(\rho)} \hat{N}_\rho (\hat{N}_\rho - 1)] + a_0 \hat{N}_\pi \hat{N}_\nu \\ & + x_6 (C_{\overline{O(6)}} - 5\hat{N}) + x_5 (C_{O(5)} - 4\hat{n}_d) + x_3 (C_{O(3)} - 6\hat{n}_d) \\ & + \sum_\rho [x_6^{(\rho)} (C_{\overline{O(6)}}^{(\rho)} - 5\hat{N}_\rho) + x_5^{(\rho)} (C_{O(5)}^{(\rho)} - 4\hat{n}_{d\rho}) + x_3^{(\rho)} (C_{O(3)}^{(\rho)} - 6\hat{n}_{d\rho})], \end{aligned} \tag{3.5}$$

where terms of the type $\hat{N}_\rho - N_\rho$ or $[N_\nu(\hat{N}_\pi - 1)/(N_\pi - 1) - \hat{N}_\nu] \hat{n}_{d_\pi}$ have been omitted, since they vanish identically in the states of fixed N_π, N_ν considered here. The coefficients x in Eq. (3.5) are most easily written $x_3 = (b_1 - b_3)/20$, $x_3^{(\rho)} = (c_4^{(\rho)} - c_2^{(\rho)})/7 - x_3$; $x_5 = (b_3 - 2a_2')/4$, $x_5^{(\rho)} = v_0^{(\rho)} - (7c_0^{(\rho)} - 10c_2^{(\rho)} + 3c_4^{(\rho)})/35 - x_5$; $x_6 = \frac{1}{2}a_2'$, $x_6^{(\rho)} = -v_0^{(\rho)} - x_6$. So any Hamiltonian with a flat energy surface is constructed from trivial number-operator terms and the two-body parts of the quadratic Casimir operators associated with $\overline{O(6)}_\pi \times \overline{O(6)}_\nu$ and its subalgebras.

3.1. *Intrinsic Boson Basis*

The condensate bosons $b_c^\dagger$, $\hat{b}_c^\dagger$ defined in Eq. (3.3) are members of a complete, alternative, intrinsic-boson basis [20, 22] which can be used instead of the spherical basis $s_\rho^\dagger$, $d_{\rho\mu}^\dagger$. Consider the unitary operators

$$R_\beta \equiv \exp[-\alpha(s_\rho^\dagger d_{\rho 0} - d_{\rho 0}^\dagger s_\rho)] = \exp[i\alpha \bar{\Pi}_0^{(2)}], \qquad \beta = \tan\alpha \quad (0 \leqslant \alpha \leqslant \pi/2) \tag{3.6a}$$

$$\begin{aligned} R_\gamma &\equiv \exp\{-\gamma[d_{\rho 0}^\dagger(d_{\rho 2} + d_{\rho -2})/\sqrt{2} - (d_{\rho 2}^\dagger + d_{\rho -2}^\dagger)/\sqrt{2} \cdot d_{\rho 0}]\} \\ &= \exp[-i\gamma \cdot i(P_2^{(3)} - P_{-2}^{(3)})], \end{aligned} \tag{3.6b}$$

where R_β is a specific element of the group $\overline{O(6)}_\rho$ and R_γ is a specific element of the group $O(5)_\rho \subset \overline{O(6)}_\rho$. It is easily checked that $b_c^\dagger$ is an $\overline{O(6)}_\pi$ transform of $s_\pi^\dagger$, i.e., $b_c^\dagger = R_{\gamma_\pi} R_{\beta_\pi} s_\pi^\dagger R_{\beta_\pi}^{-1} R_{\gamma_\pi}^{-1}$. Similarly, $\hat{b}_c^\dagger$ is an $\overline{O(6)}_\nu$ transform of $s_\nu^\dagger$, having in addition to R_β and R_γ also a spatial rotation R_Ω belonging to $O(3)_\nu \subset O(5)_\nu \subset \overline{O(6)}_\nu$. By applying the same unitary transformations to $d_{\rho\mu}^\dagger$, a complete alternative basis can be generated. The form found to be most useful is

$$b_c^\dagger = [s_\pi^\dagger + \beta_\pi \cos\gamma_\pi \cdot d_{\pi 0}^\dagger + \beta_\pi \sin\gamma_\pi \cdot (d_{\pi 2}^\dagger + d_{\pi -2}^\dagger)/\sqrt{2}]/(1+\beta_\pi^2)^{1/2} \tag{3.7a}$$

$$b_\beta^\dagger = [\cos\gamma_\pi d_{\pi 0}^\dagger + \sin\gamma_\pi \cdot (d_{\pi 2}^\dagger + d_{\pi -2}^\dagger)/\sqrt{2} - \beta_\pi s_\pi^\dagger]/(1+\beta_\pi^2)^{1/2} \tag{3.7b}$$

$$b_\gamma^\dagger = \cos\gamma_\pi \cdot (d_{\pi 2}^\dagger + d_{\pi -2}^\dagger)/\sqrt{2} - \sin\gamma_\pi \cdot d_{\pi 0}^\dagger \tag{3.7c}$$

$$b_x^\dagger = (d_{\pi 1}^\dagger + d_{\pi -1}^\dagger)/\sqrt{2} \tag{3.7d}$$

$$b_y^\dagger = i(d_{\pi 1}^\dagger - d_{\pi -1}^\dagger)/\sqrt{2} \tag{3.7e}$$

$$b_z^\dagger = (d_{\pi 2}^\dagger - d_{\pi -2}^\dagger)/\sqrt{2}. \tag{3.7f}$$

For neutrons, the basis $\hat{b}_i^\dagger$ $(i = c, \beta, \gamma, x, y, z)$ is obtained by replacing the subscript π by ν in Eqs. (3.7) and rotating the result through the Euler angles Φ, Θ, Ψ.

It has been found, in the framework of IBM-1, [12, 20, 22] that the time-even bosons are associated with intrinsic shape degrees of freedom ($b_c^\dagger$ with the condensate, $b_\beta^\dagger$ with β-vibrations, $b_\gamma^\dagger$ with γ-vibrations), while the time-odd bosons are associated with collective rotations about the corresponding axes ($b_x^\dagger$ with rotations about the x-axis, $b_y^\dagger$ and $b_z^\dagger$ about the y-axis and the z-axis, respectively). Any IBM-2 operator may be expressed in the intrinsic basis by using the inverse of transformation (3.7) and its neutron analogue. In particular, this is true of the Hamiltonian H, and the energy surface can be read off from the coefficients of the terms $b_c^\dagger b_c$, $\hat{b}_c^\dagger \hat{b}_c$, $(b_c^\dagger)^2 b_c^2$, $(\hat{b}_c^\dagger)^2 \hat{b}_c^2$ and $\hat{b}_c^\dagger b_c^\dagger b_c \hat{b}_c$ in the intrinsic form of H.

The intrinsic basis, and the double condensate, may be defined with arbitrary values of β_ρ, γ_ρ, Ω, but it is clearly most reasonable to choose these shape parameters at the global minimum of the energy surface. The resulting equilibrium condensate and equilibrium intrinsic basis will then evidently have dynamical significance, and may be expected to be particularly useful in discussing the dynamics of the model.

4. INTRINSIC/COLLECTIVE RESOLUTION OF THE HAMILTONIAN

Given any IBM-2 Hamiltonian H, it is straightforward to construct its energy surface $E(\beta_\rho, \gamma_\rho, \Omega)$, Eq. (3.4), and to find the equilibrium shape parameters, defined as the values of β_π, β_ν, γ_π, γ_ν, Φ, Θ, and Ψ at the global minimum of $E(\beta_\rho, \gamma_\rho, \Omega)$. The equilibrium parameters determine the intrinsic basis, Eq. (3.7), and the equilibrium condensate $|C\rangle$, Eq. (3.3). There exist IBM-2 Hamiltonians H' for which the equilibrium condensate is an eigenstate. Since the eigenvalue can be shifted at will, for any fixed values of N_π and N_ν, for example by adding a term proportional to $\hat{N}_\pi \hat{N}_\nu$, it is convenient to take it to be zero. Then the Hamiltonians H' are those which annihilate the equilibrium condensate,

$$H' |C\rangle = 0. \tag{4.1}$$

By rewriting H' in terms of the equilibrium intrinsic basis, Eq. (4.1) can be recognized as requiring that the coefficients of all terms of H' of the form $b_i^\dagger b_c$, $\hat{b}_i^\dagger \hat{b}_c$, $b_i^\dagger b_j^\dagger b_c^2$, $\hat{b}_i \hat{b}_j^\dagger \hat{b}_c^2$, and $\hat{b}_i^\dagger b_j^\dagger b_c \hat{b}_c$ should vanish, for all i and j. There is generally a whole family of Hamiltonians H' whose parameters satisfy these conditions.

For each Hamiltonian H' satisfying Eq. (4.1), it is possible to construct the corresponding energy surface, $E'(\beta_\rho, \gamma_\rho, \Omega)$. This will generally differ from the energy surface E of H, but the equilibrium shape parameters of E will fall at an extremum of E'. There may be some member of the family H' whose energy surface E' differs from that of H by a constant, independent of β_ρ, γ_ρ, Ω. Since E' and E have the same shape in such a case, their equilibrium shape parameters coincide. In most cases of physical interest, such a Hamiltonian H' can be found. (Sometimes, the full energy surface of H can be reproduced, up to an overall constant shift, by that of H' only if certain restrictions are imposed on the original parameters of H. Since IBM-2 has so many parameters in its most general form, this is unlikely to be a serious obstacle.) This specific H' has an energy surface of exactly the same shape as the energy surface of H, and the equilibrium condensate is its exact ground state. (It appears that the conditions for the equilibrium shape parameters to lie at a global minimum of the energy surface are the same as the conditions of H' to be positive semi-definite.) It is defined to be the intrinsic part of H, denoted H_{int}.

When the equilibrium shape parameters are such that $\beta_\pi \neq 0$ and/or $\beta_\nu \neq 0$, the equilibrium condensate does not have a well-defined angular momentum, but is a superposition of many angular momenta. Since H_{int} is a rotational scalar, while its (deformed) ground state does not have good angular momentum, this is a case of spontaneous symmetry breaking. Any rotation of the condensate will produce a new, degenerate, ground state. Components of good angular momentum can be projected from the condensate. Since the projection operators are constructed from angular-momentum generators, and hence commute with the scalar H_{int}, each such projected state is a zero-energy ground state with well-defined angular momentum. This case thus corresponds to an exactly-degenerate ground-state band for H_{int}. In cases where H has additional symmetries (e.g., it may be an $O(5)$ scalar), they are generally shared by H_{int}, but broken by the condensate. The phenomenon of spontaneous symmetry breaking is thus extended, and much larger multiplets become degenerate. Usually, the higher (excited) states of H_{int} do not form exactly-degenerate bands, except in the dynamic-symmetry limits, where H_{int} is a sum of appropriate Casimir operators. But numerical calculations have shown [20–22] that they do tend to cluster into recognizable bands of states close to one another in energy and connected by particularly large $E2$ matrix elements.

Thus, given a Hamiltonian, it is possible to define its intrinsic part H_{int}, which determines the shape of the energy surface and has the equilibrium condensate as an exact ground state. The remainder of H, called its collective part H_c, is defined by the equation

$$H = H_{\text{int}} + H_c. \tag{4.2}$$

Since, by definition, the energy surface of H_c is flat, it is necessarily of the $\overline{O(6)}_\pi \times \overline{O(6)}_\nu$ form, Eq. (3.5), its parameters being given by the difference between those of H and H_{int}. It is responsible for splitting the degenerate ground-state band and near-degenerate excited bands of H_{int}, and may be interpreted as incorporating the collective motion of the intrinsic structures determined by H_{int}. This collective motion is not only rotational (of $O(3)$ type), but can include also $O(5)$ or $\overline{O(6)}$ dynamics. The transformation (3.6) to the intrinsic basis, also of the $O(3) \subset O(5) \subset \overline{O(6)}$ type, may be thought of as a kind of "unfolding" of the collective motion in order to expose the building blocks of the intrinsic structure.

In general, the intrinsic and collective parts of H do not commute, $[H_{\text{int}}, H_c] \neq 0$, so that H_c not only splits and shifts the intrinsic bands, but may also mix them. The persistence of band structure in nuclei away from dynamical symmetries (where H_{int} and H_c do commute and the bands are exact) is thus dependent on the degree to which H_c mixes the intrinsic bands. It is a quantitative feature, dependent on the details of the dynamics, and not an automatic consequence of the existence of an underlying intrinsic structure. In the collective nuclei where the IBM has been successful, it is empirically observed that band structure persists quite strongly. It is thus likely that the band mixing induced by H_c is quite weak in these cases, though experience indicates that H_c can bring about appreciable shifts in band-head energies.

Given the richness and complexity of IBM-2, it is unreasonable to attempt anything like a complete survey of all possible intrinsic/collective resolutions, for all possible types of condensates. However, some cases of physical interest can be presented as illustrative examples of the technique.

4.1. *Spherical Condensate*

The point $\beta_\pi = 0 = \beta_\nu$ is always an extremum of the energy surface, i.e., $\partial E/\partial \beta_\rho = 0$, $\partial E/\partial \gamma_\rho = 0$, $\partial E/\partial \Omega = 0$ at this point, for any values of the parameters of the Hamiltonian H. For suitable choices of the parameters of H, this point can be a minimum of the energy surface, and in some cases it will be the global minimum. When this occurs, the equilibrium condensate is just $(N_\pi!\, N_\nu!)^{-1/2}\, (s_\pi^\dagger)^{N_\pi}\, (s_\nu^\dagger)^{N_\nu}\, |0\rangle$, a spherical condensate with angular momentum zero. There is no spontaneous symmetry breaking, and the ground-state "band" is a single state.

The Hamiltonian H' (with primed parameters (2.5)) annihilates the spherical condensate provided $\varepsilon_s^{(\rho)'}=0$, $u_0^{(\rho)'}=0$, $v_0^{(\rho)'}=0$, $u_0'=0$, and $v_0'=0$ ($\rho=\nu$ or π). Such a Hamiltonian can always be rewritten in the form

$$\begin{aligned} H_{\text{int}} = \sum_{\rho=\nu,\pi} & \{\zeta_\rho[s_\rho^\dagger d_\rho^\dagger + \eta_\rho(d_\rho^\dagger d_\rho^\dagger)^{(2)}]\cdot[\tilde{d}_\rho s_\rho + \eta_\rho(\tilde{d}_\rho \tilde{d}_\rho)^{(2)}] + \zeta_\rho' \hat{n}_{d_\rho}(\hat{n}_{d_\rho}-1)\} \\ & + \zeta_0 \hat{n}_{d_\pi}\hat{n}_{d_\nu} + \sum_{L=1,3} \zeta_L (d_\pi^\dagger d_\nu^\dagger)^{(L)}\cdot(\tilde{d}_\nu \tilde{d}_\pi)^{(L)} \\ & + \zeta_2[s_\pi^\dagger d_\nu^\dagger + \eta_2 s_\nu^\dagger d_\pi^\dagger + \eta_2'(d_\pi^\dagger d_\nu^\dagger)^{(2)}]\cdot[\tilde{d}_\nu s_\pi + \eta_2 \tilde{d}_\pi s_\nu + \eta_2'(\tilde{d}_\nu \tilde{d}_\pi)^{(2)}], \end{aligned} \tag{4.3}$$

where ζ_ρ, ζ_ρ', η_ρ, ζ_i, η_2, η_2' are arbitrary real parameters. This form is not unique, and other representations are occasionally useful. In arriving at this form terms have been discarded if they vanish identically for fixed values of N_π, N_ν or if they involve the Casimir operators of $O(5)$ and $O(3)$, which do not contribute to the energy surface and are more naturally included in the collective part H_c. The 12 parameters of H_{int} determine its energy surface, and can be chosen to reproduce the shape of the energy surface of H. In terms of the energy-surface coefficients of H they are given by

$$\zeta_\pi = N_\nu(q_\pi - 2r_{11}r_{21}/r_{12})/(N_\pi - 1) \tag{4.4a}$$

$$\zeta_\nu = N_\pi(q_\nu - 2r_{11}r_{12}/r_{21})/(N_\nu - 1) \tag{4.4b}$$

$$\eta_\rho = v_2^{(\rho)}/\zeta_\rho \qquad (\rho = \nu, \pi) \tag{4.4c}$$

$$\zeta_\rho' = N_\sigma p_\rho/(N_\rho - 1) + \zeta_\rho(1 - 2\eta_\rho^2/7) \qquad (\rho, \sigma = \nu, \pi; \sigma \neq \rho) \tag{4.4d}$$

$$\zeta_1 = 4r_{22} - 8192r_5/7 + 5r_{12}r_{21}/r_{11} \tag{4.4e}$$

$$\zeta_2 = 2r_{11}r_{12}/r_{21} \tag{4.4f}$$

$$\zeta_3 = -16r_{22} - 3072r_5/7 \tag{4.4g}$$

$$\eta_2 = r_{21}/r_{12} \tag{4.4h}$$

$$\eta_2' = -\sqrt{7/2}\cdot r_{21}/r_{11} \tag{4.4i}$$

$$\zeta_0 = q + 4r_{22} + 9216r_5/35 + 2r_{11}r_{21}/r_{12} + 2r_{11}r_{12}/r_{21} - 2r_{12}r_{21}/r_{11}. \tag{4.4j}$$

Equations (4.3) and (4.4) define H_{int} for all cases when the equilibrium shape parameters are $\beta_\pi = 0 = \beta_\nu$. (Modifications may be necessary in specific cases, such as $r_{11}=0$, $r_{12}=0$ or $r_{21}=0$.) The structure of Eq. (4.3) is of general interest—each term is the scalar product of a pair-creation operator of definite rank with its conjugate pair-destruction operator. Each term is thus positive semi-definite if its coefficient ζ is positive. The intrinsic Hamiltonian annihilates the spherical condensate because each individual pair-destruction operator does so. When all coefficients

ζ are positive, $\beta_\rho = 0$ is a global minimum of the energy surface. Experience has shown that H_{int} always takes this particular form, so its construction is made simpler, being simply a search for all two-body destruction operators of fixed angular-momentum rank which annihilate the appropriate condensate.

Two dynamic-symmetry limits [41, 44, 45] relevant to the spherical condensate are (I) $U(6)_\pi \times U(6)_\nu \supset U(6) \supset U(5) \supset O(5) \supset O(3)$ and (II) $U(6)_\pi \times U(6)_\nu \supset U(5)_\pi \times U(5)_\nu \supset U(5) \supset O(5) \supset O(3)$. The corresponding Hamiltonians, when treated according to Eqs. (4.3), (4.4), and (4.2), separate naturally into mutually-commuting intrinsic and collective parts below the $U(5)$ link in the chain of algebras. Then

$$H_{\text{int}}^{(I)} = \varepsilon \hat{n}_d + A \hat{n}_d(\hat{n}_d - 1) + A_1 (s_\pi^\dagger d_\nu^\dagger - s_\nu^\dagger d_\pi^\dagger) \cdot (\tilde{d}_\nu s_\pi - \tilde{d}_\pi s_\nu) + A_2 \mathscr{M}_5 \tag{4.5a}$$

$$H_{\text{c}}^{(\mathrm{I})} = B_1 (C_{O(5)} - 4\hat{n}_d) + B_2 (\mathbf{J}^2 - 6\hat{n}_d) \tag{4.5b}$$

$$H_{\text{int}}^{(\mathrm{II})} = \varepsilon'_\pi \hat{n}_{d_\pi} + \varepsilon'_\nu \hat{n}_{d_\nu} + A' \hat{n}_{d_\pi} \hat{n}_{d_\nu} + A_\pi \hat{n}_{d_\pi}(\hat{n}_{d_\pi} - 1) + A_\nu \hat{n}_{d_\nu}(\hat{n}_{d_\nu} - 1) + A'' \mathscr{M}_5 \tag{4.5c}$$

$$H_{\text{c}}^{(\mathrm{II})} = B'_1 (C_{O(5)} - 4\hat{n}_d) + B'_2 (\mathbf{J}^2 - 6\hat{n}_d) \tag{4.5d}$$

with energy-surface coefficients (I) $p_\rho = (N_\rho - 1) A / N_\sigma$, $q_\rho = \varepsilon / N_\sigma + A_1$, $v_2^{(\rho)} = 0$ ($\rho, \sigma = \nu, \pi; \sigma \neq \rho$); $q = 2A - 2A_1 + 4A_2/5$, $r_{11} = -A_1/2$, $r_{12} = 0 = r_{21}$, $r_{22} = -A_2/14$, $r_5 = -A_2/512$; (II) $p_\rho = (N_\rho - 1) A_\rho / N_\sigma$, $q_\rho = \varepsilon'_\rho / N_\sigma$, $v_2^{(\rho)} = 0$ ($\rho, \sigma = \nu, \pi$; $\sigma \neq \rho$); $q = A' + 4A''/5$, $r_{11} = 0 = r_{12} = r_{21}$, $r_{22} = -A''/14$, $r_5 = -A''/512$.

4.2. *Aligned Axial Condensates*

When the global minimum of the energy surface of H falls at non-zero values of the shape parameters β_ρ, the condensate is deformed. If at this global minimum $\gamma_\rho = 0$ or $\pi/3$, each individual condensate, neutron or proton, is axially symmetric (prolate if $\gamma = 0$, symmetry axis in z-direction; oblate if $\gamma = \pi/3$, symmetry axis in y-direction). The symmetry axes of the two axial condensates may be parallel (aligned), at right angles (orthogonal) or at some arbitrary relative orientation (skew). In view of the strong attractive neutron–proton force in nuclei, it is to be anticipated that the neutron and proton condensates will be both spherical or both deformed, and that when they are deformed they will be both prolate or both oblate (if axially symmetric), and aligned. In specific nuclei, other cases could occur, and the method described here could be applied also to them, but only the more likely cases will be dealt with at any length below. The prototype case is that of aligned prolate condensates, with equilibrium shape parameters $\beta_\rho > 0$, $\gamma_\rho = 0$, $\Omega = 0$. This is a case of spontaneous rotational-symmetry breaking, so the double condensate will correspond to an exactly-degenerate ground-state band of the intrinsic Hamiltonian H_{int}.

It is noteworthy that all points in shape-parameter space on the two-dimensional surface $\gamma_\rho = 0$, $\Omega = 0$ satisfy the five extremum equations $\partial E / \partial \gamma_\rho = 0$, $\partial E / \partial \Omega = 0$, while the remaining two extremum equations $\partial E / \partial \beta_\rho = 0$ determine the values of β_ρ at extrema of the energy surface.

The intrinsic Hamiltonian which annihilates the aligned prolate condensate can be constructed from condensate-annihilating pair-destruction operators, as discussed in the previous subsection, and has the general form

$$\begin{aligned} H_{\text{int}} = \sum_{\rho} \{ & \zeta_\rho [\beta_\rho^2 (s_\rho^\dagger)^2 - d_\rho^\dagger \cdot d_\rho^\dagger][\beta_\rho^2 s_\rho^2 - \tilde{d}_\rho \cdot \tilde{d}_\rho] \\ & + \zeta'_\rho [\beta_\rho s_\rho^\dagger d_\rho^\dagger + \sqrt{7/2}\,(d_\rho^\dagger d_\rho^\dagger)^{(2)}] \cdot [\beta_\rho \tilde{d}_\rho s_\rho + \sqrt{7/2}\,(\tilde{d}_\rho \tilde{d}_\rho)^{(2)}]\} \\ & + \zeta_0 (\beta_\pi \beta_\nu s_\pi^\dagger s_\nu^\dagger - d_\pi^\dagger \cdot d_\nu^\dagger)(\beta_\pi \beta_\nu s_\nu s_\pi - \tilde{d}_\nu \cdot \tilde{d}_\pi) \\ & + \sum_{L=1,3} \zeta_L (d_\pi^\dagger d_\nu^\dagger)^{(L)} \cdot (\tilde{d}_\nu \tilde{d}_\pi)^{(L)} \\ & + \zeta_2 (\beta_\pi s_\pi^\dagger d_\nu^\dagger - \beta_\nu s_\nu^\dagger d_\pi^\dagger) \cdot (\beta_\pi \tilde{d}_\nu s_\pi - \beta_\nu \tilde{d}_\pi s_\nu) \\ & + \zeta'_2 [\beta_\pi s_\pi^\dagger d_\nu^\dagger + \sqrt{7/2}\,(d_\pi^\dagger d_\nu^\dagger)^{(2)}] \cdot [\beta_\pi \tilde{d}_\nu s_\pi + \sqrt{7/2}\,(\tilde{d}_\nu \tilde{d}_\pi)^{(2)}] \\ & + \zeta''_2 [\beta_\nu s_\nu^\dagger d_\pi^\dagger + \sqrt{7/2}\,(d_\nu^\dagger d_\pi^\dagger)^{(2)}] \cdot [\beta_\nu \tilde{d}_\pi s_\nu + \sqrt{7/2}\,(\tilde{d}_\pi \tilde{d}_\nu)^{(2)}], \end{aligned} \tag{4.6}$$

where the 10 ζ coefficients are arbitrary. The energy surface of H_{int} will reproduce the shape of the energy surface of H when the coefficients ζ are determined by the energy-surface parameters of H as follows:

$$\begin{aligned} \zeta_\rho = {} & [N_\sigma p_\rho/(N_\rho - 1) - \sqrt{2/7}\, v_2^{(\rho)}(1 - \beta_\rho^2)/\beta_\rho](1 + \beta_\rho^2)^{-2} \\ & (\rho, \sigma = \pi, \nu; \rho \neq \sigma) \end{aligned} \tag{4.7a}$$

$$\zeta'_\rho = \sqrt{2/7}\, v_2^{(\rho)}/\beta_\rho \qquad (\rho = \pi, \nu) \tag{4.7b}$$

$$\begin{aligned} \zeta_0 = {} & [q + 4r_{22} + 9216 r_5/35 + 2r_{12}(1 - \beta_\pi^2)/\beta_\pi + 2r_{21}(1 - \beta_\nu^2)/\beta_\nu \\ & - 2r_{11}(\beta_\pi^2 + \beta_\nu^2)/\beta_\pi \beta_\nu]/(1 + \beta_\pi^2)(1 + \beta_\nu^2) \end{aligned} \tag{4.7c}$$

$$\zeta_1 = 2\zeta_0 + 4r_{22} - 5(r_{12}/\beta_\pi + r_{21}/\beta_\nu) - 8192 r_5/7 \tag{4.7d}$$

$$\zeta_2 = -\zeta_0 - 2r_{11}/\beta_\pi \beta_\nu \tag{4.7e}$$

$$\zeta'_2 = -2r_{12}/\beta_\pi \tag{4.7f}$$

$$\zeta''_2 = -2r_{21}/\beta_\nu \tag{4.7g}$$

$$\zeta_3 = 2\zeta_0 - 16 r_{22} - 3072 r_5/7. \tag{4.7h}$$

Since 10 parameters ζ are determined by 12 energy-surface parameters, there remain two conditions which must be satisfied by the energy-surface parameters, and these are just the extremum conditions $\partial E/\partial \beta_\rho = 0$ which fix the values of β_ρ.

All other cases of aligned axial condensates can be obtained from the aligned prolate case above by simple manipulations of the results. The aligned oblate case ($\gamma_\rho = \pi/3$, $\Omega = 0$) is obtained by reversing the sign of the operators $s_\rho^\dagger$, s_ρ everywhere in Eq. (4.6) and of β_ρ everywhere in Eqs. (4.7). Similarly the aligned prolate/oblate case $\gamma_\pi = 0$, $\gamma_\nu = \pi/3$, $\Phi = 0$, $\Theta = \pi/2$, $\Psi = \pi/2$) is obtained by reversing the signs of the operators $s_\nu^\dagger$, s_ν everywhere in Eq. (4.6) and of β_ν everywhere in Eqs. (4.7). (The aligned oblate/prolate case receives obvious analogous treatment.) This is a reflection of the general property of the IBM that the distinction between prolate and oblate shapes is dependent on the choice of the s-boson phase. Reversal of this phase converts prolate into oblate and vice versa. The distinction between the two shapes is thus conventional, and can be traced to the assumed form of the $E2$ transition operator.

$$T^{(E2)} = q[s^\dagger \tilde{d} + d^\dagger s + \chi(d^\dagger \tilde{d})^{(2)}], \tag{4.8}$$

where it is customarily assumed that $q > 0$, while χ can have any sign. A reversal of the phase of $s^\dagger$, s would effectively correspond to a reversal of the sign of χ and of q, so that $q < 0$. It is the adoption of the convention that $q > 0$ that confers a meaning on the distinction between prolate (positive quadrupole moment) and oblate (negative quadrupole moment) shapes once a phase has been chosen for the s-boson. The formal reversal of the s-boson phase can then be used to convert expressions appropriate to prolate shapes into those appropriate to oblate shapes and vice versa (as was done at the beginning of this paragraph), without blurring the physical distinction.

Dynamic-symmetry limits of IBM-2 to which the case of aligned axial condensates applies include the $SU(3)$, $\overline{SU(3)}$, and $O(6)$ limits [41, 44, 45]. For the former two, the minimum of the energy surface occurs at $\beta_\pi = \sqrt{2} = \beta_\nu$, and $\gamma_\pi = \gamma_\nu = 0$ or $\pi/3$ respectively, while for the last-named it occurs at $\beta_\pi = 1 = \beta_\nu$ and arbitrary $\gamma_\pi = \gamma_\nu$, so it is not really axial. (Note that the one-body parts of $\mathbf{J}^2$ and $C_{O(5)}$ contribute to the energy surface and can shift the exact minimum of the energy surface away from the β_ρ values quoted by small amounts, of order $1/N_\rho$.) it should be noted that this statement depends on the choice of the sign of the Casimir operator of the algebra defining the dynamic symmetry. The choice which is relevant to nuclear spectra makes the coefficients of $C_{SU(3)}$, $C_{\overline{SU(3)}}$ or $C_{O(6)}$ negative. This is an illustration of a general property of IBM-2. Although it is a very limited model, it contains within itself, as well-defined mathematical entities, forms of dynamics which are irrelevant to nuclear spectroscopy (such as repulsive pairing or "wrong-sign" $SU(3)$ limits). It is important to restrict the parameters of the model to physically-relevant ranges of values in discussing general properties of the model.

The aligned axial condensate has the prototype form $(s_\pi^\dagger + \beta_\pi d_{\pi 0}^\dagger)^{N_\pi}$ $(s_\nu^\dagger + \beta_\nu d_{\nu 0}^\dagger)^{N_\nu} |0\rangle$, so although it does not have well-defined angular momentum, it does have a well-defined projection $K = 0$ (made up of $K_\pi = 0 = K_\nu$) along the intrinsic z-axis (the axis of symmetry). It is invariant also under 180° rotation about the y-axis, so it has positive signature. Because the Clebsch–Gordan coefficient $(J_1 0 J_2 0 | J_3 0)$ with J_1 and J_2 even vanishes for J_3 odd, the aligned axial condensate has only even-J components, so the exactly-degenerate ground band of H_{int} contains only states $0^+, 2^+, 4^+, \ldots, (2N)^+$ (one of each).

4.3. *Other Deformed Condensates*

Although the aligned axial condensate is the one most likely to be relevant in nuclear spectroscopy, it is illuminating to consider the intrinsic part of the

Hamiltonian in some other cases. For example, there might be a case where the global minimum of the energy surface occurred with $\beta_\rho > 0$, $\gamma_\pi = 0$, $\gamma_\nu = \pi/3$, $\Omega = 0$. The double condensate is made up of a prolate proton condensate (axially symmetric about the intrinsic z-axis) and an oblate neutron condensate (axially symmetric about the intrinsic y-axis). This triaxial "cigar on an ashtray" configuration of orthogonal axial condensates is of the form

$$(s_\pi^\dagger + \beta_\pi d_{\pi 0}^\dagger)^{N_\pi} \{s_\nu^\dagger + \tfrac{1}{2}\beta_\nu [d_{\nu 0}^\dagger + \sqrt{3}\,(d_{\nu 2}^\dagger + d_{\nu -2}^\dagger)/\sqrt{2}]\}^{N_\nu} |0\rangle$$

and is a positive-signature combination of $K = 0$ and $|K| = 2, 4, \ldots, 2N_\nu$ components. The Hamiltonian which annihilates this condensate is

$$\begin{aligned} H_{\text{int}} = \sum_\rho \{ & \zeta_\rho [\beta_\rho^2 (s_\rho^\dagger)^2 - d_\rho^\dagger \cdot d_\rho^\dagger][\beta_\rho^2 s_\rho^2 - \tilde{d}_\rho \cdot \tilde{d}_\rho] \\ & + \zeta'_\rho [\beta_\rho s_\rho^\dagger d_\rho^\dagger + \sqrt{7/2} \cos 3\gamma_\rho \cdot (d_\rho^\dagger d_\rho^\dagger)^{(2)}] \\ & \quad \cdot [\beta_\rho \tilde{d}_\rho s_\rho + \sqrt{7/2} \cos 3\gamma_\rho \cdot (\tilde{d}_\rho \tilde{d}_\rho)^{(2)}]\} \\ & + \zeta_0 (\beta_\pi \beta_\nu s_\pi^\dagger s_\nu^\dagger - 2 d_\pi^\dagger \cdot d_\nu^\dagger)(\beta_\pi \beta_\nu s_\nu s_\pi - 2 \tilde{d}_\nu \cdot \tilde{d}_\pi) \\ & + \zeta_1 (d_\pi^\dagger d_\nu^\dagger)^{(1)} \cdot (\tilde{d}_\nu \tilde{d}_\pi)^{(1)} \\ & + \zeta_2 [\beta_\pi s_\pi^\dagger d_\nu^\dagger - \beta_\nu s_\nu^\dagger d_\pi^\dagger - \sqrt{7/2}\,(d_\pi^\dagger d_\nu^\dagger)^{(2)}] \\ & \quad \cdot [\beta_\pi \tilde{d}_\nu s_\pi - \beta_\nu \tilde{d}_\pi s_\nu - \sqrt{7/2}\,(\tilde{d}_\nu \tilde{d}_\pi)^{(2)}], \end{aligned} \tag{4.9}$$

where the coefficients ζ are arbitrary. In order for $\gamma_\pi = 0$, $\gamma_\nu = \pi/3$, $\Omega = 0$ to be an extremum of the energy surface of the full Hamiltonian H, its energy-surface parameters must satisfy the two conditions.

$$r_{12}\beta_\nu + r_{21}\beta_\pi = 0 \tag{4.10a}$$

$$r_{11} + r_{12}\beta_\nu + (2r_{22} + 384 r_5/7)\beta_\pi \beta_\nu = 0 \tag{4.10b}$$

which arise from $\partial E/\partial \gamma_\rho = 0$. The values of β_ρ are determined by the two further equations $\partial E/\partial \beta_\rho = 0$.

This is one of the cases alluded to earlier where H_{int} cannot reproduce the shape of the most general energy surface with a global minimum of the type considered. This can be seen by a simple counting argument. According to Eq. (4.9), H_{int} has seven coefficients ζ, while the general energy surface has 12. The extremum conditions $\partial E/\partial \gamma_\rho = 0 = \partial E/\partial \beta_\rho$ produce four relations among energy-surface coefficients (the three conditions $\partial E/\partial \Omega = 0$ are then automatically satisfied), two of which are displayed in Eq. (4.10). For H_{int} to reproduce the shape of the energy surface, there must thus be one additional constraint on the energy-surface coefficients. The intrinsic/collective resolution is allowed in this case only if the Hamiltonian parameters are chosen such that $q + r_{11}(2 + \beta_\pi^2 \beta_\nu^2)/\beta_\pi \beta_\nu + r_{12}(2\beta_\pi^2 + 2\beta_\nu^2 + \beta_\pi^2 \beta_\nu^2)/\beta_\pi + 768 r_5/5 = 0$. This is a very mild constraint indeed, and there is likely to be no loss of physical relevance if it is imposed. Subject to this constraint (on the original

Hamiltonian), H_{int} reproduces the shape of the energy surface provided its coefficients are chosen such that

$$\zeta'_\rho = \sqrt{2/7}\, v_2^{(\rho)} \cos 3\gamma_\rho/\beta_\rho \qquad (\rho = \pi, \nu) \tag{4.11a}$$

$$\zeta_\rho = [N_\sigma p_\rho/(N_\rho - 1) - \zeta'_\rho(1-\beta_\rho^2)]/(1-\beta_\rho^2)^2 \qquad (\rho, \sigma = \pi, \nu; \sigma \neq \rho) \tag{4.11b}$$

$$\zeta_0 = 2r_{22} + 384r_5/7 \tag{4.11c}$$

$$\zeta_1 = 20r_{22} - 5120r_5/7 + 5\zeta_2/2 \tag{4.11d}$$

$$\zeta_2 = 2r_{12}/\beta_\pi = -2r_{21}/\beta_\nu. \tag{4.11e}$$

The $SU(3)^*$ dynamic-symmetry limit of IBM-2 [43] falls into this category, and does satisfy the energy-surface constraint, so the above treatment is applicable in this limit.

Another case of possible interest, even though there is as yet no evidence that it might be relevant to nuclear spectroscopy, is the case of the aligned non-uniform triaxial condensate, with $\beta_\rho > 0$, $0 < \gamma_\rho < \pi/3$, $\Omega = 0$, $\gamma_\pi \neq \gamma_\nu$. An intrinsic Hamiltonian for this condensate would have the form

$$\begin{aligned}
H_{\text{int}} = \sum_\rho \zeta_\rho [\beta_\rho^2 (s_\rho^\dagger)^2 - d_\rho^\dagger \cdot d_\rho^\dagger][\beta_\rho^2 s_\rho^2 - \tilde{d}_\rho \cdot \tilde{d}_\rho] \\
+ \zeta_0[\beta_\pi \beta_\nu \cos(\gamma_\pi - \gamma_\nu) s_\pi^\dagger s_\nu^\dagger - d_\pi^\dagger \cdot d_\nu^\dagger][\beta_\pi \beta_\nu \cos(\gamma_\pi - \gamma_\nu) s_\nu s_\pi - \tilde{d}_\nu \cdot \tilde{d}_\pi] \\
+ \zeta_1 (d_\pi^\dagger d_\nu^\dagger)^{(1)} \cdot (\tilde{d}_\nu \tilde{d}_\pi)^{(1)} \\
+ \zeta_2 [\beta_\pi \sin(2\gamma_\pi + \gamma_\nu) s_\pi^\dagger d_\nu^\dagger - \beta_\nu \sin(\gamma_\pi + 2\gamma_\nu) s_\nu^\dagger d_\pi^\dagger \\
+ \sqrt{7/2} \sin(\gamma_\pi - \gamma_\nu)(d_\pi^\dagger d_\nu^\dagger)^{(2)}] \\
\cdot [\beta_\pi \sin(2\gamma_\pi + \gamma_\nu) \tilde{d}_\nu s_\pi - \beta_\nu \sin(\gamma_\pi + 2\gamma_\nu) \tilde{d}_\pi s_\nu \\
+ \sqrt{7/2} \sin(\gamma_\pi - \gamma_\nu)(\tilde{d}_\nu \tilde{d}_\pi)^{(2)}],
\end{aligned} \tag{4.12}$$

where the five coefficients ζ are arbitrary. Reproduction of the shape of the energy surface of the original Hamiltonian H requires matching 12 energy-surface parameters. These obey four relations imposed by the extremum equations $\partial E/\partial \beta_\rho = 0$, $\partial E/\partial \gamma_\rho = 0$, but it will still generally be impossible to choose the values of the ζ's to reproduce the eight independent energy-surface parameters unless the parameters of the original H happen to satisfy three additional constraints. It is easy to see that two of these constraints are $v_2^{(\rho)} = 0$, while the third is $q - 4r_{22} + 1536r_5/35 - 8(r_{22} + 192r_5/7)\beta_\pi^2 \beta_\nu^2 \cos^2(\gamma_\pi - \gamma_\nu) - 2r_{12}[\beta_\pi^2 \sin^2(2\gamma_\pi + \gamma_\nu) + \beta_\nu^2 \sin^2((\gamma_\pi + 2\gamma_\nu) - \sin^2(\gamma_\pi - \gamma_\nu)]/\beta_\pi \sin(2\gamma_\pi + \gamma_\nu) \sin(\gamma_\pi - \gamma_\nu) = 0$. Similarly, the extremum conditions $\partial E/\partial \gamma_\rho = 0$ impose the simple relation $r_{12}\beta_\nu \sin(\gamma_\pi + 2\gamma_\nu) = -r_{21}\beta_\pi \sin(2\gamma_\pi + \gamma_\nu)$, and a further, more complicated, relation. Subject to these relations and constraints, the parameters of H_{int} are

$$\zeta_\rho = N_\sigma p_\rho/(N_\rho - 1)(1 + \beta_\rho^2)^2 \qquad (\rho, \sigma = \pi, \nu; \rho \neq \sigma) \tag{4.13a}$$

$$\zeta_0 = 8r_{22} + 1536r_5/7 \tag{4.13b}$$

$$\zeta_1 = 20r_{22} - 5120r_5/7 + 5\zeta_2 \sin^2(\gamma_\pi - \gamma_\nu)/2 \tag{4.13c}$$

$$\zeta_2 = -2r_{12}/\beta_\pi \sin(2\gamma_\pi + \gamma_\nu) \sin(\gamma_\pi - \gamma_\nu). \tag{4.13d}$$

This particular example, with all its limitations, indicates another aspect of this approach—it allows the construction of IBM-2 Hamiltonians with predetermined properties. Thus, by choosing a Hamiltonian of the form of Eq. (4.12), with fixed values of β_ρ and γ_ρ and suitable positive values of the ζ coefficients, and adding a reasonable $\mathbf{J}^2$ term, it is possible to produce an IBM-2 Hamiltonian which is guaranteed to have an aligned, non-uniform triaxial intrinsic structure. The procedure for choosing suitable ζ values will become clear below.

5. NORMAL MODES AND INTRINSIC EXCITATIONS

The procedure described in the previous section allows any IBM-2 Hamiltonian to be resolved into intrinsic (H_{int}) and collective (H_{c}) parts. All Hamiltonians having the same shape energy surface (recall that there are only 12 combinations of the 30 Hamiltonian parameters which fix the shape of the energy surface) will have the same intrinsic Hamiltonian, but their final spectra will differ because of the differences between their collective parts. However, since they have the same H_{int}, they will have the same equilibrium condensate and the same normal modes of intrinsic excitation. The structure of these modes is easily extracted from H_{int} via the well-known Bogoliubov prescription for interacting-boson systems [39].

When the boson numbers N_ρ become large, the boson system approaches a classical limit. The equilibrium condensate is a good approximation to the ground state of the interacting system, with the correlations between the original $s_\rho^\dagger$ and $d_\rho^\dagger$ bosons partially subsumed in the mean-field hybrid bosons $b_c^\dagger$ and $\hat{b}_c^\dagger$. For large N_ρ, the action of the condensate operators b_c, $\hat{b}_c$, $b_c^\dagger$ and $\hat{b}_c^\dagger$ is to multiply the normalized condensate by a factor $\sqrt{N_\rho}$, up to corrections of order $1/N_\rho$. The intrinsic basis is thus rewritten [22] in the form $b_c^\dagger = \sqrt{N_\pi} + c^\dagger, b_i^\dagger$; $\hat{b}_c^\dagger = \sqrt{N_\nu} + \hat{c}^\dagger, \hat{b}_i^\dagger$ $(i = \beta, \gamma, x, y, z)$, where the dominant terms are the c-numbers $\sqrt{N_\rho}$, and all the operators $c^\dagger$, $\hat{c}^\dagger$, $b_i^\dagger$, $\hat{b}_i^\dagger$ are of lower order in $1/N_\rho$. Any operator can be rewritten in terms of the intrinsic basis and expanded into a finite series of terms of decreasing order, with $1/\sqrt{N_\rho}$ playing the role of small parameter.

In particular, the intrinsic Hamiltonian H_{int} can be expanded in this manner, with the following general consequences. (It will be assumed that one-body terms $\hat{n}_\rho$ $(= \hat{n}_{s_\rho}$ or $\hat{n}_{d_\rho})$, are rewritten as equivalent two-body operators $(\hat{N}_\rho - 1)\hat{n}_\rho/(N_\rho - 1)$, for fixed values of N_ρ, so the ensuing discussion is couched solely in terms of two-body operators.) The highest-order terms, of order N^2 (either N_ρ^2 or $N_\pi N_\nu$), arise only from operators containing condensate bosons alone. They are c-numbers, and their sum is proportional to the expectation value of the intrinsic Hamiltonian in the equilibrium condensate—zero, by definition. Next follow terms of order $N^{3/2}$.

These have a single lower-order operator ($c^\dagger$, c, $\hat{c}^\dagger$, $\hat{c}$, $b_i^\dagger$, b_i, $\hat{b}_i^\dagger$, $\hat{b}_i$; $i=\beta, \gamma, x, y, z$), and their coefficients are proportional to the derivatives of the energy surface with respect to the shape parameters. Since the whole procedure is carried out with equilibrium shape parameters, these terms all vanish. The leading-order surviving terms are of order N, and each contains two operators. The fact that equilibrium shape parameters are used leas to the vanishing of boson-number non-conserving terms like bb' or $b^\dagger b'^\dagger$, so the leading terms in the Bogoliubov expansion of H_{int} are Hermitian one-body number-conserving operators, and the resulting form is amenable to diagonalization. The leading terms constitute the Bogoliubov approximation to H_{int}, to be denoted H_{int}^B.

After diagonalization, H_{int}^B is in harmonic form, a sum of terms $\omega a^\dagger a$, where $a^\dagger$ is a specific linear combination of intrinsic bosons and ω is a positive number. (The coefficients of H_{int}^B are related to the second derivatives of the energy surface with respect to the shape parameters. Since the equilibrium shape parameters are chosen at a minimum of the energy surface, the second-derivative matrix is positive there, and this ensures that the eigenvalues ω in the diagonalized H_{int}^B are positive.) The combination $a^\dagger$ of intrinsic bosons defines a normal mode of excitation of the system, of intrinsic excitation energy ω.

The number of terms in the harmonic form of H_{int}^B is at most 10, there being precisely 10 shape parameters in the formalism. Usually, the number actually appearing is less. This can be interpreted as the occurrence of zero-energy modes, modes of excitation for which $\omega=0$. These are Goldstone modes, associated with spontaneous breaking of symmetries in the equilibrium condensate. The method described here automatically distinguishes between physical modes of intrinsic excitation ($\omega>0$) and modes of collective motion (Goldstone modes, $\omega=0$). The number and nature of the intrinsic modes come naturally from the formalism, and need not be guessed in advance.

Although H_{int}, via its Bogoliubov approximation H_{int}^B, dictates the form of the normal modes, it does not determine their observed excitation energies. The collective part H_{c}, expressed in terms of the normal-mode creation and destruction operators, will contain diagonal terms which shift the observed normal-mode energies. In addition, H_{c}^B will contain Goldstone-mode terms giving the leading approximation to collective energy shifts (such as band splitting) and, since H_{int} and H_{c} do not generally commute, non-diagonal terms which can mix different normal modes. Also, non-leading terms, of lower order in N, in both H_{int} and H_{c} will generally destroy the harmonicity of the normal-mode spectrum. Nonetheless, the harmonic form of H_{int}^B, together with the diagonal shifts from H_{c}^B, does determine the nature of the intrinsic normal modes and, at least semi-quantitatively (corrections of order $1/N_\rho$ are not negligible in IBM-2), their excitation energies.

5.1. *Spherical Condensate*

When $\beta_\rho=0$ at the global minimum of the energy surface, the condensate is made purely of s_ρ-bosons, and H_{int} is given in Eq. (4.3). The Bogoliubov approximation is obtained by replacing each $s_\rho^\dagger$ and s_ρ by $\sqrt{N_\rho}$ and keeping only the leading terms (of order N). The result is obviously

$$H_{\text{int}}^B = \sum_\rho \zeta_\rho N_\rho d_\rho^\dagger \cdot \tilde{d}_\rho + \zeta_2(\sqrt{N_\pi}\, d_\nu^\dagger + \eta_2 \sqrt{N_\nu}\, d_\pi^\dagger) \cdot (\sqrt{N_\pi}\, \tilde{d}_\nu + \eta_2 \sqrt{N_\nu}\, \tilde{d}_\pi), \quad (5.1)$$

where ζ_ρ, ζ_2, and η_2 are given in terms of energy-surface parameters in Eqs. (4.4). This quadratic form is easily diagonalized, and the result is

$$H_{\text{int}}^B = \omega_+ B_p^\dagger \cdot \tilde{B}_p + \omega_- B_m^\dagger \cdot \tilde{B}_m \quad (5.2\text{a})$$

$$\omega_\pm = \tfrac{1}{2}(\zeta_\pi N_\pi + \zeta_\nu N_\nu) + \tfrac{1}{2}\zeta_2(\eta_2^2 N_\nu + N_\pi) \pm [\Delta^2 + 4N_\pi N_\nu r_{11}^2]^{1/2} \quad (5.2\text{b})$$

$$\Delta = \tfrac{1}{2}(\zeta_\pi N_\pi - \zeta_\nu N_\nu) + \tfrac{1}{2}\zeta_2(\eta_2^2 N_\nu - N_\pi) \quad (5.2\text{c})$$

$$B_p^\dagger = (d_\nu^\dagger - \eta d_\pi^\dagger)/\sqrt{1+\eta^2} \quad (5.2\text{d})$$

$$B_m^\dagger = (d_\pi^\dagger + \eta d_\nu^\dagger)/\sqrt{1+\eta^2} \quad (5.2\text{e})$$

$$\eta = -(\Delta + \sqrt{\Delta^2 + 4N_\pi N_\nu r_{11}^2})/2r_{11}\sqrt{N_\pi N_\nu}. \quad (5.2\text{f})$$

Not surprisingly, the harmonic approximation to the intrinsic Hamiltonian for a spherical condensate is a sum of two (five-dimensional) quadrupole harmonic oscillators, one symmetric between proton and neutron bosons, the other antisymmetric [46]. Which lies lower in excitation energy (note $\omega_- < \omega_+$, always) depends on the sign of the mixing parameter η, which in turn is opposite to the sign of the energy-surface parameter r_{11} (or the sum of $H_{\pi\nu}$ parameters $u_2'' + v_0$). If $r_{11} < 0$, then $\eta > 0$, $B_m^\dagger$ is neutron–proton symmetric, and the symmetric mode is lower in energy.

There are several interesting features of this result. Since the condensate does not break rotational symmetry, there are 10 intrinsic normal modes of well-defined angular momentum (two quadrupoles) and no Goldstone modes. There is not much point in introducing the intrinsic shape modes here (such as distinguishing between β modes, γ modes, etc.), since all are equivalent. The quadrupole excitation mode has five equivalent components, and a unitary transformation among the different μ components can only confuse the issue. The coupling between proton–boson and neutron–boson modes arises solely from the parameter r_{11}. If $r_{11} = 0$, the modes decouple, and the normal modes become just the unperturbed neutron and proton modes. Although the method developed conserves total boson number, the normal-mode creation operators $B_p^\dagger$, $B_m^\dagger$ involve combinations of neutron and proton bosons, and so do not conserve N_π and N_ν separately. The correct number-conserving form of the leading terms in excited intrinsic states is obtained by inserting appropriate factors $b_c/\sqrt{N_\pi}$ or $\hat{b}_c/\sqrt{N_\nu}$. For example, the lowest normal-mode state is obtained by acting on the s-boson condensate with the (unnormalized) operator $(\sqrt{N_\nu}\, d_\pi^\dagger s_\pi + \eta \sqrt{N_\pi}\, d_\nu^\dagger s_\nu)$.

The structure of the normal modes is determined by H_{int}, but their excitation energies can be shifted by H_c. Thus the values $\omega_\pm$ must be corrected by adding the diagonal part of H_c. This can be done in either of two ways. The form of H_c can be determined by subtracting H_{int} from H. The resulting H_{c} has a part involving only operators $\hat{N}_\rho$, which affects the intrinsic ground state (the condensate) and excited states (normal modes) in exactly the same way, and hence does not contribute to excitation energies. The rest of H_{c} can be rewritten in terms of condensate and normal-mode creation and destruction operators, and its Bogoliubov approximation will generally contain harmonic normal-mode terms and terms mixing the normal modes. The coefficients of the harmonic terms must be added to the corresponding coefficients of H_{int} to get the correct normal-mode excitation energies. Alternatively, the expectation value of the full Hamiltonian H can be computed in the condensate (intrinsic ground state) and in the normal-mode state (intrinsic excited state), and the difference, to leading order (order N) in boson numbers, taken as the normal-mode excitation energy. Both methods lead to identical results. For the spherical condensate, the full normal-mode excitation energies are

$$\begin{aligned} E_m = \{&\varepsilon_d^{(\pi)} - \varepsilon_s^{(\pi)} + \eta^2(\varepsilon_d^{(\nu)} - \varepsilon_s^{(\nu)}) + N_\pi[u_2^{(\pi)} - 2u_0^{(\pi)} + \eta^2(u_2 - u_0)] \\ &+ N_\nu[\eta^2(u_2^{(\nu)} - 2u_0^{(\nu)}) + u_2' - u_0] + 2\eta\sqrt{N_\pi N_\nu}\, u_2''\}/(1+\eta^2) \end{aligned} \tag{5.3a}$$

$$\begin{aligned} E_p = \{&\eta^2(\varepsilon_d^{(\pi)} - \varepsilon_s^{(\pi)}) + \varepsilon_d^{(\nu)} - \varepsilon_s^{(\nu)} + N_\pi[\eta^2(u_2^{(\pi)} - 2u_0^{(\pi)}) + u_2 - u_0] \\ &+ N_\nu[u_2^{(\nu)} - 2u_0^{(\nu)} + \eta^2(u_2' - u_0)] - 2\eta\sqrt{N_\pi N_\nu}\, u_2''\}/(1+\eta^2) \end{aligned} \tag{5.3b}$$

with η defined in Eq. (5.2). [It is generally true in the IBM that single-particle energies are of a higher order in N than two-body interaction energies. This is evident from the transcription $\hat{n} \to (\hat{N}-1)\hat{n}/(N-1)$ with $\hat{n} = \hat{n}_s$ or $\hat{n}_d$, so that the one-body coefficient ε is replaced in the equivalent two-body description by the coefficient $\varepsilon/(N-1)$. Thus the one-body coefficient ε is of the same order in N as N times a typical two-body coefficient.]

For the standard IBM-2 Hamiltonian, defined in Eq. (2.9), when the parameters N_ρ, ε_ρ, χ_ρ, κ, κ', α_i are such that the global minimum of the energy surface occurs at $\beta_\rho = 0$, the above treatment produces the normal-mode energies

$$\begin{aligned} E_m = &\tfrac{1}{2}(\varepsilon_\pi + \varepsilon_\nu) + \tfrac{1}{2}(N_\pi + N_\nu)\alpha_2 \\ &+ [\Delta(1-\eta^2) + 2\sqrt{N_\pi N_\nu}\,\eta(\kappa - \alpha_2)]/(1+\eta^2) \end{aligned} \tag{5.4a}$$

$$\begin{aligned} E_p = &\tfrac{1}{2}(\varepsilon_\pi + \varepsilon_\nu) + \tfrac{1}{2}(N_\pi + N_\nu)\alpha_2 \\ &- [\Delta(1-\eta^2) + 2\sqrt{N_\pi N_\nu}\,\eta(\kappa - \alpha_2)]/(1+\eta^2) \end{aligned} \tag{5.4b}$$

$$\Delta = \tfrac{1}{2}(\varepsilon_\pi - \varepsilon_\nu) + \tfrac{1}{2}(N_\nu - N_\pi)\alpha_2 \tag{5.4c}$$

$$\eta = -(\Delta + \sqrt{\Delta^2 + N_\pi N_\nu(2\kappa - \alpha_2)^2})/\sqrt{N_\pi N_\nu}\,(2\kappa - \alpha_2). \tag{5.4d}$$

These depend only on the single-boson energies ε_ρ, the quadrupole–quadrupole strength parameter κ and the single Majorana parameter α_2. In the special case $\varepsilon_\pi = \varepsilon_\nu$, $\kappa = 0$, these reduce to $\eta = \sqrt{N_\nu/N_\pi}$, $E_m = \varepsilon_\rho$, $E_p = \varepsilon_\rho + (N_\pi + N_\nu)\alpha_2$ for $\alpha_2 > 0$, and to $\eta = -\sqrt{N_\pi/N_\nu}$, $E_m = \varepsilon_\rho + (N_\pi + N_\nu)\alpha_2$, $E_p = \varepsilon_\rho$ for $\alpha_2 < 0$.

5.2. *Aligned Axial Condensate*

When the global minimum of the energy surface occurs at $\beta_\rho > 0$, $\gamma_\rho = 0$, $\Omega = 0$, the intrinsic part of the Hamiltonian is given by Eq. (4.6), and the intrinsic boson basis by Eqs. (3.7). (As discussed in Section 4.2, the results for all aligned axial condensates can easily be obtained from the aligned prolate case, to which the following discussion will be restricted.) Since in this case $b_c^\dagger = (s_\pi^\dagger + \beta_\pi d_{\pi 0}^\dagger)/\sqrt{1+\beta_\pi^2}$ and $\hat{b}_c^\dagger = (s_\nu^\dagger + \beta_\nu d_{\nu 0}^\dagger)/\sqrt{1+\beta_\nu^2}$, the leading terms in the Bogoliubov approximation to H_{int} will be those containing the most factors $s_\rho^\dagger$, s_ρ, $d_{\rho 0}^\dagger$, or $d_{\rho 0}$. The Bogoliubov approximation in this case is

$$\begin{aligned} H_{\text{int}}^B = {} & \varepsilon_\beta b_\beta^\dagger b_\beta + \hat{\varepsilon}_\beta \hat{b}_\beta^\dagger \hat{b}_\beta + m_\beta (b_\beta^\dagger \hat{b}_\beta + \hat{b}_\beta^\dagger b_\beta) \\ & + \varepsilon_\gamma (b_\gamma^\dagger b_\gamma + b_z^\dagger b_z) + \hat{\varepsilon}_\gamma (\hat{b}_\gamma^\dagger \hat{b}_\gamma + \hat{b}_z^\dagger \hat{b}_z) + m_\gamma (b_\gamma^\dagger \hat{b}_\gamma + \hat{b}_\gamma^\dagger b_\gamma + b_z^\dagger \hat{b}_z + \hat{b}_z^\dagger b_z) \\ & + \varepsilon_x (b_x^\dagger b_x + b_y^\dagger b_y) + \hat{\varepsilon}_x (\hat{b}_x^\dagger \hat{b}_x + \hat{b}_y^\dagger \hat{b}_y) + m_x (b_x^\dagger \hat{b}_x + \hat{b}_x^\dagger b_x + b_y^\dagger \hat{b}_y + \hat{b}_y^\dagger b_y) \end{aligned} \tag{5.5a}$$

$$\varepsilon_\beta = (4\zeta_\pi + \zeta'_\pi) N_\pi \beta_\pi^2 + (\zeta_0 + \zeta_2 + \zeta'_2) N_\nu \beta_\nu^2 (1 + \beta_\pi^2)/(1 + \beta_\nu^2) \tag{5.5b}$$

$$\hat{\varepsilon}_\beta = (4\zeta_\nu + \zeta'_\nu) N_\nu \beta_\nu^2 + (\zeta_0 + \zeta_2 + \zeta''_2) N_\pi \beta_\pi^2 (1 + \beta_\nu^2)/(1 + \beta_\pi^2) \tag{5.5c}$$

$$m_\beta = (\zeta_0 - \zeta_2) \beta_\pi \beta_\nu \sqrt{N_\pi N_\nu} \tag{5.5d}$$

$$\varepsilon_\gamma = 9\zeta'_\pi N_\pi \beta_\pi^2/(1 + \beta_\pi^2) + (\zeta_2 + \zeta'_2 + 4\zeta''_2 + \tfrac{1}{2}\zeta_3) N_\nu \beta_\nu^2/(1 + \beta_\nu^2) \tag{5.5e}$$

$$\hat{\varepsilon}_\gamma = 9\zeta'_\nu N_\nu \beta_\nu^2/(1 + \beta_\nu^2) + (\zeta_2 + 4\zeta'_2 + \zeta''_2 + \tfrac{1}{2}\zeta_3) N_\pi \beta_\pi^2/(1 + \beta_\pi^2) \tag{5.5f}$$

$$m_\gamma = (-\zeta_2 + 2\zeta'_2 + 2\zeta''_2 - \tfrac{1}{2}\zeta_3) \beta_\pi \beta_\nu \sqrt{N_\pi N_\nu/(1 + \beta_\pi^2)(1 + \beta_\nu^2)} \tag{5.5g}$$

$$\varepsilon_x = (\zeta_2 + \zeta'_2/4 + \zeta''_2/4 + 3\zeta_1/10 + \zeta_3/5) N_\nu \beta_\nu^2/(1 + \beta_\nu^2) \tag{5.5h}$$

$$\hat{\varepsilon}_x = (\zeta_2 + \zeta'_2/4 + \zeta''_2/4 + 3\zeta_1/10 + \zeta_3/5) N_\pi \beta_\pi^2/(1 + \beta_\pi^2) \tag{5.5i}$$

$$m_x = -(\zeta_2 + \zeta'_2/4 + \zeta''_2/4 + 3\zeta_1/10 + \zeta_3/5)\, \beta_\pi \beta_\nu \sqrt{N_\pi N_\nu/(1 + \beta_\pi^2)(1 + \beta_\nu^2)} \tag{5.5j}$$

so the normal modes fall into three groups: two β modes, four $\gamma - z$ modes and four $x - y$ modes, while only 2×2 matrices need be diagonalized. (The $\gamma - z$ and $x - y$ modes clearly occur in degenerate pairs.)

The diagonal coefficients ε and mixing coefficients m in Eqs. (5.5) are all simply related to second derivatives of the energy surface with respect to the shape parameters. As a result, the conditions that all normal-mode frequencies be positive are equivalent to the conditions that the equilibrium shape parameters fall at a minimum (not just an extremum) of the energy surface. These normal-mode frequencies will generally be shifted by H_c, even when the mixing of modes due to the off-diagonal terms in the collective part is weak.

Consider the generic case, $H = \varepsilon b^\dagger b + \hat{\varepsilon} \hat{b}^\dagger \hat{b} + m(b^\dagger \hat{b} + \hat{b}^\dagger b)$. It may be diagonalized as $H = \omega_+ b_p^\dagger b_p + \omega_- b_m^\dagger b_m$, where, defining $\Delta = \frac{1}{2}(\varepsilon - \hat{\varepsilon})$, the normal-mode frequencies are $\omega_\pm = \frac{1}{2}(\varepsilon + \hat{\varepsilon}) \pm \sqrt{\Delta^2 + m^2}$, and the normal-mode creation operators are $b_m^\dagger = (b^\dagger + \eta \hat{b}^\dagger)/\sqrt{1 + \eta^2}$, $b_p^\dagger = (\hat{b}^\dagger - \eta b^\dagger)/\sqrt{1 + \eta^2}$, with $\eta = -(\Delta + \sqrt{\Delta^2 + m^2})/m$ that $m\eta < 0$. Thus the modes will occur in pairs, one "neutron-proton symmetric," the other "neutron–proton antisymmetric," depending on the sign of η, which is opposite to that of m. Since $\omega_- < \omega_+$ in every case, the symmetric mode is lower whenever $m < 0$.

It follows from Eq. (5.5) that the aligned prolate condensate has two β modes, a "symmetric" and an "antisymmetric" one. The symmetric β mode will be below the antimsymmetric β mode (the situation to be anticipated in cases of physical interest) when $\zeta_0 < \zeta_2$. Each β mode is approximated, in lowest order, by a one-dimensional harmonic oscillator. On the other hand, the γ modes occur as degenerate pairs, or as isotropic two-dimensional harmonic oscillators. This is a well-known feature of axially-symmetric intrinsic states. The γ vibration breaks the axial symmetry by rendering the state triaxial, but the fingerprint of the axial symmetry remains in that the orientation of the other two principal axes is arbitrary. The two coupled degenerate oscillators are those in $b_\gamma^\dagger \sim d_2^\dagger + d_{-2}^\dagger$ and in $b_z^\dagger \sim d_2^\dagger - d_{-2}^\dagger$, and they may easily be transformed into degenerate $K = +2$ and $K = -2$ oscillators. This familiar situation can be thought of in terms of two degenerate orthogonal oscillators or in terms of a single isotropic two-dimensional oscillator, with one degree of freedom the "radial" oscillation ($b_\gamma^\dagger$) and the other a rotation ($b_z^\dagger$) about the axis of symmetry. In the present context, there are two such γ vibrations, a symmetric and an antisymmetric one. The symmetric γ vibration lies lower if $\zeta_2' + \zeta_2'' < (2\zeta_2 + \zeta_3)/4$. (The expressions for the ζ coefficients in terms of the parameters of H are given in Eqs. (4.7), (3.4), and (2.5).)

Finally, there remain the four $x - y$ modes, also occurring in degenerate pairs. Since, by inspection, $\varepsilon_x \hat{\varepsilon}_x - m_x^2 = 0$, one of these pairs occurs at zero energy. There are thus two Goldstone modes, associated with broken rotational symmetry in the condensate. Note that the condensate remains axially symmetric, so only two of the axes, those orthogonal to the symmetry axis, are associated with broken rotational symmetry, and there are only two Goldstone modes. The $x - y$ part of H_{int}^B is easily rewritten

$$H_{xy}^B = \omega_{xy}(B_x^\dagger B_x + B_y^\dagger B_y) \tag{5.6a}$$

$$\omega_{xy} = (\zeta_2 + \zeta_2'/4 + \zeta_2''/4 + 3\zeta_1/10 + \zeta_3/5)\mathcal{N}_{\pi\nu} \tag{5.6b}$$

$$\mathcal{N}_{\pi\nu} = N_\nu \beta_\nu^2/(1+\beta_\nu^2) + N_\pi \beta_\pi^2/(1+\beta_\pi^2) \tag{5.6c}$$

$$\begin{aligned} B_i^\dagger = [\beta_\nu \sqrt{N_\nu/(1+\beta_\nu^2)}\, b_i^\dagger \\ - \beta_\pi \sqrt{N_\pi/(1+\beta_\pi^2)}\, \hat{b}_i^\dagger]/\sqrt{\mathcal{N}_{\pi\nu}}; \qquad i = x,\ y \end{aligned} \tag{5.6d}$$

an isotropic two-dimensional harmonic oscillator plus (implicitly) a pair of zero-energy modes. The modes orthogonal to the "antisymmetric" ones displayed in Eq. (5.6d) are the "symmetric" combinations

$$\bar{B}_i^\dagger = (\beta_\pi \sqrt{N_\pi/(1+\beta_\pi^2)}\, b_i^\dagger + \beta_\nu \sqrt{N_\nu/(1+\beta_\nu^2)}\, \hat{b}_i^\dagger)/\sqrt{\mathcal{N}_{\pi\nu}}; \qquad i = x,\ y. \tag{5.6e}$$

This is precisely the creation-operator part of the Bogoliubov approximation to the angular momentum J_i (up to a numerical factor), which confirms the identification of the Goldstone modes with the collective rotations of the intrinsic system about the x and y axes. The genuine $x-y$ modes displayed in Eq. (5.6d) can thus be identified with relative rotations (or counter-rotations) of the proton and neutron condensates about axes orthogonal to the symmetry axis. This is just the famous "scissors" mode of IBM-2 [47]. It corresponds to an isotropic two-dimensional oscillator because of the axial symmetry—the orientation of the orthogonal scissor axis is arbitrary. Its "unperturbed" excitation energy (before adding in the diagonal shift due to H_c) is ω_{xy}, Eq. (5.6b).

For the standard IBM-2 Hamiltonian, Eq. (2.9), when the global minimum falls at $\beta_\rho > 0$, $\gamma_\rho = 0$, $\Omega = 0$, the parameters of H^B_{int}, as given in Eqs. (5.5), become

$$\varepsilon_\beta = N_\nu(\alpha_2 - 2\kappa + \sqrt{2/7}\,\kappa\chi_\nu\beta_\nu)\beta_\nu(1+\beta_\pi^2)/\beta_\pi(1+\beta_\nu^2) \tag{5.7a}$$

$$\hat{\varepsilon}_\beta = N_\pi(\alpha_2 - 2\kappa + \sqrt{2/7}\,\kappa\chi_\pi\beta_\pi)\beta_\pi(1+\beta_\nu^2)/\beta_\nu(1+\beta_\pi^2) \tag{5.7b}$$

$$\begin{aligned} m_\beta = \sqrt{N_\pi N_\nu}\,\Big\{ 2\kappa - \alpha_2 + 2\Big[& \alpha_2(\beta_\pi - \beta_\nu)^2 - 2\kappa(\beta_\pi^2 + \beta_\nu^2) \\ & - \sqrt{\frac{2}{7}}\,\kappa\chi_\nu\beta_\nu(1-\beta_\pi^2) - \sqrt{\frac{2}{7}}\,\kappa\chi_\pi\beta_\pi(1-\beta_\nu^2) \\ & + \frac{2}{7}\,\kappa\chi_\pi\chi_\nu\beta_\pi\beta_\nu \Big] \Big/ (1+\beta_\pi^2)(1+\beta_\nu^2) \Big\} \end{aligned} \tag{5.7c}$$

$$\begin{aligned} \varepsilon_\gamma = {} & \{\tfrac{1}{2}\alpha_3 - 4\kappa\chi_\pi\chi_\nu/7 + [\alpha_2 - 2\kappa + \sqrt{2/7}\,\kappa(\chi_\nu\beta_\nu + 4\chi_\pi\beta_\pi)]/\beta_\pi\beta_\nu\} \\ & \cdot N_\nu\beta_\nu^2/(1+\beta_\nu^2) \end{aligned} \tag{5.7d}$$

$$\begin{aligned} \hat{\varepsilon}_\gamma = {} & \{\tfrac{1}{2}\alpha_3 - 4\kappa\chi_\pi\chi_\nu/7 + [\alpha_2 - 2\kappa + \sqrt{2/7}\,\kappa(\chi_\pi\beta_\pi + 4\chi_\nu\beta_\nu)]/\beta_\pi\beta_\nu\} \\ & \cdot N_\pi\beta_\pi^2/(1+\beta_\pi^2) \end{aligned} \tag{5.7e}$$

$$\begin{aligned} m_\gamma = {} & [(4\kappa\chi_\pi\chi_\nu/7 - \tfrac{1}{2}\alpha_3)\beta_\pi\beta_\nu + 2\kappa - \alpha_2 + 2\sqrt{2/7}\,\kappa(\chi_\pi\beta_\pi + \chi_\nu\beta_\nu)] \\ & \cdot \sqrt{N_\pi N_\nu/(1+\beta_\pi^2)(1+\beta_\nu^2)} \end{aligned} \tag{5.7f}$$

$$\begin{aligned} \omega_{xy}/\mathcal{N}_{\pi\nu} = {} & 3\alpha_1/10 + \alpha_3/5 - \kappa\chi_\pi\chi_\nu/7 \\ & + [\alpha_2 - 2\kappa + \sqrt{2/7}\,\kappa(\chi_\pi\beta_\pi + \chi_\nu\beta_\nu)]/\beta_\pi\beta_\nu \end{aligned} \tag{5.7g}$$

and a harmonic estimate of the corresponding normal-mode energies and structures can easily be obtained for any given set of standard parameters.

5.3. *Other Deformed Condensates*

In Section 4.3 it was shown that an intrinsic/collective resolution of the Hamiltonian is possible in other deformed cases, in particular for the orthogonal axial condensate and for an aligned non-uniform triaxial condensate. Each of these cases has its own normal modes, which can be found by the same technique utilized above.

For the orthogonal axial condensates ($\beta_\rho > 0$, $\gamma_\pi = 0$, $\gamma_\nu = \pi/3$, $\Omega = 0$—prolate protons with symmetry axis orthogonal to that of oblate neutrons; "cigar on an ashtray" configuration), the intrinsic Hamiltonian given in Eq. (4.9) is rewritten in terms of the intrinsic basis, Eqs. (3.7), and the Bogoliubov approximation is extracted. The result is simple but lengthy, namely,

$$\begin{aligned}H^B_{\text{int}} = {} & \varepsilon_\beta b^\dagger_\beta b_\beta + \hat{\varepsilon}_\beta \hat{b}^\dagger_\beta \hat{b}_\beta + m_\beta(b^\dagger_\beta \hat{b}_\beta + \hat{b}^\dagger_\beta b_\beta) + \varepsilon_\gamma b^\dagger_\gamma b_\gamma + \hat{\varepsilon}_\gamma \hat{b}^\dagger_\gamma \hat{b}_\gamma \\ & + m_\gamma(b^\dagger_\gamma \hat{b}_\gamma + \hat{b}^\dagger_\gamma b_\gamma) + m_{\beta\gamma}(b^\dagger_\beta b_\gamma + b^\dagger_\gamma b_\beta) + \hat{m}_{\beta\gamma}(\hat{b}^\dagger_\beta \hat{b}_\gamma + \hat{b}^\dagger_\gamma \hat{b}_\beta) \\ & + m'_{\beta\gamma}(b^\dagger_\beta \hat{b}_\gamma + \hat{b}^\dagger_\gamma b_\beta) + \hat{m}'_{\beta\gamma}(\hat{b}^\dagger_\beta b_\gamma + b^\dagger_\gamma \hat{b}_\beta) + \varepsilon_x b^\dagger_x b_x + \hat{\varepsilon}_x \hat{b}^\dagger_x \hat{b}_x \\ & + m_x(b^\dagger_x \hat{b}_x + \hat{b}^\dagger_x b_x) + \omega_y \hat{b}^\dagger_y \hat{b}_y + \omega_z b^\dagger_z b_z \end{aligned} \tag{5.8a}$$

$$\varepsilon_\beta = (4\zeta_\pi + \zeta'_\pi) N_\pi \beta^2_\pi + (\zeta_0 + \zeta_2) N_\nu \beta^2_\nu (1 + \beta^2_\pi)/(1 + \beta^2_\nu) \tag{5.8b}$$

$$\hat{\varepsilon}_\beta = (4\zeta_\nu + \zeta'_\nu) N_\nu \beta^2_\nu + (\zeta_0 + \zeta_2) N_\pi \beta^2_\pi (1 + \beta^2_\nu)/(1 + \beta^2_\pi) \tag{5.8c}$$

$$m_\beta = (\zeta_0 - \tfrac{1}{2}\zeta_2) \sqrt{N_\pi N_\nu}\, \beta_\pi \beta_\nu \tag{5.8d}$$

$$\varepsilon_\gamma = 9\zeta'_\pi N_\pi \beta^2_\pi/(1 + \beta^2_\pi) + 3(\zeta_0 + \zeta_2) N_\nu \beta^2_\nu/(1 + \beta^2_\nu) \tag{5.8e}$$

$$\hat{\varepsilon}_\gamma = 9\zeta'_\nu N_\nu \beta^2_\nu/(1 + \beta^2_\nu) + 3(\zeta_0 + \zeta_2) N_\pi \beta^2_\pi/(1 + \beta^2_\pi) \tag{5.8f}$$

$$m_\gamma = -3(\zeta_0 - \tfrac{1}{2}\zeta_2)\sqrt{N_\pi N_\nu}\, \beta_\pi \beta_\nu/\sqrt{(1 + \beta^2_\pi)(1 + \beta^2_\nu)} \tag{5.8g}$$

$$m_{\beta\gamma} = \sqrt{3}\,(\zeta_0 + \zeta_2) N_\nu \beta^2_\nu \sqrt{1 + \beta^2_\pi}/(1 + \beta^2_\nu) \tag{5.8h}$$

$$\hat{m}_{\beta\gamma} = -\sqrt{3}\,(\zeta_0 + \zeta_2) N_\pi \beta^2_\pi \sqrt{1 + \beta^2_\nu}/(1 + \beta^2_\pi) \tag{5.8i}$$

$$m'_{\beta\gamma} = -\sqrt{3}\,(\zeta_0 - \tfrac{1}{2}\zeta_2) \sqrt{N_\pi N_\nu}\, \beta_\pi \beta_\nu/\sqrt{1 + \beta^2_\nu} \tag{5.8j}$$

$$\hat{m}'_{\beta\gamma} = \sqrt{3}\,(\zeta_0 - \tfrac{1}{2}\zeta_2) \sqrt{N_\pi N_\nu}\, \beta_\pi \beta_\nu/\sqrt{1 + \beta^2_\pi} \tag{5.8k}$$

$$\varepsilon_x = (3\zeta_1/10 + 9\zeta_2/4) N_\nu \beta^2_\nu/(1 + \beta^2_\nu) \tag{5.8l}$$

$$\hat{\varepsilon}_x = (3\zeta_1/10 + 9\zeta_2/4) N_\pi \beta^2_\pi/(1 + \beta^2_\pi) \tag{5.8m}$$

$$m_x = -(3\zeta_1/10 + 9\zeta_2/4) \sqrt{N_\pi N_\nu}\, \beta_\pi \beta_\nu/\sqrt{(1 + \beta^2_\pi)(1 + \beta^2_\nu)} \tag{5.8n}$$

$$\omega_y = 9\zeta'_\nu N_\nu \beta^2_\nu/(1 + \beta^2_\nu) + (3\zeta_1/10 + 9\zeta_2/4) N_\pi \beta^2_\pi/(1 + \beta^2_\pi) \tag{5.8o}$$

$$\omega_z = 9\zeta'_\pi N_\pi \beta^2_\pi/(1 + \beta^2_\pi) + (3\zeta_1/10 + 9\zeta_2/4) N_\nu \beta^2_\nu/(1 + \beta^2_\nu). \tag{5.8p}$$

In this case, in general, the β and γ modes of each condensate couple to one another and to the coupled $\beta - \gamma$ modes of the other condensate. There are thus four coupled $\beta - \gamma$ modes. The x modes of the two condensates couple only to one another, and the resulting 2×2 matrix has a vanishing determinant. There is thus a zero-energy x mode and, by inspection, a finite-energy antisymmetric x mode. The former is generated by the total angular momentum operator J_x, the latter by the relative x rotations of the two condensates. These are then, respectively, the Goldstone mode associated with the spontaneous breaking of rotational symmetry about the x-axis and the one-dimensional scissors mode of relative angular oscillation about the axis orthogonal to the symmetry axes of the prolate protons and oblate neutrons. There remain the $\hat{y}$ mode and the z mode, each the remnant of relative angular-oscillation modes involving one symmetry axis, while the orthogonal y and $\hat{z}$ modes are essentially the zero-energy Goldstone modes of collective rotation associated with spontaneous breaking of rotational symmetry about the y- and z-axes. In this case, where the total system has no axis of symmetry, there are thus three Goldstone modes—rotational symmetry is broken for all three orthogonal axes.

The scissors mode is created by the antisymmetric combination

$$B_x^\dagger = (\sqrt{N_\nu}\,\beta_\nu b_x^\dagger/\sqrt{1+\beta_\nu^2} - \sqrt{N_\pi}\,\beta_\pi \hat{b}_x^\dagger/\sqrt{1+\beta_\pi^2})/\sqrt{\mathcal{N}_{\pi\nu}} \tag{5.9a}$$

with $\mathcal{N}_{\pi\nu}$ defined in Eq. (5.6c), and its unperturbed (by H_c) frequency is

$$\omega_x = (3\zeta_1/10 + 9\zeta_2/4)\mathcal{N}_{\pi\nu}. \tag{5.9b}$$

The coupled $\beta-\gamma$ modes are generally complicated, but in the specific case $\zeta_0 = \frac{1}{2}\zeta_2$ they simplify considerably, since then $m_\beta = 0$, $m_\gamma = 0$, $m'_{\beta\gamma} = 0$ and $\hat{m}'_{\beta\gamma} = 0$. The β and γ modes of each condensate then couple to produce two normal modes, but the neutron and proton $\beta-\gamma$ modes remain decoupled from one another. In this special case, the only neutron–proton coupled mode is the scissors mode.

The dynamical symmetry $U(6)_\pi \times U(6)_\nu \supset SU(3)_\pi \times \overline{SU(3)_\nu} \supset SU(3)^* \supset O(3)$ of IBM-2 [43] belongs to this class of Hamiltonians. With the parametrization

$$H = AC_{SU(3)^*} + B_\pi C^{(\pi)}_{SU(3)} + B_\nu C^{(\nu)}_{\overline{SU(3)}} \tag{5.10}$$

the energy-surface coefficients are $p_\rho = -7(N_\rho - 1)(A + B_\rho)/N_\sigma$, $q_\rho = 8(N_\rho - 1)(A + B_\rho)/N_\sigma$ $(\rho, \sigma = \pi, \nu;\ \sigma \neq \rho)$, $q = q_\pi + q_\nu$, $r_{11} = 4A$, $r_{12} = -\sqrt{2}\,A$, $r_{21} = \sqrt{2}\,A$, $r_{22} = -\frac{1}{2}A$, $r_5 = 0$. The minimum falls at $\beta_\pi = \sqrt{2} = \beta_\nu$, $\gamma_\pi = 0$, $\gamma_\nu = \pi/3$, $\Omega = 0$ (provided $A < 0$, $A + B_\rho < 0$), and the energy-surface constraint for intrinsic/collective resolution (quoted just above Eq. (4.11)) is satisfied. The parameters of the intrinsic Hamiltonian (4.9) are $\zeta_\rho = -(A + B_\rho)$, $\zeta'_\rho = -2(A + B_\rho)$, $\zeta_0 = -A$, $\zeta_1 = -15A$, $\zeta_2 = -2A$, and all are positive. Since $\zeta_0 = \frac{1}{2}\zeta_2$, the proton and neutron $\beta-\gamma$ modes decouple. The intrinsic normal modes are then the proton $\beta-\gamma$ modes, $(b_\beta^\dagger + b_\gamma^\dagger)/\sqrt{2}$ at $-12N_\pi(A + B_\pi) - 12N_\nu A$ and $(b_\beta^\dagger - b_\gamma^\dagger)/\sqrt{2}$ at $-12N_\pi(A + B_\pi)$; the neutron $\beta-\gamma$ modes, $(\hat{b}_\beta^\dagger - \hat{b}_\gamma^\dagger)/\sqrt{2}$ at $-12N_\nu(A + B_\nu) - 12N_\pi A$ and $(\hat{b}_\beta^\dagger + \hat{b}_\gamma^\dagger)/\sqrt{2}$ at $-12N_\nu(A + B_\nu)$; the proton symmetry-axis mode $b_z^\dagger$ at $-12N_\pi(A + B_\pi) - 6N_\nu A$ (degenerate with the proton γ mode before the latter's coupling to the β mode); the neutron symmetry-axis mode $\hat{b}_y^\dagger$ at $-12N_\nu(A + B_\nu) - 6N_\pi A$ (degenerate with the neutron γ mode before the latter's coupling to the β mode); and the scissors mode $(\sqrt{N_\nu}\,b_x^\dagger - \sqrt{N_\pi}\,\hat{b}_x^\dagger)/\sqrt{N_\pi + N_\nu}$ at $-6A(N_\pi + N_\nu)$. The three Goldstone modes of collective rotation occur at zero energy. Each of the intrinsic (non-Goldstone) modes can be associated with a specific $[(\lambda_\pi, \mu_\pi)(\lambda_\nu, \mu_\nu)](\lambda\,\mu)$ representation of the dynamical symmetry, and the energies agree, to order $1/N$. For example, the scissors mode represents the $[(2N_\pi, 0)(0, 2N_\nu)](2N_\pi - 1, 2N_\nu - 1)$ band.

The above example has been given in detail because of its correspondence with a dynamical symmetry of IBM-2. A very similar treatment is applicable to the general case of aligned non-uniform triaxial condensates, as discussed in Section 4.3. The Bogoliubov approximation to the intrinsic Hamiltonian, Eq. (4.12), is very similar to Eq. (5.8a), except that the y and z terms appear, like the x terms, in the forms $b_i^\dagger b_i$, $\hat{b}_i^\dagger \hat{b}_i$ and $b_i^\dagger \hat{b}_i + \hat{b}_i^\dagger b_i$ $(i = x, y, z)$. Despite the superficial complexity of the expressions for the coefficients ε_i, $\hat{\varepsilon}_i$, m_i $(i = x, y, z)$, it can be shown that there are three zero-energy modes, the Goldstone modes of broken rotational symmetry, with normal-mode creation operators exactly the creation-operator parts of the Bogoliubov approximations to $J_i = J_i^{(\pi)} + J_i^{(\nu)}$ $(i = x, y, z)$. The three modes orthogonal to these in pairs are the one-dimensional scissors modes for relative angular oscillations about the three intrinsic axes. The remaining four modes are coupled $\beta - \gamma$, neutron–proton modes, and the extraction of their frequencies requires the diagonalization of a 4×4 matrix.

It was noted at the end of Section 4.3 that the method here described allows the tailoring of IBM-2 Hamiltonians to produce predetermined physical properties. A Hamiltonian like that of Eq. (4.12) is guaranteed to produce a global aligned-triaxial minimum in its energy surface at preset values of β_ρ, γ_ρ $(\gamma_\pi \neq \gamma_\nu)$, for any choice of positive values for the coefficients ζ. The values of ζ can then be chosen so that some of the normal modes described above fall at desirable frequencies. Upon adding reasonable collective terms (like a $\mathbf{J}^2$ term with an appropriate moment of inertia), a Hamiltonian is obtained whose exact numerical diagonalization will produce a spectrum which should reasonably approximate an aligned-triaxial nucleus with "band-heads" at reasonable excitation energies.

5.4. *The Structure of Intrinsic States*

The method described here rests on the identification of the equilibrium condensate as an approximate representation of the intrinsic structure of the ground-state band of a nucleus. This ground intrinsic state has a simple product structure, in the intrinsic basis. In the deformed case, states of well-defined angular momentum projected from it should be good approximations to the states of the ground band. Excited bands are now identified with intrinsic states in which normal modes have been excited. The leading component, in a $1/N$ expansion, of the excited intrinsic state is the one in which a single condensate boson has been replaced by a normal-mode boson. As previously mentioned, since the normal modes generally couple protons to neutrons, proper conservation of nucleon numbers requires the rewriting of a normal-mode creation operator, of generic structure $\alpha b^\dagger + \beta \hat{b}^\dagger$, as $\alpha b^\dagger b_c / \sqrt{N_\pi} + \beta \hat{b}^\dagger \hat{b}_c / \sqrt{N_\nu}$, and suitable normalization of the state obtained by acting with this on the condensate. In this way, the leading term of an excited intrinsic state is determined, and the states belonging to the corresponding excited band are obtained by projecting states of well-defined angular momentum. States of the same J projected from different intrinsic states are generally not mutually orthogonal. Components of higher order in $1/\sqrt{N}$ are needed in the intrinsic states to ensure orthogonality of projected states. The number of independent states of a given angular momentum J contained in a given band can generally be found by analysis of the K-values associated with the specific intrinsic state concerned.

In evaluating transition matrix elements between eigenstates of a given IBM-2 Hamiltonian, it is generally necessary to have explicit expressions for the eigenfunctions. However, when there is a well-defined intrinsic structure the matrix element separates, approximately, into an intrinsic factor and a collective (essentially geometric) factor. Thus some indication of the scale of matrix elements can be obtained by looking at matrix elements between intrinsic states, a task which is facilitated by use of the intrinsic basis, or even the normal-mode basis, for expressing the transition operator.

The usual forms of the $M1$ and $E2$ electromagnetic transition operators in IBM-2 are

$$T_{M1,\mu} = \sqrt{3/4\pi}\,(g_\pi J^\pi_\mu + g_\nu J^\nu_\mu) \tag{5.11a}$$

$$T_{E2,\mu} = \sum_{\rho=\pi,\nu} e_\rho [s^\dagger_\rho \tilde{d}_{\rho\mu} + d^\dagger_{\rho\mu} s_\rho + \chi_\rho (d^\dagger_\rho \tilde{d}_\rho)^{(2)}_\mu], \tag{5.11b}$$

where the g_ρ are effective boson gyromagnetic ratios and the e_ρ are generalized boson effective charges (containing implicitly information on the "mean-square radius" of the boson). For any given equilibrium intrinsic structure, these operators can be rewritten in terms of the corresponding intrinsic basis, and the latter in turn rewritten in terms of the normalized normal-mode creation and annihilation operators. In this process, the Bogoliubov approximation is invoked by the replacement $b^\dagger_c, b_c \to \sqrt{N_\pi}$; $\hat{b}^\dagger_c, \hat{b}_c \to \sqrt{N_\nu}$. The leading approximation to any intrinsic matrix element is then given by the coefficient of the appropriate product of normal-mode operators. Some illustrative examples will be presented here.

For the spherical equilibrium, where the intrinsic ground state is an s-boson condensate and the normal-mode operators are linear combinations of d-boson operators (see Eqs. (5.2)), the intrinsic states have good angular momentum, and it is easy to evaluate their g-factors and $M1$ transition rates to leading order. The relevant wavefunctions are

$$|g\rangle = (N_\pi!\,N_\nu!)^{-1/2}\,(s^\dagger_\pi)^{N_\pi}(s^\dagger_\nu)^{N_\nu}\,|\rangle \equiv |N_\pi, N_\nu\rangle \tag{5.12a}$$

$$|p\rangle = (1+\eta^2)^{-1/2}\,[d^\dagger_\nu \mid N_\pi, N_\nu - 1\rangle - \eta d^\dagger_\pi \mid N_\pi - 1, N_\nu\rangle] \tag{5.12b}$$

$$|m\rangle = (1+\eta^2)^{-1/2}\,[d^\dagger_\pi \mid N_\pi - 1, N_\nu\rangle + \eta d^\dagger_\nu \mid N_\pi, N_\nu - 1\rangle], \tag{5.12c}$$

where η is defined in Eq. (5.2f). The results are

$$g_p = (\eta^2 g_\pi + g_\nu)/(1+\eta^2) \tag{5.13a}$$

$$g_m = (g_\pi + \eta^2 g_\nu)/(1+\eta^2) \tag{5.13b}$$

$$B(M1; p \rightleftharpoons m) = 9\eta^2 (g_\nu - g_\pi)^2 / 2\pi (1+\eta^2)^2. \tag{5.13c}$$

Similarly, the leading-order approximations to intrinsic quadrupole moments and $E2$ transition rates are

$$Q_p = 4\sqrt{2\pi/35}\,(e_\nu\chi_\nu + \eta^2 e_\pi\chi_\pi)/(1+\eta^2) \tag{5.14a}$$

$$Q_m = 4\sqrt{2\pi/35}\,(e_\pi\chi_\pi + \eta^2 e_\nu\chi_\nu)/(1+\eta^2) \tag{5.14b}$$

$$B(E2;\, g \to p) = 5(e_\nu\sqrt{N_\nu} - \eta e_\pi\sqrt{N_\pi})^2/(1+\eta^2) \tag{5.14c}$$

$$B(E2;\, g \to m) = 5(e_\pi\sqrt{N_\pi} + \eta e_\nu\sqrt{N_\nu})^2/(1+\eta^2) \tag{5.14d}$$

$$B(E2;\, p \rightleftharpoons m) = \eta^2(e_\nu\chi_\nu - e_\pi\chi_\pi)^2/(1+\eta^2)^2. \tag{5.14e}$$

Recalling that $\eta > 0$ implies that the lower-lying normal mode (m) is neutron–proton symmetric, while the higher-lying mode (p) is neutron–proton antisymmetric, while the reverse is true for $\eta < 0$, it is easy to understand the pattern of reinforcement or cancellation in the transition rates. It is noteworthy that transition rates from the ground intrinsic state to the singly-excited intrinsic states are of order N, in this vibrational case, while transition rates between singly-excited intrinsic states are of order unity. The expressions in Eqs. (5.12)–(5.14) agree to leading order in N_ρ with the analytic results in the $U(5)$ dynamic symmetry limit [41, 45, 46].

For aligned prolate condensates, where the normal-mode structure is given in Eqs. (5.5) and (5.6) and the discussion between those equations, the transcription of the transition operators is somewhat more tedious, but still straightforward. Relevant intrinsic wavefunctions are

$$|g\rangle = (N_\pi!\,N_\nu!)^{-1/2}\,(b_c^\dagger)^{N_\pi}\,(\hat{b}_c^\dagger)^{N_\nu}\,|0\rangle \equiv |N_\pi, N_\nu\rangle \tag{5.15a}$$

$$|\beta p\rangle = (1+\eta_0^2)^{-1/2}\,[\hat{b}_\beta^\dagger\,|N_\pi, N_\nu - 1\rangle - \eta_0 b_\beta^\dagger\,|N_\pi - 1, N_\nu\rangle] \tag{5.15b}$$

$$|\beta m\rangle = (1+\eta_0^2)^{-1/2}\,[b_\beta^\dagger\,|N_\pi - 1, N_\nu\rangle + \eta_0\hat{b}_\beta^\dagger\,|N_\pi, N_\nu - 1\rangle] \tag{5.15c}$$

$$|\gamma p\rangle = (1+\eta_2^2)^{-1/2}\,[d_{\nu_2}^\dagger\,|N_\pi, N_\nu - 1\rangle - \eta_2 d_{\pi_2}^\dagger\,|N_\pi - 1, N_\nu\rangle] \tag{5.15d}$$

$$|\gamma m\rangle = (1+\eta_2^2)^{\;1/2}\,[d_{\pi_2}^\dagger\,|N_\pi - 1, N_\nu\rangle + \eta_2 d_{\nu_2}^\dagger\,|N_\pi, N_\nu - 1\rangle] \tag{5.15e}$$

$$|\mathrm{sc}\rangle = (1+\eta_1^2)^{-1/2}\,[d_{\nu_1}^\dagger\,|N_\pi, N_\nu - 1\rangle - \eta_1 d_{\pi_1}^\dagger\,|N_\pi - 1, N_\nu\rangle] \tag{5.15f}$$

$$\eta_1 = \beta_\nu\sqrt{N_\nu(1+\beta_\pi^2)}/\beta_\pi\sqrt{N_\pi(1+\beta_\nu^2)}, \tag{5.15g}$$

where $|\mathrm{sc}\rangle$ denotes the "scissors" mode, and η_K is the mixing coefficient for the $\beta(K=0)$, $\gamma(K=2)$, or scissors ($K=1$) mode. The two-fold degeneracy of the γ and scissors modes has been exploited to allow the use of wavefunctions with well-defined axial projection number K. The forms above have positive K ($K=+1$ for the scissors mode, $K=+2$ for the γ modes); the related $K<0$ forms are self-evident. Some representative leading-order intrinsic transition matrix elements are

$$|\langle g|\,T_{M1}\,|\mathrm{sc}\rangle|^2 = 9N_\pi N_\nu\beta_\pi^2\beta_\nu^2(g_\pi - g_\nu)^2/4\pi D_{\pi\nu} \tag{5.16a}$$

$$|\langle g|\, T_{E2}\, |\beta m\rangle|^2 = [e_\pi \sqrt{N_\pi}\,(1-\bar{\chi}_\pi\beta_\pi-\beta_\pi^2)/(1+\beta_\pi^2) + \eta_0 e_\nu \sqrt{N_\nu}\,(1-\bar{\chi}_\nu\beta_\nu-\beta_\nu^2)/(1+\beta_\nu^2)]^2/(1+\eta_0^2) \tag{5.16b}$$

$$|\langle g|\, T_{E2}\, |\beta p\rangle|^2 = [e_\nu \sqrt{N_\nu}\,(1-\bar{\chi}_\nu\beta_\nu-\beta_\nu^2)/(1+\beta_\nu^2) - \eta_0 e_\pi \sqrt{N_\pi}\,(1-\bar{\chi}_\pi\beta_\pi-\beta_\pi^2)/(1+\beta_\pi^2)]^2/(1+\eta_0^2) \tag{5.16c}$$

$$|\langle g|\, T_{E2}\, |\gamma m\rangle|^2 = [e_\pi \sqrt{N_\pi}\,(1+\bar{\chi}_\pi\beta_\pi)/\sqrt{1+\beta_\pi^2} + \eta_2 e_\nu \sqrt{N_\nu}\,(1+\bar{\chi}_\nu\beta_\nu)/\sqrt{1+\beta_\nu^2}]^2/(1+\eta_2^2) \tag{5.16d}$$

$$|\langle g|\, T_{E2}\, |\gamma p\rangle|^2 = [e_\nu \sqrt{N_\nu}\,(1+\bar{\chi}_\nu\beta_\nu)/\sqrt{1+\beta_\nu^2} - \eta_2 e_\pi \sqrt{N_\pi}\,(1+\bar{\chi}_\pi\beta_\pi)/\sqrt{1+\beta_\pi^2}]^2/(1+\eta_2^2) \tag{5.16e}$$

$$|\langle g|\, T_{E2}\, |\mathrm{sc}\rangle|^2 = N_\pi N_\nu [e_\pi \beta_\nu (1-\bar{\chi}_\pi\beta_\pi/2) - e_\nu\beta_\pi(1-\bar{\chi}_\nu\beta_\nu/2)]^2/D_{\pi\nu} \tag{5.16f}$$

$$D_{\pi\nu} = N_\pi\beta_\pi^2(1+\beta_\nu^2) + N_\nu\beta_\nu^2(1+\beta_\pi^2); \qquad \bar{\chi}_\rho = \sqrt{2/7}\,\chi_\rho. \tag{5.16g}$$

The in-band $E2$ transition rate is given in terms of

$$|\langle i|\, T_{E2}\, |i\rangle|^2 = [N_\pi e_\pi \beta_\pi (2-\bar{\chi}_\pi\beta_\pi)/(1+\beta_\pi^2) + N_\nu e_\nu \beta_\nu (2-\bar{\chi}_\nu\beta_\nu)/(1+\beta_\nu^2)]^2, \tag{5.17}$$

where i is any of the intrinsic states (g, βm, βp, γm, γp, sc). The in-band $E2$ rate is of order N^2, the ground-to-singly-excited-band $E2$ rate is of order N, and the $E2$ rate between singly-excited bands is found to be of order unity. Expressions (5.15)–(5.17) coincide to leading order in N_ρ with the corresponding analytic results in the dynamical $SU(3)$ limit [41, 45].

A number of interesting results follow from the above explicit expressions for intrinsic matrix elements. In the spherical case, the sums $g_p + g_m$, $Q_p + Q_m$, and $B(E2; g \to p) + B(E2; g \to m)$ in Eqs. (5.13)–(5.14) are independent of the mixing parameter η. Similarly, in the deformed case, adding the squares of intrinsic matrix elements from one type of band to another (e.g., $|g\rangle$ to $|\beta p\rangle$ and $|\beta m\rangle$ or $|\gamma p\rangle$ and $|\gamma m\rangle$ to $|\beta p\rangle$ and $|\beta m\rangle$) results in an expression which is independent of the mixing parameters η_i. These results provide sum-rules (appropriate for large N) for moments and transitions between the various bands.

As shown in Eqs. (5.16b)–(5.16c), intrinsic $E2$ matrix elements from $|\beta m\rangle$ or $|\beta p\rangle$ to $|g\rangle$ involve the factors $V_\rho = 1 - \bar{\chi}_\rho\beta_\rho - \beta_\rho^2$, $\rho = \pi, \nu$. If these factors are zero then the above intrinsic matrix elements vanish. This is not so for the $E2$ matrix elements from the γ-bands (type p or m) to the ground-band nor from the β-bands to the γ-bands. The equations $V_\rho = 0$ are precisely the extremum equations for the Hamiltonian $\kappa Q_\pi \cdot Q_\nu$ (defined as in (2.9)). Thus if the $E2$ parameters χ_ρ are chosen such that $V_\rho \simeq 0$, then as a direct consequence the $\beta \to g$ $E2$ transitions are predicted to be weaker than the $\beta \to \gamma$ or $\gamma \to g$ transitions. Such behaviour was first noted in the context of IBM-1 [13, 14]. Here it is seen to hold also in

IBM-2 and to apply to both proton–neutron symmetric and antisymmetric bands. It is interesting that an experimentally confirmed IBM-1 characteristic of $E2$ transitions is also present in IBM-2 (with a completely different Hamiltonian).

6. SUMMARY AND DISCUSSION

Incorporating proton–neutron degrees of freedom in the interacting boson model enlarges the set of possible one- and two-body interactions. The spectral significance of a given algebraic interaction in the abstract second quantized form of the Hamiltonian is not transparent. As a result, the role played by most of the interactions allowed has not been investigated so far. Even for the restricted IBM-2 Hamiltonians which have been used in calculations, the choice of parameters (e.g., the Majorana parameters) is not clear. Dynamical symmetries can only illuminate part of the model's capabilities and moreover are broken in most nuclei which are fitted by IBM-2. In numerical computations one deals each time with a specific choice of parameters and boson numbers. All these issues indicate a need to discuss the physical content of the general IBM-2 Hamiltonian in geometric terms. This is the aim of the approach reported in this work, which focuses on the identification of normal modes and on relating abstract algebraic terms to observables such as bandhead energies and band splitting.

The main ingredients of the approach, first developed for IBM-1, are the introduction of shape parameters through the use of non-spherical proton–neutron bases, exact resolution of the Hamiltonian into intrinsic and collective parts, the extraction of normal modes from the intrinsic part of the Hamiltonian and the construction of intrinsic states.

Two commuting sets of possibly deformed bosons are introduced, for protons and for neutrons. Each set forms a complete orthonormal basis whose members depend on two quadrupole deformation parameters, and the bases are rotated with respect to one another. One member of each set serves as a condensate boson. The overall shape of the valence-nucleon distribution is described by an intrinsic state which is a product of the proton and neutron condensate wave functions. The expectation value of the Hamiltonian in this intrinsic state defines an energy surface which depends on the $\pi - \nu$ deformation parameters as well as on the relative orientation of the proton and neutron shapes. The global minimum of the energy surface defines an equilibrium intrinsic state for the ground-state band. The latter is the key element in resolving the IBM-2 Hamiltonian H exactly into intrinsic (bandhead related) and collective (in band related) parts. The intrinsic part of the Hamiltonian H_{int} has the equilibrium intrinsic state as an exact zero-energy eigenstate and has the same shape for its energy surface as that of the full Hamiltonian. The collective part of the Hamiltonian H_{c}, obtained from $H_{\text{c}} = H - H_{\text{int}}$, has a flat energy surface and is found to be connected with particular chains of orthogonal groups. The coefficients of the various rotational terms are related to moments of inertia. By construction, the equilibrium condensate is an exact eigenstate of the rotational invariant H_{int}. In situations when this condensate is deformed, the rotation symmetry is spontaneously broken in it. As a result, all states of good angular momentum projected from the condensate form an exactly degenerate ground-state band. This degeneracy is removed by rotation terms in H_c. Other eigenstates of H_{int} also tend to cluster into bands. In general H_c and H_{int} do not commute, so that H_c can mix as well as shift and split the bands generated by H_{int}.

The normal modes appropriate to a given Hamiltonian are identified, in the limit of large boson numbers, by application of the Bogoliubov treatment to the intrinsic part of the Hamiltonian and subsequent diagonalization of the result. The normal modes of the combined proton–neutron system are determined from the dynamics, and are in general a mixture of particular members (other than the condensate boson) of the two separate bases, with the equilibrium deformation an orientation parameters. The mixing depends on these parameters and on the boson numbers and reflects the proton–neutron interactions. The normal mode frequencies are positive for a local minimum and provide an estimate, for large boson numbers, of the position of the bands. In general, the diagonalized form of the Bogoliubov image of H_{int} displays the intrinsic modes as a sum of harmonic oscillators. The spurious modes are absent (i.e., they are zero-energy modes) and therefore decoupled. The latter are the "massless" Goldstone bosons associated with spontaneously broken symmetries in the condensate and represent the modes of collective motion. Once the genuine intrinsic modes have been identified, they are used for the construction of intrinsic states by exciting the condensate ground-state wave function. This form of intrinsic states, appropriate for large boson numbers, confers an intuitive geometric interpretation. The intrinsic states are used to derive approximate expressions for intrinsic matrix elements contributing to static and dynamic moments.

There have been previous attempts at a geometric interpretation of IBM-2 [26–38]. The popular approach of Hatch and Levit [15] is based on a classical limit of the boson Hamiltonian. This is achieved by replacing the boson operators by classical commuting variables. The latter are related to nuclear deformation parameters and their conjugate momenta. The potential function is obtained by setting all the momenta to zero. Next the classical Hamiltonian is treated in the oscillator approximation by a $1/N$ expansion about the minimum of the potential. The calculation of the oscillator frequencies involves a separate calculation of a spring constant and of a reduced mass. As stated in Refs. [27, 30, 36, 38], the completely general result involving five proton and five neutron coordinates and their conjugate momenta is quite complicated and difficult to obtain. This explains why until now this approach has been confined to aligned configurations, in studies of the potential energy [27], and to simplified treatments dealing with one mode at a time: the scissors mode [30, 31, 32], 2^+ states in the $U(5)$ limit [36] and β vibrations in the $O(6)$ limit [38]. Furthermore, since the above approach is classical in nature, there is no derivation of the quantum normal modes in terms of the boson variables.

In contrast, the formalism presented in this work is fully quantal and can accomodate arbitrary $\pi - \nu$ shapes whether spherical, axially deformed or triaxial. All quantum normal modes are derived simultaneously with equal ease and thus a complete comprehensive picture is obtained. The structure of the normal modes comes automatically from the formalism, e.g., the scissors mode shows up as two dimensional in the axially-deformed case and the 2^+ symmetric and antisymmetric excitations of the spherical condensate are both five dimensional oscillators. Normal frequencies are calculated directly by a well defined procedure without the need to assume a form for the reduced mass.

A second approach to the study of the ground state and excitations in a system of interacting bosons is that of Dukelsky *et al.* [48]. Here a Hartree–Bose basis is derived self consistently as a solution of an average (distorted) one-body Hamiltonian which is obtained by minimizing the expectation value of the full boson Hamiltonian in a condensate wave-function. Excited intrinsic states are obtained by solving Tamm–Dancoff (TDA) and random-phase ((RPA) equations. A difficulty in the Hartree–Bose approach is the fact that broken symmetries in the self-consistent average distorted field lead to the appearance of spurious states. TDA energies of these spurious excited states do not vanish. This is clearly seen in Ref. [29] where the Hartree–Bose method is applied to a semiclassical description of the scissors mode. The resulting normal-mode TDA matrix has no zero eigenvalue. The spurious mode associated with a rotation of the system as a whole cannot be identified from the eigenfunctions of the above matrix since neither-normal-mode eigenvector is proportional to $J_1^\pi + J_1^\nu$ acting on the aligned axially-deformed condensate. The simple Hartree–Bose method does not naturally identify spurious, collective modes. The decoupling of the spurious states from the physical states is achieved [29] only through the use of the RPA equations. The RPA restores the symmetry and brings the spurious states to zero energy, at the cost of the loss of the simplicity in the structure of the wave functions that was inherent in the TDA. Moreover, the RPA equations do not follow from a variational principle [49].

The formalism presented in this work encompasses both the simplicity in structure of TDA wave-functions and the decoupling of spurious from physical modes. This can be achieved since in the process of deriving normal modes one deals with the intrinsic part of the Hamiltonian H_{int} and not with the full Hamiltonian H. The energy surface of H_{int} has the same shape as that of H, but in addition has the equilibrium condensate as an *exact* zero energy eigenstate. When acting on this condensate with a broken-symmetry generator (which commutes with H_{int}) the resulting new state (which contains the Goldstone boson) is still a zero energy eigenstate of H_{int}. This ensures that the Goldstone mode is indeed "massless" and is absent from the Bogoliubov image of H_{int}. Thus a clear separation and identification of genuine intrinsic and spurious collective modes of excitation is achieved. Carrying out the normal mode analysis on H_{int} rather than the full H, with the use of dynamically-determined $\pi - \nu$ bases, leads also to normal modes composed of creation operators only. This is different from the usual approach for bosonic systems [49], where the normal modes derived are quasiparticles, which are linear combinations of both creation and destruction operators. As a consequence, an inherent ingredient of IBM-2—conservation of boson number—is preserved in the structure of intrinsic states. Only genuine intrinsic modes appear in the dominant component of these states, which endows them with a transparent geometric and physical interpretation. Such a structure of intrinsic states conforms with that of known intrinsic states in the $SU(3)$ limit [35].

Van Egmond and Allart [33] have studied rotational and intrinsic excitations in IBM-2, for axially-symmetric systems, by combining a mean field approximation with a generator coordinate method. In their calculations of small oscillations about the minimum of the energy surface for symmetric and antisymmetric β vibrations, the authors assume a linear relation between β_π and β_ν. In the formalism presented in this work such an assumption is not made, but rather the route of departure from the minimum is determined from the dynamics (see the mixing parameters in Eq. (5.5)).

The symmetry preserving approach of Hahne and Scholtz [37] is based on a positional representation. The monopole bosons are eliminated by means of a Holstein–Primakoff realization of $U_\pi(6) \times U_\nu(6)$. The remaining bosons are related to shape operators whose eigenstate is used to give a geometrical interpretation for IBM-2. Excited energies, moments of inertia, and transition rates are calculated in a $1/N$ expansion. The method has been applied so far only to systems with axial symmetry. It produces normal modes composed of both creation and destruction operators and not involving the monopole bosons.

Cranking procecdures for calculating moments of inertia [34] involve a basic assumption that all collective motion is of $O(3)$ rotational character. This is also assumed in the $1/N$ expansion technique of Kuyucak and Morrison [50]. This technique involves a variation after projection, followed by a gaussian approximation for matrix elements of the Hamiltonian between states of good J projected from intrinsic states. This leads to an infinite expansion in power of $J(J+1)$ and $1/N$.

In the formalism presented in this work the variation is carried out before projection. The finite $1/N$ expansion used in a normal-mode analysis is an outcome of the Bogoliubov treatment of the Hamiltonan itself and not of the evaluation of specific matrix elements. The collective part of the Hamiltonian (see Eq. (3.5)) allows for more general types of collective rotational motions than the usual $O(3)$ rotations. The presence of these additional rotations influences the moments of inertia of the different rotational terms in H_c and dictates a splitting pattern which may differ from the $J(J+1)$ type. Furthermore, because the intrinsic and collective parts do not in general commute, their coupling may destroy the regular band-structure and the "adiabatic" nature of the spectrum.

The resolution $H = H_{\text{int}} + H_c$ of the general IBM-2 Hamiltonian into intrinsic and collective parts, as reported in this work, is exact. It is obtained without any expansion or truncation scheme. (The latter is used solely for the sake of extraction of normal modes in the limit of large boson number). Both H_{int} and H_c are full quantum mechanical, hermitian, number-conserving, rotation-invariant operators.

The resolution amounts to a rewriting of the Hamiltonian in a manner more accessible to physical interpretation. Once the form of H_{int} and H_c is given, it allows the construction of IBM-2 Hamiltonians which will have specified normal modes and frequencies. By choosing interaction terms appearing in a particular H_{int} (which annihilates a $\pi - \nu$ condensate of a given shape) and adding a reasonable J^2 term, it is possible to produce an IBM-2 Hamiltonian which is guaranteed to have a prescribed intrinsic structure. By examining the explicit expressions for the normal-mode frequencies, one can select the coefficients of the above terms to reproduce the corresponding bandhead energies (in the limit of large boson number). This can serve as a first step in a fitting procedure where one starts with an adequate intrinsic Hamiltonian and adds terms, in a controlled fashion, from the collective Hamiltonian. The efficiency of this procedure can be appreciated by comparing the small number of normal modes against the large number of possible one- and two-body interactions.

The method presented in this work is both simple and general enough to cope with any shape of the valence $\pi - \nu$ distributions (not just spherical or axially deformed) which is described within the general IBM-2 Hamiltonian without regard to limiting symmetries (e.g., dynamical symmetries or F-spin symmetry). In each case all relevant quantum intrinsic normal modes and the decoupled spurious modes are identified in a well defined procedure. These virtues allow an intuitive geometric interpretation for arbitrary algebraic interaction terms which are otherwise abstract in nature. Knowing how a given interaction is distributed among the intrinsic and collective parts of the Hamiltonian permits the study of its effect on physical observables such as bandhead energies and moments of intertia. This provides also a criterion to decide which interaction terms to choose and to reduce the number of free parameters needed for the description of specific experimental data. These ingredients give the present method the potential of being useful in exploring inherent properties and revealing the underlying intrinsic and collective structure in proton–neutron systems. It opens the possibility of investigating capabilities and limitations, choice of parameters and role of conventional and non-conventional terms in the general IBM-2 Hamiltonian. For practical applications the method may be used for interpreting numerical calculations as well as providing a suitable initial guess for multi-parameter least-squares fitting procedures.

REFERENCES

1. A. ARIMA AND F. IACHELLO, *Ann. Phys. (N.Y.)* **99** (1976), 253.
2. A. ARIMA AND F. IACHELLO, *Ann. Phys. (N.Y.)* **111** (1978), 201.
3. For a review see A. ARIMA AND F. IACHELLO, *Ann. Phys. (N.Y.)* **123** (1979), 468.
4. For a review see R. F. CASTEN AND D. D. WARNER, *Rev. Mod. Phys.* **60** (1988), 389.
5. F. IACHELLO AND I. TALMI, *Rev. Mod. Phys.* **59** (1987), 339.
6. J. N. GINOCCHIO AND M. W. KIRSON, *Phys. Rev. Lett.* **44** (1980), 1744.
7. J. N. GINOCCHIO AND M. W. KIRSON, *Nucl. Phys. A* **350** (1980), 31.
8. A. E. L. DIEPERINK, O. SCHOLTEN, AND F. IACHELLO, *Phys. Rev. Lett.* **44** (1980), 1747.

9. A. E. L. Dieperink and O. Scholten, *Nucl. Phys. A* **346** (1980), 125.
10. O. Castanos, A. Frank, P. Hess, and M. Moshinsky, *Phys. Rev. C* **24** (1981), 1367.
11. P. van Isacker and J. Q. Chen, *Phys. Rev. C* **24** (1981), 684.
12. A. Bohr and B. R. Mottelson, *Phys. Scr.* **25** (1982), 28.
13. R. Bijker and A. E. L. Dieperink, *Phys. Rev. C* **26** (1982), 2688.
14. D. D. Warner and R. F. Casten, *Phys. Rev. C* **26** (1982), 2690.
15. R. L. Hatch and S. Levit, *Phys. Rev.* C **25** (1982), 614.
16. O. S. van Roosmalen and A. E. L. Dieperink, *Phys. Lett. B* **100** (1981), 299.
17. H. T. Chen and A. Arima, *Phys. Rev. Lett.* **51** (1983), 447.
18. A. Arima, *Nucl. Phys. A* **421** (1984), 69.
19. A. Leviatan, *Phys. Lett. B* **143** (1984), 25.
20. A. Leviatan, *Z. Phys. A* **321** (1985), 467.
21. M. W. Kirson and A. Leviatan, *Phys. Rev. Lett.* **55** (1985), 2846.
22. A. Leviatan, *Ann. Phys. (N.Y.)* **179** (1987), 201.
23. A. Leviatan and M. W. Kirson, *Ann. Phys. (N.Y.)* **188** (1988), 142.
24. A. Arima, T. Otsuka, F. Iachello, and I. Talmi, *Phys. Lett. B* **66** (1977), 205.
25. T. Otsuka, A. Arima, F. Iachello, and I. Talmi, *Phys. Lett. B* **76** (1978), 139.
26. A. E. L. Dieperink, *Prog. Part. Nucl. Phys.* **9** (1983), 121.
27. A. B. Balantekin, B. R. Barrett, and S. Levit, *Phys. Lett. B* **129** (1983), 153.
28. A. E. L. Dieperink, *Nucl. Phys. A* **421** (1984), 189.
29. S. Pittel and J. Dukelsky, *Phys. Rev. C* **32** (1985), 335.
30. A. B. Balantekin and B. R. Barrett, *Phys. Rev. C* **32** (1985), 288; Erratum **33** (1986), 1842.
31. R. Bijker, *Phys. Rev. C* **32** (1985), 1442.
32. N. R. Walet, P. J. Brussard, and A. E. L. Dieperink, *Phys. Lett. B* **163** (1985), 1.
33. A. van Egmond and K. Allart, *Phys. Lett. B* **164** (1985), 1.
34. H. Schaaser and D. M. Brink, *Nucl. Phys. A* **452** (1986), 1.
35. H. C. Wu, A. E. L. Dieperink, and S. Pittel, *Phys. Rev. C* **34** (1986), 703.
36. A. B. Balantekin and B. R. Barrett, *Phys. Rev. C* **35** (1987), 1878.
37. F. J. W. Hahne and F. G. Scholtz, *Nucl. Phys. A* **483** (1988), 23.
38. A. B. Balantekin, B. R. Barett, and P. Halse, *Phys. Rev. C* **38** (1988), 1392.
39. N. H. March, W. H. Young, and S. Samphanthar, "The Many Body Problem in Quantum Mechanics," Cambridge Univ. Press, London, 1967.
40. A. Leviatan, *in* "Proceedings of the International Conference on Nuclear Structure through Static and Dynamic Moments" (H. H. Bolotin, Ed.), Vol. II, p. 148, 1987.
41. F. Iachello and A. Arima, "The Interacting Boson Model," Cambridge Univ. Press, 1987.
42. P. van Isacker, A. Frank, and H. Z. Sun, *Ann. Phys. (N.Y.)* **157** (1984), 183.
43. A. E. L. Dieperink and R. Bijker, *Phys. Lett. B* **116** (1982), 77.
44. A. E. L. Dieperink and I. Talmi, *Phys. Lett. B* **131** (1983), 1.
45. P. van Isacker, K. Heyde, J. Jolie, and A. Servin, *Ann. Phys. (N.Y.)* **171** (1986), 253.
46. For an experimental observation of such mixed symmetry states see W. D. Hamilton, A. Irbäck, and J. P. Elliott, *Phys. Rev. Lett.* **53** (1984), 2469.
47. D. Bohle, A. Richter, W. Steffen, A. E. L. Dieperink, N. Lo Iudice, F. Palumbo, and O. Scholten, *Phys. Lett. B* **137** (1984), 27.
48. J. Dukelsky, G. G. Dussel, R. P. J. Perazzo, S. L. Reich, and H. M. Sofia, *Nucl. Phys. A* **425** (1984) 93.
49. P. Ring and P. Schuck, "The Nuclear Many-Body Problem," Springer-Verlag, New York/Heidelberg/Berlin, 1980.
50. S. Kuyucak and I. Morrison, *Ann. Phys. (N.Y.)* **181** (1988), 79.

ANNALS OF PHYSICS **201**, 51–82 (1990)

Photon Magnetic Mass and Meissner Effect in the Bose–Einstein Condensate of W-Mesons

E. J. FERRER,* V. DE LA INCERA,* AND A. E. SHABAD

P. N. Lebedev Physical Institute, Moscow, USSR

Received September 1, 1989

It is shown that in the W-condensate phase reached in the electroweak plasma when the fermion density J_L is increased above some critical value ($J_L \simeq M_W^3/6\pi$) the residual $U_{\mathrm{EM}}(1)$ symmetry of the Weinberg–Salam model is spontaneously broken. Starting from the effective action of the W-condensate phase, calculated within the approximation known to guarantee the Bose–Einstein condensation of $W^{\pm}$-mesons, we diagonalize the mass matrix of bosons and calculate the photon magnetic mass that proves to be different from zero as a consequence of the spontaneous violation of the $U_{\mathrm{EM}}(1)$-symmetry. By solving the linearized set of coupled equations for the photon, W- and Z-boson fields, we find that a small magnetic field applied from outside penetrates into the W-condensate medium down to the Londons' depth equal to the photon magnetic mass inversed and also induces W- and Z-fields in the same layer of the medium. This Meissner effect is performed by a polarization charge of weak nature induced on the surface and by an electric and weak supercurrents concentrated at the depth of inversed weak mesons masses ($M_W \sim \mathscr{M}_{\mathscr{Z}}$). © 1990 Academic Press, Inc.

1. INTRODUCTION

Considering electroweak matter with high density of leptons at zero temperature, Linde [1] found a new nontrivial ground state characterized by a nonvanishing average value of the charged vector meson field W, present together with the usual Higgs average. This result is understood as the Bose–Einstein (BE) condensation of W-mesons and it has stimulated various investigations [3–12] in the recent years.

The BE W-condensation, which gives rise to the W-meson condensate phase, can be simpliest understood for the case which includes only leptons [1] along the following lines. Let one have a degenerate gas of neutrinos whose density, J_L, exceeds the critical value of $J_L^c = M_W^3/6\pi$, where M_W is the mass of the W-boson. Then, among the neutrinos occupying the Fermi sphere, there are such whose energy exceeds M_W. Every neutrino of this sort is able to convert into a W^+-meson and an electron (the neutrino chemical potential exceeds the W-boson mass). The

---

* Address after Oct. 1990: Institute of Mathematics, Cibernetics and Physics, Academy of Sciences of Cuba, Havana, Cuba.

0003-4916/90 $7.50

Copyright © 1990 by Academic Press, Inc.
All rights of reproduction in any form reserved.

W^+-mesons and electrons thus created may take part in the inverse reaction to convert back into neutrinos. However, the first reaction $\nu \rightarrow W^+ + e^-$ is energetically favorable as compared with the inverse one. The final state is characterized by a finite density of the W-mesons forming a BE condensate, a Fermi sphere of electrons that balance the electric charge of the W-condensate and the correspondingly reduced (remember, that the overall number of neutrinos and electrons conserves) Fermi sphere of neutrinos. In Section 2 we outline formally the derivation of the W-condensation following Ref. [1]. Analogous results concerning the BE condensation of W-mesons, hold true for electroweak matter with baryons (quarks) included [2].

The study of the condensation phenomena at finite temperature was realized in [3, 4] (see also [5, 6]). It has been demonstrated in [4, 6] that for the system with electric and weak-neutral net charges equal to zero the W-condensate present at $T=0$ for $J_L \geqslant J_L^c$ evaporates prior to the Higgs condensate when the temperature increases.

The above-mentioned results have been obtained neglecting the effects of the fermion anomalies, because they are $O(g^2)$ corrections to the values of the condensates, and therefore insignificant for the determination of the phase transition curves. The inclusion of fermion anomalies gives rise to a spatial inhomogeneity of the W-condensate [7]. The behaviour of the inhomogeneity of the W-condensate at high temperature has been studied in [8], with the result that it is weakened by the heating of the system. We do not find it timely to take into account these small effects in the present work, however.

The appearance of an electrically charged condensate in the electroweak system must bring new consequences in what concerns the long- or short-ranged behaviour of the gauge fields. It is already known from the way the Higgs mechanism operates in the Weinberg–Salam (WS) model that all the fields whose associated charge operator transforms the average value of the condensate field $\langle \phi \rangle = \xi$ turn massive. It was the case, that as ξ remained invariant under the action of the electric charge operator, the photon field remained massless. Thus, once the W-condensate appears and transforms nontrivially under the action of the electric charge operator, it is expected that the photon should become massive through a mechanism analogous to the one which served the Z_μ and $W_\mu^\pm$ fields under the Higgs condensation. These expectations have been realized in our brief publication [11], where also it was argued that the Meissner screening associated to the photon magnetic mass is due mostly to the effect of an induced polarization charge of weak nature. We shall further develop this theme in the present article. In Refs. [9, 10] we went beyond the simplest approximation capable of producing the W-condensate and took into account the influence the latter has on the fermion spectrum and hence on the fermion loop contribution into the polarization tensor responsible for the appearance of a superconducting electromagnetic current. We are going to present a more detailed and up-to-dated version of that investigation in a forthcoming paper [12].

The fermion densities necessary for the W-condensate to appear are very high. In [13] a scenario is suggested for the evolution of the post-inflationary universe with very high densities of baryons and leptons. In spite of the large fermion asymmetries present in the scenario [13] they are erased at temperatures about 200 GeV, thanks to the action of a mechanism described by Affleck and Dine [14] and Linde [15], the baryon asymmetry $n_B/n_\gamma \sim 10^{\;9}$ observed at present being finally obtained.

Within this scenario the W-condensate phase could be passed in the course of the evolution, giving rise to interesting physical effects, as for instance, gravitational waves [16, 8] caused by the small effects of the inhomogeneity of the W-condensate [7, 8], as well as of the above-mentioned effects of superconductivity, as was pointed out in [9, 10] and the Meissner screening by induced weak charge [11].

The phenomenology of the W-condensate phase present in some stages of the universe in evolution might have important consequences for cosmology. In addition to the just-mentioned physical effects, this phase could supply the natural conditions for annihilation of the monopoles produced together with cosmological strings and other objects [17] at the end of the inflationary era. This point will be discussed in more detail in the concluding section.

In the present paper we deal with the high-leptonic-density WS plasma in a simplest approximation capable of reproducing the W-condensation phenomenon. This approximation may be roughly reffered to as a tree approximation with respect to bosons and one-loop approximation with respect to leptons. One of our main results is that already in the approximation under study all the bosons, including the photon, acquire (electric and magnetic) masses through a Higgs-like mechanism, as a result of the shift of the Lagrangian by the average vector boson field of the condensate. These masses provide the infrared finiteness of the theory in the W-condensed phase and the short-range character of all interactions mediated by vector particles, in other words, the spatial damping of all the field strength, including the conventional electric and magnetic fields, known as Debye and Meissner screening. The latter effect, is gained through a spontaneous symmetry break down of the residual $U_{\mathrm{EM}}(1)$-symmetry.

In analogy with the way adopted in the usual theory of the Meissner effect, we consider the response of the W-condensate medium to an application of a (small) magnetic field by studing the (linearized) field equations characteristic of this medium. We give the solutions of these equations showing that the applied magnetic field, together with the induced quasimagnetic field associated to the weak-neutral field component Z_3 and the induced quasielectric field associated to the weak-charged component $W_0^{(2)}$, fall down exponentially inwards the W-condensate phase as it is usual for the Meissner screening. The fields inside the W-condensate phase change on two essentially different scales: the shorten one is of the order of the inverse W-meson mass and the longer one is given by the inverse of the photon magnetic mass, found. The cooperative screening effect is attributed to induced weak charge concentrated near the surface of the medium and to accompanying electromagnetic and weak nondamping currents flowing in a somewhat deeper layer. Thus, already in the lowest approximation able to produce the W-condensation solution, there appears the superconducting behaviour of the

W-condensate phase, earlier obtained in a more sphisticated approximation in our publications [9, 10].

We organize the main results of the paper as follows. In Section 2 the effective action for the many-particle *WS* model is presented (Subsection 2.1) and we shortly discuss the derivation of the W-condensate solution obtained in Ref. [1], emphasizing the approximation used and the symmetries of the W-condensate phase broken (subsection 2.2). Working within the lowest approximation especified above, we prove in Section 3 the massiveness of all the physical bosons involved in the *WS* theory. We also find in the weak condensate approximation the new combination of fields that forms the photon in such a phase, together with other eigenfields diagonalizing the mass matrix. It is proved that in the W-condensate phase not only B_μ and W^3_μ enter to form the photon field as it was the case in the Higgs phase of the *WS* model but also the weak component $W^{(2)}_0$ gives its contribution to this combination, where the mixing angles depend now on the W-condensate amplitude (Subsection 3.3). The behaviour of the applied magnetic field when it penetrates inside the W-condensate phase is investigated in Section 4. We obtain the linearised field equations and solve them with the boundary conditions provided by a small magnetic field applied from outside of the W-condensate medium. Finally, in Section 5 we discuss a possible cosmological implication of the nonvanishing photon magnetic mass and summarize the main results of the paper.

2. *W*-CONDENSATE PHASE

2.1. *The Many-Particle Weinberg–Salam Effective Action*

Introducing the chemical potentials relative to each of the conserved and mutually commuting charges into the Hamiltonian of the *WS* system [4, 6] the following many-particle *WS* Lagrangian is found after the continual integration over canonical momenta

$$\mathcal{L} = \mathcal{L}^B + \mathcal{L}^F. \tag{2.1.1}$$

Here the effective Lagrangian of the boson sector $\mathcal{L}^B$ is

$$\mathcal{L}^B(W^a_\mu, B_\mu, \phi) = -\tfrac{1}{4}\tilde{G}^a_{\mu\nu}\tilde{G}^{\mu\nu}_a - \tfrac{1}{4}B_{\mu\nu}B^{\mu\nu} + |\tilde{D}_\mu\phi|^2 - \lambda\phi^4 + m^2\phi^2, \tag{2.1.2}$$

where

$$\tilde{G}^a_{\mu\nu} = \partial_\mu \tilde{W}^a_\nu - \partial_\nu \tilde{W}^a_\mu + g\varepsilon^{abc}\tilde{W}^b_\mu \tilde{W}^c_\nu \tag{2.1.3}$$

$$B_{\mu\nu} = \partial_\mu B_\nu - \partial_\nu B_\mu \tag{2.1.4}$$

$$\tilde{D}_\nu = \partial_\nu - \frac{ig}{2}\tilde{W}^a_\nu \tau^a - \frac{ig'}{2}\tilde{B}_\nu \tag{2.1.5}$$

$$\widetilde{W}^a_\nu = W^a_\nu + \frac{1}{g}(\mu_e - \mu_w \cos^2\theta_w)\,\delta_{\nu 0}\delta^{a3} \tag{2.1.6}$$

$$\widetilde{B}_\nu = B_\nu + \frac{1}{g'}(\mu_e + \mu_w \sin^2\theta_w)\,\delta_{\nu 0}; \tag{2.1.7}$$

μ_e and μ_w are chemical potentials associated to the electric and weak-neutral charges which enter effectively in the theory as the shifts to the $W^{(3)}_0$ and B_0 components of the fields in (2.1.6), (2.1.7) through the combinations

$$\mu_3 = \mu_e - \mu_w \cos^2\theta_w \tag{2.1.8}$$

$$\mu = \mu_e + \mu_w \sin^2\theta_w, \tag{2.1.9}$$

respectively. θ_w is the known Weinberg angle.

The effective Lagrangian of the fermion sector is given as

$$\mathscr{L}^F(W^a_\mu, B_\mu, \phi, \Psi) = \bar{\Psi}_L \gamma^\mu \widetilde{\mathscr{D}}_\mu \Psi_L + \bar{e}_R \gamma^\mu (i\partial_\mu - g'\widetilde{B}_\mu + \mu_L \delta_{\mu 0})\, e_R$$
$$- \lambda_1(\bar{\Psi}_L \phi e_R + \bar{e}_R \phi^+ \Psi_L) \tag{2.1.10}$$

with

$$\Psi_L = \begin{pmatrix} \nu_L \\ e_L \end{pmatrix} \tag{2.1.11}$$

$$\widetilde{\mathscr{D}}_\nu = i\partial_\nu + \frac{g}{2}\widetilde{W}^a_\nu \tau^a - \frac{g'}{2}\widetilde{B}_\nu + \mu_L \delta_{\nu 0}, \tag{2.1.12}$$

where μ_L is the leptonic chemical potential which has entered in the many-particle *WS* Hamiltonian as the Lagrange multiplier to the conserved leptonic charge density

$$J_L = \bar{e}\gamma_0 e + \tfrac{1}{2}\bar{\nu}_e \gamma_0 (1 + \gamma_5)\, \nu_e. \tag{2.1.13}$$

2.2. *W-meson Bose–Einstein Condensation*

The *W*-meson BE condensation phenomenon found by Linde in [1] when an increase of the lepton number is considered can be obtained in our description as the solution of the extremum equation for the zero-temperature effective action Γ of the many-particle *WS* model with only one generation of massless leptons[1]

$$\frac{\delta\Gamma}{\delta\varphi_a} = 0, \tag{2.2.1}$$

---

[1] It is considered that λ_1 is small with respect to the rest of the parameters of the theory. We do not include hadrons as they will not change the qualitative properties of the *W*-condensation with leptonic density alone, as has been shown in [2].

where φ_a represents all the boson fields of the theory. With the disregard of virtual bosons, which makes a valid approximation in weakly coupled theories ($\lambda \gg e^4$) the zero-temperature effective action Γ is given by

$$\Gamma = \Gamma_B^{(0)} + \lim_{\beta \to \infty} \Gamma_F^{(1)}; \tag{2.2.2}$$

$\Gamma_B^{(0)}$ denotes the bosonic part of the effective action taken in the tree approximation, i.e., $\Gamma_B^{(0)} = \mathscr{L}^B$ (2.1.2), and $\lim_{\beta \to \infty} \Gamma_F^{(1)}$ is the one-loop fermionic contribution in the effective action taken at zero-temperature (β is the inverse of the absolute temperature). The leptonic density enters into $\Gamma_F^{(1)}$ through the chemical potential μ_L via (2.1.10)–(2.1.12). Further, in $\Gamma_F^{(1)}$ we neglect the contribution of the W-condensate amplitude C considering that we work close to the W-condensate phase-transition point where $C \ll \mu_L$ [1]. This is what we referred to above as the simplest approximation capable to produce the BE condensation of the W-mesons [1]. (The inclusion of the W-condensate amplitude into the fermion loops is important as long as the contribution of the restructured fermion spectrum, producing the supercurrent [9, 10], is concerned, but they give small corrections, as long as we work close enough to the W-condensation phase transition point as not to be taken into account in the present paper.)

It was shown in [1] that if the leptonic charge density is larger than the critical value $J_L \geqslant J_L^c = M_W^3/6\pi^2$ the solution of (2.2.1) with Γ given by (2.2.2) is found in the class of constant fields and chemical potentials to be the set of nonzero values

$$S = \{\bar{\varphi}_a\} = \left\{\bar{\phi} = \begin{pmatrix} 0 \\ \xi \end{pmatrix},\ \bar{W}_3^{(2)} = C,\ \mu_e,\ \mu_w,\ \mu_L \right\}, \tag{2.2.3}$$

where ϕ is the Higgs field, while $W_3^{(2)}$ is one of the electrically charged $SU(2)$-field components; the bar over the field means that the latter belongs to the equilibrium solution (the ground state average of the field). The zero components of the gauge fields which in [1] have average values different from zero, are represented in (2.2.3) by the nonzero chemical potentials μ_e (2.1.8) and μ_w (2.1.9). The point is that Eq. (2.2.1) also contain among them the equations for the electric and weak-neutral charge equilibrium, with the averages of these charges being equal to zero.

The solutions (2.2.3) can be expressed in general as functions of the leptonic chemical potential μ_L, the Higgs mass, and coupling constants. Their explicit dependences can be found for the limiting situation of superdense matter $\mu_L \gg m$ in Ref. [7]. The chemical potential μ_L can be equivalently reexpressed as a function of the leptonic charge density J_L, taking into account the additional equation

$$\lim_{\beta \to \infty} \frac{\partial \Gamma_F^{(1)}}{\partial \mu_L} = J_L. \tag{2.2.4}$$

Now we can introduce the following definitions: the W-condensate phase is the one characterized by the nonzero values of the average fields and chemical potentials (2.2.3), while the phase with $C=0$, which occurs for $J_L < L_L^c$, we name the finite-density Higgs phase, to be distinguished from the Higgs vacuum characterized by $\xi \neq 0$, $C=\mu_e=\mu_w=\mu_L=0$.

It is interesting to note that the solution (2.2.3) of the extremum equations (2.2.1)–(2.2.2) is a pure many-particle effect, i.e., the fermion one-loop correction to the effective action leads to the nonzero average solution of the fields (2.2.3) because precisely the fermion one-loop level possesses an additional parameter, the leptonic chemical potential μ_L, which may be large enough to equalize the one-loop and the tree contributions of the effective action, although the one-loop contribution is smaller by a coupling constant factor. This compensation is a common event in the situation with phase transitions, the role of the large parameter being sometimes also played by the temperature (we refer to the symmetry restoration in the *WS* theory [18, 19]).

Let us now discuss the symmetry of the *W*-condensate phase and the choice of the components in (2.2.3). Whereas the vacuum Higgs-solution implies the spontaneous breaking of the global $SU(2)$ symmetry, the solution (2.2.3) is characterized by further breakdowns. The introduction of the (external) leptonic current J_L has caused the violation of the Lorentz invariance that is not spontaneous. Even before J_L reaches the *W*-condensation critical value the vector components $\bar{W}_0^{(3)}$, $\bar{B}_0$ appear. They characterize the finite-density Higgs phase, together with the Higgs field $\bar{\phi}$. The component $\bar{W}_0^{(3)}$ specializes, apart from the special Lorentz frame, also the isotopic direction 3. This fact however, does not mean any further violation of the isotopic invariance as compared to that already inherent in the Higgs vacuum, since the Higgs average $\bar{\phi}=\binom{0}{\xi}$ is an eigenstate of the matrix τ^3. After J_L exceeds the critical value J_L^c the appearance of the isotopic vector component $\bar{W}_3^{(2)}$ specialized in an occassional way an extra isotopic direction 2 in the (1, 2) plane (as well as the spatial direction 3). This means that at this step we face the further spontaneous breakdown of the isotopic (and rotational) symmetries. Namely, what is broken now is the $U_{\mathrm{EM}}(1)$ symmetry, left after the Higgs breakdown, as the one under global rotations in the (1, 2) isotopic space. To see more directly the $U_{\mathrm{EM}}(1)$ noninvariance of the *W*-condensate phase note the transformation law of the *W*-field

$$\delta W_\mu^a = [Q_e, W_\mu^a] = \varepsilon^{3ba} W_i^b \delta_{i\mu} \tag{2.2.5}$$

induced by the electric charge operator Q_e

$$Q_e = \int d^3x \left[\varepsilon^{3bc} W_i^b \pi^{ic} + i\left(\phi^+ \frac{\tau^3+I}{2} p - p^+ \frac{\tau^3+I}{2} \phi\right) - \bar{e}\gamma^0 e \right] \tag{2.2.6}$$

via the canonical commutation relations. Here π_i^b and p, p^+ are the canonical momenta conjugated to the fields W_i^b, ϕ^+, and ϕ, respectively:

$$\pi^{ie} = -G^{oic} = \frac{\delta \mathscr{L}}{\delta \partial_0 W_\nu^c} \tag{2.2.7a}$$

$$p = D^0\phi = \frac{\delta\mathscr{L}}{\delta\partial_0\phi^+} \tag{2.2.7b}$$

$$p^+ = (D^0\phi)^+ = \frac{\delta\mathscr{L}}{\delta\partial_0\phi}. \tag{2.2.7c}$$

Equation (2.2.5), in particular, reads

$$\delta W_3^{(1)} = [Q_e, W_3^{(1)}] = -W_3^{(2)}. \tag{2.2.8}$$

By taking the ground state average of Eq. (2.2.8) we conclude that according to the Fabri–Picasso theorem (see Appendix A for an explanation how this theorem works in the case of quantum statistical theory) it implies that the ground state is taken out of the space of physical states by the action of the charge operator Q_e (which is just the $U_{\mathrm{EM}}(1)$-symmetry generator), once $\bar{W}_3^{(2)} \neq 0$ is solution (2.2.3).

Therefore the initial $SU(2)\times U(1)$ global symmetry inherent in the WS model, after being broken at the first (Higgs-condensation) step, down to $U_{\mathrm{EM}}^{(1)}$, breaks down completely at the second (W-condensation) step. It is, therefore, naturally expected that the $U_{\mathrm{EM}}^{(1)}$ (electromagnetic) field should become massive under the W-condensation through the same mechanism as the one that served the non-Abelian vector fields to acquire their masses under the Higgs-condensation. We shall trace this mechanism explicitly in the next section.

3. Massive Photon in the Dense Weinberg–Salam Model

Our goal now is to find the infrared mass matrix of the boson fields against the background of the W-condensate solution (2.2.3) and specifically to study its sector which contains the spatial photon field components A_i, $i = 1, 2, 3$, responsible for the magnetic mass. Once this matrix is known, then the corresponding mass eigenvalues and eigenvectors can be obtained.

Taking in mind that the W-condensate solution (2.2.3) is obtained from the effective action Γ (2.2.2), that contains the contribution from the fermionic loop, the mass matrix of the fields in the condensed phase must be defined as

$$\begin{aligned}\Pi_{ab} &= \lim_{\substack{|K|\to 0\\ K_4=0}} \left.\frac{\delta^2\Gamma}{\delta\varphi_a\delta\varphi_b}\right|_S \\ &= \Pi^B_{\varphi_a\varphi_b}(K_4=0, |\mathbf{K}|\to 0) + \Pi^F_{\varphi_a\varphi_b}(K_4=0, |\mathbf{K}|\to 0),\end{aligned} \tag{3.1}$$

where φ_a again runs the set of all the boson fields, the subscript S designates that the corresponding quantities are taken on the solution (2.2.3), $\Pi^B_{\varphi_a\varphi_b}$ is the boson part of the polarization operator (3.1) at the tree level,

$$\Pi^B_{\varphi_a\varphi_b}(K_4=0, |\mathbf{K}|\to 0) = \left.\frac{\delta^2\Gamma_B^{(0)}}{\delta\varphi_a\delta\varphi_b}\right|_S, \tag{3.2}$$

where $\Gamma_B^{(0)}$ is the tree *WS* action on the general class of constant fields, and

$$\Pi^F_{\varphi_a\varphi_b}(K_4=0, |\mathbf{K}|\to 0) = \lim_{\beta\to\infty} \left.\frac{\delta^2\Gamma_F^{(1)}}{\delta\varphi_a\delta\varphi_b}\right|_S \tag{3.3}$$

is the zero temperature, zero-momentum one-loop polarization operator with boson fields for external legs and fermions for internal ones.

The fermion propagators, taken for the internal lines, in the adopted approximation are calculated against the background fields (2.2.3) neglecting the W-condensate amplitude ($C\simeq 0$).

The infrared limit $K_4=0$, $|\mathbf{K}|\to 0$ taken in (3.1) is the one required to establish the screening of static configurations of electric and magnetic charge and the presence of infrared divergencies. This limit is provided within the temperature Green functions method once the functional Γ in (3.1) is calculated on the class of constant homogeneous fields φ_a, to which class the solution (2.2.3) also belongs. The point is that when working in the temperature Green function formalism we deal only with discrete values of K_4. Therefore, K_4 may either be or not be strictly equal to zero, the limiting transition $K_4\to 0$ not being possible. The other limit $|\mathbf{K}|=0$, $K_0\to 0$ in the analytically continued polarization operator serves the elementary excitation or plasmon masses of various transverse and longitudinal modes. This is not our concern in the present paper. The absence of zero eigenvalues of the mass matrix (3.1), that we are going to prove in Subsection 3.3, implies the short range of all fields, electric and magnetic screening, as well as the infrared convergence of the theory.

3.1. *Mass Matrix; Boson Contribution*

In order to obtain the tree contribution to the mass-matrix (3.1), we must perform the shift of $\mathscr{L}_B$ (2.1.2), omitting the terms that contain derivatives, in the average fields (2.2.3),

$$W^a_\mu = C\delta_{\mu 3}\delta^{a2} + \hat{W}^a_\mu \tag{3.1.1a}$$

$$\phi = \begin{pmatrix} 0 \\ \xi \end{pmatrix} + \sigma \tag{3.1.1b}$$

The quadratic part $\mathscr{L}^B_q$ of the shifted Lagrangian thus obtained contains the first matrix of the l.h.s. of (3.1) as

$$\mathscr{L}^B_q = \varphi_a \left.\frac{\delta^2\Gamma_B^{(0)}}{\delta\varphi_a\delta\varphi_b}\right|_S \varphi_b.$$

$$\begin{aligned}\mathscr{L}^B_q = {} & \tfrac{1}{2}\hat{W}^{(1)}_\mu[g^2C^2(g_{\mu\nu}+\delta_{\mu 3}\delta_{\nu 3}) + \mu_3^2(\delta_{\mu 0}\delta_{\nu 0} - g_{\mu\nu}) + 2M_W^2 g_{\mu\nu}]\,\hat{W}^{\nu(1)} \\ & + \tfrac{1}{2}\hat{W}^{(2)}_\mu[\mu_3^{(2)}(\delta_{\mu 0}\delta_{\nu 0} - g_{\mu\nu}) + 2M_W^2 g_{\mu\nu}]\,\hat{W}^{\nu(2)} \\ & + \tfrac{1}{2}A_\mu[g^2C^2\sin^2\theta_w(g_{\mu\nu}+\delta_{\mu 3}\delta_{\nu 3})]\,A^\nu\end{aligned}$$

$$
\begin{aligned}
&+\tfrac{1}{2}Z_\mu[g^2C^2\cos^2\theta_w(g_{\mu\nu}+\delta_{\mu3}\delta_{\nu3})+2M_Z^2 g_{\mu\nu}]\,Z^\nu\\
&-\tfrac{1}{2}A_\mu[g^2C^2\sin 2\theta_w(g_{\mu\nu}+\delta_{\mu3}\delta_{\nu3})]\,Z^\nu\\
&+A_\mu[2gC\mu_3\sin\theta_w\delta_{\mu0}\delta_{\nu3}]\,\hat{W}^{\nu(2)}\\
&-\hat{W}^{(2)}_\mu[gC\mu_3\cos\theta_w\delta_{\mu0}\delta_{\nu3}]\,A^\nu\\
&-Z_\mu[2gC\mu_3\cos\theta_w\delta_{\mu0}\delta_{\nu3}]\,\hat{W}^{\nu(2)}\\
&+\hat{W}^{(2)}_\mu[g^2C\xi\delta_{\mu3}]\,\sigma-M_\sigma^2\sigma^2\\
&+Z_\mu[\xi\sqrt{g^2+g'^2}\,(\mu-\mu_3)\,\delta_{\mu0}]\,\sigma.
\end{aligned}
\tag{3.1.2}
$$

In (3.1.2) the $SU(2)$ unitary gauge [20] and the Feynman gauge $\partial_\mu B^\mu=0$ for the $U(1)$ gauge symmetry have been taken; the metric $g_{\mu\nu}=(1,-\vec{1})$ is used. In the unitary gauge, the field σ has only the bottom component. The fluctuating A_μ and Z_μ fields in (3.1.2) are the known combinations

$$A_\mu=\cos\theta_w B_\mu+\sin\theta_w \hat{W}^{(3)}_\mu \tag{3.1.3a}$$

$$Z_\mu=\sin\theta_w B_\mu+\cos\theta_w \hat{W}^{(3)}_\mu. \tag{3.1.3b}$$

In (3.1.3), $W^{(3)}_\mu=\hat{W}^{(3)}_\mu$, since $\bar{W}^{(3)}_\mu$ does not exist. The combinations (3.1.3a), (3.1.3b) coincide in form with the fields that diagonalize the quadratic Lagrangian of the Higgs vacuum $\tilde{B}_\mu=B_\mu$, $\tilde{W}^{(a)}_\mu=W^{(a)}_\mu=\hat{W}^{(a)}_\mu$. The same combinations (3.1.3) for A_μ and Z_i ($i=1,2,3$) continue to diagonalize the quadratic Lagrangian of the finite-density Higgs phase, i.e., $\mathscr{L}^B_q$ (3.1.2) with $C=0$, $W^{(a)}_\mu=\hat{W}^{(a)}_\mu$ in it, but Z_0 (3.1.3) does not. It is seen from (3.1.2) with $C=0$, that Z_0 mixes with σ. Further, M_W and M_z in (3.1.2) are the W- and Z-meson masses, respectively, ($M_W^2=\frac{1}{2}g^2\xi^2$, $M_Z^2=\frac{1}{2}(g^2+g'^2)\,\xi^2$), and M_σ^2 is given by

$$M_\sigma^2=6\lambda\xi^2-m^2+\tfrac{1}{4}g^2C^2-\tfrac{1}{4}(\mu-\mu_3)^2. \tag{3.1.4}$$

The other notations in (3.1.2) are standard.

In (3.1.2) the breakdown of all the symmetries that we had pointed out above can be explicitly observed. This is, the appearance of the W-condensate, given by C in (3.1.2), produces the symmetry breaking in the isotopic (1, 2) plane, as well as the rotational noninvariance among different components of the vector fields. Only the invariance under the rotation in the spatial (1, 2)-plane is retained.

The matrix elements $\delta^2\Gamma^{(0)}_B/\delta\varphi_a\,\delta\varphi_b$ in (3.1.2) will be used in calculating the complete mass matrix (3.1) in what follows.

3.2. *Mass Matrix; Fermion Contribution*

The only diagrams that can contribute to the one-loop fermion polarization operators (3.3) are drawn in Fig. 1. In accord with what was mentioned above, the condensate field C is put equal to zero in the fermion propagators.

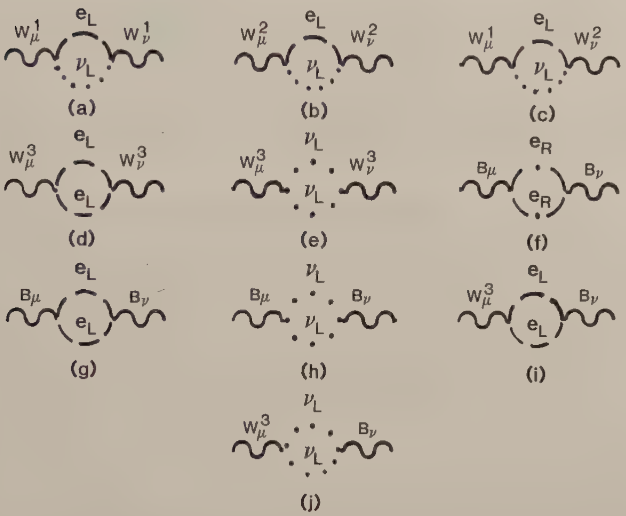
W_μ^1 e_L W_ν^1 ν_L
(a)
W_μ^2 e_L W_ν^2 ν_L
(b)
W_μ^1 e_L W_ν^2 ν_L
(c)
W_μ^3 e_L W_ν^3 e_L
(d)
W_μ^3 ν_L W_ν^3 ν_L
(e)
B_μ e_R B_ν e_R
(f)
B_μ e_L B_ν e_L
(g)
B_μ ν_L B_ν ν_L
(h)
W_μ^3 e_L B_ν e_L
(i)
W_μ^3 ν_L B_ν ν_L
(j)

FIG. 1. One-loop fermion diagrams for the polarization operator components: (a) $\Pi^F_{W_\mu^{(1)}W_\nu^{(1)}}$; (b) $\Pi^F_{W_\mu^{(2)}W_\nu^{(2)}}$, (c) $\Pi^F_{W_\mu^{(1)}W_\nu^{(2)}}$, $\Pi^F_{W_\mu^{(2)}W_\nu^{(1)}}$; (d), (e) $\Pi^F_{W_\mu^{(3)}W_\nu^{(3)}}$; (f), (g), (h) $\Pi^F_{B_\mu B_\nu}$; (i), (j) $\Pi^F_{B_\mu W_\nu^{(3)}}$. The meanings of the lines are indicated in the drawing.

The Green functions of each internal line are given by the expressions

– – – – – – – – – – – – – – – $$\frac{i}{(p_\nu - i\mu_{e_L}\delta_{\nu 4})\gamma_\nu},$$ left electron (3.2.1a)

———•———•——— $$\frac{i}{(p_\nu - i\mu_{e_R}\delta_{\nu 4})\gamma_\nu},$$ right electron (3.2.1b)

• • • • • • • • • • • • • • • • $$\frac{i}{(p_\nu - i\mu_{\nu_L}\delta_{\nu 4})\gamma_\nu},$$ left neutrino, (3.2.1c)

where the chemical potentials of the left electron, μ_{e_L}, right electron, μ_{e_R}, and left neutrino, μ_{ν_L}, are given by

$$\mu_{e_L} = \mu_e - \tfrac{1}{2}\mu_w \cos 2\theta_w + \mu_L \tag{3.2.2a}$$

$$\mu_{e_R} = \mu_e + \mu_w \sin^2\theta_w + \mu_L \tag{3.2.2b}$$

$$\mu_{\nu_L} = \tfrac{1}{2}(\mu_w + 2\mu_L). \tag{3.2.2c}$$

All the polarization operator components of the type of $\Pi^F_{W_\mu^{(a)}W_\nu^{(b)}}$ contain only left massless leptons in the loop and are gathered in the following expression, corresponding to the diagrams (a) to (e) in Fig. 1. (This expression is obtained using a common propagator G for the left fermion coloumn Ψ_L,

$$G(p^*)=\left[i\not{p}^*+\frac{\mu_3}{2}\tau^3\gamma_4\right]^{-1}, \qquad p^*_\mu=p_\mu-\left(\frac{\mu}{2}-\mu_L\right)\delta_{\mu 4}.$$

$$\begin{aligned}\Pi^F_{W^{(a)}_\mu W^{(b)}_\nu}(\Psi_L,\bar{\Psi}_L)={}&-\frac{g^2}{(2\pi)^4}\left[\delta_{\mu\rho}\delta_{\lambda\nu}+\delta_{\mu\lambda}\delta_{\nu\rho}-\delta_{\mu\nu}\delta_{\rho\lambda}+\varepsilon_{\mu\nu\rho\lambda}\right]\\&\times\left\{\left[\delta^{ab}-\delta^{a3}\delta^{b3}\right]\left[\sum\!\!\!\!\!\!\int\frac{A_\rho A'_\lambda}{D}\,d^4p-\sum\!\!\!\!\!\!\int\frac{B_\rho B'_\lambda}{D}\,d^4p\right]\right.\\&+\delta^{a3}\delta^{b3}\left[\sum\!\!\!\!\!\!\int\frac{A_\rho A'_\lambda}{D}\,d^4p+\sum\!\!\!\!\!\!\int\frac{B_\rho B'_\lambda}{D}\,d^4p\right]\\&\left.+i\varepsilon^{ab3}\left[\sum\!\!\!\!\!\!\int\frac{A_\rho B'_\lambda}{D}\,d^4p-\sum\!\!\!\!\!\!\int\frac{B_\rho A'_\lambda}{D}\,d^4p\right]\right\},\end{aligned} \tag{3.2.3a}$$

where

$$A_\rho=-i\left[\left(p^{*2}-\frac{1}{4}\mu_3^2\right)p^*_\rho+\frac{\mu_3^2}{2}p^*_4\delta_{\rho 4}\right]; \qquad A'_\rho=A_\rho(p^*\to p^*+K) \tag{3.2.3b}$$

$$B_\rho=\left[\mu_3 p^*_4 p^*_\rho-\frac{\mu_3}{2}\left(p^{*2}-\frac{1}{4}\mu_3^2\right)\delta_{\rho 4}\right]; \qquad B'_\rho=B_\rho(p^*\to p^*+K) \tag{3.2.3c}$$

and

$$\sum\!\!\!\!\!\!\int\frac{d^4p}{(2\pi)^4}=\frac{i}{\beta}\sum_{p_4}\int\frac{d^3p}{(2\pi)^3}$$

as it is usual for the Feynman rules in statistics (taking the limit $\beta\to\infty$ in (3.2.3) we obtain the $T=0$ many-particle contribution).

Now, the polarization operators represented in Fig. 1, (d) to (j) are of the type of the many-particle QED polarization operator; it is a known fact that the static $K_4=0$, and homogeneous $|\mathbf{K}|\to 0$ limit of their space–space components both at high [21] and at zero temperature [10], is zero. This conclusion cannot be directly extended to the space–space components $\Pi^F_{W^{(1,2)}_i W^{(1,2)}_j}$ presented in Fig. 1a–c, since the latter differ both from the polarization operator components of the many-particle QED [21] and also from the many-particle $SU(3)$ QCD with only one chemical potential included for which case the calculations are available [22]. We shall not, however, need to know the components $\Pi^F_{W^{(1,2)}_i W^{(1,2)}_j}$ for our present purposes for the reasons to become clear later.

Next, using the covariant decomposition [21, 23] of the polarization operator $\Pi^F_{B_\mu B_\nu}$ valid also for $\Pi^F_{B_\mu W^{(3)}_\nu}$ and $\Pi^F_{W^{(3)}_\mu W^{(3)}_\nu}$ that are at least within the one-loop approximation [22] similar to the polarization operator of finite-density QED and hence transversal, one can prove that once there is not spatial vector at one's disposal, the space-time components $\Pi^F_{B_0 B_i}$, $\Pi^F_{W^{(3)}_0 W^{(3)}_i}$, $\pi^F_{B_i W^{(3)}_i}$ obey the relation $\Pi_{i0}=(K_i K_0/\mathbf{K}^2)\,\Pi_{00}$ and hence disappear in the point $K_0=0$.

For the static and homogeneous limit of the polarization operator components $\Pi^F_{W_0^{(1,2)}W_i^{(1,2)}}$, the same manipulations cannot be done, because, as we have underlined above (see Fig. 1a–c), this case is not equivalent to the many-particle QED [21]. Out of these components only $\Pi^F_{W_0^{(2)}W_i^{(2)}}$ might be important for our purposes. It is demonstrated in Appendix B that this component disappears in the static and homogeneous limit.

We are to calculate now the time–time components of (3.3). To this end we will start with the effective action $\Gamma^{(1)}_F$ which includes only the fourth components of the gauge fields as the arguments for the differentiations. Thus, to serve the derivatives with respect to B_0, $W_0^{(3)}$, one can use μ, μ_3 (2.1.8)–(2.1.9), respectively. After introducing, moreover, $\mu_{1,2} = gW_0^{(1,2)} = \text{const}$, we have the complete set of auxiliary parameters needed to make the required derivatives in (3.3).

The corresponding one-loop fermion contribution in the effective action with all the mentioned parameters included is

$$\Gamma^{(1)}_F = \beta^{-1} \int \frac{d^3p}{(2\pi)^3} \{2\beta E + \ln(1 + e^{\beta(E+\mu^+)}) + \ln(1 + e^{-\beta(E-\mu^+)})$$

$$+ \ln(1 + e^{-\beta(E+\mu^-)}) + \ln(1 + e^{-\beta(E-\mu\ )})$$

$$+ \ln(1 + e^{-\beta[E+(\mu-\mu_L)]}) + \ln(1 + e^{-\beta[E-(\mu-\mu_L)]})\}, \tag{3.2.4}$$

where

$$E = |\mathbf{p}| \tag{3.2.5a}$$

$$\mu^{\pm} = \frac{\mu}{2} - \mu_L \pm \frac{|\vec{\mu}|}{2} \tag{3.2.5b}$$

and $\vec{\mu}$ is the vector with the components (μ_1, μ_2, μ_3).

The nonzero time–time components of the static homogeneous polarization operators in the zero-temperature limit obtained from (3.2.4) via (3.3) are summarized in the following expressions:

$$\Pi^F_{W_0^{(1)}W_0^{(1)}} = \Pi^F_{W_0^{(2)}W_0^{(2)}} = \frac{g^2}{6\pi^2} \frac{\mu^3_{e_L} - \mu^3_{\nu_L}}{\mu_3} \tag{3.2.6a}$$

$$\Pi^F_{A_0A_0} = (g^2 \sin\theta_w + g'^2 \cos\theta_w) \frac{\mu^2_{e_L} + \mu^2_{\nu_L}}{4\pi^2}$$

$$+ 2g'^2 \cos^2\theta_w \frac{\mu^2_{e_R}}{\pi^2} - \frac{1}{2} gg' \sin 2\theta_w \frac{\mu^2_{e_L} - \mu^2_{e_R}}{4\pi^2} \tag{3.2.6b}$$

$$\Pi^F_{Z_0Z_0} = (g^2 \cos^2\theta_w + g'^2 \sin^2\theta_w) \frac{\mu^2_{e_L} + \mu^2_{\nu_L}}{4\pi^2}$$

$$+ 2g'^2 \sin^2\theta_w \frac{\mu^2_{e_R}}{\pi^2} - \frac{1}{2} gg' \sin 2\theta_w \frac{\mu^2_{e_L} + \mu^2_{\nu_L}}{4\pi^2} \tag{3.2.6c}$$

$$\Pi^F_{A_0 Z_0} = (g^2 - g'^2) \sin 2\theta_w \frac{\mu^2_{e_L} + \mu^2_{\nu_L}}{4\pi^2} - 2g' \sin 2\theta_w \frac{\mu^2_{e_R}}{\pi^2}$$
$$+ gg' \cos 2\theta_w \frac{\mu^2_{e_L} - \mu^2_{\nu_L}}{4\pi^2}. \tag{3.2.6d}$$

3.3. *Magnetic and Debye Masses of the Photon*

The infrared masses of the fields of the many-particle *WS* theory in the approximation considered are to be found by diagonalizing the quadratic matrix obtained as (3.1) from the effective action Γ (2.2.2) in the static and homogeneous limit. The static, or infra-red, electric, and magnetic masses, which are our only concern here should be distinguished, in the case of finite temperature and/or density, when we go beyond the tree approximation, from the plasmon masses, i.e., the masses of longitudinal and transversal elementary electromagnetic excitations obtained as the poles of the Green function $G^{(K)}_{\mu\nu}$ at $T \neq 0$ in the limit $K_0 \neq 0$, $|\mathbf{K}| = 0$ [24]. The latter are normally (already in QED [21]) both nonzero, but it is irrelevant to the problem of the screening of the corresponding fields or to the infrared divergency [19].

Let us represent the quadratic part of the effective action (2.2.2) in the $K_4 = 0$, $|\mathbf{K}| \to 0$ limit as

$$\Gamma_q = \Phi_i \Pi_{ij} \Phi_j, \qquad i, j = 1, 2. \tag{3.3.1}$$

Since our main purpose is to investigate the mass of the photon field components the following arrangement for the generalized fields Φ_i is taken

$$\Phi = \begin{pmatrix} \Phi_1 \\ \Phi_2 \end{pmatrix} \tag{3.3.2}$$

in such a way that Φ_1 includes all the fields that are mixed with the magnetic (spatial) components of the photon potential (3.1.3a), $\Phi_1^+ = (A_3, Z_3, \hat{W}^{(2)}_0, A_1, Z_1, A_2, Z_2)$, while Φ_2 includes the rest of the boson field components $\Phi_2^+ = (A_0, Z_0, \hat{W}^{(2)}_3, \sigma, \hat{W}^{(1)}_\mu, \hat{W}^{(2)}_2, \hat{W}^{(2)}_1)$. It follows from (3.1.2) and (3.2.6) that in this representation the mass matrix Π has the following box form

$$\Pi = \begin{pmatrix} \mathbf{\Pi}_{11} & 0 \\ 0 & \mathbf{\Pi}_{22} \end{pmatrix} \tag{3.3.3}$$

Following the order of the field components given in Φ_1 the matrix $\mathbf{\Pi}_{11}$ is expressed as

$$\mathbf{\Pi}_{11} = \begin{pmatrix} \mathcal{M}_1 & & \\ & \mathcal{M}_2 & \\ & & \mathcal{M}_3 \end{pmatrix} \tag{3.3.4}$$

with the matrix $\mathscr{M}_1$, which is related to the field components A_3, Z_3, $W_0^{(2)}$, given by

$$\mathscr{M}_1=\begin{pmatrix} 0 & 0 & \frac{1}{4}\Pi^{B}_{A_3 W_0^{(2)}} \\ 0 & -\frac{1}{2}M_Z^2 & \frac{1}{4}\Pi^{B}_{Z_3 W_0^{(2)}} \\ \frac{1}{4}\Pi^{B}_{W_0^{(2)} A_3} & \frac{1}{4}\Pi^{B}_{W_6^{(2)} Z_3} & \frac{1}{2}[M_W^2+\Pi^{F}_{W_0^{(2)} W_0^{(2)}}] \end{pmatrix} \tag{3.3.5}$$

$$\Pi^{B}_{A_3 W_0^{(2)}}=\Pi^{B}_{W_0^{(2)} A_3}=-2gC\mu_3 \sin\theta_w, \qquad \Pi^{B}_{Z_3 W_0^{(2)}}=\Pi^{B}_{W_0^{(2)} Z_3}=2gC\mu_3 \cos\theta_w$$

and the matrices $\mathscr{M}_2$ and $\mathscr{M}_3$, related respectively to the two pairs of components A_1, Z_1 and A_2, Z_2, given by the coinciding expressions

$$\mathscr{M}_2=\mathscr{M}_3=\begin{pmatrix} -\frac{1}{2}g^2C^2\sin^2\theta_w & \frac{1}{4}g^2C^2\sin 2\theta_w \\ \frac{1}{4}g^2C^2\sin 2\theta_w & -\frac{1}{2}g^2C^2\cos^2\theta_w-\frac{1}{2}M_Z^2 \end{pmatrix}. \tag{3.3.6}$$

It follows from (3.3.4), (3.3.5), and (3.3.6) that

$$\det \mathbf{\Pi}_{11}=\frac{1}{2^7}g^6C^6\mu_3^2M_Z^6\sin^6\theta_w. \tag{3.3.7}$$

This is positively definite, which means that all fields linearly combined of the fields from the set Φ_1 are massive, including the spatial part of the photon field. Here the following important remark is in order. Formally, in obtaining the matrix $\mathbf{\Pi}$ above, the condensate field was, as a matter of fact, treated as external. The external field like (2.2.3) particularly breaks the gauge invariance of the system [25], so the appearance of extra nonzero masses in the spectrum of gauge particles is not unexpected and sounds trivial. Moreover, the use of gauge conditions is not justified, since there are fewer degrees of freedom [25]. Only when taken on the extremum, i.e., on solutions of Eq. (2.2.1), the effective action restores its gauge-invariance properties (in the present context this general theorem [26] is directly checked in Appendix C). That was the reason why we kept the one-loop fermion contribution to $\mathbf{\Pi}$; only this contribution makes the field (2.2.3) spontaneous and not external. Now, to get a final conclusion about the masses we must use the extremum solution in (3.3.7). It is technically difficult to perform this substitution explicitly. Nevertheless, the evident positive definiteness of (3.3.7) guarantees the fact that (3.3.7) remains nonzero after the parameters C, μ_3, and ξ (hidden inside M_z) are all expressed in terms of μ_L according to the extremum solution.

The photon temporal component mass squared $m^2(A_0)$ is one of the eigenvalues of the matrix $\mathbf{\Pi}_{22}$. This eigenvalue is already nonzero in the finite-density Higgs phase and is responsible for the Debye screening. The appearance of such an infrared-massive component of the A_μ field in this phase is a finite-density effect for which the nonvanishing of the four–four components of the zero-temperature polarization operators (3.2.6) is responsible (also finite temperature alone would give the same). We neglect the small correction introduced by C in the W-condensate phase to write

$$m^2(A_0)=[\Pi^F_{A_0A_0}+\Pi^F_{Z_0Z_0}+M_Z^2]-\{[\Pi^F_{A_0A_0}-\Pi^F_{Z_0Z_0}-M_Z^2]^2+4[\Pi^F_{A_0Z_0}]^2\}^{1/2}. \tag{3.3.8}$$

In obtaining this result we have also neglected the quantity $\tilde{Z}_0=\mu-\mu_3$ because it is of the higher order in e^2 compared with the other average values of the fields, as it can be corroborated from the extremum equations equivalent to (2.2.1) given in Ref. [1].

It is worth stressing that in the W-condensate phase a redefinition of the mixing angles is needed as it is evident from the non-diagonal character of the mass matrix $\mathbf{\Pi}$. Thus, by diagonalizing the mass matrices $\mathcal{M}_{1,2,3}$ the following eigenvectors and eigenvalues in the small condensate $(J_L \sim J^c_L)$ approximation are found:

$$A'_{1,2}=A_{1,2}+\frac{g^2C^2\sin 2\theta_w}{2M_Z^2}Z_{1,2} \tag{3.3.9a}$$

$$-m^2(A'_{1,2})=-\tfrac{1}{2}g^2C^2\sin^2\theta_w \tag{3.3.9b}$$

$$A'_3=A_3+\frac{g^2C^2\mu_3^2\sin 2\theta_w}{2M_Z^2[M_W^2+\Pi^F_{W_0^{(2)}W_0^{(2)}}]}Z_3+\frac{gC\mu_3\sin\theta_w}{M_W^2+\Pi^F_{W_0^{(2)}W_0^{(2)}}}W_0^{(2)} \tag{3.3.10a}$$

$$-m^2(A'_3)=-\frac{g^2C^2\mu_3^2\sin^2\theta_w}{2[M_W^2+\Pi^F_{W_0^{(2)}W_0^{(2)}}]} \tag{3.3.10b}$$

$$Z'_{1,2}=-\frac{g^2C^2\sin 2\theta_w}{2M_Z^2}A_{1,2}+Z_{1,2} \tag{3.3.11a}$$

$$-m^2(Z'_{1,2})=-M_Z^2-\tfrac{1}{2}g^2C^2\cos^2\theta_w \tag{3.3.11b}$$

$$\begin{aligned}Z'_3=&-\frac{g^2C^2\mu_3^2\sin 2\theta_w}{2M_Z^2[M_Z^2+M_W^2+\Pi^F_{W_0^{(2)}W_0^{(2)}}]}A_3\\&+Z_3-\frac{gC\mu_3\cos\theta_w}{M_Z^2+M_W^2+\Pi^F_{W_0^{(2)}W_0^{(2)}}}W_0^{(2)}\end{aligned} \tag{3.3.12a}$$

$$-m^2(Z'_3)=-M_Z^2-\frac{g^2C^2\mu_3^2\cos^2\theta_w}{M_Z^2+M_W^2+\Pi^F_{W_0^{(2)}W_0^{(2)}}} \tag{3.3.12b}$$

$$W_0^{(2)'}=-\frac{gC\mu_3\sin\theta_w}{M_W^2+\Pi^F_{W_0^{(2)}W_0^{(2)}}}A_3-\frac{gC\mu_3\cos\theta_w}{M_Z^2+M_W^2+\Pi^F_{W_0^{(2)}W_0^{(2)}}}Z_3+W_0^{(2)} \tag{3.3.13a}$$

$$\begin{aligned}m^2(W_0^{(2)'})=&\,M_W^2+\Pi^F_{W_0^{(2)}W_0^{(2)}}\\&+\frac{g^2\mu_3^2[M_W^2+\Pi^F_{W_0^{(2)}W_0^{(2)}}+M_Z^2\sin^2\theta_w]\,C^2}{[M_Z^2+M_W^2+\Pi^F_{W_0^{(2)}W_0^{(2)}}][M_W^2+\Pi^F_{W_0^{(2)}W_0^{(2)}}]}.\end{aligned} \tag{3.3.13b}$$

For the spatial field components the eigenvalues of the mass matrix are their squared masses taken with the opposite sign, due to the Minkowskian metrics effect (cf. the standard mass term $m^2(A_0^2 - A^2)$). Here the primed fields are the eigenvectors of the $\mathbf{\Pi}_1$ matrix. In these notations A_i' denote the new photon field spatial components in the W-condensate phase, and Z_i', $W_0^{(2)\prime}$, are the weak-neutral spatial field components and the zeroth component of the weak-charged field, respectively, in the W-condensate phase. The criterion for adopting this terminology is that each new eigenfield must turn into its counterpart in the many-particle Higgs phase in the limit $C \to 0$, i.e., $A_i' \to_{C\to 0} A_i$, $Z_i' \to_{C\to 0} Z_i$, and $W_0^{(2)\prime} \to_{C\to 0} W_0^{(2)}$, as well as their mass eigenvalues should also turn into their counterparts, i.e., $m^2(A_i') \to_{C\to 0} 0$, $m^2(Z_i') \to_{C\to 0} M_Z^2$, and $m^2(W_0^{(2)\prime}) m_{C\to 0} M_W^2$.

It ought to be noted as peculiar characteristics of the system in presence of a charged background, that the new mixing angles depend on the condensate solution as it is evident from (3.3.9)–(3.3.13) and that the rotational symmetry in the 1–2 plane is the only remnant of the Lorentz invariance.

The eigenfields of the matrix $\mathbf{\Pi}_{22}$ will not be given here, since they were already all massive in the many-particle Higgs phase, as we have pointed out before, for the zeroth-component of the photon field, A_0, and then the contribution of the W-meson condensate amplitude, C, is not crucial for them.

Thus, from (3.3.8), (3.3.9b), (3.3.10b), and (3.2.6) we have that when the phase transition from the W-condensate phase to the finite-density Higgs phase occurs ($C \to 0$), the static electric mass squared (3.3.8) of the photon survives, while the magnetic masses (3.3.9b), (3.3.10b) do not.

It must be stressed that the acquirement of the magnetic mass by the photon in the course of the W-condensation does not contradict the principle of conservation of the number of degrees of freedom. The point is that the mass that matters in the degrees of freedom counting is not the infrared mass, determined by the static homogeneous limit $K_4 = 0$, $|\mathbf{K}| \to 0$ which is the main concern of our investigation, but the "plasmon" mass determined by the opposite limit in the polarization operator $|\mathbf{K}| = 0$, $K_4 \to 0$. The extra degree of freedom that appears when a vector field becomes "plasmon-massive" is that connected with the medium oscillations, e.g., there are the well-known longitudinal charge-density (Langmuir) waves in the electrodynamical plasma. The plasmon mass becomes nonzero when the density and/or temperature are introduced [27], and so it is not connected with the W-condensation phase transition, the number of degrees of freedom remaining unchanged under this transition.

4. Meissner Screening

In this section we will investigate the penetration of an applied magnetic field into the region occupied by the W-condensate phase of the dense electroweak matter. True enough, the short range of the electromagnetic field inside the W-condensate region, found in the previous section, is already sufficient for concluding that the screening of an applied magnetic field takes place. The reason is that an applied external field penetrating the *W*-condensate medium, must split into the new modes characteristic of this medium (3.3.9a)–(3.3.13a) which are all massive, once the only gauge particle, which remained massless in the common *WS* model, the photon, has turned massive in the dense medium.

In analogy with the study of the common Meissner effect in solid state physics we have to solve the field equations in the medium of interest with the boundary condition corresponding to a constant magnetic field applied at the border. The field equations in our case are nonlinear, so we shall handle only the small amplitude applied field case and employ the correspondingly linearized field equations. The other peculiarity is provided by mixing the electromagnetic field with other fields. This will give rise to the effect of induction of quasielectric and quasimagnetic fields by the applied magnetic field, whose damping in the depth of the medium is described by the same field equations. The same mixing will be shown to become responsible for appearance of a weak surface charge, which is more important in providing the Meissner screening than the superconducting current. The corresponding mechanisms are studied here in more detail as compared with our previous publication [11].

By solving the field equations we will establish the connection between the photon magnetic mass found above and the Londons' penetration depth which characterizes the screening of the applied magnetic field. We also establish the connection of the damping parameters of the induced accompanying fields with the photon, *W*- and *Z*-masses.

As pointed out above, we consider that the dense electroweak region has a border, beyond which the dense Higgs phase is spread. There are, in principle, various ways to realize this border. As an example we can suppose that the lepton density or temperature beyond the border may be lesser than their critical values needed for the *W*-condensation to appear [1, 2, 4, 6]. The density or temperature inhomogeneity does not seem unprobable in the cosmological matter distribution in the course of the Universe evolution.

4.1. *Linearized Set of Field Equations in the Dense Electroweak Matter*

Before writing the set of field equations we should take into account that, once an external magnetic field is switched on it breaks the spatial isotropy of the free system, which means that the condensate solution loses its freedom in orientation (i.e., the system in absence of external field cannot distinguish any spatial direction for the condensed solution, only the modulus of $\bar{W}_i^{(2)}$ being determined by Eqs. (2.2.1)).

Specifically, it has been demonstrated in Ref. [10] that once and external field is applied, the condensate field $\tilde{\mathbf{W}}^{(2)}$ alignes parallel or antiparallel to the vector potential $\hat{\mathbf{A}}$. So, in the equilibrium case we only need to consider the component $\hat{A}_3$, as long as the *W*-condensate field has been chosen in (2.2.3) to possess only this spatial component $\bar{W}_3^{(2)}$.

In order to obtain the needed linear field equations we must start from the quadratic many-particle effective action of the W-condensate phase.

$$\begin{aligned}\Gamma^q_{\hat{A}_3} = {} & \tfrac{1}{2}\hat{A}_3\partial^2_{x_1}\tilde{A}_3 - \tfrac{1}{2}\tilde{W}^{(2)}_0\partial^2_{x_1}\tilde{W}^{(2)}_0 + \tfrac{1}{2}\tilde{Z}_3\partial^2_{x_1}\tilde{Z}_3 \\ & + \tfrac{1}{2}\tilde{A}_3\Pi^B_{A_3W^{(2)}_0}\tilde{W}^{(2)}_0 + \tfrac{1}{2}\tilde{W}^{(2)}_0[M^2_W + \Pi^F_{W^{(2)}_0W^{(2)}_0}]\,\tilde{W}^{(2)}_0 \\ & - \tfrac{1}{2}\tilde{Z}_3M^2_Z\tilde{Z}_3 + \tfrac{1}{2}\tilde{Z}_3\Pi^B_{Z_3W^{(2)}_0}\tilde{W}^{(2)}_0, \end{aligned} \qquad (4.4.1)$$

which is obtained from (2.2.2), taking into account all the quadratic terms of the fields that are mixed with $\tilde{A}_3$ and making the supposition that the potentials $\tilde{A}_3$, $\tilde{W}^{(2)}_0$, and $\tilde{Z}_3$ depend only on the coordinate x_1, orthogonal to the border. The subscript 1 for this coordinate will be henceforth omitted. Inside the W-condensate region $x \geqslant 0$.

From the extremal conditions $\delta\Gamma^q_{\tilde{A}_3}/\delta\tilde{A}_3 = 0$, $\delta\Gamma^q_{\tilde{A}_3}/\delta\tilde{W}^{(2)}_0 = 0$, and $\delta\Gamma^q_{\tilde{A}_3}/\delta\tilde{Z}_3 = 0$, we obtain the mentioned linearized equations which are respectively given by

$$\partial^2_x\tilde{A}_3 = -\tfrac{1}{2}\Pi^B_{A_3W^{(2)}_0}\tilde{W}^{(2)}_0 \qquad (4.1.2a)$$

$$-\partial^2_x\tilde{W}^{(2)}_0 = -[M^2_W + \Pi^F_{W^{(2)}_0W^{(2)}_0}]\,\tilde{W}^{(2)}_0 - \tfrac{1}{2}\Pi^B_{A_3W^{(2)}_0}\tilde{A}_3 - \tfrac{1}{2}\Pi^B_{Z_3W^{(2)}_0}\tilde{Z}_3 \qquad (4.1.2b)$$

$$\partial^2_x\tilde{Z}_3 = M^2_Z\tilde{Z}_3 - \tfrac{1}{2}\Pi^B_{Z_3W^{(2)}_0}\tilde{W}^{(2)}_0. \qquad (4.1.2c)$$

Now, considering that the border coincides with the (y, z)-plane we may define the magnetic $H^{A_3}_2$, quasimagnetic $H^{Z_3}_2$ and quasielectric $E^{W^{(2)}_0}_1$ fields respectively

$$H^{A_3}_2 = -\partial_x\tilde{A}_3 \qquad (4.1.3a)$$

$$H^{Z_3}_2 = -\partial_x\tilde{Z}_3 \qquad (4.1.3b)$$

$$E^{W^{(2)}_0}_1 = -\partial_x\tilde{W}^{(2)}_0. \qquad (4.1.3c)$$

Then, introducing the definitions (4.1.3) into (4.1.2) we can arrive at the following equations for the magnetic, quasimagnetic, and quasielectric fields:

$$\begin{aligned}&\{[\partial^2_x - M^2_Z][-\partial^2_x + M^2_W + \Pi^F_{W^{(2)}_0W^{(2)}_0}] + \tfrac{1}{4}(\Pi^B_{Z_3W^{(2)}_0})^2\}\,\partial^2_x\mathscr{F}_j \\ &\quad = \tfrac{1}{4}(\Pi^B_{A_3W^{(2)}_0})^2\,[\partial^2_x - M^2_Z]\,\mathscr{F}_j, \qquad j = 1, 2, 3.\end{aligned} \qquad (4.1.4)$$

Here, for brevity we have denoted by $\mathscr{F}_j$, $j = 1, 2, 3$, the fields $\tilde{H}^{A_3}_2$, $\tilde{H}^{Z_3}_2$, and $\tilde{E}^{W^{(2)}_0}_1$, respectively. That is, we have obtained a similar differential equation (4.1.4) for each field (4.1.3).

Being higher order differential equations, the three equations (4.1.4) contain an ampler class of solutions than the three original equations (4.1.2). It can be shown that in order to exclude the redundant solutions it is sufficient to supplement equations (4.1.4) by the following two equations also derived from (4.1.2):

$$[\partial^2_x - M^2_Z]\,\tilde{H}^{Z_3}_2 = -\tfrac{1}{2}\Pi^B_{Z_3W^{(2)}_0}\tilde{E}^{W^{(2)}_0}_1 \qquad (4.1.5a)$$

$$\partial^2_x\tilde{H}^{A_3}_2 = \frac{\Pi^B_{A_3W^{(2)}_0}}{\Pi^B_{Z_3W^{(2)}_0}}\,(\partial^2_x - M^2_Z)\,\tilde{H}^{Z_3}_2. \qquad (4.1.5b)$$

A nonzero solution of Eqs. (4.1.4), (4.1.5) may be provided by fixing a nonzero value for the magnetic field on the inside border of the W-condensate region $\hat{H}_2^{A_3}$ and zero values for $H_2^{Z_3}$ and $E_1^{W_0^{(2)}}$.

This formulation just corresponds to the problem of penetration of a magnetic field applied to the W-condensate from outside accompanied by an induction of the quasielectric and quasimagnetic fields inside it.

4.2. *Londons' Penetration Depths*

The solution of Eqs. (4.1.4), (4.1.5) must not grow infinitely at large distance and must satisfy the boundary conditions pointed out above,

$$\tilde{H}_2^{A_3}|_{x=0}=\hat{H}_2^{A_3}, \qquad \tilde{H}_2^{Z_3}|_{x=0}=0, \qquad \tilde{E}_1^{W_0^{(2)}}|_{x=0}=0. \tag{4.2.1}$$

Once we impose all these restrictions we arrive at the solution of the set (4.1.4), (4.1.5),

$$\tilde{H}_2^{A_3}(x)=\gamma(A)\,\gamma(Z)\,\bar{B}_W e^{-\alpha(W)x}+\gamma(A)\,\gamma(W)\,\bar{B}_Z e^{-\alpha(Z)x}+\gamma(Z)\,\gamma(W)\,\bar{B}_A e^{-\alpha(A)x} \tag{4.2.2a}$$

$$\tilde{H}_2^{Z_3}(x)=\gamma(A)\,\gamma(Z)\,\gamma(W)[\bar{B}_W e^{-\alpha(W)x}+\bar{B}_Z e^{-\alpha(Z)x}+\bar{B}_A e^{-\alpha(A)x}] \tag{4.2.2b}$$

$$\tilde{E}_1^{W_0^{(2)}}(x)=-\gamma(A)\gamma(Z)\gamma(W)[\beta(W)\,\bar{B}_W e^{-\alpha(W)x}+\beta(Z)\,\bar{B}_Z e^{-\alpha(Z)x}+\beta(A)\,\bar{B}_A e^{-\alpha(A)x}] \tag{4.2.2c}$$

with

$$\bar{B}_i=\frac{1}{2}\varepsilon_{ijK}\frac{\hat{H}_2^{A_3}}{D}[\beta(j)-\beta(k)], \qquad i, j, k=1, 2, 3, \tag{4.2.3}$$

where we assume following order $1 \leftrightarrow W$, $2 \leftrightarrow Z$, $3 \leftrightarrow A$ and ε_{ijK} is the unit totally antisymmetric tensor with $\varepsilon_{123}=1$. Further,

$$\begin{aligned} D=&\,[\gamma(A)-\gamma(W)][\beta(Z)-\beta(W)]\,\gamma(Z)\\ &-[\gamma(Z)-\gamma(W)][\beta(A)-\beta(W)]\,\gamma(A) \end{aligned} \tag{4.2.4}$$

and $\gamma(i)$ and $\beta(i)$ are given as functions of $\alpha(i)$ as

$$\gamma(i)=\frac{\Pi^B_{Z_3W_0^{(2)}}}{\Pi^B_{A_3W_0^{(2)}}}\,\frac{\alpha^2(i)}{\alpha^2(i)-M_Z^2} \tag{4.2.5}$$

$$\beta(i)=-\frac{2[\alpha^2(i)-M_Z^2]}{\Pi^B_{Z_3W_0^{(2)}}}. \tag{4.2.6}$$

The exponents $\alpha^2(i)=y$ are the three roots of the cubic equation

$$y^3+ay^2+by+c=0, \tag{4.2.7}$$

where

$$a = M_W^2 + M_Z^2 + \Pi^F_{W_0^{(2)}W_0^{(2)}} \tag{4.2.8}$$

$$b = M_Z^2(M_W^2 + \Pi^F_{W_0^{(2)}W_0^{(2)}}) + g^2C^2\mu_3^2 \tag{4.2.9}$$

$$c = M_Z^2(g^2C^2\mu_3^2 \sin^2\theta_w). \tag{4.2.10}$$

In finding an explicit expression for $\alpha(i)$ we will restrict ourselves to the small-condensate approximation ($g^2C^2 \ll M_Z^2 \sim M_W^2$) already used in writing Eqs. (3.3.9)–(3.3.13). So we find

$$\alpha(W) \simeq M_W \tag{4.2.11}$$

$$\alpha(Z) \simeq M_Z \tag{4.2.12}$$

$$\alpha(A) \simeq m(A_3') \ll M_Z \sim M_W. \tag{4.2.13}$$

In this approximation the general solution (4.2.2) reduces to

$$\tilde{H}_2^{A_3}(x) \simeq \hat{H}_2^{A_3} e^{-m(A_3')x} \tag{4.2.14a}$$

$$\tilde{H}_2^{Z_3}(x) \simeq \frac{m^2(A_3')\,\Pi^B_{Z_3W_0^{(2)}}\,\hat{H}_2^{A_3}}{M_Z^2\,\Pi^B_{A_3W_0^{(2)}}}\left[\frac{M_W^2}{M_W^2-M_Z^2}e^{-M_Zx} - \frac{M_Z^2}{M_W^2-M_Z^2}e^{-M_Wx} - e^{-m(A_3')x}\right] \tag{4.2.14b}$$

$$\tilde{E}_1^{W_0^{(2)}} \simeq \frac{-2m^2(A_3')\,\hat{H}_2^{A_3}}{\Pi^B_{A_3W_0^{(2)}}}\left[e^{-M_Wx} - e^{-m(A_3')x}\right] \tag{4.2.14c}$$

from where we can assert that, while in the given approximation the applied magnetic field $\tilde{H}_2^{A_3}$ falls down inside the W-condensate phase with Londons' penetration depth given by $\lambda_L^{(2)} \simeq m^{-1}(A_3')$, the induced weak quasimagnetic $\tilde{H}_2^{Z_3}$ and weak quasielectric $\tilde{E}_1^{W_0^{(2)}}$ fields fall down on two essentially different scales: the short one, $\lambda_L^{(s)} \simeq M_Z^{-1} \sim M_W^{-1}$, and the long one, $\lambda_L^{(2)} \simeq m^{-1}(A_3')$. We must remember that we are considering the small-condensate approximation ($C \sim 0$), where the photon magnetic mass $m(A_3')$ (see Eq. (3.3.10b) is much smaller than the meson masses $M_W \sim M_Z$.

The grafical representations of solution (4.2.14) are given in Fig. 2, where we can observe how the applied magnetic field falls from its boundary value $\hat{H}_2^{A_3}$ down to zero at the distance $\lambda_L^{(2)}$ (Fig. 2a), while the weak-quasimagnetic $\tilde{H}_2^{Z_3}$ and weak-quasielectric $\tilde{E}_1^{W_0^{(2)}}$ fields combine their different decay velocities (the ones related with $\lambda_L^{(2)}$ and $\lambda_L^{(s)}$) to make the following picture: they grow first from their zero values on the boundary to their respective maximum values at a length approximately equal to $\lambda_L^{(s)}$, to fall then to zero at $\lambda_L^{(l)}$ (Figs. 2b,c). The sign in front of $\tilde{E}_1^{W_0^{(2)}}$ will change if one reverses the direction of the vector C, since the polarization operators Π^B_{ZW} and Π^B_{AW} depend linearly on C. Remember the statement made

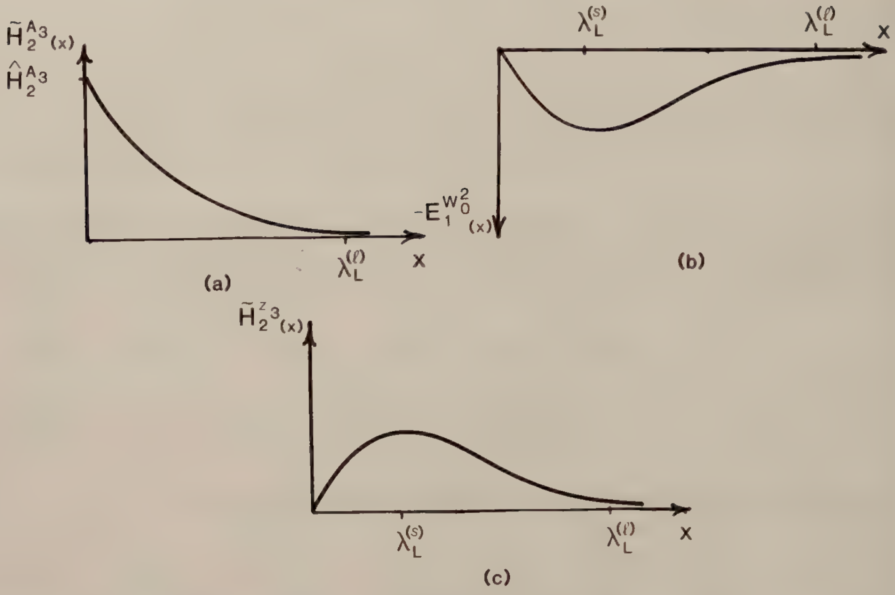

FIG. 2. Behaviour of the magnetic, $\tilde{H}_2^{A_3}$, (a); quasielectric, $\tilde{E}_1^{W_0^{(2)}}$, (b); and quasimagnetic, $\tilde{H}_2^{Z_3}$, (c); fields inside the W-condensate medium as given by Eqs. (4.2.14). The coordinate x is directed from the boundary ($x=0$) into the interior of the W-condensate medium. $\lambda_L^{(l)}$ is the Londons' penetration depth, which coincides with the inverse of the photon magnetic mass. $\lambda_L^{(s)}$ is the Londons' penetration depth, which coincides with the inverse of the photon magnetic mass. $\lambda_L^{(s)}$ is a second characteristic length of the order of $M_W^{-1} \sim M_Z^{-1}$. In drawing (b) we accepted **C** to be oriented anti-parallel to **A**.

in Section 4.1 that both the orientations of the W-condensate are possible, parallel and antiparallel, with the vector potential of the applied magnetic field.

The appearance of induced weak quasimagnetic $\tilde{H}_2^{Z_3}$ and weak quasielectric $\tilde{E}_1^{W_0^{(2)}}$ fields tangled with the applied magnetic field $\hat{H}_2^{A_3}$ through the mechanism of the Meissner screening in the W-condensate phase (i.e., as solutions of the set of Eq. (4.1.2)) can be understood as a reflection of the fact that the magnetic screening in the present approximation is realized at first instance by the generation of an induced charge of weak nature $\tilde{J}_0^{W_0^{(2)}} = \frac{1}{2}\Pi^B_{W_0^{(2)}A_3}\tilde{A}_3$, as it has been reported in Ref. [11]. Taking into account the definitions (4.1.3) we see that once the induced charge $\tilde{J}_0^{W_0^{(2)}}$ is nonzero, already at the border, where it makes the only non-vanishing contribution into the r.h.s. of Eq. (A.1.2), it starts the development of the screening process via equation (4.1.2b) giving rise to the field $W_0^{(2)}$, which in its turn produces the change of the magnetic field by contributing to the r.h.s. of Eq. (4.1.2a). The latter makes an electromagnetic superconducting current induced by the field $W_0^{(2)}$. These two quantities have their maximum at a depth of about $\lambda_L^{(s)}$. In this point we face a difference with the ordinary Meissner effect in solid state physics, where it is completely due to the supercurrent whose maximum density is at the surface. The superconducting currents carrying weak charge in Eq. (4.1.2) are

$-\frac{1}{2}\Pi^{B}_{Z_3 W_0^{(2)}} \tilde{W}_0^{(2)}$ and $M_Z^2 \tilde{Z}_3$ and the weak charges taking part in the screening process are $(M_W^2 + \Pi^{F}_{W_0^{(2)} W_0^{(2)}}) \tilde{W}_0^{(2)} + \frac{1}{2}\Pi^{B}_{Z_3 W_0^{(2)}} Z_3$.

Finally, we want to call attention to the fact that the appearance of a photon magnetic mass in the W-condensate phase and the possibility of realizing the Meissner effect, in such a phase, are not independent events. This can be corroborated in a rough way, making $m(A_3') \to 0$ in Eqs. (4.2.14). Then the magnetic field in the W-condensate phase $\tilde{H}_2^{A_3}$ does not suffer any screening, maintaining at any depth its boundary value $\hat{H}_2^{A_3}$, while there is not any other induced field, i.e., $\tilde{H}_2^{Z_3} = 0$ and $\tilde{E}_1^{W_0^{(2)}} = 0$.

5. CONCLUDING REMARKS

As was discussed in Refs. [4, 6] the WS model in presence of a finite density of leptons exhibits two phase transitions when the temperature is decreased. The first one is from the totally symmetrical phase to the finite-density Higgs phase, and the second, obtained for lower temperatures, requires that the lepton number density be larger than the critical one at zero temperature ($J_L^c = M_W^3/6\pi^2$), is the one which turns the finite-density Higgs phase ($\xi \neq 0$, $C = 0$) to the W-condensate phase ($\xi \neq 0$, $C \neq 0$).

In the finite-density Higgs phase, as well as in the Higgs vacuum, some boson fields acquire masses (those of the $W_\mu^{\pm}$-mesons ad Z_μ-mesons) and become thereby short-range, which implicates that some weak current superconductivity appears responsible for the Meissner screening of the sources of the meson fields $W_\mu^{\pm}$ and Z_μ [28], which may be thought of as providing the short-range character of these fields. But even in this phase the $U_{\mathrm{EM}}(1)$ subgroup remained unbroken, and this was interpreted as the permanence of a long-range character of the $U_{\mathrm{EM}}(1)$-gauge field: the photon. Therefore, an electric current superconductivity could not be expected in this phase.

What is peculiar for the phase transition towards the W-condensate phase is that all the gauge symmetries break down and no boson remains massless. Thus, we found that in this phase the photon acquires the infrared mass providing the Meissner effect for the WS medium with a high density of leptons.

The nonzero magnetic mass of the photon obtained certainly implies the finiteness of the penetration depth of the magnetic field inside the region occupied by the W-condensate phase. As distinct from the usual Meissner effect, this screening is in first place due to the weak charge $J_0^{W_0^{(2)}} = \Pi^{B}_{W_0^{(2)} A_3} A_3$ induced on the surface of the W-condensate phase by a magnetic field applied from outside of this phase. Here the applied magnetic field is contained in the potential A_3. The polarization operator $\Pi^{B}_{W_0^{(2)} A_3}$ is one of the components of the matrix $\mathscr{M}_1$ (3.3.5). This polarization operator also provides the existence of an electromagnetic supercurrent $-\Pi^{B}_{W_0^{(2)} A_3} W_0^{(2)}$ that flows inside the W-condensate at the depth of the order of inverse W-meson mass. However, this current should not be thought of as carrying charged fermions because $\Pi^{B}_{W^{(2)}_{0} A_3}$ does not contain the fermion contribution. The role of fermion within the approximation adopted in the present paper is only to maintain the existence of the W-condensate phase. However, when we went beyond this approximation by calculating the polarization operator as a loop of fermions considered against the background of the W-condensate [9, 10] we saw that electrically charged fermions do contribute directly into the magnetic screening by forming a usual supercurrent, flowing along the surface. This fermionic superconductivity is accompanied by the restructuring of the fermion spectrum. The full investigation of the related phenomena will be published in a forthcoming paper [12].

In accord with the promise given in the Introduction we shall discuss now how the existence of the W-condensate phase may bring a solution for the problem of relic monopoles [29].

As is known, the primordial monopole problem [29] is one of the most difficult problems in compatibilizing cosmology and the theory of elementary particles [30]. Despite the great success of the standard hot universe scenario, the primordial monopole problem together with others makes such a scenario incomplete.[2]

The problem is that the 't Hooft–Polyakov monopoles [32] can be copiously produced during the phase transitions in GUTs at temperatures $T \sim 10^{14}-10^{15}$ GeV [29] and their ulterior annihilation is very slight [30]. This leads to catastrophic cosmological consequences, since the consequent increase of the density of matter, would have made the universe collapse a long time ago.

With the advent of the inflationary universe scenarios [33] this contradiction was overcome. The inflation stage of the universe is able to dilute the density of all objects which existed before the exponential expansion, including monopoles.

But recently it was proved [17] in the context of the new [33] and chaotic [34] inflationary scenarios, that some phase transitions may occur during the last stages of inflation (due to the change of the inflation field Φ and the Hubble parameters) which may lead to the creation of strings, monopoles, and other objects.

Particularly important here is the fact that if monopoles are produced towards the end of inflation, their density, being not totally suppressed, should survive this stage to resurrect the primordial monopole problem.

In this sense the existence of the W-condensate phase as a post-inflationary stage of the expanding universe [13] may bring the possible solution to this problem. The matter is that starting from the mechanism of monopole confinement in a superconductor suggested by Nambu [35], Linde found the way through which the confined monopoles may be annihilated [36]. Within Linde's mechanism [36] it was proposed that the temperature may become responsible for the infrared cutoff needed to generate the superconducting medium. But up to now the thermic photon mass doubtlessly has not been found. In contrast, if the universe really passed after the inflation [13] through the dense phase, $J_L \sim M_W^3$ [1], the photon gained the magnetic mass in that time in a natural way, as we have proved in this work, bringing an adequate context for Linde's mechanism [36] to work, thereby cleaning the universe from the excess of relic monopoles.

---

[2] For a discussion of the general incompatibility between cosmology and elementary particle theories see Ref. [31].

APPENDIX A

Here we present the following special character of the spontaneous symmetry breaking mechanism in quantum statistical theory (i.e., the generalization to statistics of the Fabri–Picasso theorem). Let Q be an infinitesimal operator of a symmetry transformation, $[Q, \rho]=0$, with ρ being the density matrix. Let a field φ be transformed nontrivially by Q in a linear way, i.e., $\delta\varphi \equiv [Q, \varphi]=\alpha\varphi$ with α a matrix coefficient. Then, the nonvanishing of the statistical average $\bar{\varphi}=\operatorname{Tr}(\rho\varphi)\neq 0$ implies that the operator Q cannot leave vectors of the full space of physical states in this space (this wording just expresses the notion of the spontaneous symmetry breakdown). To see why this happens, consider the average of the symmetry field transformation

$$\alpha\bar{\varphi} \equiv \alpha \operatorname{Tr} \rho\varphi = \operatorname{Tr} \rho[Q, \varphi]_- = \operatorname{Tr}(Q\rho\varphi) - \operatorname{Tr}(\rho\varphi Q). \tag{A.1}$$

To maintain the nonvanishing of the l.h.s. of this equation one must point to a reason why the operator Q cannot be cyclically permuted under the sign of trace without changing the value of the trace, since if it could the r.h.s. of (A.1) would be zero. If every vector $|n\rangle$ of the full space of physical states might be transformed by the action of Q into a linear combination of other vectors $|n'\rangle$ of the same space

$$Q\,|n\rangle = \sum_{n'} q_{nn'}\ |n'\rangle, \qquad \langle n|\, Q = \sum_{n'} q_{n'n}\langle n'|, \tag{A.2}$$

the freedom of the cyclic permutation would be proven in a direct way. So, to forbid this permutation is to forbid Eqs. (A.2) for at least one vector $|n\rangle$. When the temperature is zero the only state that contributes to the trace (A.1) is the ground state; i.e., the statistical and ground state averages become the same. Then, for $T=0$ the spontaneous symmetry breakdown means, naturally, the violation of (A.2) for $|n\rangle$ being the ground state. It is unclear whether this situation can occur when (A.2) is violated, not for a ground state but for excited states. If that were the case, the spontaneous symmetry breakdown might appear for a nonzero temperature although it did not for a zero one. The case of W-condensation under study in the body of the paper is characterized by the fact that the vacuum is not taken out of the physical space of states by Q, whereas the ground state is. Normally, as the temperature increases Eq. (A.1) may become zero at the symmetry restoration point, although Eqs. (A.2) cannot be restored, since they are temperature independent. This is not surprising; once the violation of (A. 2) is only a necessary, but not sufficient, condition for (A.1) to be nonzero.

APPENDIX B

As was promised in Subsection 3.2, here we shall show that in the limit $K_4=0$, $|\mathbf{K}|\to 0$ the polarization operator $\Pi^F_{W_0^{(2)}W_i^{(2)}}$ is equal to zero. To this end we apply the method of Refs. [9, 10]. Thus, we introduce the auxiliary coordinate-independent parameters μ_2 and κ in the fermion WS effective Lagrangian (2.1.10), as the shift to the fields $W_0^{(2)}$ and $W_i^{(2)}$,

$$W_\mu^{(2)} \to W_\mu^{(2)\prime} + \bar{W}_\mu^{(2)}$$

$$\bar{W}_\mu^{(2)} \to \frac{\mu_2}{g}\,\delta_{\mu 0} + \kappa\delta_{\mu i}; \tag{B.1}$$

$W_\mu^{(2)\prime}$ is the fluctuating field remaining after the shift. We have specialized $\bar{W}_i^{(2)}$ to be directed along the spatial third component ($i=3$) appealing to the rotational invariance of the problem (remember that $C=0$ within the present calculation).

Then the polarization operator component under consideration can be calculated as

$$\Pi^F_{W_0^{(2)}W_3^{(2)}} = \lim_{\beta\to\infty} \left.\frac{\partial^2 \Gamma^{(1)}_{\Psi_L}}{\partial\mu_2\,\partial\kappa}\right|_{\mu_2=\kappa=0}, \tag{B.2}$$

where

$$\Gamma^{(1)}_{\Psi_L} = \tfrac{1}{2}\beta^{-1}\ln\det G^{-1} \tag{B.3}$$

and G^{-1} is the Dirac operator in the external fields $\bar{W}_\mu^{(2)}=(\mu_2)/g)\,\delta_{\mu 0}+\kappa\delta_{\mu 3}$, $\bar{W}_0^{(3)}=\mu_3/g$, $\bar{B}_0=\mu$ and with the leptonic chemical potential

$$G^{-1} = -i\gamma\cdot(p^* - E) \tag{B.4}$$

$$p_\mu^* = \begin{cases} p_j^* = p_j, & j=1,2,3, \\ p_4^* = p_4 - i(\frac{\mu}{2}-\mu_L) \end{cases} \tag{B.5}$$

$$E_\mu = \begin{cases} E_j = g\kappa\,\dfrac{\tau^2}{2}\,\delta_{j3}, & i=1,2,3 \\[2ex] E_4 = -i\mu_a\,\dfrac{\tau^a}{2}, & a=2,3 \end{cases} \tag{B.6}$$

Taking into account that the functional determinant in (B.3) includes the operations $i\beta^{-1}\sum_{p_4}\int (d^3p/(2\pi)^3)$, after the sum over p_4 is carried out (B.3) is given by

$$\begin{aligned}\Gamma_{\Psi_L}=\int\frac{d^3p}{(2\pi)^3}\bigg\{&\frac{1}{2}\varepsilon_+ +\beta^{-1}\ln(1+e^{-\beta(\varepsilon_+-\tilde{\mu})})\\ &+\frac{1}{2}\varepsilon_- +\beta^{-1}\ln(1+e^{-\beta(\varepsilon_-+\tilde{\mu})})\\ &+\frac{1}{2}\bar{\varepsilon}_+ +\beta^{-1}\ln(1+e^{-\beta(\bar{\varepsilon}_++\tilde{\mu})})\\ &+\frac{1}{2}\bar{\varepsilon}_- +\beta^{-1}\ln(1+e^{-\beta(\bar{\varepsilon}_--\tilde{\mu})})\bigg\},\end{aligned}\qquad\text{(B.7)}$$

where the spectrum of the Dirac operator is presented implicitly as

$$\varepsilon_\pm=\tfrac{1}{2}\sqrt{q^2+4r}\pm\tfrac{1}{2}q\qquad\text{(B.8)}$$

$$\bar{\varepsilon}_\pm=\tfrac{1}{2}\sqrt{q^2+4\bar{r}}\pm\tfrac{1}{2}q\qquad\text{(B.9)}$$

$$\tilde{\mu}=\frac{\mu}{2}-\mu_L\qquad\text{(B.10)}$$

$$r=\left(\omega^2+\frac{\mu_a^2}{4}\right)-\frac{q^2}{2}-\sqrt{q^4/4-q^2(\omega^2+\mu_a^2/4)+\mu_a^2\omega^2-H}\qquad\text{(B.11)}$$

$$\bar{r}=\left(\omega^2+\frac{\mu_a^2}{4}\right)-\frac{q^2}{2}+\sqrt{q^4/4-q^2(\omega^2+\mu_a^2/4)+\mu_a^2\omega^2-H}\qquad\text{(B.12)}$$

$$q=g\kappa\mu_2 p_3\left[\frac{q^4}{4}-q^2\left(\omega^2+\frac{\mu_a^2}{4}\right)+\mu_a^2\omega^2-H\right]^{-1/2}\qquad\text{(B.13)}$$

$$\omega^2=p^2+\tfrac{1}{4}g^2\kappa^2\qquad\text{(B.14)}$$

$$H=\tfrac{1}{4}g^2\kappa^2\mu_3^2-g^2\kappa^2p_3^2.\qquad\text{(B.15)}$$

In the same way as in Refs. [9,10], instead of solving Eq. (B.13) for q we shall list the first derivatives of q with respect to μ_2 ($\dot{q}=\partial q/\partial\mu_2$), and to κ ($q'=\partial q/\partial\kappa$), at $\mu_2=\kappa=0$, which is enough for the task we are involved in

$$\dot{q}(0)\equiv\dot{q}|_{\mu_2=\kappa=0}=0\qquad\text{(B.16)}$$

$$q'(0)\equiv q'|_{\mu_2=\kappa=0}=0\qquad\text{(B.17)}$$

$$\dot{q}'(0)\equiv\dot{q}'|_{\mu_2=\kappa=0}=g\cos\alpha/|\mu_3|,\qquad\text{(B.18)}$$

α being the angle between p and the axis 3. From (B.16), (B.17), (B.18) and the fact that r and $\bar{r}$ only depend on κ^2 and $(\mu_2)^2$ we have at $\mu_2=\kappa=0$,

$$\varepsilon_\pm(0)=\sqrt{r(0)}=|p-|\mu_3|/2|\qquad\text{(B.19)}$$

$$\bar{\varepsilon}_\pm(0)=\sqrt{\bar{r}(0)}=|p+|\mu_3|/2|\qquad\text{(B.20)}$$

$$\dot{\varepsilon}_{\pm}(0)=\dot{\bar{\varepsilon}}_{\pm}(0)=\varepsilon'_{\pm}(0)=\bar{\varepsilon}'_{\pm}(0)=0 \tag{B.21}$$

$$\dot{\varepsilon}'_{\pm}(0)=\dot{\bar{\varepsilon}}'_{\pm}(0)=\pm\tfrac{1}{2}\dot{q}'(0)=\pm g\cos\alpha/2\,|\mu_3|. \tag{B.22}$$

Then, carring out the derivatives with respect to μ_2 and κ in (B.7), and making the substitutions $\mu_2=\kappa=0$ we obtain

$$\begin{aligned}\left.\frac{\partial^2\Gamma^{(1)}_{\Psi_L}}{\partial\mu_2\partial\kappa}\right|_{\mu_2=\kappa=0}=\int\frac{d^3p}{(2\pi)^3}\Bigg\{&\dot{\varepsilon}'_{+}(0)\frac{1}{1+e^{\beta[\varepsilon_{+}(0)+\tilde{\mu}]}}\\&-\dot{\varepsilon}'_{-}(0)\frac{1}{1+e^{\beta[\varepsilon_{-}(0)-\tilde{\mu}]}}+\dot{\bar{\varepsilon}}'_{+}\frac{1}{1+e^{\beta[\bar{\varepsilon}_{+}(0)-\tilde{\mu}]}}\\&-\dot{\bar{\varepsilon}}'_{-}\frac{1}{1+e^{\beta[\bar{\varepsilon}_{-}(0)+\tilde{\mu}]}}\Bigg\}\end{aligned} \tag{B.23}$$

Finally, the zero-temperature limit gives the polarization operator in question

$$\begin{aligned}\Pi^{F}_{W_0^{(2)}W_3^{(2)}}=\Pi^{F}_{W_3^{(2)}W_0^{(2)}}&=\lim_{\beta\to\infty}\left.\frac{\partial\Gamma^{(1)}_{\Psi_L}}{\partial\mu_2\partial\kappa}\right|_{\mu_2=\kappa=0}\\&=\int\frac{d^3p}{(2\pi)^3}\{\dot{\varepsilon}'_{-}(0)\,\theta[\tilde{\mu}-\varepsilon_{-}(0)]+\dot{\bar{\varepsilon}}'_{+}(0)\,\theta[\tilde{\mu}-\bar{\varepsilon}_{+}(0)]\}\\&=-\frac{1}{(2\pi)^2}\int_0^{\pi}\sin\alpha\,d\alpha\int_0^{\infty}p^2\,dp\left\{\frac{g\cos\alpha}{2|\mu_3|}\theta[\tilde{\mu}-\varepsilon_{-}(0)]\right.\\&\qquad\left.-\frac{g\cos\alpha}{2|\mu_3|}\theta[\tilde{\mu}-\bar{\varepsilon}_{+}(0)]\right\}\end{aligned} \tag{B.24}$$

which turns to zero after the integration in the α-angle. θ is the step function.

APPENDIX C

Let us now show that on the mass shell, the product of the masses of physical particles (3.3.7) does not depend on the gauge fixing conditions. With this purpose, instead of working in the unitary gauge used in developing the result (3.3.7), we will employ the covariant gauge conditions which depend on an arbitrary parameter α,

$$F^a=\partial^{\mu}W^a_{\mu}+ig\alpha\left(\tilde{\phi}^{+}\frac{\tau^a}{2}\bar{\phi}-\bar{\phi}^{+}\frac{\tau^a}{2}\tilde{\phi}\right)=0 \tag{C.1}$$

$$a=1,\ 2,\ 3$$

$$f=\partial^{\mu}B_{\mu}+ig'\frac{\alpha}{2}(\tilde{\phi}^{+}\bar{\phi}-\bar{\phi}^{+}\tilde{\phi})=0, \tag{C.2}$$

where

$$\tilde{\phi} = \begin{pmatrix} \varphi_1 \\ \varphi_2 \end{pmatrix} \tag{C.3}$$

$$\bar{\phi} = \begin{pmatrix} 0 \\ \xi \end{pmatrix}. \tag{C.4}$$

When we repeat all of the procedure carried out in Section 3.3, but introducing in the *WS* Lagrangian (2.1.1) the gauge contribution, L_g, corresponding to the conditions (C.1)–(C.2),

$$\begin{aligned} L_g = &-\frac{1}{2\alpha}\left[\partial^\mu W^a_\mu + ig\alpha\left(\tilde{\phi}^+ \frac{\tau^a}{2}\bar{\phi} - \bar{\phi}^+ \frac{\tau^a}{2}\tilde{\phi}\right)\right]^2 \\ &-\frac{1}{2\alpha}\left[\partial^\mu B_\mu + \frac{ig'\alpha}{2}(\tilde{\phi}^+\bar{\phi} - \bar{\phi}^+\tilde{\phi})\right]^2, \end{aligned} \tag{C.5}$$

we find that the isolated block in the mass matrix, where the contribution of A_3 is contained is now a 4×4 matrix (instead of 3×3 matrix (3.3.5)), whose new row and column refer to the Goldstone field h,

$$\hat{\mathbf{\Pi}} = \begin{bmatrix} 0 & 0 & \frac{1}{4}\Pi^B_{A_3 W_0^{(2)}} & \frac{1}{4}\Pi^B_{A_3 h} \\ 0 & -\frac{1}{2}M_Z^2 & \frac{1}{4}\Pi^B_{Z_3 W_0^{(2)}} & \frac{1}{4}\Pi^B_{Z_3 h} \\ \frac{1}{4}\Pi^B_{W_0^{(2)} A_3} & \frac{1}{4}\Pi^B_{W_0^{(2)} Z_3} & \frac{1}{2}M_W^2 + \frac{1}{2}\Pi^F_{W_0^{(2)} W_0^{(2)}} & \frac{1}{4}\Pi^B_{W_0^{(2)} h} \\ \frac{1}{4}\Pi^B_{hA_3} & \frac{1}{4}\Pi^B_{hZ_3} & \frac{1}{4}\Pi^B_{hW_0^{(2)}} & \frac{1}{2}m_h^2 \end{bmatrix}, \tag{C.6}$$

where apart from the known polarization operator components given in (3.3.5), (3.2.6) we have

$$\Pi^B_{hA_3} = \Pi^B_{A_3 h} = 2gg'C\xi\cos\theta_w \tag{C.7}$$

$$\Pi^B_{hZ_3} = \Pi^B_{Z_3 h} = 2gg'C\xi\sin\theta_w \tag{C.8}$$

$$\Pi^B_{hW_0^{(2)}} = \Pi^B_{W_0^{(2)} h} = -2g\mu\xi \tag{C.9}$$

$$m_h^2 = \tfrac{1}{2}(\mu+\mu_3)^2 - \tfrac{1}{2}g^2C^2 + 2m^2 - (4\lambda + \alpha g^2)\,\xi^2. \tag{C.10}$$

The contribution of (C.6) to the quadratic part of the effective action (2.2.2) in the infrared limit is given by

$$\Gamma_q^s = \chi^+ \hat{\mathbf{\Pi}} \chi \tag{C.11}$$

with

$$\chi^+ = (A_3, Z_3, W_0^{(2)}, h) \tag{C.12}$$

$$h = \frac{1}{2i}(\varphi_1 - \varphi_1^*). \tag{C.13}$$

On the other hand, the contributions given by A_1, Z_2 and A_2, Z_2 to the mass matrix in the covariant gauge (C.1)–(C.2) remains an isolated diagonal blocks which coincide with those obtained in the unitary gauge (3.3.6).

Taking the determinant of the new matrix $\hat{\Pi}$ (C.8) we obtain

$$\det \hat{\Pi} = \left(\frac{g}{2} C\mu_3\right)^2 \left(\frac{gg'}{2} C\xi\right)^2 + e^2C^2 \frac{M_Z^2}{2} \times \left[\left(\frac{\mu_3}{2}\right)^2 \frac{m_h^2}{2} - \frac{g^2\mu\mu_3}{4}\xi^2 + \frac{1}{2}\left(\frac{g\xi}{2}\right)^2 \left(M_W^2 + \Pi^F_{W_0^{(2)} W_0^{(2)}}\right)\right]. \tag{C.14}$$

Now in order to take into account the mass shell conditions let us write explicitly the extremum equations for the W-condensate phase (2.2.1),

$$\frac{\partial v^{(0)}}{\partial \xi^2} = \frac{1}{4} g^2C^2 - \frac{1}{4}(\mu - \mu_3)^2 - m^2 + 2\lambda\xi^2 = 0 \tag{C.15}$$

$$\frac{\partial v^{(0)}}{\partial C^2} = \frac{1}{4} g^2\xi^2 - \frac{1}{2}\mu_3^2 = 0 \tag{C.16}$$

$$\frac{\partial v^{(0)}}{\partial \mu_3} = -\mu_3 C^2 + \frac{1}{2}(\mu - \mu_3)\,\xi^2 + \frac{1}{6\pi^2}(\mu^3_{\nu_L} - \mu^3_{e_L}) = 0 \tag{C.17}$$

$$\frac{\partial v^{(0)}}{\partial \mu} = -\frac{1}{2}(\mu - \mu_3)\,\xi^2 - \frac{1}{6\pi^2}[\mu^3_{\nu_L} + \mu^3_{e_L} + 2\mu^3_{e_R}] = 0. \tag{C.18}$$

Then, taking into account Eq. (C.15), we have that

$$\mu_3^2 = \tfrac{1}{2} g^2\xi^2 = M_W^2 = M_Z^2 \cos^2\theta_w \tag{C.19}$$

and from Eq. (C.15) the Goldstone mass m_h, Eq. (C.10), reduces to

$$m_h^2 = 2\mu\mu_3 - 2\alpha\mu_3^2. \tag{C.20}$$

Therefore, substituting Eqs. (C.19) and (C.20) in Eq. (C.14), we arrive at

$$\det \hat{\Pi} = \frac{M_Z^2}{2} \frac{M_W^2}{2} \frac{e^2C^2}{2} \left[g^2C^2 + (1-\alpha)\,\mu_3^2 - \mu\mu_3 + \tfrac{1}{2}\Pi^F_{W_0^{(2)} W_0^{(2)}}\right]. \tag{C.21}$$

Now, from Eq. (C.17) and the definition of $\Pi^F_{W_0^{(2)} W_0^{(2)}}$ given in Eq. (3.2.6a), which is not affected by the change of the gauge, we have that

$$\Pi^F_{W_0^{(2)} W_0^{(2)}} = -2g^2C^2 + 2\mu\mu_3 - 2\mu_3^2. \tag{C.21}$$

Finally, substituting Eq. (C.22) in (C.21) and taking into account (C.19) we find that $\det \hat{\Pi}$, on the mass shell, reduces to

$$\det \hat{\Pi} = (\det \hat{\Pi})_{\text{phys}} \cdot (\det \hat{\Pi})_{\text{Goldstone}}, \tag{C.23}$$

where

$$(\det \hat{\Pi})_{\text{phys}} = \frac{M_Z^2}{2} \frac{M_W^2}{2} \frac{e^2 C^2}{2} \tag{C.24}$$

$$(\det \hat{\Pi})_{\text{Goldstone}} = -\alpha M_W^2. \tag{C.25}$$

Here we have written $\det \hat{\Pi}$ as the product of two terms: one, $(\det \hat{\Pi})_{\text{Goldstone}}$, which includes the gauge parameter α, and the other, $(\det \hat{\Pi})_{\text{phys}}$, which coincides with $\det \mathscr{M}_1$, where $\mathscr{M}_1$ is given by Eq. (3.3.5) in the unitary gauge. The latter coincidence must be understood as a reflection of the fact that the masses of the physical modes (in this case corresponding to the components A_3, Z_3, and $W_0^{(2)}$ are independent of the gauge-fixing conditions when evaluated on the mass shell. We must observe that the extremum equations (C.15)–(C.18) coincide in the covariant and in the unitary gauges, so the evaluation of C, ξ, μ_3, and μ on the mass shell, i.e., as functions of μ_L (once the system (C.15)–(C.18) is solved) will give equivalent results in both gauges.

The dependence of $\det \hat{\Pi}$ on α, as a factor, is natural, because $\det \hat{\Pi}$ includes as one of its eigenvalues the mass of the nonphysical Goldstone h (this is what we have denoted by $(\det \hat{\Pi})_{\text{Goldstone}}$ in (C.23)), which on the mass shell must be a pure gauge quantity (i.e., a quantity proportional to the arbitrary parameter α).

From (C.23), (C.24), and (C.25) we can conclude that the magnetic mass of the photon third component $m(A'_3)$, which is one of the eigenvalues of $\hat{\Pi}$, is on the mass shell nonzero independently of the gauge conditions. The masses of the other components $m(A'_{1,2})$ remain nonzero since the determinants of $\mathscr{M}_1$ and $\mathscr{M}_2$ coincide in this general covariant gauge with their values in the unitary gauge, as we have already pointed out.

ACKNOWLEDGMENTS

The authors are grateful to Professor E. S. Fradkin for valuable discussions during the work and to Professor A. D. Linde for instructive conversations. It is also a pleasure for the authors to thank Professor V. L. Ginzburg for the hospitality extended to two of them at the Theoretical Department of the Lebedev Physical Institute, where this work was fulfilled.

REFERENCES

1. A. D. Linde, *Phys. Lett. B* **86** (1979), 39.
2. I. V. Krive, *Yad. Fiz.* **31** (1980), 1279.
3. O. K. Kalashnikov and H. Perez-Rojas, *Kratk. Soobshch. Fiz.* **2** (1986), 23; *Sov. Phys. Lebedev Inst. Rep.* (*Engl. Transl.*)
4. E. J. Ferrer, V. de la Incera, and A. E. Shabad, *Phys. Lett. B* **185** (1987), 407.
5. O. K. Kalashnikov and H. Perez Rojas, *Nucl. Phys. B* **293** (1987), 241.
6. E. J. Ferrer, V. de la Incera, and A. E. Shabad, *Nucl. Phys. B* **309** (1988), 170.
7. D. I. Deryagin, D. Yu. Grigoriev and V. A. Rubakov, *Phys. Lett. B* **178** (1986), 385; *Int. J. Mod. Phys. A* **3** (1988), 1199.

8. E. J. Ferrer and V. de la Incera, *Phys. Lett. B* **205** (1988), 381.
9. E. J. Ferrer, V. de la Incera, and A. E. Shabad, *Mod. Phys. Lett. A* **3** (1988), 623.
10. E. J. Ferrer, V. de la Incera, and A. E. Shabad, *in* "Proceedings 11th International School of Theoret. Phys.: Testing of the Standard Model, Szczyrk-Bila, Poland, Sept. 1987," (M. Zralek and R. Manka, Eds.), p. 443, World Sci., Singapore, 1988.
11. E. J. Ferrer, V. de la Incera, and A. E. Shabad, *Phys. Lett. B* **220** (1989), 623.
12. E. J. Ferrer, V. de la Incera, and A. E. Shabad, Fermionic superconductivity in the dense Weinberg–Salam model, (*Int. J. Mod. Phys. A* (1990)). To appear.
13. E. J. Ferrer and V. de la Incera, Preprint 223, Moscow, FIAN, 1988; *Int. J. Mod. Phys. A* **4** (1989), 5539.
14. I. Affleck and M. Dine, *Nucl. Phys. B* **249** (1985), 361.
15. A. D. Linde, *Phys. Lett. B* **160** (1985), 243.
16. D. I. Deryagin, D. Yu. Grigoriev, V. A. Rubakov, and M. V. Sazhin, *Mod. Phys. Lett. A* **1** (1986), 593.
17. L. A. Kofman and A. D. Linde, *Nucl. Phys. B* **282** (1987), 555.
18. D. A. Kirzhnits and A. D. Linde, *Phys. Lett. B* **42** (1972), 471; *Ann. Phys.*, (*N.Y.*) **101** (1976), 195.
19. A. D. Linde, *Rep. Prog. Phys.* **42** (1979), 389.
20. E. Abers and B. W. Lee, *Phys. Rep. C* **9** (1973), 1.
21. E. S. Fradkin, "Quantum Field Theory and Hydrodynamics," Consultants Bureau, New York, 1967.
22. O. K. Kalashnikov and V. V. Klimov, *Sov. J. Nucl. Phys.* **31** (1980), 1357.
23. E. J. Ferrer, V. de la Incera, and A. E. Shabad, *Fortsch. Phys.* **32** (1984), 261.
24. M. B. Kislinger and P. D. Morley, *Phys. Rev. D* **13** (1976), 2765.
25. E. J. Ferrer, V. de la Incera, and A. E. Shabad, *Nuovo Cimento A* **98** (1987), 245.
26. R. Fukuda and T. Kugo, *Phys. Rev. D* **13** (1976), 3469.
27. V. N. Tsytovich, *Zh. Eksp. Teor. Fiz.* **40** (1961), 1775; M. M. Kislinger and P. D. Morley, *Phys. Rev. D* **13** (1976), 2765, 2771.
28. G. M. Shore, *Ann. Phys.* **134** (1981), 259.
29. T. W. Kibble, *J. Phys. A Math. Gen.* **9** (1976), 1387; *Phys. Rep.* **67** (1980), 183.
30. Ya. B. Zeldovich and M. Yu. Khlopov, *Phys. Lett. B* **79** (1978), 239; J. P. Preskill, *Phys. Rev. Lett.* **43** (1979), 1365.
31. A. D. Linde, *Rep. Prog. Phys.* **47** (1984), 925.
32. G. 't Hooft, *Nucl. Phys. B* **79** (1974), 279; A. M. Poliakov, *JETP Lett.* **20** (1974), 194.
33. E. B. Gliner, *Sov. Phys. JETP* **22** (1965), 378; *Dokl. Akad. Nauk. SSSR* **192** (1970), 771; A. A. Starobinsky, *Phys. Lett. B* **91** (1980), 99; A. H. Guth, *Phys. Rev. D* **23** (1981), 347; A. D. Linde, *Phys. Lett. B* **108** (1982), 389; **144** (1982), 431; **116** (1982), 335; A. Albrecht and P. J. Steinhardt, *Phys. Rev. Lett.* **48** (1982), 1220.
34. A. D. Linde, *JETP Lett.* **38** (1983), 176; *Phys. Lett. B* **129** (1983), 177.
35. Y. Nambu, *Phys. Rev. D* **10** (1974), 4262.
36. A. D. Linde, *Phys. Lett. B* **96** (1980), 293.

ANNALS OF PHYSICS **201**, 83–116 (1990)

Dynamical Symmetry of the Magnetic Vortex*

R. JACKIW[†]

Department of Physics, Columbia University,
538 West 120th Street, New York, New York 10027

Received November 27, 1989

The dynamics of charged point particles interacting with point vortices, as in the idealized Aharonov–Bohm experiment or in Chern–Simons physics, possesses a dynamical $SO(2, 1)$ symmetry. Ramifications of this symmetry for the physical problem are presented. We also find an integral representation for the scattering wave function, discuss the angular momentum spectrum, and establish the absence of self-interactions in Chern–Simons electrodynamics, for which the two-body scattering state is explicitly constructed as a definite superposition of free one-body states. © 1990 Academic Press, Inc.

I. INTRODUCTION

The dynamics of a charged point-particle interacting with a magnetic point-vortex (flux tube) arises in various physically interesting circumstances. It provides an idealization for charged particle motion around a solenoid, and therefore captures the essence of the Aharonov–Bohm effect. When free motion along the (infinite) vortex is ignored, the description becomes essentially planar (two-dimensional) and summarizes center-of-mass dynamics for two point-particles that carry charge as well as magnetic flux and interact according to the laws of planar, Chern–Simons electrodynamics. It has been conjectured that such structures enter into the physics of the quantized Hall effect and of high T_c superconductivity. Equations identical to the particle-vortex system are encountered also in the context of $(2+1)$-dimensional gravity, which is physically realized with infinite cosmic strings.

The quantum mechanical theory of the particle-vortex system is governed by the time-dependent Schrödinger equation, defined on the two-dimensional plane,

$$i\hbar \frac{\partial}{\partial t} \psi(t; \mathbf{r}) = H\psi(t; \mathbf{r}). \tag{1.1}$$

---

* This work is supported in part by funds provided by the U.S. Department of Energy (D.O.E.) under contract #DE-AC02-72.116ER03069.

[†] On sabbatical leave from the Center for Theoretical Physics, Laboratory for Nuclear Science and Department of Physics, Massachusetts Institute of Technology, Cambridge, MA 02139.

0003-4916/90 $7.50

Copyright © 1990 by Academic Press, Inc.
All rights of reproduction in any form reserved.

The Hamiltonian

$$H = \frac{1}{2M}\left(\mathbf{p} - \frac{e}{c}\,\mathbf{A}(\mathbf{r})\right)^2 \tag{1.2}$$

is determined from the Lorentz-force Lagrangian

$$L = \frac{1}{2}\,Mv^2 + \frac{e}{c}\,\mathbf{v}\cdot\mathbf{A}(\mathbf{r}). \tag{1.3}$$

Here M, e, $\mathbf{v} \equiv \dot{\mathbf{r}}$ are the particle's mass, charge, and velocity. The vector potential $\mathbf{A}$ in (1.2) and (1.3) is externally prescribed,

$$A^i(\mathbf{r}) = -\frac{\Phi}{2\pi}\,\varepsilon^{ij}\,\frac{\hat{r}^j}{r} \tag{1.4a}$$

and gives rise to a vortex concentrated at the origin, carrying magnetic field B

$$B(\mathbf{r}) = \nabla\times\mathbf{A} = \Phi\,\delta^2(\mathbf{r}) \tag{1.4b}$$

and flux Φ,

$$\Phi = \int d^2\mathbf{r}\,B(\mathbf{r}). \tag{1.4c}$$

The magnetic field is invisible when the Hamiltonian is expressed in terms of the velocity $\mathbf{v}$, rather than the canonical momentum $\mathbf{p}$,

$$\mathbf{p} \equiv \frac{\partial L}{\partial\mathbf{v}} = M\mathbf{v} + \frac{e}{c}\,\mathbf{A} \tag{1.5}$$

$$H = \frac{1}{2}\,Mv^2. \tag{1.6}$$

However, B reappears in the dynamical quantum algebra,

$$[r^i, r^j] = 0 \tag{1.7a}$$

$$[r^i, Mv^j] = i\hbar\,\delta^{ij} \tag{1.7b}$$

$$[Mv^i, Mv^j] = i\varepsilon^{ij}\hbar\,\frac{e}{c}\,B(\mathbf{r}) = i\varepsilon^{ij}2\pi\nu\hbar^2\,\delta^2(\mathbf{r}). \tag{1.7c}$$

The velocity commutator (1.7c) is extended by an (infinitesimal) 2-cocycle that involves the flux quantum,

$$\nu \equiv \frac{e\Phi}{2\pi\hbar c}. \tag{1.8}$$

However, since the 2-cocycle does not obstruct quantization, ν can be arbitrary; if it happens to be an integer, the vortex has no physical effect.

The energy eigenvalue problem that emerges when time is separated in the usual way in (1.1),

$$\begin{aligned} \psi(t; \mathbf{r}) &= e^{\ itE/\hbar}\psi_E(\mathbf{r}) \\ H\psi_E(\mathbf{r}) &= E\psi_E(\mathbf{r}) \end{aligned} \tag{1.9}$$

has of course been solved in many ways: first by Aharonov and Bohm [1], again by Ruijsenaars [2] who made use of a partial wave expansion. More recently, solutions on a conical surface have been given [3]; these are relevant when gravitational interactions are included [4].

Here we demonstrate that the problem admits a hidden, dynamical $SO(2, 1)$ symmetry group of conformal transformations, which has not been previously identified. The symmetry group is present because, as we show below, the action $I = \int dt L$, is left invariant not only by translations ($t \to t + t_0$) but also by dilations ($t \to \lambda t$) and special conformal transformations ($1/t \to 1/t + 1/t_0$) of the time coordinate t. Commutators of the three associated constants of motion, H, D, and K, respectively, close on the conformal $SO(2, 1)$ Lie algebra. We describe the ramifications of this higher symmetry for the particle-vortex quantum theory and present a group theoretic analysis, which supplements the known [1–3] "direct" treatments, and in a sense explains "why" an analytic solution is available.

The role of $SO(2, 1)$ as a dynamical symmetry was first recognized for the inverse-square potential [5]. More relevant to the present research is our earlier discussion of the $SO(2, 1)$ dynamical symmetry enjoyed by the charged particle-magnetic monopole interaction [6]. Indeed much of the present paper consists of a transcription to the vortex problem of formulas developed for the magnetic monopole. Evidently the vortex is in many ways the planar analog of the three-dimensional magnetic monopole. (Another point of similarity, which will not concern us here, is that the Dirac operators for both systems require self-adjoint extensions [3, 7, 8].)

The paper is organized as follows. In Section II, we establish the symmetries of the vortex Lagrangian (1.3)–(1.4): the obvious rotational invariance and the hidden conformal $SO(2, 1)$ invariance. Also the constants of motion and their algebra are obtained, and the conventional nature of the angular momentum spectrum is stressed. Section III is devoted to a review of the known [1–3] "direct" solution to the energy eigenvalue problem (1.9). Since the spectrum is continuous, interest resides in the eigenfunctions. We derive a contour integral representation for the scattering solution, which separates in a natural way into an incoming wave and a scattered wave, with explicitly determined scattering amplitude. Our analysis takes over techniques developed for the gravitational problem [3, 4], complementing and clarifying the older treatments [1, 2]. The group theoretic discussion based on representations of $SO(2, 1)$ is given in Section IV. In particular we show that quantum motion at fixed angular momentum is described by a single, irreducible, unitary, and infinite-dimensional representation. (This is also true for the magnetic monopole problem [6].) The group theoretic analysis can be alternatively motivated by an unconventional separation of variables in (1.1) or by an unconventional quantization procedure, wherein quantum mechanical evolution is not effected by the Hamiltonian, but by another generator of the conformal group. This is demonstrated in Section V, where it is also shown that our group theoretic approach provides a natural infrared (long-distance) regularization for the particle-vortex interaction. The last Section VI is devoted to Chern–Simons theory. In contrast to the earlier discussions in Sections II–V, which concern a particle moving in the externally prescribed vector potential **A** of (1.4), we now allow **A** to be an independent dynamical variable, governed by Chern–Simons dynamics. After a careful treatment of self-interactions, which are found to be absent, we show that space-translation symmetries and Galileo boosts supplement the conformal and rotational symmetries, with rotations generated by an angular momentum operator that acquires an additional contribution from the gauge field. As a consequence, the angular momentum carries in units of $\hbar$ non-integer eigenvalues, unlike in the external field case, where the spectrum comprises the conventional integers. Also we confirm that two-body center-of-mass motion obeys the external-field equations discussed earlier [9], and we show how the two-body wave function is constructed by superposing products of one-body wave functions.

Various formulas involving special functions that are used in the analysis are collected in an appendix.

II. INVARIANCES OF THE ACTION

A. *Spatial Rotation Symmetry*

The charged particle-vortex Lagrangian (1.3), (1.4) is rotationally invariant; it does not change when the dynamical variable is rotated. Infinitesimally we have

$$\begin{aligned} \delta r^i &= -\varepsilon^{ij} r^j \\ \delta L &= 0 \qquad \text{(rotation)}. \end{aligned} \tag{2.1}$$

The conserved constant of motion, whose general form for invariant Lagrangians is

$$C = \frac{\partial L}{\partial \mathbf{v}} \cdot \delta \mathbf{r} = \mathbf{p} \cdot \delta \mathbf{r} \tag{2.2}$$

becomes in the present case the angular momentum,

$$J = \mathbf{r} \times \mathbf{p}. \tag{2.3a}$$

According to (1.4) and (1.5) this may also be written as

$$\begin{aligned} J &= M\mathbf{r}\times\mathbf{v} - \frac{e\Phi}{2\pi\hbar c} \\ &= M\mathbf{r}\times\mathbf{v} + \hbar\nu. \end{aligned} \tag{2.3b}$$

Nevertheless, the spectrum of J comprises integer multiples of $\hbar$ because in the quantum theory, where $\mathbf{p}$ is realized by $-i\hbar\nabla$, J is realized in circular coordinates $\mathbf{r}=(x, y)=(r\cos\theta, r\sin\theta)$, by $-i\hbar\,\partial/\partial\theta$ acting on single-valued functions of θ. Thus contrary to occasional statements in the literature [10], the angular momentum spectrum of a charged particle in an external field is conventional [11]. The situation changes when the vector potential becomes an independent variable with Chern–Simons dynamics, see Section VI.

B. *Conformal Symmetries*

A transformation may be a symmetry operation, giving rise to a constant of motion, even if the Lagrangian is not invariant, but the action is; i.e., if under a transformation $\delta\mathbf{r}$ of the dynamical variable $\mathbf{r}$, it is determined *without using equations of motion* that the Lagrangian changes by a total time derivative,

$$\delta L = \frac{d}{dt}X, \tag{2.4}$$

then the constant of motion acquires an addition to (2.2),

$$C = \mathbf{p}\cdot\delta\mathbf{r} - X. \tag{2.5}$$

It is in this extended sense that conformal redefinition of time is a symmetry operation for (1.3), (1.4).

To see this, let us consider first the interaction part of (1.3),

$$L_{\text{interaction}} = \frac{e}{c}\,\mathbf{v}\cdot\mathbf{A}(\mathbf{r}). \tag{2.6}$$

With arbitrary $\delta\mathbf{r}$, $L_{\text{interaction}}$ changes as follows:

$$\begin{aligned} \delta L_{\text{interaction}} &= \frac{e}{c}\,\delta v^i A^i + \frac{e}{c}\,v^i\,\partial_j A^i\,\delta r^j \\ &= \frac{e}{c}\left(\frac{d}{dt}\,\delta r^i\right)A^i + \frac{e}{c}\,v^i\,\partial_i A^j\,\delta r^j + \frac{e}{c}\,v^i(\partial_j A^i - \partial_i A^j)\,\delta r^j \\ &= \frac{d}{dt}\left(\frac{e}{c}\,\mathbf{A}\cdot\delta\mathbf{r}\right) + \frac{e}{c}\,\delta\mathbf{r}\times\mathbf{v}\,\Phi\,\delta^2(\mathbf{r}). \end{aligned} \tag{2.7}$$

The first term in the final equality is a total time derivative for arbitrary $\delta\mathbf{r}$ and time-independent external vector potentials **A**. For an evaluation of the last contribution to $\delta L_{\text{interaction}}$, whose form is specific to the vortex, we take $\delta\mathbf{r}$ as arising from an arbitrary redefinition of time. If

$$t \rightarrow T = T(t) \tag{2.8}$$

the dynamical variable also changes

$$\mathbf{r} \rightarrow \mathbf{R} \tag{2.9a}$$

by a transformation that can involve a Jacobian factor with arbitrary weight ε,

$$\mathbf{R}(T) = \left(\frac{dt}{dT}\right)^{\varepsilon} \mathbf{r}(t). \tag{2.9b}$$

Infinitesimally, this gives

$$T(t) - t \equiv \delta_f t = -f(t) \tag{2.10}$$

$$\mathbf{R}(t) - \mathbf{r}(t) \equiv \delta_f \mathbf{r}(t) = f(t)\,\mathbf{v}(t) + \varepsilon \dot{f}(t)\,\mathbf{r}(t) \tag{2.11}$$

and we see that the last term in (2.7) vanishes. Thus the particle-vortex interaction is invariant against arbitrary time reparametrization, and **r** transforming with *arbitrary* weight. (This large invariance is also enjoyed by the charged particle-magnetic monopole interaction in three dimensions [6].)

Note that for arbitrary, time-independent vector potentials $\mathbf{v} \cdot \mathbf{A}(\mathbf{r})$ changes by a total derivative, and its action $\int dt\, \mathbf{v} \cdot \mathbf{A}(\mathbf{r})$ is invariant, when time is reparametrized and $\mathbf{r}(t)$ transforms as in (2.11) with *zero* weight, $\varepsilon = 0$. This is most readily seen by rewriting the time integral as a line integral $\int d\mathbf{r} \cdot \mathbf{A}(\mathbf{r})$, which is obviously reparametrization invariant. The special and additional feature of the vortex (and of the magnetic monopole [6]) is that the interaction remains time reparametrization invariant when $\mathbf{r}(t)$ changes with *arbitrary* weight ε.[1]

The charged particle's kinetic energy

$$L_{\text{particle}} = \tfrac{1}{2} M v^2 \tag{2.12}$$

changes under (2.11) by a total derivative only when $\varepsilon = -\frac{1}{2}$ and f corresponds to the $SO(2, 1)$ conformal group: $f = 1,\ t,\ t^2$,

$$\delta\mathbf{r} = \mathbf{v} \qquad \text{(time translation)} \tag{2.13a}$$

$$\delta\mathbf{r} = t\mathbf{v} - \tfrac{1}{2}\mathbf{r} \qquad \text{(time dilation)} \tag{2.13b}$$

$$\delta\mathbf{r} = t^2\mathbf{v} - t\mathbf{r} \qquad \text{(time special conformal transformation).} \tag{2.13c}$$

---

[1] In fact, an even larger invariance holds for both systems: for the vortex, we can allow $\delta\mathbf{r} = f\mathbf{v} + \Delta(\mathbf{r})$, because the last term in (2.7) vanishes provided the arbitrary quantity $\Delta(\mathbf{r})$ vanishes at the origin; for the magnetic monopole, see [6, 12].

For these, the change of L_{particle} is a total time derivative,

$$\delta_f L_{\text{particle}} = \frac{d}{dt}\left(f L_{\text{particle}} - \frac{1}{4} \ddot{f} M r^2 \right). \tag{2.14}$$

By putting together (2.5), (2.11), and (2.14), we arrive at expressions for the three constants of motion that arise, respectively, from the three symmetries (2.13),

$$H = \tfrac{1}{2} M v^2 \tag{2.15a}$$

$$D = tH - \tfrac{1}{4} M(\mathbf{r} \cdot \mathbf{v} + \mathbf{v} \cdot \mathbf{r}) \tag{2.15b}$$

$$K = -t^2 H + 2tD + \tfrac{1}{2} M r^2. \tag{2.15c}$$

These are also generators of the transformations (2.13), as is seen by using the quantum algebra (1.7) to reproduce (2.13) by commutation,

$$\frac{i}{\hbar}[H, \mathbf{r}] = \mathbf{v} \tag{2.16a}$$

$$\frac{i}{\hbar}[D, \mathbf{r}] = t\mathbf{v} - \tfrac{1}{2}\mathbf{r} \tag{2.16b}$$

$$\frac{i}{\hbar}[K, \mathbf{r}] = t^2 \mathbf{v} - t\mathbf{r}. \tag{2.16c}$$

The quantum algebra (1.7) also establishes that the generators satisfy the $SO(2, 1)$ commutation relations,

$$[D, H] = -i\hbar H \tag{2.17a}$$

$$[D, K] = i\hbar K \tag{2.17b}$$

$$[H, K] = 2i\hbar D \tag{2.17c}$$

which can be presented in the Cartan basis by forming linear combinations with the help of a fixed, positive parameter a of time dimensionality,

$$\mathcal{R} = \frac{1}{2}\left(\frac{1}{a} K + aH\right) \tag{2.18a}$$

$$\mathcal{S} = \frac{1}{2}\left(\frac{1}{a} K - aH\right) \tag{2.18b}$$

$$L_{\pm} = \frac{1}{\hbar}(\mathcal{S} \pm iD). \tag{2.18c}$$

$\mathcal{S}$ and D act as non-compact two-dimensional boost generators, while $\mathcal{R}$ generates the rotations that form the compact $SO(2)$ subgroup of $SO(2, 1)$,

$$[\hbar^{-1}\mathcal{R}, L_{\pm}] = \pm L_{\pm} \tag{2.19a}$$

$$[L_{+}, L_{-}] = -2\hbar^{-1}\mathcal{R}. \tag{2.19b}$$

With these commutators, the time independence of the generators may be established by use of the formula

$$\frac{dC}{dt} = \frac{i}{\hbar}[H, C] + \frac{\partial C}{\partial t}. \tag{2.20}$$

It follows from (2.20) that all three generators are time-independent. Note however, D and K do not commute with the Hamiltonian; their total time derivative vanishes owing to the explicit time-dependence seen in (2.15b) and (2.15c).

C. *Combined Symmetries*

The Casimir operator for $SO(2, 1)$ is

$$\mathcal{J}^2 = \mathcal{R}^2 - \mathcal{S}^2 - D^2 = \tfrac{1}{2}(KH + HK) - D^2. \tag{2.21}$$

The angular momentum (2.3) commutes with the conformal generators since they are rotational scalars, and the total symmetry group is $SO(2, 1) \times U(1)$. The $SO(2, 1)$ Casimir (2.21) may be expressed in terms of the angular momentum. From (2.3b) and (2.15) it follows that (2.21) also is given by

$$\mathcal{J}^2 = \frac{1}{4}(J - \hbar\nu)^2 - \frac{\hbar^2}{4}. \tag{2.22}$$

Therefore, $\mathcal{J}^2$ is diagonalized when angular momentum is,

$$\begin{gathered} J = \hbar j \qquad j = 0, \pm 1, \pm 2, \ldots \\ \mathcal{J}^2 = \frac{\hbar^2}{4}(j - \nu)^2 - \frac{\hbar^2}{4}. \end{gathered} \tag{2.23}$$

Upon defining the Casimir eigenvalue by

$$\mathcal{J}^2 = \hbar^2 d(d-1) \tag{2.24a}$$

we find

$$d = \tfrac{1}{2} \pm \tfrac{1}{2}|j - \nu|. \tag{2.24b}$$

We shall show below that only the upper sign is acceptable, hence

$$2d - 1 = |j - \nu| \geqslant 0. \tag{2.24c}$$

III. SCHRÖDINGER THEORY

Group theory is not needed to solve the time-independent Schrödinger equation (1.9). Here we reproduce known results [1–3] by techniques used to solve related problems in $(2+1)$-dimensional gravity [3, 4].

Observe that the vector potential (1.4) can also be written as

$$\mathbf{A}(\mathbf{r}) = \frac{\Phi}{2\pi} \nabla\theta = \frac{c\hbar}{e} \nu \nabla\theta. \tag{3.1}$$

Hence (1.9) requires

$$-\frac{\hbar}{2M} (\nabla - i\nu \nabla\theta)^2 \psi_E(\mathbf{r}) = E\psi_E(\mathbf{r}) \tag{3.2}$$

whose solutions necessarily have the form

$$\psi_E(\mathbf{r}) = e^{i\nu\theta} \psi_k^0(r, \theta), \tag{3.3}$$

where ψ_k^0, although satisfying the free equation,

$$(\nabla^2 + k^2) \psi_k^0(r, \theta) = 0, \qquad k^2 = 2ME/\hbar^2 \tag{3.4}$$

is not a conventional plane wave owing to a non-trivial boundary condition,

$$\psi_k^0(r, 2\pi) = e^{-i2\pi\nu} \psi_k^0(r, 0) \tag{3.5}$$

which must be met so that $\psi_E(\mathbf{r})$ be single-valued. Since (3.4) holds, ψ_k^0 may be expressed as a superposition of plane waves; we choose a contour integral representation [3, 4],

$$\psi_k^0(r, \theta) = \oint_C \frac{dz}{2\pi} e^{i\mathbf{k}(z)\cdot\mathbf{r}} \rho(z). \tag{3.6a}$$

Here $\mathbf{k}(z) = (k \cos z, k \sin z)$, and (3.4) is obviously obeyed. The contour C and the weight function ρ must still be determined so that (3.5) is satisfied; alternatively so that $\psi_E(\mathbf{r})$, given by

$$\psi_E(\mathbf{r}) = e^{i\nu\theta} \oint_C \frac{dz}{2\pi} e^{i\mathbf{k}(z)\cdot\mathbf{r}} \rho(z) \tag{3.6b}$$

will be single-valued.

We determine C and ρ by considering the scattering problem, the radial equation and the phase shifts.

The *Ansatz* $u_E^j(r)\, e^{ij\theta}/\sqrt{2\pi}$ is made for $\psi_E(\mathbf{r})$ in (3.2); j is an arbitrary integer to insure single valuedness, $j=0, \pm 1, \pm 2, \ldots$; $u_E^j(r)$ satisfies the radial equation,

$$\left(-\frac{1}{r}\frac{d}{dr}r\frac{d}{dr}+\frac{(j-\nu)^2}{r^2}\right)u_E^j(r)=k^2u_E^j(r) \tag{3.7}$$

and is given by a Bessel function,

$$u_E^j(r)=\frac{\sqrt{M}}{\hbar}J_{|j-\nu|}(kr). \tag{3.8}$$

The normalization is fixed by

$$\int_0^\infty r\,dr u_E^j(r)\,u_{E'}^j(r)=\delta(E-E') \tag{3.9a}$$

and insures

$$\int_0^\infty dE u_E^j(r)\,u_E^j(r')=\frac{1}{r}\,\delta(r-r') \tag{3.9b}$$

(see Eqs. (A.2), (A.4), (A.8), and (A.12) in the Appendix).

When the plane wave identity

$$e^{ikr\cos\theta}=\sum_{j=-\infty}^{\infty} e^{ij(\theta+\pi/2)}J_j(kr) \tag{3.10}$$

is recalled, we are led to form the scattering solution by

$$\psi_E(\mathbf{r})=\sum_{j=-\infty}^{\infty} e^{i(\delta_j+(\pi/2)j)}u_E^j(r)\frac{e^{ij\theta}}{\sqrt{2\pi}}, \tag{3.11}$$

where the phase shift δ_j of $u_E^j(r)$ relative to $J_j(kr)$ is identified from their large r asymptotes,

$$\delta_j=\begin{cases}\nu\pi/2 & j>[\nu]\\ -\nu\pi/2-j\pi & j\leqslant[\nu]\end{cases}. \tag{3.12}$$

Here the brackets [ ] indicate integer part. Thus

$$\begin{aligned}\psi_E(\mathbf{r})=&\sqrt{\frac{M}{2\pi\hbar^2}}\sum_{j=[\nu]+1}^{\infty} e^{i\pi(\nu+j)/2}J_{j-\nu}(kr)e^{ij\theta}\\ &+\sqrt{\frac{2M}{\pi\hbar^2}}\sum_{j=-\infty}^{[\nu]} e^{-i\pi(\nu+j)/2}J_{\nu-j}(kr)e^{ij\theta}.\end{aligned} \tag{3.13}$$

The sums are performed by using the Schläfli contour representation for the Bessel function,

$$J_\alpha(kr) = e^{i\pi\alpha/2} \oint_{C_s} \frac{dz}{2\pi} e^{-ikr\cos z} e^{iz\alpha}. \tag{3.14}$$

The Schläfli contour C_s begins at $z = -3\pi/2 + i\infty$, descends to slightly above the real axis, passes from $z = -3\pi/2 + i(0^+)$ to $z = \pi/2 + i(0^+)$, and ascends to $z = \pi/2 + i\infty$. The sums are now geometric, and give for the two terms in (3.13), respectively,

$$\begin{aligned}
\psi_E(\mathbf{r}) &= \left(\frac{M}{2\pi\hbar^2}\right)^{1/2} \oint_{C_s} \frac{dz}{2\pi} e^{-ikr\cos z} e^{i([\nu]\pi - \{\nu\}z + [\nu]\theta)} \frac{-1}{1+e^{-i(z+\theta)}} \\
&\quad + \left(\frac{M}{2\pi\hbar^2}\right)^{1/2} \oint_{C_s} \frac{dz}{2\pi} e^{-ikr\cos z} e^{-i([\nu]\pi - \{\nu\}z - [\nu]\theta)} \frac{1}{1+e^{i(z-\theta)}} \\
&= \left(\frac{M}{2\pi\hbar^2}\right)^{1/2} \oint_{C_{-s}} \frac{dz}{2\pi} e^{-ikr\cos z} e^{i([\nu]\pi + \{\nu\}z + [\nu]\theta)} \frac{1}{1+e^{i(z-\theta)}} \\
&\quad + \left(\frac{M}{2\pi\hbar^2}\right)^{1/2} \oint_{C_s} \frac{dz}{2\pi} e^{-ikr\cos z} e^{i([\nu]\pi + \{\nu\}z + [\nu]\theta)} \frac{1}{1+e^{i(z-\theta)}}
\end{aligned} \tag{3.15a}$$

$$\{\nu\} \equiv \nu - [\nu].$$

In passing from the first to the second equality, the change of variable $z \to -z$ is performed in the first integral. As a consequence, the integration contour for that integral, now called C_{-s}, becomes the mirror image of the Schläfli contour C_s. (C_{-s} starts from $3\pi/2 - i\infty$, ascends to $3\pi/2$ below the real axis, passes to $-\pi/2$ and descends to $-\pi/2 - i\infty$.) As a further consequence, the integrands of the two contour integrals become identical (we use $e^{i[\nu]\pi} = e^{-i[\nu]\pi}$). To proceed, contours are shifted: C_{-s} is shifted by $\pi/2$ to the left, and C_s by $\pi/2$ to right, so that the vertical portions of both contours are at $z = \pm\pi$. The last step is to redefine the integration variable by $z = -z' + \theta - \pi$. The z' integral now runs over the contour C depicted in Fig. 1a, and $\psi_E(\mathbf{r})$ is represented by (z' is renamed z)

$$\begin{aligned}
\psi_E(\mathbf{r}) &= \left(\frac{M}{2\pi\hbar^2}\right)^{1/2} e^{i\nu\theta} \oint_C \frac{dz}{2\pi} e^{ikr\cos(z-\theta)} \frac{e^{-i\{\nu\}z}}{1-e^{-iz}} \\
&= \left(\frac{M}{2\pi\hbar^2}\right)^{1/2} e^{i\nu\theta} \oint_C \frac{dz}{2\pi} e^{i\mathbf{k}(z)\cdot\mathbf{r}} \frac{e^{-i\{\nu\}z}}{1-e^{-iz}}.
\end{aligned} \tag{3.15b}$$

(A constant phase factor has been suppressed.)

Thus we have derived the representation (3.6b) with the contour C as in Fig. 1a, and $\rho(z)$ given by

$$\rho(z) = \left(\frac{M}{2\pi\hbar^2}\right)^{1/2} \frac{e^{-i\{\nu\}z}}{1-e^{-iz}}. \tag{3.16}$$

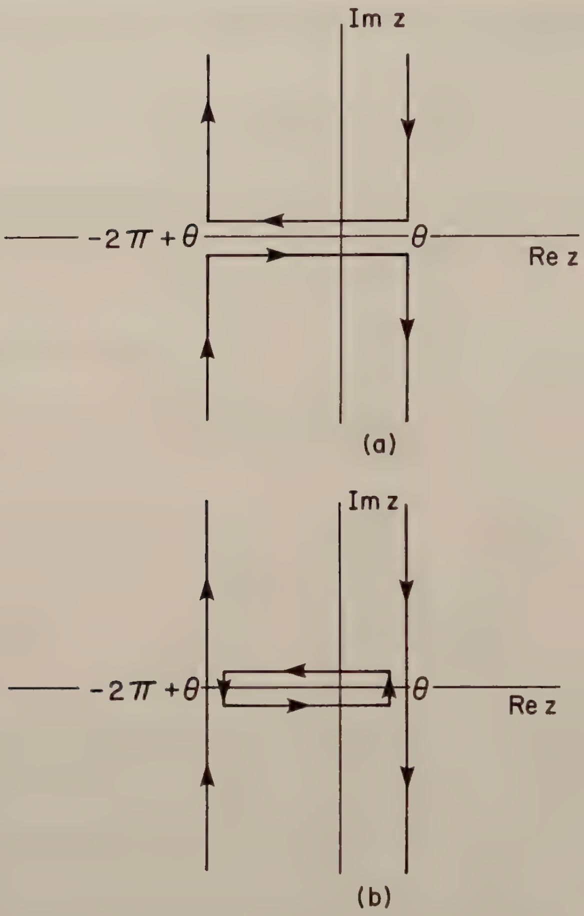

FIG. 1. (a) Integration contour C for the scattering wave function (3.15b). The pole at the origin in avoided. (b) Contour $\tilde{C}$ equivalent to contour C. The pole at the origin is enclosed giving rise to the incoming wave. The vertical contours produce the scattered wave.

That $\psi_E(\mathbf{r})$ as given by (3.15b) satisfies (3.2) is obvious from (3.15b); that it is single-valued—periodic in θ with 2π period—is more easily seen in (3.15a).

The contour C avoids the pole in $\rho(z)$ at $z=0$. However, we may alternatively enclose the pole, and replace the contour C by the three-segmented contour $\tilde{C}$, depicted in Fig. 1b. The portion encircling the pole is evaluated by Cauchy's residue theorem, contributing $(M/2\pi\hbar^2)^{1/2}\, e^{i(kr\cos\theta+\nu\theta)}$; the portions arising from the vertical axes are presented in terms of real integrals by setting $z=\theta-2\pi+iy$ and $z=\theta+iy$. Evidently this separation decomposes the total scattering wave function $\psi_E(\mathbf{r})$ into an incoming wave (pole contribution) and the scattered wave (vertical contour contributions),

$$\psi_E(\mathbf{r})=\left(\frac{M}{2\pi\hbar^2}\right)^{1/2}\left(\psi_E^{(\mathrm{in})}(\mathbf{r})+\psi_E^{(\mathrm{sc})}(\mathbf{r})\right) \tag{3.17a}$$

$$\psi_E^{(\mathrm{in})}(\mathbf{r})=e^{i(kr\cos\theta+\nu\theta)} \tag{3.17b}$$

$$\psi_E^{(\mathrm{sc})}(\mathbf{r})=e^{i[\nu]\theta}e^{i\nu\pi}\sin\nu\pi\int_{-\infty}^{\infty}\frac{dy}{\pi}\,e^{ikr\cosh y}\,\frac{e^{\{\nu\}y}}{e^{y-i\theta}-1}. \tag{3.17c}$$

The large-r asymptote of $\psi_E^{(\mathrm{sc})}(\mathbf{r})$ defines the scattering amplitude $f(\theta)$ through the formula

$$\psi_E^{(\mathrm{sc})}(\mathbf{r})\xrightarrow[r\to\infty]{}\sqrt{\frac{i}{r}}\,f(\theta)\,e^{ikr}. \tag{3.18}$$

Although the integral (3.17c) for $\psi_E^{(\mathrm{sc})}(\mathbf{r})$ cannot be performed, its limit at large r can be evaluated. The circular wave form (3.18) is found, with scattering amplitude

$$f(\theta)=\frac{1}{\sqrt{2\pi k}}\,e^{-i\{\nu\}\theta}e^{i(\nu+1/2)(\theta+\pi)}\,\frac{\sin\nu\pi}{\sin\theta/2}. \tag{3.19}$$

Equations (3.17b) and (3.19) are essentially the results of Aharonov and Bohm [1]; note especially that the incoming wave is not a plane wave, but is modulated by the additional phase $e^{i\nu\theta}$. Ruijsenaars [2] finds a plane incoming wave $e^{ikr\cos\theta}$ and a scattering amplitude containing δ-functions. This can be reconciled with the above by writing (3.17a) as

$$\psi_E(\mathbf{r})=\left(\frac{M}{2\pi\hbar^2}\right)^{1/2}\left(e^{ikr\cos\theta}+\tilde{\psi}_E^{(\mathrm{sc})}(\mathbf{r})\right), \tag{3.20a}$$

where by construction

$$\tilde{\psi}_E^{(\mathrm{sc})}(\mathbf{r})=e^{ikr\cos\theta}(e^{i\nu\theta}-1)+\psi_E^{(\mathrm{sc})}(\mathbf{r}). \tag{3.20b}$$

Since a plane wave possesses in its large-r asymptote a circular wave times a "scattering" amplitude that is a delta function, Ruijsenaars' result can be understood as an alternative description of the solution (3.17).

Finally we remark that the energy independence of the phase shifts (3.12), and of the scattering amplitude (3.19) (apart from a kinematical $1/\sqrt{k}$ factor) is a consequence of scale symmetry [5], (2.13b).

IV. GROUP THEORY

We give an algebraic analysis of the charged particle-vortex system, using its $SO(2,1)\times U(1)$ invariance group. The spectrum of $SO(2,1)$ generators is known to be continuous or discrete, depending whether one is considering the non-compact generators or the compact one.[2] Since the Hamiltonian belongs to the former category, it has a continuous spectrum. An algebraic approach is therefore more interesting in the diagonalization of the compact generator $\mathscr{R}$, and then the properties of H follow by further group theoretical reasoning.

A. *Spectrum of $\mathscr{R}$*

The unitary, irreducible representations that diagonalize $\mathscr{J}^2$ and $\mathscr{R}$ are determined by the group algebra (2.17), (2.18), and (2.19), and are well-known [13]. They are labeled by $\hbar\lambda_n$, the eigenvalues of $\mathscr{R}$, and are divided into four distinct types. Two spectral families for $\mathscr{R}$ are unbounded above and below; they are called the *continuous* series. In the other two, the $\mathscr{R}$ spectra are bounded, respectively below or above by $\pm d$, where d is related to the Casimir eigenvalue by (2.24); these are the *discrete* series $D_d^{\pm}$.

$$\begin{aligned} D_d^+ &: \lambda_n = d+n \\ D_d^- &: \lambda_n = -d-n \qquad n=0, 1, 2, \ldots. \end{aligned} \tag{4.1}$$

To ascertain which representation is appropriate to the magnetic vortex, we examine the explicit form of $\mathscr{R}$, given by (2.15) and (2.18). Since it is time independent, we may set $t=0$ to find

$$\mathscr{R} = \frac{Ma}{4}\left(v^2 + \frac{r^2}{a^2}\right). \tag{4.2}$$

This is a non-negative operator, hence its eigenvalues must also be non-negative. Consequently, only the D_d^+ series can occur in our problem. Moreover, the lowest eigenvalue must be non-negative, which means that $d \geqslant 0$. In fact, as we show below, $d \geqslant \frac{1}{2}$, in agreement with (2.24c).

Of course, the angular momentum J is also diagonalized with eigenvalues $\hbar j$, $j=0, \pm 1, \pm 2, \ldots$. Therefore, the eigenstates of $\mathscr{R}$ and J can be represented by $|n, j\rangle$, where we have suppressed the label d, which determines the Casimir eigenvalue, since it is given by j and v. In the coordinate representation (always at $t=0$) we have

$$\langle \mathbf{r} | n, j\rangle = \varphi_n^j(r) \frac{e^{ij\theta}}{\sqrt{2\pi}}, \tag{4.3}$$

where $\varphi_n^j(r)$ is a function, determined below.

An equation for $\varphi_n^j(r)$ follows by considering the eigenvalue equation in the coordinate representation,

$$\langle \mathbf{r} | \mathscr{R} | n, j\rangle = \hbar\lambda_n \langle \mathbf{r} | n, j\rangle = \hbar(d+n)\langle \mathbf{r} | n, j\rangle. \tag{4.4}$$

---

[2] The $SO(2, 1)$ group, its properties and representations are discussed and applied to quantum problems in [13]. However, care must be exercised in using formulas from this reference since some are garbled.

$\mathscr{R}$ is expressed, with the help of (2.15), (2.18), and (2.21), by operators that have simple matrix elements,

$$\mathscr{R} = \frac{1}{2a} K + \frac{a}{2K} (D^2 - i\hbar D + \mathscr{J}^2). \tag{4.5}$$

The coordinate representation of the conformal generator K, at $t = 0$, is easy,

$$K = \frac{Mr^2}{2}, \tag{4.6}$$

that of the dilation operator D is obtained by observing that $\mathbf{r} \cdot M\mathbf{v} = \mathbf{r} \cdot \mathbf{p}$, since $\mathbf{A}$ has no radial component, see (1.4) and (1.5). Thus

$$D = \frac{i\hbar}{2} \left(r \frac{\partial}{\partial r} + 1 \right). \tag{4.7}$$

Of course $\mathscr{J}^2$ is given by its eigenvalue $\hbar^2 d(d-1)$. In this way (4.4) implies

$$\left\{ -\frac{1}{r} \frac{d}{dr} r \frac{d}{dr} + \frac{(2d-1)^2}{r^2} + \frac{M^2}{a^2 \hbar^2} r^2 \right\} \varphi_n^j(r) = \frac{4M}{a\hbar} (d+n)\, \varphi_n^j(r) \tag{4.8}$$

whose normalized solution is given by generalized Laguerre polynomials L_n^{2d-1}.

$$\varphi_n^j(r) = e^{i\alpha_n} \left(\frac{M}{a\hbar} \right)^d \left(\frac{2n!}{\Gamma(n+2d)} \right)^{1/2} r^{2d-1} e^{-Mr^2/2a\hbar} L_n^{2d-1} \left(\frac{M}{a\hbar} r^2 \right). \tag{4.9}$$

Here α_n is a phase, which is still to be determined. It follows from formulas (A.1), (A.2), (A.5), (A.6), and (A.13) given in the Appendix that

$$\int_0^\infty r\, dr \varphi_n^{j*}(r)\, \varphi_{n'}^j(r) = \delta_{nn'} \tag{4.10a}$$

$$\sum_{n=0}^{\infty} \varphi_n^j(r)\, \varphi_n^{j*}(r') = \frac{1}{r} \delta(r - r'). \tag{4.10b}$$

The phase is fixed by considering the operators $L_\pm$, (2.18), which raise and lower eigenvalues of $\mathscr{R}$.[3]

$$L_\pm\, |n, j\rangle = ((d+n)(d+n \pm 1) - d(d-1))^{1/2}\, |n \pm 1, j\rangle. \tag{4.11}$$

---

[3] There is a sign misprint in the corresponding formula (3.13) of Ref. [6].

To evaluate the above in the coordinate representation, we set

$$\hbar L_{\pm} = K/a - \mathscr{R} \pm iD \tag{4.12}$$

and use (4.5), (4.6), and (4.7) to obtain differential recursion relations between φ_n^j and $\varphi_{n\pm 1}^j$. By exploiting known properties of generalized Laguerre polynomials, we learn that the wave functions alternate in sign with n.

Therefore, the eigenfunctions $\varphi_n^j(r)$ are

$$\varphi_n^j(r) = (-1)^n \left(\frac{M}{a\hbar}\right)^d \left(\frac{2n!}{\Gamma(n+2d)}\right)^{1/2} r^{2d-1} e^{-Mr^2/2a\hbar} L_n^{2d-1}\left(\frac{M}{a\hbar} r^2\right). \tag{4.13}$$

For small r they are proportional to r^{2d-1}; requiring regularity at $r=0$ gives $2d-1 \geqslant 0$, as anticipated in (2.24c).

B. *Spectrum of H*

If we were dealing with a compact group, one could reach H from $\mathscr{R}$ by a group rotation, and then the eigenvalues and eigenfunctions of H would be simply determined. In our non-compact problem, this is not possible. One way of reaching the non-compact generators is by analytic continuation [13]. We prefer, however, to use a different method, based on group theoretic reasoning.

Consider the eigenstates of H,

$$H\,|E\rangle = E\,|E\rangle. \tag{4.14}$$

(We take angular momentum also to be diagonal, but do not exhibit the relevant label.) From (2.17) is follows that the effect of D and K on $|E\rangle$ may be realized by differentiation with respect to the continuous eigenvalue E. For D we have from (2.17a)

$$D\,|E\rangle = i\hbar\left(E\frac{d}{dE} + \frac{1}{2}\right)|E\rangle, \tag{4.15}$$

where the inhomogenous term is chosen so that the operator will be Hermitian. The action of K is now uniquely determined by the remaining commutators (2.17b) and (2.17c), as well as by (2.21) and (2.24a),

$$K\,|E\rangle = \hbar^2\left(-E\frac{d^2}{dE^2} - \frac{d}{dE} + \frac{(d-1/2)^2}{E}\right)|E\rangle. \tag{4.16}$$

In order to obtain the eigenfunctions of H in terms of those of $\mathscr{R}$, we need the overlap $\langle n|E\rangle$.

$$|E\rangle = \sum_{n=0}^{\infty} |n\rangle\langle n|E\rangle. \tag{4.17}$$

An equation for $\langle n|E\rangle$ is derived by taking matrix elements of $\mathscr{R}$ and using (2.18a), (4.4), (4.14), and (4.16).

$$\begin{aligned}\langle n|\,\mathscr{R}\,|E\rangle &= \hbar(d+n)\langle n|E\rangle \\ &= \left\{\frac{\hbar^2}{2a}\left(-E\frac{d^2}{dE^2}-\frac{d}{dE}+\frac{(d-\frac{1}{2})^2}{E}\right)+\frac{a}{2}E\right\}\langle n|E\rangle. \end{aligned} \tag{4.18}$$

By consulting the Appendix, it is recognized that $\langle n|E\rangle$ also involves generalized Laguerre polynomials, see (A.1) and (A.3).

$$\langle n|E\rangle = e^{i\beta_n}\left(\frac{n!}{E\Gamma(n+2d)}\right)^{1/2}\left(\frac{2aE}{\hbar}\right)^d e^{-aE/\hbar}L_n^{2d-1}\left(\frac{2aE}{\hbar}\right). \tag{4.19}$$

It further follows from formulas (A.5) and (A.6) given in the Appendix that

$$\sum_{n=0}^{\infty}\langle E|n\rangle\langle n|E'\rangle = \delta(E-E') \tag{4.20a}$$

$$\int_0^{\infty} dE\langle n|E\rangle\langle E|n'\rangle = \delta_{nn'}. \tag{4.20b}$$

The phase $e^{i\beta_n}$ is again evaluated with the help of $L_\pm$, except in the energy representation it is not convenient to use (4.12), but rather

$$\hbar L_\pm = \mathscr{R} - aH \pm iD. \tag{4.21}$$

One finds no variation of phase with n. The overlap therefore is

$$\langle n|E\rangle = \left(\frac{n!}{E\Gamma(n+2d)}\right)^{1/2}\left(\frac{2aE}{\hbar}\right)^d e^{-aE/\hbar}L_n^{2d-1}\left(\frac{2aE}{\hbar}\right). \tag{4.22}$$

This amplitude is non-singular at $E=0$ when $d \geqslant \frac{1}{2}$.

It remains to evaluate the sum (4.17). In the coordinate representation, restoring the angular momentum label, we have

$$\begin{aligned}\langle \mathbf{r}|E, j\rangle &= u_E^j(r)\frac{e^{ij\theta}}{\sqrt{2\pi}} \\ u_E^j(r) &= \sum_{n=0}^{\infty}\varphi_n^j(r)\langle n|E\rangle. \end{aligned} \tag{4.23}$$

Again formulas (A.7), (A.12), (A.13), and (A.14) in the Appendix are used to evaluate the sum. We find

$$u_E^j(r) = \frac{\sqrt{M}}{\hbar}J_{2d-1}(kr). \tag{4.24}$$

That this agrees with (3.8) is established by (2.24c).

In conclusion, we see that the entire quantum mechanical problem of the particle-vortex interaction is described at fixed angular momentum by a single, irreducible, unitary and infinite-dimensional representation of $SO(2, 1)$, with Casimir eigenvalue determined by the difference between angular momentum j and flux quantum ν.

V. ALTERNATE APPROACHES

A. *Alternate Separation of Variables*

While the calculation in the previous Section IV is motivated by the $SO(2, 1)$ invariance group enjoyed by the particle-vortex system, it is also possible to arrive at our equations by separating variables in the time-dependent Schrödinger equation (1.1), not in the conventional fashion (1.9), but in a different way, which is available because of the higher symmetry. We set in (1.1)

$$\psi(t; \mathbf{r}) = \left(1 + \frac{t^2}{a^2}\right)^{-1/2} \exp\left(\frac{i}{2\hbar}\frac{Mr^2 t}{a^2 + t^2}\right) \Psi\left(a \tan^{-1}\frac{t}{a}; \left(1 + \frac{t^2}{a^2}\right)^{-1/2} \mathbf{r}\right). \tag{5.1}$$

Upon defining (compare (2.8) and (2.9))

$$T = a \tan^{-1}\frac{t}{a} \tag{5.2a}$$

$$\mathbf{R} = \left(1 + \frac{t^2}{a^2}\right)^{-1/2} \mathbf{r} = \left(\frac{dt}{dT}\right)^{-1/2} \mathbf{r} \tag{5.2b}$$

it is readily established that $\Psi(T; \mathbf{R})$ satisfies

$$i\hbar \frac{\partial}{\partial T} \Psi(T; \mathbf{R}) = \left\{\frac{1}{2M}\left(\frac{\hbar}{i}\nabla_R - \frac{e}{c}\mathbf{A}(\mathbf{R})\right)^2 + \frac{1}{2a^2} MR^2\right\} \Psi(T; \mathbf{R}). \tag{5.3}$$

Here $\mathbf{A}$ is still the vortex potential (1.4), but now taken as a function of $\mathbf{R}$. The differential operator on the right-hand side of (5.3) may be viewed as a "T-Hamiltonian" H_T, which is T independent; hence the T variable can be separated.

$$\Psi(T; \mathbf{R}) = e^{-2iT\lambda_n/a} \Psi_n(\mathbf{R}). \tag{5.4}$$

We see that $\Psi_n(\mathbf{R})$ is an H_T eigenfunction with eigenvalue $2\hbar\lambda_n/a$. Since H_T may be written as

$$\begin{aligned} H_T &= \frac{M}{2}\left(V^2 + \frac{R^2}{a^2}\right) \\ M\mathbf{V} &= \mathbf{P} - \frac{e}{c}\mathbf{A}(\mathbf{R}) \\ \mathbf{P} &= \frac{\hbar}{i}\nabla_R \end{aligned} \tag{5.5}$$

we further recognize from (4.2) that H_T coincides with $(2/a)\mathscr{R}$, at $t=0$, so that λ_n is just the $\mathscr{R}$ eigenvalue in the D_d^+ discrete series of (4.1). The factor $(1+t^2/a^2)^{-1/2}$ in (5.1) insures that the probability density normalization is unchanged

$$\psi^*(t;\mathbf{r})\,\psi(t;\mathbf{r})\,d^2\mathbf{r}=\Psi^*(T;\mathbf{R})\,\Psi(T;\mathbf{R})\,d^2\mathbf{R}. \tag{5.6}$$

We now see that a solution to the time-dependent Schrödinger equation (1.1) can be constructed from (5.1), (5.2), and (5.4),

$$\begin{aligned}\psi_n(t;\mathbf{r})=&\left(1+\frac{t^2}{a^2}\right)^{-1/2}\exp\left(\frac{i}{2\hbar}\frac{Mr^2t}{a^2+t^2}\right)\\&\times\exp\left(-2i\lambda_n\tan^{-1}\frac{t}{a}\right)\Psi_n\left(\left(1+\frac{t^2}{a^2}\right)^{-1/2}\mathbf{r}\right).\end{aligned} \tag{5.7}$$

Here $\Psi_n(\mathbf{r})$ is an $\mathscr{R}$ eigenfunction, e.g., $\varphi_n^j(r)\,e^{ij\theta}/\sqrt{2\pi}$ of (4.3) and (4.13). The solution (5.7) gives the coordinate representation for a state that has evolved in ordinary time t from an eigenstate of $\mathscr{R}$,

$$\psi_n(t;\mathbf{r})=\langle\mathbf{r}|\,e^{-itH/\hbar}\,|n\rangle. \tag{5.8}$$

B. *Alternate Dynamics*

In the unconventional separation of variables described above, $\mathscr{R}$ emerges as the evolution operator, see (5.3) and (5.5). This may also be achieved in an alternate formulation of dynamics for the particle-vortex system, where a manifestly $SO(2)$ invariant formalism is used. To this end, we define variables,

$$\begin{aligned}\xi_1&=\frac{2ta}{a^2+t^2}\\ \xi_2&=\frac{a^2-t^2}{a^2+t^2}\end{aligned} \tag{5.9a}$$

which form a circle,

$$\xi_1^2+\xi_2^2=1. \tag{5.9b}$$

$\mathscr{R}$ acts linearly on ξ_i by rotation

$$\delta_{\mathscr{R}}\xi_i=-\varepsilon^{ij}\xi_j. \tag{5.10}$$

The circle may be parametrized by an angle $2T/a$, compare (5.2),

$$\begin{aligned}\xi_1&=\sin\frac{2T}{a}\\ \xi_2&=\cos\frac{2T}{a}\\ T&=a\tan^{-1}\frac{t}{a}\end{aligned} \tag{5.11}$$

and $\mathscr{R}$ translates T,

$$\delta_{\mathscr{R}} T = -\frac{a}{2}. \tag{5.12}$$

Also the dynamical variable is redefined as in (5.2),

$$\mathbf{R}(T) = \left(1 + \frac{t^2}{a^2}\right)^{-1/2} \mathbf{r}(t). \tag{5.13}$$

$\mathbf{R}(T)$ transforms under $\mathscr{R}$ with zero weight,

$$\delta_{\mathscr{R}} \mathbf{R} = \frac{a}{2} \frac{d}{dT} \mathbf{R} = \frac{a}{2} \mathbf{V}. \tag{5.14}$$

The action, which in terms of old variables, reads

$$I = \int dt \left(\frac{1}{2} M v^2 + \frac{e}{c} \mathbf{v} \cdot \mathbf{A}(\mathbf{r})\right) \tag{5.15}$$

is expressed in terms of the new variables (5.11) and (5.12) as

$$I = \int dT \left(\frac{1}{2} M V^2 + \frac{e}{c} \mathbf{V} \cdot \mathbf{A}(\mathbf{R}) - \frac{1}{2a^2} M R^2 + \frac{d}{dT}\left(\frac{M R^2}{2a} \tan \frac{T}{a}\right)\right). \tag{5.16}$$

The total derivative contribution may be dropped, leaving a T-translation invariant "T-Lagrangian,"

$$L_T = \frac{1}{2} M V^2 + \frac{e}{c} \mathbf{V} \cdot \mathbf{A}(\mathbf{R}) - \frac{1}{2a^2} M R^2. \tag{5.17}$$

A Legendre transform on L_T gives rise to the "T-Hamiltonian" of (5.5),

$$\begin{aligned} H_T &= \frac{\partial L_T}{\partial \mathbf{V}} \cdot \mathbf{V} - L_T = \frac{1}{2} M \left(V^2 + \frac{R^2}{a^2}\right) \\ \mathbf{P} &= \frac{\partial L_T}{\partial \mathbf{V}} = M\mathbf{V} + \frac{e}{c} \mathbf{A}(\mathbf{R}). \end{aligned} \tag{5.18}$$

Canonical quantization then leads to (5.3).

The above exemplifies the Dirac program of alternative quantization [14], which in quantum field theory is realized by light-cone quantization [15] and radial quantization [16], while another quantum mechanical application is provided by the magnetic monopole [6].

In conclusion we note that there is also available a manifestly $SO(2, 1)$ invariant formalism which makes use of a null three-vector η_A, $\eta_1^2 + \eta_2^2 - \eta_3^2 = 0$, with $\eta_i/\eta_3 = \xi_i$. We do not pursue this here.

C. *Infrared Regularization*

Because

$$\lim_{a \to \infty} \frac{2}{a} \mathscr{R} = H, \tag{5.19}$$

$\mathscr{R}$ provides an infrared (long-range) regularization for the Hamiltonian. The continuous spectrum of H is attained from the discrete spectrum of $\mathscr{R}$ at large quantum numbers. According to (4.4) and (5.19), $\lim_{a \to \infty} (2/a)\, \hbar(d+n) = E$, which is satisfied if a grows as $2\hbar n/E$ for large n. The eigenfunctions of $\mathscr{R}$, $\varphi_n^j(r)$, determine those of H, $u_E^j(r)$, as $\lim_{n \to \infty} \varphi_n^j(r)|_{a=2\hbar n/E}$. The limit is evaluated from (A.11),

$$\varphi_n^j(r) \to (-1)^n \sqrt{\frac{E}{n}}\, u_E^j(r). \tag{5.20}$$

The mismatch in the normalization reflects the fact that φ_n^j is normalized to unity, while u_E^j is continuum orthonormalized to an energy delta function.

VI. CHERN–SIMONS DYNAMICS

Rather than considering the vector potential in (1.2) and (1.3) to be the externally given field (1.4), one may take A_μ as a dynamical variable, governed by the kinetic action of an Abelian gauge theory. The posited action need not consist solely of the conventional Maxwell electrodynamical term,

$$I_{EM} = -\frac{1}{4c} \int d^3x F^{\mu\nu}(x)\, F_{\mu\nu}(x) \tag{6.1}$$

$$F_{\mu\nu} \equiv \partial_\mu A_\nu - \partial_\nu A_\mu \tag{6.2a}$$

$$F_{ij} \equiv -\varepsilon^{ij} B, \qquad F_{0i} \equiv E^i \tag{6.2b}$$

(metric: $g^{\mu\nu} = \mathrm{diag}(1, -1, -1)$), but can also include the Chern–Simons term [17, 18],

$$I_{CS} = \frac{\kappa}{2c} \int d^3x \varepsilon^{\alpha\beta\gamma}\, \partial_\alpha A_\beta(x)\, A_\gamma(x). \tag{6.3}$$

When the action for the matter-gauge field interaction, $I_{\text{interaction}}$, is presented in terms of a conserved matter current, $j^\mu \equiv (c\rho, \mathbf{j})$,

$$-\frac{c^2\, \delta I_{\text{interaction}}}{\delta A_\mu(x)} = j^\mu(x) \tag{6.4}$$

the gauge field equations

$$\partial_\alpha F^{\alpha\mu} + \frac{\kappa}{2} \varepsilon^{\mu\alpha\beta} F_{\alpha\beta} = j^\mu / c \tag{6.5}$$

have an important consequence, which follows from the time component of (6.5),

$$\nabla \cdot \mathbf{E} - \kappa B = \rho. \tag{6.6a}$$

Integrating this Chern–Simons modified Gauss law over all space produces a formula summarizing all that is topologically interesting about the Chern–Simons interaction,

$$\Phi = -\frac{1}{\kappa} Q. \tag{6.6b}$$

(The spatial integral of $\nabla \cdot \mathbf{E}$ vanishes, because the gauge invariant electric field $\mathbf{E}$ decreases at large distance due to damping by the mass κ.) According to (6.6) particles carrying charge Q necessarily possess magnetic flux $\Phi = -(1/\kappa) Q$. Since $B = \nabla \times \mathbf{A}$, we further see that the gauge-variant vector potential $\mathbf{A}$ is long range (so that $\int d^2\mathbf{x}\, \nabla \times \mathbf{A}$ is non-zero) while the gauge-invariant magnetic field B is short-range (so that $\int d^2\mathbf{x}\, B$ converges). In other words we are dealing with a vortex-like object [18].

Since (6.6b) encapsulates the non-routine aspects of three-dimensional gauge theories, it is plausible to consider a truncation of (6.5) so that (6.6b) holds locally in space. This is achieved when the kinetic action for the gauge field is just the Chern–Simons term, with no Maxwell term [19]. Such a model can be viewed as the $\kappa \to \infty$ limit of (6.5); it is a physically meaningful truncation at low energy, or equivalently at large distance, where the lower-derivative Chern–Simons term dominates the higher-derivative Maxwell term.

A. *Equations of Motion and Canonical Formulation*

According to the above, we take for the gauge field kinetic Lagrangian the Chern–Simons term,

$$\begin{aligned} L_{\mathrm{CS}} &= \frac{\kappa}{2c} \int d^2\mathbf{x}\, \varepsilon^{ij} \dot{A}_i(x) A_j(x) - \kappa \int d^2\mathbf{x}\, A_0(x) B(x) \\ I_{\mathrm{CS}} &= \int dt\, L_{\mathrm{CS}}. \end{aligned} \tag{6.7}$$

(Spatial, but not temporal, integration by parts if freely performed.) This shows that the gauge field dynamical variables are the spatial components $A_i(x) \equiv A_i(t, \mathbf{x})$, which depend on the three-vector $x^\mu = (ct, \mathbf{x})$ (denoted for short also by x), while A_0 acts as a Lagrange multiplier.

The matter kinetic Lagrangian for N point particles with masses m_p, $p = 1, \ldots, N$ and coordinates $\mathbf{r}_p(t)$, which serve as the matter dynamical variables, is

$$L_{\text{matter}} = \frac{1}{2} \sum_{p=1}^{N} m_p v_p^2(t). \tag{6.8}$$

(Our use of x as the first component of $\mathbf{r} = (x, y)$ should not be confused with shorthand notation for the three-vector.)

In the interaction Lagrangian

$$L_{\text{interaction}} = \frac{1}{c} \sum_{p=1}^{N} e_p \mathbf{v}_p(t) \cdot \mathbf{A}(t, \mathbf{r}_p(t)) - \sum_{p=1}^{N} e_p A_0(t, \mathbf{r}_p(t)) \tag{6.9a}$$

the e_p are the charges carried by the particles and the notation $A_\mu(t, \mathbf{r}_p(t))$ or $A_\mu(\mathbf{r}_p)$ for short, denotes an object that acts as a dynamical variable in two ways: as a field A_μ and also through its dependence on $\mathbf{r}_p(t)$. This double function may be separated by presenting the interaction Lagrangian as

$$L_{\text{interaction}} = -\frac{1}{c} \int d^2\mathbf{x}\, A_\mu(x)\, j^\mu(x), \tag{6.9b}$$

where the conserved current j^μ depends on the matter dynamical variables,

$$j^\mu(x) = \sum_{p=1}^{N} e_p v_p^\mu(t)\, \delta^2(\mathbf{x} - \mathbf{r}_p(t)) = (c\rho(x), \mathbf{j}(x)) \tag{6.10a}$$

$$v_p^\mu \equiv (c, \mathbf{v}_p). \tag{6.10b}$$

The Euler–Lagrange equations of motion consist of the Lorentz force equation for the matter variables,

$$m_p \dot{v}_p^i = e_p \left(E^i(\mathbf{r}_p) + \frac{1}{c} \varepsilon^{ij} v_p^j B(\mathbf{r}_p) \right) \tag{6.11}$$

and a field-current identity that relates the electromagnetic fields to the matter currents,

$$E^i(x) = \frac{1}{c\kappa} \varepsilon^{iju} j^j(x) \tag{6.12a}$$

$$B(x) = -\frac{1}{\kappa} \rho(x). \tag{6.12b}$$

In a canonical formulation, we recognize from (6.7), (6.8), and (6.9) that the phase-space variables are $\mathbf{r}_p$, $\mathbf{p}_p = m_p \mathbf{v}_p + (e_p/c)\, \mathbf{A}(\mathbf{r}_p)$ and $\mathbf{A}(\mathbf{x})$. The symplectic structure of the matter coordinates is conventional, leading to conventional Poisson brackets for $\mathbf{r}_p$ and $\mathbf{p}_p$. Not so for the gauge fields: since the Lagrangian (6.7) is first order in time-derivatives, the Poisson bracket is [20]

$$[A_i(\mathbf{x}), A_j(\mathbf{y})]_{\mathrm{PB}} = -\frac{c}{\kappa}\,\varepsilon^{ij}\,\delta(\mathbf{x}-\mathbf{y}). \tag{6.13}$$

(Quantities that are bracketed are at equal time, so their time argument is suppressed.)

The Hamiltonian arising from the total Lagrangian—the sum of (6.7), (6.8), and (6.9)—is

$$H = \frac{1}{2}\sum_{p=1}^{N} m_p v_p^2 + \int d^2\mathbf{x}\, A_0(x)(\kappa B(x) + \rho(x)). \tag{6.14a}$$

It is recognized that the Lagrange multiplier A_0 may be set to zero (by choosing the Weyl gauge) provided Eq. (6.12b) is imposed as a constraint. Thus the Hamiltonian is just the free particle one,

$$H = \frac{1}{2}\sum_{p=1}^{N} m_p v_p^2. \tag{6.14b}$$

Let us now discuss the equations of motion for a single particle, $N=1$ and subscript p suppressed. The force in Eq. (6.11) arises from the electromagnetic fields at the particle position $\mathbf{r}$; by (6.12) they are given by the charge and current densities evaluated at $\mathbf{x}=\mathbf{r}$. However, from (6.10) we see that at $\mathbf{x}=\mathbf{r}$ there appears the undefined quantity $\delta(\mathbf{r}-\mathbf{r})$—the density function of a point particle at its position. Fortunately this singular object is multiplied by a factor that vanishes, since according to (6.10) and the field-current identity (6.12)

$$E^i(\mathbf{x}) + \frac{1}{c}\,\varepsilon^{ij}v^j B(\mathbf{x}) = \frac{1}{c\kappa}\,\varepsilon^{ij}(j^j(x) - v^j\rho(x)) = \frac{1}{c\kappa}\,\varepsilon^{ij}(v^j - v^j)\,\delta(\mathbf{x}-\mathbf{r}).$$

This vanishes unambiguously; therefore we shall take it to be zero also at $\mathbf{x}=\mathbf{r}$. In other words the charge and current densities are regulated by non-singular expressions for the evaluation of the self-interaction, which is then shown to vanish.

With this prescription, particles interacting through Chern–Simons gauge fields do not experience self-interactions. Equations (6.10), (6.11), and (6.12) combine to give for the particle coordinates a closed equation of motion, free from undefined contributions,

$$m_p \dot{v}_p^i = \varepsilon^{ij}\frac{e_p}{c\kappa}\sum_{q\neq p} e_q(v_q^j - v_p^j)\,\delta^2(\mathbf{r}_p - \mathbf{r}_q). \tag{6.15a}$$

The remaining gauge field equation (6.12a) leaves in the gauge $A_0=0$

$$\dot{A}^i(\mathbf{x}) = -\frac{1}{\kappa}\,\varepsilon^{ij}\sum_{p=1}^{N} e_p v_p^j\,\delta(\mathbf{x}-\mathbf{r}_p). \tag{6.15b}$$

To derive (6.15) as a Hamiltonian equation from (6.14b), the brackets with velocities are needed. It follows from the canonical brackets that

$$[m_p v_p^i, m_p v_q^j]_{\mathrm{PB}} = -\frac{1}{c}\,\varepsilon^{ij}\left(\delta_{pq} e_p B(\mathbf{r}_p) + \frac{1}{\kappa}\, e_p e_q\, \delta^2(\mathbf{r}_p - \mathbf{r}_q)\right). \tag{6.16a}$$

The first term in the right-hand side parentheses is present because velocities differ from momenta by the vector potential, see (1.7c), the second because the vector potentials possess a non-vanishing bracket, see (6.13). Also we have

$$[m_p v_p^i, A^j(\mathbf{x})]_{\mathrm{PB}} = \frac{1}{\kappa}\,\varepsilon^{ij} e_p\, \delta^2(\mathbf{x} - \mathbf{r}_p). \tag{6.16b}$$

Brackening **A** with the Hamiltonian given in (6.14b) readily reproduces (6.15b) with the help of (6.16b), but the equation for $m_p \dot{\mathbf{v}}_p$ emerges with the help of (6.16a) in the form (6.11), beset by self-interactions and ambiguities, rather than in the well-defined from (6.15a). Indeed, we see that (6.16a) itself suffers from ill-defined self-interaction ($p = q$) expressions. To remedy this defect and to reproduce (6.15a) canonically, we replace the magnetic field in (6.16a) by the charge density, thus satisfying the constraint (6.12b).

At this stage we can pass to quantum mechanics. The Hamiltonian operator H is taken without field and interaction contributions as in (6.14b), and the velocity commutator is postulated from (6.16a), with the constrained B field expressed in terms of the charge density.

$$\begin{aligned}[m_p v_p^i, m_q v_q^j] &= i\frac{\hbar}{c\kappa}\,\varepsilon^{ij}\left(e_p e_q\, \delta^2(\mathbf{r}_p - \mathbf{r}_q) - \delta_{pq} \sum_{n=1}^{N} e_p e_n\, \delta^2(\mathbf{r}_p - \mathbf{r}_n)\right) \\ &= i\frac{\hbar}{c\kappa}\,\varepsilon^{ij}\left((1 - \delta_{pq})\, e_p e_q\, \delta^2(\mathbf{r}_p - \mathbf{r}_q) - \delta_{pq} \sum_{n \neq p} e_p e_n\, \delta^2(\mathbf{r}_p - \mathbf{r}_n)\right).\end{aligned} \tag{6.17a}$$

The remaining commutators are conventional

$$[r_p^i, m_q v_q^j] = i\hbar\, \delta^{ij}\, \delta_{pq} \tag{6.17b}$$

$$[r_p^i, r_q^j] = 0. \tag{6.17c}$$

It is straightforward to verify that the equation of motion (6.15a), properly symmetrized, is reproduced by commuting $m_p v_p^i$ with H. The consistency of the postulated commutator (6.17a) is established by recognizing that (6.17a) is realized in the formula

$$m_p v_p^i = p_p^i - \frac{e_p}{c}\frac{1}{2\pi\kappa}\,\varepsilon^{ij} \sum_{q \neq p} e_q \frac{(r_p^j - r_q^j)}{|\mathbf{r}_p - \mathbf{r}_q|^2}. \tag{6.18}$$

This in turn shows that the effective Lagrangian for particle motion is [9]

$$L_{\text{effective}} = \sum_{p=1}^{N} \left(\frac{1}{2} m_p v_p^2 + \frac{e_p}{c} \mathbf{v}_p \cdot \mathbf{a}_p \right) \tag{6.19a}$$

$$\begin{aligned} \mathbf{a}_p^i(\mathbf{r}_1, \ldots, \mathbf{r}_N) &= \frac{1}{2\pi\kappa} \varepsilon^{ij} \sum_{q \neq p} e_q \frac{(r_p^j - r_q^j)}{|\mathbf{r}_p - \mathbf{r}_q|^2} \\ &= \frac{1}{2\pi\kappa} \varepsilon^{ij} \frac{\partial}{\partial r_p^j} \sum_{q \neq p} e_q \ln |\mathbf{r}_p - \mathbf{r}_q| \\ &= -\frac{1}{2\pi\kappa} \frac{\partial}{\partial r_p^i} \sum_{q \neq p} e_q \theta_{pq} \end{aligned} \tag{6.19b}$$

$$\tan \theta_{pq} \equiv \frac{y_p - y_q}{x_p - x_q}$$

$$L_{\text{effective}} = \frac{1}{2} \sum_{p=1}^{N} m_p v_p^2 + \frac{1}{2\pi c\kappa} \sum_{p,q=1,\, p<q}^{N} e_p e_q \frac{(\mathbf{v}_p - \mathbf{v}_q) \times (\mathbf{r}_p - \mathbf{r}_q)}{|\mathbf{r}_p - \mathbf{r}_q|^2} \tag{6.19c}$$

and the gauge fields are eliminated.

In the Schrödinger equation, the interaction may be removed at the expense of redefining phases of the N-particle wave function.

$$\Psi(\mathbf{r}_1, \ldots, \mathbf{r}_N) = e^{-i\Theta} \Psi^0(\mathbf{r}_1, \ldots, \mathbf{r}_N) \tag{6.20a}$$

$$\Theta = \sum_{p,q=1,\, p<q}^{N} \nu_{pq} \theta_{pq} \tag{6.20b}$$

$$\nu_{pq} \equiv e_p e_q / 2\pi c\kappa\hbar. \tag{6.20c}$$

The wave function Ψ^0 is governed by the free N-body Hamiltonian,

$$H^0 = \sum_{p=1}^{N} \frac{p_p^2}{2m_p}. \tag{6.21}$$

Nevertheless, Ψ^0 is not a trivial product of free one-body wavefunctions, owing to the complicated boundary conditions obeyed by Ψ^0 as a consequence of its definition in (6.20). These boundary conditions insure that Ψ is single-valued. Of course Ψ^0 is a *superposition* of free, one-body wave functions and in the two-body case can be explicitly determined as follows.

Because total momentum is a constant of motion, see below, it is clear that in the two-body problem, motion in the relative coordinate $\mathbf{r} = \mathbf{r}_1 - \mathbf{r}_2$ is governed by the Hamiltonian (1.2) with M reduced mass, $M^{-1} = m_1^{-1} + m_2^{-1}$ and $\nu = e_1 e_2 / 2\pi c\kappa\hbar$. In the center-of-mass frame [vanishing total momentum] the superposition which determines Ψ^0 is explicitly known from (3.15),

$$\Psi^0(\mathbf{r}_1, \mathbf{r}_2) = \oint dz\, \psi_1^{(z)}(\mathbf{r}_1)\, \psi_2^{(z)}(\mathbf{r}_2)\, \rho(z). \tag{6.22a}$$

The contour is that of Fig. 1a; the weight function is given in (3.16b), and the one-body wave functions are plane waves, with vanishing total momentum,

$$\psi_1^{(z)}(\mathbf{r}) = e^{i\mathbf{k}(z)\cdot\mathbf{r}} \tag{6.22b}$$

$$\psi_2^{(z)}(\mathbf{r}) = e^{-i\mathbf{k}(z)\cdot\mathbf{r}}. \tag{6.22c}$$

As yet we do not have a similar closed form for the N-body wave function. The problem is reminiscent of the δ-function interaction in one dimension. There too the many-body wave function is obtained by superposing one-body wave functions in a fashion prescribed by the Bethe *Ansatz*. Perhaps similar ideas will prove useful here.

B. *Symmetries—General Discussion*

A transformation, which may be a symmetry operation, is effected on the particle coordinates,

$$\mathbf{r}_p(t) \to \mathbf{r}_p(t) + \delta\mathbf{r}_p(t, \mathbf{r}_p(t)). \tag{6.23}$$

Also the gauge potential $A_\mu(x)$ transforms: we assume that associated with (6.23), there is a diffeomorphism of the $(2+1)$-dimensional parameter space x,

$$\delta x^\mu = -g^\mu(x) \tag{6.24a}$$

and that the vector potential transforms by the Lie derivative,

$$\delta A_\mu = g^\nu\, \partial_\nu A_\mu + \partial_\mu g^\nu A_\nu = g^\nu F_{\nu\mu} + \partial_\mu (g^\nu A_\nu). \tag{6.24b}$$

Regardless of the form of g^μ, the kinetic action for the gauge field does not change under (6.24b), because the Chern–Simons term is a topological invariant; the kinetic Lagrangian (6.7) changes by a time derivative,

$$\delta L_{\mathrm{CS}} = \frac{\kappa}{2c} \frac{d}{dt} \int d^2\mathbf{x}\, g^0 \varepsilon^{\alpha\beta\gamma}\, \partial_\alpha A_\beta A_\gamma. \tag{6.25}$$

The interaction Lagrangian, presented as in (6.9a), transforms according to

$$\delta L_{\text{interaction}} = -\sum_{p=1}^{N} e_p \Big\{ (\delta r_p^i\, \partial_i + g^\mu\, \partial_\mu)\, A_0(\mathbf{r}_p) + \frac{v_p^i}{c} (\delta r_p^j\, \partial_j + g^\mu\, \partial_\mu)\, A_i(\mathbf{r}_p)$$
$$+ \left(\frac{d}{cdt}\, \delta r_p^i\right) A_i(\mathbf{r}_p) + \left(\frac{v_p^i}{c}\, \partial_i g^\mu + \partial_0 g^\mu\right) A_\mu(\mathbf{r}_p) \Big\}. \tag{6.26a}$$

The terms involving g^μ, which is evaluated on t and $\mathbf{r}_p$: $g^\mu(t, \mathbf{r}_p(t))$, arise from the Lie derivative (6.24b); the remaining terms are the transformation of the particle coordinates, (6.23). In the last contribution to (6.26a) we recognize the total time derivative of $g^\mu(t, \mathbf{r}_p(t))$; hence the final expression for the response of the interaction Lagrangian to the transformation (6.23), (6.24b) is

$$\delta L_{\text{interaction}} = -\sum_{p=1}^{N} e_p \left\{ (\delta r_p^i\, \partial_i + g^\mu\, \partial_\mu)\, A_0(\mathbf{r}_p) + \left(\frac{d}{c\,dt} g^0\right) A_0(\mathbf{r}_p) + \frac{v_p^i}{c} (\delta r_p^j\, \partial_j + g^\mu\, \partial_\mu)\, A_i(\mathbf{r}_p) + \left(\frac{d}{c\,dt}\delta r_p^i + \frac{d}{c\,dt} g^i\right) A_i(\mathbf{r}_p) \right\}. \tag{6.26b}$$

Finally there is the transformation of the particle kinetic Lagrangian,

$$\delta L_{\text{particle}} = \sum_{p=1}^{N} m_p \mathbf{v}_p \cdot \frac{d}{dt} \delta \mathbf{r}_p. \tag{6.27}$$

We now consider several interesting symmetry transformations, for which $\delta L_{\text{interaction}}$ and $\delta L_{\text{particle}}$ are a total time derivative,

$$\delta L_{\text{interaction}} + \delta L_{\text{particle}} = \frac{d}{dt} X \tag{6.28}$$

and evaluate the corresponding constant of motion, using the formula

$$C = \int d^2\mathbf{x}\, \frac{\partial L}{\partial \dot{\mathbf{A}}} \cdot \delta \mathbf{A} + \sum_{p=1}^{N} \frac{\partial L}{\partial \mathbf{v}_p} \cdot \delta \mathbf{r}_p - \frac{\kappa}{2c} \int d^2\mathbf{x}\, g^0 \varepsilon^{\alpha\beta\gamma}\, \partial_\alpha A_\beta A_\gamma - X. \tag{6.29a}$$

The last term is present as a consequence of (6.28). The next-to-last term arises because of (6.25), but it combines with the first term, which is evaluated from (6.7) and (6.24b). With the help of (6.8) and (6.9) we find

$$C = \sum_{p=1}^{N} \left(m_p \mathbf{v}_p + \frac{e_p}{c} \mathbf{A}(\mathbf{r}_p) \right) \cdot \delta \mathbf{r}_p + \frac{\kappa}{c} \int d^2\mathbf{x}\, g^\mu A_\mu B - X. \tag{6.29b}$$

This may be alternatively presented in terms of the canonical momentum $\mathbf{p}_p = m_p \mathbf{v}_p + (e_p/c)\, \mathbf{A}(\mathbf{r}_p)$,

$$C = \sum_{p=1}^{N} \mathbf{p}_p \cdot \delta \mathbf{r}_p + \frac{\kappa}{c} \int d^2\mathbf{x}\, g^\mu A_\mu B - X. \tag{6.29c}$$

C. *Spatial Translation and Rotation Symmetries*

For translations and rotations of the spatial coordinate $\mathbf{r}_p$ we take

$$\delta r_p^i = a^i \qquad \text{(translation)} \tag{6.30}$$

$$\delta r_p^i = -\varepsilon^{ij} r_p^j \qquad \text{(rotation).} \tag{6.31}$$

Moreover, for the associated infinitesimal diffeomorphism g^μ we take a three vector with vanishing time component (time is not reparametrized in (6.30) and (6.31)) and spatial component equal to $-\delta\mathbf{r}_p$,

$$g^\mu(x) = \begin{pmatrix} 0 \\ -a^i \end{pmatrix} \qquad \text{(translation)} \tag{6.32}$$

$$g^\mu(x) = \begin{pmatrix} 0 \\ \varepsilon^{ij} x^j \end{pmatrix} \qquad \text{(rotation).} \tag{6.33}$$

As a consequence, the gauge potential transforms under rotations and translations as expected,

$$\delta A_\mu(t, \mathbf{x}) = -a^i\, \partial_i A_\mu(t, \mathbf{x}) \qquad \text{(translation)} \tag{6.34}$$

$$\begin{aligned} \delta A_0(t, \mathbf{x}) &= -\varepsilon^{j\kappa} x^j\, \partial_\kappa A_0(t, \mathbf{x}) \\ \delta A_i(t, \mathbf{x}) &= -\varepsilon^{j\kappa} x^j\, \partial_\kappa A_i(t, \mathbf{x}) - \varepsilon^{ij} A_j(t, \mathbf{x}) \qquad \text{(rotation).} \end{aligned} \tag{6.35}$$

$L_{\text{interaction}}$ and L_{particle} are invariant, $[X = 0]$. From (6.29b) and (6.29c) we find the constants of motion: momentum $\mathbf{P}$ and angular momentum J,

$$\begin{aligned} \mathbf{P} &= \sum_{p^2}^{N} \left(m_p \mathbf{v}_p + \frac{e_p}{c} \mathbf{A}(\mathbf{r}_p) \right) + \frac{\kappa}{c} \int d^2\mathbf{x}\, \mathbf{A}\, B \\ &= \sum_{n=1}^{N} \mathbf{p}_p + \frac{\kappa}{c} \int d^2\mathbf{x}\, \mathbf{A}\, B \end{aligned} \tag{6.36}$$

$$\begin{aligned} J &= \sum_{p=1}^{N} \left(\mathbf{r}_p \times \left(m_p \mathbf{v}_p + \frac{e_p}{c} \mathbf{A}(\mathbf{r}_p) \right) \right) + \frac{\kappa}{c} \int d^2\mathbf{x} (\mathbf{x} \times \mathbf{A}) B \\ &= \sum_{p=1}^{N} \mathbf{r}_p \times \mathbf{p}_p + \frac{\kappa}{c} \int d^2\mathbf{x} (\mathbf{x} \times \mathbf{A}) B. \end{aligned} \tag{6.37}$$

The second formula in both expressions makes use of the canonical momentum; the last term is the contribution from the gauge field kinetic Lagrangian. Thus the above formulae for J differs from the corresponding external field expression (2.3) precisely by this field contribution.

The angular momentum for particles interacting through a Chern–Simons gauge field possesses a contribution not present in the external field problem. As explained above and contrary to occasional statements in the literature [10], angular momentum eigenvalues in the external field problem are quantized in conventional integer multiplets of $\hbar$ [11]. Correspondingly, when the gauge field obeys Chern–Simons dynamics the additional contribution to the angular momentum—the last, field-dependent term in (6.37)—lifts the quantization condition by an amount determined by the Chern–Simons coupling.

Next we observe that the magnetic field B in (6.36) and (6.37), may be evaluated using the subsidiary condition (6.12b). This has the effect of removing from the constants of motion all the field contributions, both those coming from the field kinetic term and those coming from the interaction Lagrangian, leaving only the contribution arising from the particle kinetic Lagrangian,

$$\mathbf{P} = \sum_{p=1}^{N} m_p \mathbf{v}_p \tag{6.38}$$

$$J = \sum_{p=1}^{N} m_p \mathbf{r}_p \times \mathbf{v}_p. \tag{6.39}$$

However, it should be reiterated that $m_p \mathbf{v}_p$ is not the canonical momentum, hence the eigenvalues of $J/\hbar$ are not integers, compare with (2.3b).

A physical characterization for the difference between the external field problem and the Chern–Simons dynamical field situation may be given. In the former case, the externally and arbitrarily prescribed gauge field configuration can in fact be physically supported only by the dynamics of a Maxwell gauge field. As a consequence, constants of motion possess gauge field contributions which arise from the momentum, angular momentum, etc., stored in the field. These contributions can frequently (but not always [21]) be collected in the canonical momentum, which differs from the kinematical momentum. On the other hand, as is well-known, Chern–Simons gauge fields give rise only to ephemeral, statistics-changing interactions and particles do not experience the usual electrodynamical forces [22]—a situation familiar from (2+1)-dimensional gravity [3, 4]. As a consequence, constants of motion can be expressed solely in terms of the kinematical, particle coordinates as in (6.38) and (6.39).

The generators (6.38) and (6.39) commute with the Hamiltonian (6.14b) and satisfy the Euclidean algebra

$$[P^i, P^j] = 0 \tag{6.40a}$$

$$[J, P^i] = i\hbar\varepsilon^{ij} P^j. \tag{6.40b}$$

This can be verified with the help of the dynamical algebra (6.17).

D. *Conformal Symmetries*

We consider time reparametrizations for which, as in (2.9),

$$\delta_f t = -f(t) \tag{6.41a}$$

$$\delta_f \mathbf{r}_p(t) = f(t)\, \mathbf{v}_p(t) + \varepsilon \dot{f}(t)\, \mathbf{r}_p(t) \tag{6.41b}$$

and the associated infinitesimal diffeomorphism g^μ is chosen to be

$$g_f^\mu(x) = \begin{pmatrix} cf(t) \\ -\varepsilon \dot{f}(t) x^i \end{pmatrix}. \tag{6.42}$$

It then follows from the general expression (6.26b) that

$$\delta_f L_{\text{interaction}} = \frac{d}{dt}(fL_{\text{interaction}}). \tag{6.43}$$

Just as for the external field problem, the interaction is invariant against arbitrary time reparametrization, with the particle coordinate transforming with arbitrary weight.

The particle kinetic term (6.27) transforms as a total derivative only with the conformal transformations, $f = 1,\ t,\ t^2$ and weight $\varepsilon = -\frac{1}{2}$. In that case

$$\delta_f L_{\text{particle}} = \frac{d}{dt}\left(fL_{\text{particle}} - \frac{1}{4}\ddot{f}\sum_{p=1}^{N} m_p r_{pm}^2\right). \tag{6.44}$$

The constants of motion may then be represented according to (6.29) by

$$\begin{aligned} C_f = {} & \sum_{p=1}^{N}\left(f\frac{1}{2}m_p\mathbf{v}_p^2 - \frac{1}{4}\dot{f}m_p\frac{d}{dt}r_p^2 + \frac{1}{4}\ddot{f}m_p r_p^2\right) \\ & + f\int d^2\mathbf{x}\, A_0(\kappa B + \rho) - \frac{1}{2c}\dot{f}\int d^2\mathbf{x}\mathbf{x}\cdot\mathbf{A}(\kappa B + \rho). \end{aligned} \tag{6.45}$$

Here again the gauge field contribution disappears once the constraint (6.12b) is imposed, leaving for the three respective constants the N-body generalizations of (2.16),

$$H = \frac{1}{2}\sum_{p=1}^{N} m_p v_p^2 \tag{6.46a}$$

$$D = tH - \frac{1}{4}\sum_{p=1}^{N} m_p(\mathbf{r}_p\cdot\mathbf{v}_p + \mathbf{v}_p\cdot\mathbf{r}_p) \tag{6.46b}$$

$$K = -t^2H + 2tD + \frac{1}{2}\sum_{p=1}^{N} m_p r_p^2. \tag{6.46c}$$

Of course H above agrees with the Hamiltonian (6.14b). That the conformal algebra (2.17) is satisfied by these generators follows from (6.17).

E. *Combined Symmetries*

The commutators of the spatial generators **P** and J with the conformal generators H, D, and K can be evaluated, to produce new generators. J commutes with the conformal generators, because they are rotational scalars and **P** commutes with H because momentum is conserved. The remaining commutators of **P** with D and K are

$$[D, \mathbf{P}] = -\frac{i\hbar}{2}\mathbf{P} \tag{6.47}$$

$$[K, \mathbf{P}] = -i\hbar\left(t\mathbf{P} - \sum_{p=1}^{N} m_p\mathbf{r}_p\right). \tag{6.48}$$

Equation (6.47) shows that the scale dimension of the momentum is $\frac{1}{2}$, opposite to that of the coordinate $\mathbf{r}_p$. Since the commutator of two constants of motion is again a constant of motion, the right-hand side of (6.48) shows that center-of-mass motion is free. This is a consequence of the evident invariance of our theory against Galileo boosts, which are generated by $t\mathbf{P} - \sum_{p=1}^{N} m_p \mathbf{r}_p$.

F. *Discussion*

The external field problem possesses the symmetry group of transformations $SO(2, 1) \times U(1)$, the $U(1)$ factor arising from the rotational symmetry. When the vector potential is dynamical, this symmetry is enlarged to include spatial translations and Galileo boosts. The kinematics of the point-particle is always taken to be non-relativistic; only the non-relativistic point-particle kinetic term admits the dilation and special conformal transformation.

When the particle kinetic term is taken to be relativistic

$$L_{\text{particle}} = -\sum_{p=1}^{N} m_p c^2 \sqrt{1 - v_p^2/c^2} \tag{6.49}$$

the two conformal symmetries are lost. On the other hand, in the classical theory the two boosts in the two independent spatial directions are symmetry operations leading to an $ISO(2, 1)$ invariance group—the (2 + 1)-dimensional Poincaré group. However, quantization appears to spoil the Lorentz algebra owing to ordering ambiguities of non-commuting operators. This should be expected, since a relativistic quantum theory with a fixed number of interacting charged particles (and no anti-particles) is not believed to exist. This appears to be still the case even when the interactions are of the ephemeral Chern–Simons variety [23].

APPENDIX: SPECIAL FUNCTIONS

We collect here formulas obeyed by the special functions that arise in our analysis. Derivations can be found in mathematical reference books, and also in Ref. [6], where similar results are recorded.[4]

Define functions related to generalized Laguerre polynomials L_n^α and Bessel functions J_α,

$$f_n^\alpha(z) = \left(\frac{2n!}{\Gamma(n+\alpha+1)}\right)^{1/2} z^{\alpha+1/2} e^{-z^2/2} L_n^\alpha(z^2) \tag{A.1}$$

$$K_\alpha(z) = z^{1/2} J_\alpha(z). \tag{A.2}$$

---

[4] However there is a normalization error $\sqrt{2}$ in the formula of Ref. [6] corresponding to (A.2).

These are the regular solutions to the differential equations

$$\frac{d^2}{dz^2} f_n^\alpha(z) + \left(\frac{\frac{1}{4} - \alpha^2}{z^2} + 2\alpha + 2 + 4n - z^2\right) f_n^\alpha(z) = 0 \tag{A.3}$$

$$\frac{d^2}{dz^2} K_\alpha(z) + \left(\frac{\frac{1}{4} - \alpha^2}{z^2} + 1\right) K_\alpha(z) = 0 \tag{A.4}$$

and obey the following summation/integration formulas,

$$\int_0^\infty dz f_n^\alpha(z)\, f_{n'}^\alpha(z) = \delta_{nn'} \tag{A.5}$$

$$\sum_{n=0}^\infty f_n^\alpha(z)\, f_n^\alpha(z') = \delta(z - z') \tag{A.6}$$

$$\sum_{n=0}^\infty (-1)^n f_n^\alpha(z)\, f_n^\alpha(z') = K_\alpha(zz') \tag{A.7}$$

$$\int_0^\infty dz\, K_\alpha(zz')\, K_\alpha(zz'') = \delta(z' - z'') \tag{A.8}$$

$$\int_0^\infty dz'\, K_\alpha(zz')\, f_n^\alpha(z') = (-1)^n f_n^\alpha(z). \tag{A.9}$$

An integral representation for the Laguerre polynomials

$$L_n^\alpha(z) = \frac{e^z z^{-\alpha/2}}{n!} \int_0^\infty dt e^{-t} t^{n+\alpha/2} J_\alpha(2\sqrt{zt}) \tag{A.10}$$

allows deriving of the following asymptotic formula that links f with K,

$$\lim_{n \to \infty} n^{1/4} f_n^\alpha(z/\sqrt{4n}) = K_\alpha(z). \tag{A.11}$$

The functions f and K are relevant to our analysis because various wave functions/overlaps are expressed by them,

$$u_E^j(r) = \frac{1}{\hbar}\sqrt{\frac{M}{kr}}\, K_{|j-v|}(kr) \tag{A.12}$$

$$\varphi_n^j(r) = (-1)^n \left(\frac{M}{a\hbar r}\right)^{1/4} f_n^{2d-1}\left(\left(\frac{M}{a\hbar}\right)^{1/2} r\right) \tag{A.13}$$

$$\langle n|E\rangle = \left(\frac{a}{2E\hbar}\right)^{1/4} f_n^{2d-1}\left(\left(\frac{2Ea}{\hbar}\right)^{1/2}\right). \tag{A. 14}$$

ACKNOWLEDGMENTS

I thank G. Feinberg for discussing with me relativistic quantum mechanics and acquainting me with Ref. [23]. The help of P. Gerbert in checking several formulas is also acknowledged.

REFERENCES

1. Y. AHARONOV AND D. BOHM, *Phys. Rev.* **115** (1959), 485.
2. S. RUIJSENAARS, *Ann. Phys. (N.Y.)* **146** (1983), 1.
3. P. GERBERT AND R. JACKIW, *Commun. Math. Phys.* **124** (1989), 229.
4. S. DESER, R. JACKIW, AND G. T'HOOFT, *Ann. Phys. (N.Y.)* **152** (1984), 220; G. T'HOOFT, *Commun. Math. Phys.* **117** (1988), 685; S. DESER AND R. JACKIW, *Commun. Math. Phys.* **118** (1988), 495.
5. R. JACKIW, *Phys. Today* **25**, No. 1 (1972), 23; V. DE ALFARO, S. FUBINI, AND G. FURLAN, *Nuovo Cimento A* **34** (1976), 569.
6. R. JACKIW, *Ann. Phys. (N.Y.)* **129** (1980), 183.
7. A. GOLDHABER, *Phys. Rev. D* **16** (1977), 1815; C. CALLIAS, *Phys. Rev. D* **16** (1977), 3068.
8. P. GERBERT, *Phys. Rev. D* **40** (1989), 1346.
9. D. AROVAS, J. SCHRIEFFER, F. WILCZEK, AND A. ZEE, *Nucl. Phys. B* **251** (1985), 117; S. ZHANG, T. HANSON, AND S. KIVELSON, *Phys. Rev. Lett.* **62** (1989), 82; Y.-W. CHEN, F. WILCZEK, E. WITTEN, AND B. HALPERN, *Int. J. Mod. Phys. B* **3** (1989), 1001.
10. F. WILCZEK, *Phys. Rev. Lett.* **48** (1982), 1144; A. GOLDHABER AND R. MACKENZIE, *Phys. Lett. B* **214** (1988), 471; CHEN *et al.*, Ref. [9].
11. A. GOLDHABER, *Phys. Rev. Lett.* **49** (1982), 905; H. LIPKIN AND M. PESHKIN, *Phys. Lett. B* **118** (1982), 385; R. JACKIW AND N. REDLICH, *Phys. Rev. Lett.* **50** (1983), 555.
12. R. FLOREANINI, R. PERCACCI, AND E. SEZGIN, *Nucl. Phys. B* **322** (1989), 255.
13. B. WYBOURNE, "Classical Groups for Physicists," Wiley, New York, 1974.
14. P. DIRAC, *Rev. Mod. Phys.* **21** (1949), 392.
15. J. KOGUT AND D. SOPER, *Phys. Rev. D* **1** (1970), 2901; F. ROHRLICH, *Acta Phys. Austriaca* **32** (1970), 87.
16. S. FUBINI, A. HANSON, AND R. JACKIW, *Phys. Rev. D* **7** (1973), 1732.
17. W. SIEGEL, *Nucl. Phys. B* **156** (1979), 135; R. JACKIW AND S. TEMPLETON, *Phys. Rev. D* **23** (1981), 2291.
18. J. SCHONFELD, *Nucl. Phys. B* **185** (1981), 157; S. DESER, R. JACKIW, AND S. TEMPLETON, *Phys. Rev. Lett.* **48** (1982), 975, *Ann. Phys. (N.Y.)* **140** (1982), 373, (E) **185** (1988), 406.
19. C. HAGEN, *Ann. Phys. (N.Y.)* **157** (1984), 342.
20. S. DESER AND R. JACKIW, *Phys. Lett. B* **139** (1984), 371; L. FADDEEV AND R. JACKIW, *Phys. Rev. Lett.* **60** (1988), 1692.
21. R. JACKIW AND N. MANTON, *Ann. Phys. (N.Y.)* **127** (1980), 257.
22. A. POLYAKOV, *Mod. Phys. Lett. A* **3** (1988), 325; G. DUNNE, R. JACKIW, AND C. TRUGENBERGER, *Ann. Phys. (N.Y.)* **194** (1989), 197; ZHANG *et al.*, CHEN *et al.*, Ref. [9].
23. J. SUCHER, *J. Math. Phys.* **4** (1963), 17.

ANNALS OF PHYSICS **201**, 117–151 (1990)

Ondelettes: The Spinor QED_3 Connection*

GUY BATTLE

Mathematics Department, Texas A& M University,
College Station, Texas 77843

Received September 27, 1989; revised December 14, 1989

It is known that the formal perturbation theory of spinor quantum electrodynamics in *three* space-time dimensions requires no ultraviolet renormalization. We introduce an ondelette cluster expansion (with an infrared cutoff) which converges without counter-terms for weak coupling, thus making the knowledge rigorous. Following the formalism of Lesniewski, we integrate out the bosons at the outset to make the genuine absence of a large-field problem transparent. The combinatoric part of the convergence proof—indeed the *precise* case-by-case definition of the inductive expansion—is reserved for a subsequent paper. In this paper we publicize the language of ondelette diagrams—originally introduced by Federbush—and describe the correspondence to Feynman diagrams. © 1990 Academic Press, Inc.

1. INTRODUCTION

There has been a recent flurry of interest in the theory of spinor quantum electrodynamics in three space-time dimensions [1–9] in spite of the fact that this theory is not the "real thing." The major reason is that it seems to have properties peculiar to its dimension. For example, the topological mass—the abelian version of the Chern–Simons invariant—is defined only in three dimensions [1–3]. Another example could be the nature of the phase transition, which is unknown, although the results of [4, 5] are suggestive, and peculiar to three dimensions.

In spite of the motivation, however, no one has been able to construct the infinite volume limit of this model for either strong or weak coupling, even in the (non-compact) lattice approximation. (For the compact lattice approximation, of course, one can control the limit for strong coupling [10, 11], but the situation avoids the hardest part of the infrared problem.) In the case of weak coupling, the infrared non-renormalizability of spinor QED in $2+1$ dimensions has posed a serious problem.

By contrast, the continuum limit of the theory in a finite volume of space-time for weak coupling is much better understood because spinor QED_3 is also ultraviolet super-renormalizable. In fact, a striking feature of this model is that there are no ultraviolet renormalizations except for the usual Wick-ordering! This means that it should be possible to control the ultraviolet limit of normalized

---

* Supported in part by the National Science Foundation under Grant DMS-8904197.

0003-4916/90 $7.50

Copyright © 1990 by Academic Press, Inc.
All rights of reproduction in any form reserved.

vacuum expectations with a phase cell expansion containing no counter-terms, but even this has never been done. Magnen and Seneor (private communication) controlled the limit with a very complicated expansion several years ago when the technology of constructive field theory was more primitive, but they had to use a number of counter-terms. No publication—nor even a preprint—of their result exists, but their approach is very similar to their treatment of the Yukawa$_3$ model [12].

In this paper and its sequel we introduce an ultraviolet spinor QED_3 cluster expansion with no counter-terms. Our phase cell decomposition is based on ondelettes [13–16], and our expansion is an order of magnitude simpler than any previous expansion of this model.

Let $A_\mu(x)$ denote the Euclidean gauge potential for the free electromagnetic field in three space-time dimensions. We fix the Feynman gauge, so this field is just the vector-valued Gaussian field with mean zero and covariance

$$\langle A_\mu(x) A_\nu(y) \rangle_0 = \delta_{\mu\nu}(-\Delta^{-1})(x, y). \tag{1.1}$$

Consider the $\|\nabla \cdot \|_2$-orthonormal basis in [13] truncated but not completed at the unit-scale level. As we have already pointed out in [13], some of the unit-scale functions needed for the completion do not have exponential fall-off, but this is the result of throwing away functions whose exponential decay have arbitrarily large scale. Here we are imposing our infrared cutoff in the form of an incomplete basis by excluding ondelettes of either type. Thus every ondelette in the expansion has exponential localization with characteristic volume 0(1) or less. Now it is clear from the phase factors in the momentum expressions [13] that the ondelettes are only permuted by the action of the symmetry $Px = -x$. Thus for every pair f, Pf in the incomplete orthonormal set, we substitute

$$\frac{f + Pf}{\sqrt{2}}, \frac{f - Pf}{\sqrt{2}} \tag{1.2}$$

and let $\mathscr{B}$ denote the new orthonormal set. The point is that every function in $\mathscr{B}$ is either odd or even with respect to the symmetry. This choice will be very convenient for a symmetry argument later. Let $\mathscr{B} = \{u_l\}$, where l runs over the even and odd modes. We expand the field in these massless Sobelev ondelettes—i.e.,

$$A_\mu(x) = \sum_l \alpha_{l\mu} u_l(x). \tag{1.3}$$

More precisely, we define the random variables

$$\alpha_{l\mu} = -\int A_\mu \, \Delta u_l, \tag{1.4}$$

which have the simple property

$$\langle \alpha_{k\mu}\alpha_{l\nu}\rangle_0 = \delta_{\mu\nu}\delta_{kl}. \tag{1.5}$$

Our cluster expansion requires no decoupling of boson covariances.

Let $\Psi_\iota(x)$, $\bar{\Psi}_\iota(x)$ be the Osterwalder–Schrader fields [17] and $\langle\cdot\rangle_f$ the free fermi expectation functional. Since we are considering a three-dimensional Euclidean world, the fields are two-component spinors. Consider the Lemarié basis [14, 15] modified at the unit-scale level as described in [13, 16]. Let $\mathscr{F} = \{\psi_k\}$ denote the basis derived from this by the pair replacement (1.2). We expand the fermion field in these L^2-ondelettes,

$$\Psi_\iota(x) = \sum_k L_k^{1/2}\beta_{k\iota}\psi_k(x), \tag{1.6}$$

where L_k denotes the length scale of ψ_k, or rather we define the smeared operators

$$\beta_{k\iota} = L_k^{-1/2}\int \Psi_\iota\psi_k. \tag{1.7}$$

We expand the anti-fermion field—which is independent in the Euclidean world—a little differently,

$$\bar{\Psi}_\varepsilon(x) = \sum_k\sum_\iota L_k^{-1/2}\bar{\beta}_{k\iota}\int S_{\varepsilon\iota}(x-y)\psi_k(y)\,dy \equiv \sum_k\sum_\iota \bar{\beta}_{k\iota}w_k^{(\varepsilon\iota)}(x), \tag{1.8}$$

where

$$S = (-\not\nabla + m)^{-1}, \tag{1.9}$$

m is the fermion mass, and

$$\not\nabla = \sum_{\mu=0}^{2}\gamma_\mu\frac{\partial}{\partial x_\mu}. \tag{1.10}$$

The 2×2 matrices γ_μ, $\mu = 0, 1, 2$, are the Euclidean Dirac matrices in three dimensions—indeed they are the Pauli spin matrices. Thus we are actually defining

$$\bar{\beta}_{k\iota} = L_k^{1/2}\sum_\varepsilon\int \bar{\Psi}_\varepsilon(-\not\nabla + m)_{\iota\varepsilon}\psi_k. \tag{1.11}$$

Since

$$\langle \Psi_\iota(x)\bar{\Psi}_\varepsilon(y)\rangle_f = S_{\iota\varepsilon}(x-y), \tag{1.12}$$

it follows from (1.7) and (1.11) that

$$\langle \beta_{k\iota}\bar{\beta}_{l\varepsilon}\rangle_f = \delta_{kl}\delta_{\iota\varepsilon}. \tag{1.13}$$

Our cluster expansion requires no decoupling of fermi covariances either. The only part of the Feynman–Kac formula [17] that is ever modified by the expansion is the electromagnetic interaction term in the Euclidean Lagrangian. Our choice of scale factors is motivated by [17]

$$\|\Psi_\iota(f)\| = \|\bar{\Psi}_\iota(f)\| = \|D_m^{-1/2} f\|_2, \tag{1.14}$$

$$D_m = (-\Delta + m^2)^{1/2}. \tag{1.15}$$

What we have done is normalize the operator coefficients.

$$\|\beta_{k\iota}\| = L_k^{-1/2}\, \|D_m^{-1/2}\psi_k\|_2 \leqslant c, \tag{1.16}$$

$$\|\bar{\beta}_{k\iota}\| \leqslant \sum_{\varepsilon} L_k^{1/2}\, \|(-\not{\nabla} + m)_{\iota\varepsilon} D_m^{-1/2}\psi_k\|_2 \leqslant c L_k^{1/2}\, \|D_m^{1/2}\psi_k\|_2 \leqslant c, \tag{1.17}$$

where the estimations are easily done in momentum space.

In the a priori definition of our interacting theory we must impose regularizations on the interaction. We then control the vacuum expectation values with a cluster expansion as the regularizations are removed. The convergent expansion *without cutoffs* is the a posteriori definition of the theory.

We choose a finite $\Lambda \subset \mathscr{B}$ and an $M > 0$ for our regularization of the interaction.

$$I_M^\Lambda = \lambda \sum_\mu \sum_{\varepsilon, \iota} \int A_\mu^\Lambda \gamma_\mu^{\iota\varepsilon} : \Psi_\iota \bar{\Psi}_{\varepsilon, M} :, \tag{1.18}$$

where λ is the coupling constant, : : denotes Wick ordering for fermions [17], and

$$A_\mu^\Lambda = \sum_{l \in \Lambda} \alpha_{l\mu} u_l, \tag{1.19}$$

$$\bar{\Psi}_{\varepsilon, M} = M^2 D_M^{-2} \bar{\Psi}_\varepsilon. \tag{1.20}$$

We are leaving all fermi modes and anti-fermi modes in the interaction, in contrast to our choice of cutoff for the boson field. We are imposing the ultraviolet cutoff (1.20) instead, because we need it for the regularization of a Ward identity. Clearly $M^2(p^2 + M^2)^{-1} \to 1$ pointwise as $M \to \infty$, but this particular ultraviolet cutoff preserves the approximate scaling of the estimates on the ordinary integrals in I_M^Λ. Since

$$\bar{\Psi}_{\varepsilon, M} = \sum_k \sum_\iota \bar{\beta}_{k\iota} M^2 D_M^{-2} w_k^{(\varepsilon\iota)} \equiv \sum_k \sum_\iota \bar{\beta}_{k\iota} v_k^{(\varepsilon\iota)}, \tag{1.21}$$

we have

$$I_M^\Lambda = \lambda \sum_\mu \sum_{\varepsilon, \iota} \gamma_\mu^{\iota\varepsilon} \sum_l \alpha_{l\mu} \sum_{k, \bar{k}} \sum_{\iota} : \beta_{k\iota} \bar{\beta}_{\bar{k}\iota} : L_k^{1/2} \int u_l \psi_k v_{\bar{k}}^{(\varepsilon\iota)}, \tag{1.22}$$

where we suppress the dependence of v_k on M. In Section 2 we derive

M-independent bounds on $L_k^{1/2}\int u_l\psi_k v_k^{(\varepsilon\bar{\imath})}$. Clearly $\alpha_{l\mu}$, $\beta_{k\iota}$, $\bar{\beta}_{k\iota}$ are the most natural kinematic observables to use in this phase cell description, and smeared fields can certainly be expanded in these. We consider the normalized expectation

$$\left\langle \prod_{i=1}^{p} \alpha_{l_i\mu_i} \prod_{j=1}^{q} \beta_{k_j\iota_j}\bar{\beta}_{\bar{k}_j\varepsilon_j} \right\rangle_{M,\Lambda}$$

$$\equiv Z_{M,\Lambda}^{-1}\left\langle\left\langle \exp(-I_M^{\Lambda})\cdot \prod_{i=1}^{p} \alpha_{l_i\mu_i} \prod_{j=1}^{q} \beta_{k_j\iota_j}\bar{\beta}_{\bar{k}_j\varepsilon_j} \right\rangle_f\right\rangle_0, \tag{1.23}$$

where

$$Z_{M,\Lambda} = \langle\langle \exp(-I_M^{\Lambda})\rangle_f\rangle_0. \tag{1.24}$$

Remark. $Z_{M,\Lambda}$ and the un-normalized expectation $Z_{M,\Lambda}\cdot$ (1.23) are well-defined because the formal perturbation series actually converges for fixed r and Λ.

THEOREM 1.1. *For sufficiently small* λ, *the limit of* (1.23) *as* $M\to\infty$ *and* Λ *approaches* $\mathscr{B}$ (*in the sense of set inclusion*) *exists.*

We prove this theorem in this paper and its sequel by developing a phase cell cluster expansion for this model. The convergence of the expansion will be uniform in both Λ and M, while each term converges with the removal of these cutoffs. These facts establish the theorem, and the limiting identity can be regarded as an a posteriori definition of the theory with no cutoffs (except the infrared cutoff $\mathscr{B}$).

We are working in an infinite volume, but we are avoiding the long-distance problem with the cutoff $\mathscr{B}$. The fermi fields require no infrared cutoff because they have a mass. At a more technical level, we observe that the fermi mass renders harmless the consequences of completing the Lemarié basis at the unit-scale—i.e., some of the exponentially localized functions ψ_k at the unit-scale level do not have enough vanishing moments, but the corresponding potentials $v_k^{(\varepsilon\iota)}$ still has rapid fall-off.

This paper is more expository than its sequel, which is more concerned with the organization of cases, the precise case-by-case definition of our inductive expansion, and the combinatoric estimation. In this paper we concentrate on the perturbative aspect, which involves just a few expansion steps (two, three, five, etc.), but which motivates the expansion rules. Our expository motivation is three-fold:

(a) We wish to isolate the description of the Ward identity and Furry's Theorem in the ondelette formalism. The application of these identities introduces a new type of inductive expansion step, which we have dubbed an *expansion step of the third kind.*

(b) The issue of renormalization is a perturbative one, so we can argue here that the Wick-ordering of the fermi current is the only renormalization that our expansion needs.

(c) The perturbation theory in our cluster expansion is conveniently described by "ondelette diagrams," which were first suggested by Paul Federbush (private communication). We wish to highlight the correspondence between ondelette diagrams and Feynman diagrams.

Actually, the first major issue to be addressed in the construction of any boson-fermion theory is whether to use the Matthews–Salam formalism [12, 20–24] or the "Gross–Neveu" formalism [25]. In the former case, one "integrates out" the fermions before one develops the expansion, and in the latter case the a priori step is to integrate out the bosons instead. *In the development of our cluster expansion we use the latter.* Since this model does not really have a large field problem, any formalism that allows boson number divergences to develop is not very natural, even if such factorial growths can be cancelled. Thus we have become a convert from the Matthews–Salam formula to the Gross–Neveu-like formula. Moreover, the estimates associated with the former choice seem to require boson mass counterterms for stability as well as for ultraviolet renormalizations. This disease becomes serious in the case of our model, where there are no ultraviolet renormalizations but a stability bound is still needed. In the latter formalism we are rescued by the boundedness of the operators $\beta_{k\iota}$, $\bar{\beta}_{k\iota}$.

Accordingly, we write

$$\prod_{i=1}^{p} \alpha_{l_i\mu_i} = \prod_{l,\mu} \alpha_{l\mu}^{n_{l\mu}} \tag{1.25}$$

and note that (1.23) is just $\prod_{l,\mu} (\partial^{n_{l\mu}}/\partial z_{l\mu}^{n_{l\mu}})[\ \ ]_{z=0}$ applied to

$$Z_{\Lambda,M}^{-1} \left\langle \left\langle \exp(-I_M^{\Lambda}) \prod_{(l,\mu)\in\Lambda_0} e^{z_{l\mu}\alpha_{l\mu}} \right\rangle_0 \prod_{j=1}^{q} \beta_{k_j\iota_j} \bar{\beta}_{k_j\varepsilon_j} \right\rangle_f . \tag{1.26}$$

But explicit computation of the Gaussian expectation yields the operator (with $z_{l\mu}=0$ for $(l,\mu)\in\Lambda\backslash\Lambda_0$)

$$\exp \sum_{(l,\mu)\in\Lambda} \left(z_{l\mu} - \lambda \sum_{\varepsilon,\iota} \gamma_{\mu}^{\iota\varepsilon} \int u_l :\Psi_{\iota} \bar{\Psi}_{\varepsilon,M}: \right)^2 . \tag{1.27}$$

This expression is immediate because the Gaussian is diagonal and the regularized currents commute. Dropping the numerical factor $\exp \sum_{(l,\mu)\in\Lambda_0} z_{l\mu}^2$, we have reduced the problem to controlling

$$\begin{aligned} Z_{\Lambda,M}^{-1} \Bigg\langle \exp\Bigg[&\sum_{(l,\mu)\in\Lambda} \left(\lambda \sum_{\varepsilon,\iota} \gamma_{\mu}^{\iota\varepsilon} \int u_l :\Psi_{\iota} \bar{\Psi}_{\varepsilon,M}: \right)^2 \\ &+ 2 \sum_{(l,\mu)\varepsilon\Lambda_0} z_{l\mu} \lambda \sum_{\varepsilon,\iota} \gamma_{\mu}^{\iota\varepsilon} \int u_l :\Psi_{\iota} \bar{\Psi}_{\varepsilon,M}: \Bigg] \prod_{j=1}^{q} \beta_{k_j\iota_j} \bar{\beta}_{k_j\varepsilon_j} \Bigg\rangle_f . \end{aligned} \tag{1.28}$$

Our cluster expansion is defined in terms of this purely fermionic—but equivalent—theory.

As in the ϕ_3^4 case [19] the cluster expansion includes two basic kinds of expansion steps: decoupling variables to generate factorized expectations and integrating by parts to control the singularities at small length scales. However, unlike the ϕ_3^4 model, this model demands a third kind of expansion step which implements the Ward identity and Furry's Theorem. We reserve the description of this additional kind of step for Section 5. The first step in the expansion is the application of the identity

$$e^{-J^{\Lambda}(z)}=e^{-J^{\Lambda}_{A^c}}e^{J_A(z)}-\int_0^1 ds_1\, e^{-s_1 J^{\Lambda}(z)-(1-s_1)(J_A(z)+J^{\Lambda}_{A^c})}(J^{\Lambda}(z)-J^{\Lambda}_{A^c}-J_A(z)), \tag{1.29}$$

where A is the initial set of fermi modes—including Λ_0—that one is trying to decouple from the rest of the universe, $J^{\Lambda}(z)$ denotes the bracketed quantity in (1.28),

$$J^{\Lambda}_{A^c}=\sum_{l\in\Lambda\setminus A}\sum_{\mu}\left(\lambda\sum_{\varepsilon,\iota}\gamma_{\mu}^{\iota\varepsilon}\sum_{k,\bar{k}\in\mathscr{F}\setminus A}\sum_{\bar{\iota}}{:}\beta_{k\iota}\bar{\beta}_{\bar{k}\bar{\iota}}{:}\, L_k^{1/2}\int u_l\psi_k v_{\bar{k}}^{(\varepsilon\bar{\iota})}\right)^2 \tag{1.30}$$

and $J_A(z)$ is defined by restricting all mode contributions in the $J^{\Lambda}(z)$-expression to A. (The exponental law holds for (1.29) because $J_A(z)$, $J^{\Lambda}_{A^c}$, and $J^{\Lambda}(z)$ commute.) The point of (1.29) is that for an observable $\mathscr{G}$ whose modes are in A,

$$\langle e^{J^{\Lambda}_{A^c}}e^{J_A(z)}\mathscr{G}\rangle_f=\langle e^{J^{\Lambda}_{A^c}}\rangle_f\,\langle e^{J_A(z)}\mathscr{G}\rangle_f. \tag{1.31}$$

This factorization follows from the fact that the free covariance is diagonal with respect to our fermi "variables." Since there is no measure-theoretic notion of functional integration for the fermi expectation, we should be a little more explicit. Expand each exponential in an operator-valued power series and observe that the resulting expansions of expectations converge for fixed Λ. Thus, it suffices to show that

$$\begin{aligned}&\left\langle\prod_{j=1}^{p}{:}\beta_{k_j\iota_j}\bar{\beta}_{\bar{k}_j\bar{\iota}_j}{:}\prod_{j=1}^{n}{:}\beta_{k'_j\iota'_j}\bar{\beta}_{\bar{k}'_j\bar{\iota}'_j}{:}\prod_{j=1}^{N}\beta_{k''_j\iota''_j}\bar{\beta}_{\bar{k}''_j\bar{\iota}''_j}\right\rangle_f\\&\qquad=\left\langle\prod_{j=1}^{p}{:}\beta_{k_j\iota_j}\bar{\beta}_{\bar{k}_j\iota_j}{:}\right\rangle_f\left\langle\prod_{j=1}^{n}{:}\beta_{k'_j\iota'_j}\bar{\beta}_{\bar{k}'_j\bar{\iota}'_j}{:}\prod_{j=1}^{N}\beta_{k''_j\iota''_j}\bar{\beta}_{\bar{k}''_j\bar{\iota}''_j}\right\rangle_f\end{aligned} \tag{1.32}$$

for $k_1,\bar{k}_1,\ldots,k_p,\bar{k}_p\in\mathscr{F}\setminus A$, $k'_1\bar{k}'_1,\ldots,k'_n,\bar{k}'_n$, $k''_1,\bar{k}''_1,\ldots,k''_N,\bar{k}''_N\in A$, provided that the observable $\mathscr{G}$ is also expanded in applying this assertion. As for verifying (1.32), we observe that since these Wick orderings each amount to substraction of a constant, we may drop them from (1.32) without loss. Now by the nature of the free Euclidean fermi expectation [17] and by (1.13) we have

$$\left\langle\prod_{j=1}^{q}\beta_{k_j\iota_j}\bar{\beta}_{\bar{k}_j\bar{\iota}_j}\right\rangle_f=\det_{ij}(\delta_{\iota_i\bar{\iota}_j}\delta_{k_i\bar{k}_j}). \tag{1.33}$$

If $k_1, \bar{k}_1, \ldots, k_p, \bar{k}_p \in \mathscr{F} \setminus A$ and $k_{p+1}, \bar{k}_{p+1}, \ldots, k_q, \bar{k}_q \in A$, then obviously

$$\det_{ij} (\delta_{\iota_i \bar{\iota}_j} \delta_{k_i \bar{k}_j}) = \det_{i,j \leqslant p} (\delta_{\iota_i \bar{\iota}_j} \delta_{k_i \bar{k}_j}) \det_{i,j > p} (\delta_{\iota_i \bar{\iota}_j} \delta_{k_i \bar{k}_j}), \tag{1.34}$$

and so the claim is verified.

In the course of the expansion process, the repeated attempts to decouple variables are occasionally interrupted by a need to "integrate by parts." When one integrates by parts with respect to a fermi "variable" $\beta_{k_0 \iota_0}$, one applies the formula

$$\begin{aligned}
&\Big\langle :\beta_{k_0 \iota_0} \bar{\beta}_{\bar{k}_0 \bar{\iota}_0}: \mathscr{G} \exp \Big(\sum_{k,\bar{k}} \sum_{\iota,\bar{\iota}} P_{k\bar{k},\iota\bar{\iota}}(z) :\beta_{k\iota} \bar{\beta}_{\bar{k}\bar{\iota}}: \\
&\qquad + \sum_{k,\bar{k},k',\bar{k}'} \sum_{\iota,\bar{\iota},\iota',\bar{\iota}'} Q_{k\bar{k}k'\bar{k}',\iota\bar{\iota}\iota'\bar{\iota}'} :\beta_{k\iota} \bar{\beta}_{\bar{k}\bar{\iota}}: :\beta_{k'\iota'} \bar{\beta}_{\bar{k}'\bar{\iota}'}: \Big) \Big\rangle_f \\
&= -\sum_{k} \sum_{\iota} P_{kk_0,\iota\iota_0}(z) \langle \beta_{k\iota} \bar{\beta}_{\bar{k}_0 \bar{\iota}_0} \mathscr{G} \exp(\text{ditto}) \rangle_f \\
&\quad - \sum_{k,k',\bar{k}} \sum_{\iota,\iota',\bar{\iota}} Q_{k\bar{k}k'k_0,\iota\bar{\iota}\iota'\iota_0} \langle :\beta_{k\iota} \bar{\beta}_{\bar{k}\bar{\iota}}: \beta_{k'\iota'} \bar{\beta}_{\bar{k}_0 \bar{\iota}_0} \mathscr{G} \exp(\text{ditto}) \rangle_f \\
&\quad - \sum_{k,k',\bar{k}'} \sum_{\iota,\iota',\bar{\iota}'} Q_{kk_0k'\bar{k}',\iota\iota_0\iota'\bar{\iota}'} \langle \beta_{k_\iota} \bar{\beta}_{\bar{k}_0 \bar{\iota}_0} :\beta_{k'\iota'} \bar{\beta}_{\bar{k}'\bar{\iota}'}: \mathscr{G} \exp(\text{ditto}) \rangle_f,
\end{aligned} \tag{1.35}$$

where the exponent is the interpolated interaction. This identity follows from (1.13) together with the abstract formulation discussed in [26, Sect. 2]. As before, the exponential is expanded and we verify the formula term by term, using anti-commutativity as well as the basic Berezin rules. Similarly our "integration by parts" with respect to $\bar{\beta}_{\bar{k}_0 \bar{\iota}_0}$ is given by

$$\begin{aligned}
&\Big\langle :\beta_{k_0 \iota_0} \bar{\beta}_{\bar{k}_0 \bar{\iota}_0}: \mathscr{G} \exp \Big(\sum_{k,\bar{k}} \sum_{\iota,\bar{\iota}} P_{k\bar{k},\iota\bar{\iota}}(z) :\beta_{k\iota} \bar{\beta}_{\bar{k}\bar{\iota}}: \\
&\qquad + \sum_{k,\bar{k},k',\bar{k}'} \sum_{\iota,\bar{\iota},\iota',\bar{\iota}'} Q_{k\bar{k}k'\bar{k}',\iota\bar{\iota}\iota'\bar{\iota}'} :\beta_{k\iota} \bar{\beta}_{\bar{k}\bar{\iota}}: :\beta_{k'\iota'} \bar{\beta}_{\bar{k}'\bar{\iota}'}: \Big) \Big\rangle_f \\
&= -\sum_{\bar{k}} \sum_{\bar{\iota}} P_{\bar{k}_0\bar{k},\bar{\iota}_0\bar{\iota}}(z) \langle \beta_{k_0 \iota_0} \bar{\beta}_{\bar{k}\bar{\iota}} \mathscr{G} \exp(\text{ditto}) \rangle_f \\
&\quad - \sum_{k,\bar{k},\bar{k}'} \sum_{\iota,\iota',\bar{\iota}} Q_{k\bar{k}\bar{k}_0\bar{k}',\iota\bar{\iota}\bar{\iota}_0\bar{\iota}'} \langle :\beta_{k\iota} \bar{\beta}_{\bar{k}\bar{\iota}}: \beta_{k_0 \iota_0} \bar{\beta}_{\bar{k}'\bar{\iota}'} \mathscr{G} \exp(\text{ditto}) \rangle_f \\
&\quad - \sum_{\bar{k},k',\bar{k}'} \sum_{\bar{\iota},\iota',\bar{\iota}'} Q_{\bar{k}_0\bar{k}k'\bar{k}',\bar{\iota}_0\bar{\iota}\iota'\bar{\iota}'} \langle \beta_{k_0 \iota_0} \bar{\beta}_{\bar{k}\bar{\iota}} :\beta_{k'\iota'} \bar{\beta}_{\bar{k}'\bar{\iota}'}: \mathscr{G} \exp(\text{ditto}) \rangle_f,
\end{aligned} \tag{1.36}$$

where $\mathscr{G}$ does not include $\bar{\beta}_{\bar{k}_0 \bar{\iota}_0}$ when expanded.

Our expansion process is inductive and results in a sum over histories of successive expansion steps, where each step selects a term on the rhs of the decoupling formula or of one of the integration by parts formulae as the case may be. Our

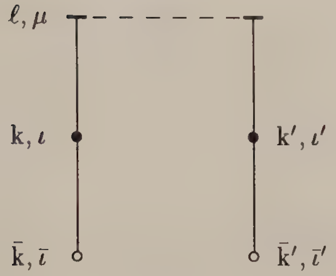
ℓ, μ
k, ι
k′, ι'
$\bar{\mathrm{k}}, \bar{\iota}$
$\bar{\mathrm{k}}', \bar{\iota}'$

FIGURE 1

definition of a *term* is based on expanding the interpolated interaction in boson modes as well as fermi modes. A term has one of the following forms (sometimes with a fermi variable erased):

$$2z_{l\mu}\lambda \sum_{\varepsilon} \gamma_{\mu}^{\iota\varepsilon} L_k^{1/2} :\beta_{k\iota}\bar{\beta}_{\bar{k}\bar{\iota}}: \int u_l \psi_k v_{\bar{k}}^{(\varepsilon\bar{\iota})}, \tag{1.37}$$

$$\lambda^2 \sum_{\varepsilon, \varepsilon'} \gamma_{\mu}^{\iota\varepsilon} \gamma_{\mu}^{\iota'\varepsilon'} :\beta_{k\iota}\bar{\beta}_{\bar{k}\bar{\iota}}: :\beta_{k'\iota'}\bar{\beta}_{\bar{k}'\bar{\iota}'}: L_k^{1/2} L_{k'}^{1/2} \int u_l \psi_k v_{\bar{k}}^{(\varepsilon\bar{\iota})} \int u_l \psi_{k'} v_{\bar{k}'}^{(\varepsilon'\bar{\iota}')}, \tag{1.38}$$

ignoring the product of interpolation parameters that will automatically appear with such terms for an arbitrary expansion step. The next step is applied with this interaction term absorbed into the observable as a factor that has just been "differentiated down." We now introduce ondelette diagrams to facilitate discussion of our expansion rules in the next section. We use a dash if a given ondelette is bosonic, a solid dot if it is fermionic, and a hollow dot if it is anti-fermionic. These marks are connected by a line if the corresponding variables appear in the same trilinear interaction term differentiated down as a factor in the developing observable $\mathscr{G}$. Further, the length scales of the ondelettes will be calibrated by the vertical coordinates of the corresponding marks, where the marks in the lower part of a diagram correspond to smaller length scales. Thus the ondelette diagram that appears when a term of the form (1.38) is differentiated down looks like the diagram shown in

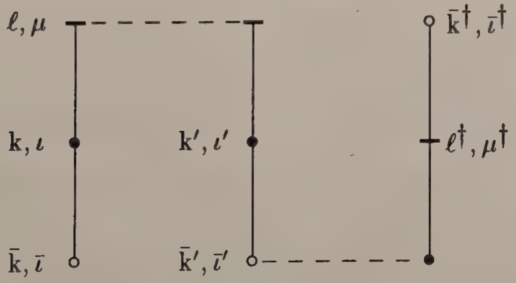
ℓ, μ
k, ι
k′, ι'
$\bar{\mathrm{k}}, \bar{\iota}$
$\bar{\mathrm{k}}', \bar{\iota}'$
$\bar{\mathrm{k}}^{\dagger}, \bar{\iota}^{\dagger}$
$\ell^{\dagger}, \mu^{\dagger}$

FIGURE 2

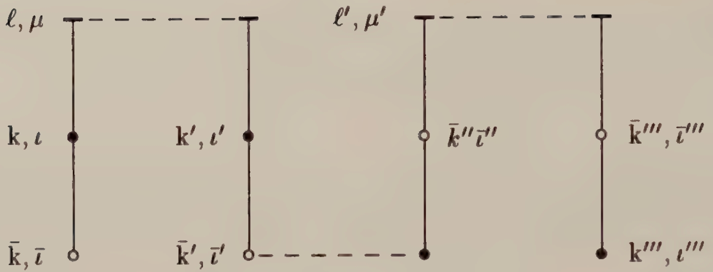

FIGURE 3

Fig. 1 in the case $L_{\bar{k}} = L_{\bar{k}'} < L_k = L_{k'} < L_l$, for example, where the dashed line denotes identification.

Now a "new" mode is understood to be a mode in the diagram just differentiated down which has never appeared in the observable $\mathscr{G}$ before, Note that we sometimes integrate by parts with respect to a variable associated with a new mode. In the diagram above, suppose $\bar{k}$ is a new mode and we integrate by parts with respect to $\bar{\beta}_{\bar{k}\bar{\imath}}$. The expansion step may possibly choose a term of the form (1.37), in which case we now have the composite diagram shown in Fig. 2 if $L_{l^\dagger} = L_{k'}$ and $L_{\bar{k}^\dagger} = L_l$, where the second dashed line is an identification in the sense that a fermi mode is pushed into its "hole." As the formula (1.37) implies, both variables $\beta_{\bar{k}\bar{\imath}}$ and $\bar{\beta}_{\bar{k}\bar{\imath}}$ are wiped out, leaving their numerical imprints behind, so our integration by parts for fermions is an "annihilation." The surviving product of variables is $:\beta_{k\iota}\bar{\beta}_{\bar{k}\bar{\imath}}:\ \beta_{k'\iota'}\bar{\beta}_{\bar{k}^\dagger\bar{\imath}^\dagger}$ and the missing variables $\beta_{\bar{k}\bar{\imath}}$ and $\bar{\beta}_{\bar{k}\bar{\imath}}$ will never be "new" again.

Typically we integrate by parts with respect to the variable which is both "new" and smallest scale in the solid line it belongs to, but there are important variations. For example, if the diagram in Fig. 3 develops instead of that in Fig. 2 and if $\bar{k}''$, $\bar{\imath}''$ is "new" while k''', ι''' is "old," then our expansion rules may dictate an integration by parts with respect to $\bar{\beta}_{\bar{k}'',\bar{\imath}''}$ because the preceding integration by parts wiped out $\bar{\beta}_{\bar{k}'\bar{\imath}'}$ and $\beta_{\bar{k}'\bar{\imath}'}$ and—as we shall see in Section 2—another integration by parts may be needed for the central part of this graph. As another example, suppose the diagram in Fig. 4 is differentiated down and k is "new." Then our expansion rules

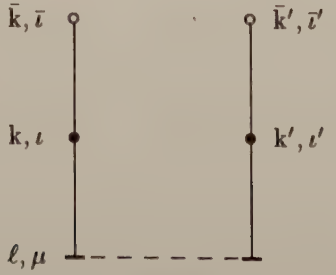

FIGURE 4

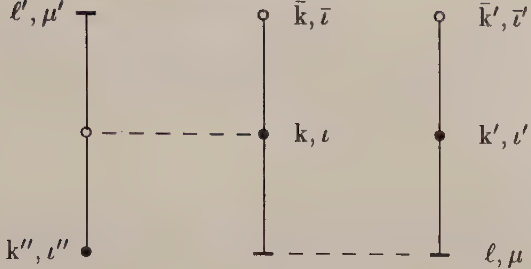

FIGURE 5

may dictate an integration by parts with respect to $\beta_{k\iota}$. The step may choose the composite diagram in Fig. 5 where the dashed line pushes the fermi mode into its "hole." The surviving product of variables in this case is clearly $:\beta_{k'\iota'}\bar{\beta}_{\bar{k}'\bar{\iota}'}:\ \beta_{k''\iota''}\bar{\beta}_{\bar{k}\bar{\iota}}$, by Formula (1.35).

In Section 2 we state the basic estimates on the numerical factors associated with ondelette contributions to the interaction. We use these estimates to motivate our expansion rules and tabulate the diagrams that we have to worry about.

In Section 3 we state and prove the basic mode stability bound for the interaction in the "Gross-Neveu" formalism. The bound is linear in the number of modes, and the basic ondelette estimates are the input bounds. This is similar in spirit to the α-stability and α-positivity established in [18] for the ϕ^4 interaction.

In Section 4 we exploit a symmetry to control an apparently divergent fermi mass diagram, and in Section 5 we use a Ward identity to solve a similar problem with a boson mass diagram. We introduce our *expansion step of the third kind* in this latter context. In Section 6 we show how Furry's Theorem is applied to our expansion. In the Appendix we review the ondelette cluster expansion for a scalar field.

2. ESTIMATES ON NUMERICAL FACTORS

When pieces of the interaction are differentiated down by the expansion, the most basic part of the convergence proof is to estimate the numerical factors $L_k^{1/2} \int u_l \psi_k v_k^{(\varepsilon i)}$ that accumulate. We now establish the estimates on these configuration integrals and demonstrate the implications for the perturbation theory of the expansion. Let κ denote the ondelette construction parameter [13, 15]. For any ondelette $\psi_k \in \mathscr{F}$ or $u_k \in \mathscr{B}$, we denote the centers of the two approximate localization cells by $x_k^{\pm}$ (recall that all of our functions are even or odd).

LEMMA 2.1. *For an arbitrary integer $N > 0$, the parameter κ can be chosen large enough such that*

$$|[(\nabla + 1)^{-n} u_l](x)| \leqslant c L_l^{n-1/2} \sum_{\# = \pm} (1 + L_l^{-1} |x - x_l^{\#}|)^{-N+n} \tag{2.1}$$

for $n<\kappa$, *where the bound is on a matrix norm. Moreover,*

$$|\partial^{\delta} u_l(x)| \leqslant cL_l^{-|\delta|-1/2} \sum_{\#=\pm} \exp(-cL_l^{-1}\,|x-x_l^{\#}|) \tag{2.2}$$

for all multi-indices δ *for which* $\delta_\mu<\kappa-1$.

The second bound follows from the analyticity properties of the momentum space construction of the function u_l [13]. As for the first bound, the Bessel-like potential destroys the scale- commensurate exponential decay. The potential we propose to use has a "mass" but it is tied to the unit scale. At small length scales the potential is practically Coulomb-like, so the small-scale fall-off is only an inverse power of degree determined by the number of vanishing moments arranged for u_l. The proof of this first bound is just standard estimation and scaling in momentum space using the momentum expressions for u_l [13].

LEMMA 2.2. *Given* $N>0$, *the parameter* κ *can be chosen such that*

$$|[\nabla+1)^{-n}\psi_k](x)| \leqslant cL_k^{n-3/2} \sum_{\#=\pm} (1+L_k^{-1}\,|x-x_k^{\#}|)^{-N+n} \tag{2.3}$$

for $n<\kappa$, *while*

$$|[(\nabla+1)^{-n} M^2 D_M^{-2} S_m \psi_k](x)| \leqslant cL_k^{n-1/2} \sum_{\#=\pm} (1+L_k^{-1}\,|x-x_k^{\#}|)^{-N+n+1} \tag{2.4}$$

uniformly in M *for* $n<\kappa-1$. *On the other hand,*

$$|\partial^{\delta}\psi_k(x)| \leqslant cL_k^{-|\delta|-3/2} \sum_{\#=\pm} (1+L_k^{-1}\,|x-x_k^{\#}|)^{-N-|\delta|} \tag{2.5}$$

for all multi-indices δ *for which* $\delta_\mu<\kappa-1$, *while*

$$|\partial^{\delta}[M^2 D_M^{-2} S_m \psi_k](x)| \leqslant cL_k^{|\delta|-1/2} \sum_{\#=\pm} (1+L_k^{-1}\,|x-x_k^{\#}|)^{-N-|\delta|+1} \tag{2.6}$$

uniformly in M *for* $\delta_\mu<\kappa$.

Estimates (2.3) and (2.5) hold by the same kind of momentum space estiation that proves (2.1)—the vanishing moments yield the scale-commensurate power law decay. There are unit-scale ψ_k without enough vanishing moments [13], but the potential has a unit-scale exponential decay anyway. The proof of Estimates (2.4) and (2.6) is similar because $S_m\psi_k$ is also a Bessel-like potential of an L^2-ondelette and because $M^2(p^2+M^2)^{-1}$ as well as $(\partial^{\delta}/\partial p^{\delta})$-derivatives are bounded uniformly in M.

We can easily derive the basic estimates (uniform in M):

$$L_k^{1/2}\left|\int u_l\psi_k v_{\bar{k}}^{(\varepsilon\bar{i})}\right| \leqslant cL_k^2 L_{\bar{k}}^{-1} L_l^{-1/2} h_s(l,k,\bar{k}), \tag{2.7}$$

$$\leqslant cL_{\bar{k}}^2 L_k^{-1} L_l^{-1/2} h_s(l,k,\bar{k}), \tag{2.8}$$

$$\leqslant cL_l^{5/2} L_k^{-2} L_{\bar{k}}^{-1} h_s(l,k,\bar{k}), \tag{2.9}$$

where s depends on N, we have set $n=0$ and $\delta=0$, and

$$h_s(l,k,\bar{k}) = h_s(k,l)h_s(l,\bar{k})h_s(k,\bar{k}), \tag{2.10}$$

$$h_s(k,l) = \sum_{\# = \pm} (1 + L_{kl}^{-1}\,|x_k^{\#} - x_l^{\#}|)^{-s}, \tag{2.11}$$

$$L_{kl} = \max\{L_k, L_l\}. \tag{2.12}$$

Obviously (2.7) is applied when k has the smallest length scale, and so on.

In some cases we will need a refinement of these estimates readily obtained from integrating by parts inside this ordinary integral and applying our lemmas with non-zero values of n and δ.

$$L_k^{1/2}\left|\int u_l\psi_k v_{\bar{k}}^{(\varepsilon\bar{i})}\right| \leqslant cL_k^{2+n} L_{\bar{k}}^{-1} L_l^{-1/2}(L_{\bar{k}}^{-n} + L_l^{-n}) h_{\tilde{s}}(k,\bar{k},l), \tag{2.13}$$

$$\leqslant cL_{\bar{k}}^{2+n} L_k^{-1} L_l^{-1/2}(L_{\bar{k}}^{-n} + L_l^{-n}) h_{\tilde{s}}(k,\bar{k},l), \tag{2.14}$$

$$\leqslant cL_l^{5/2+n} L_k^{-1} L_{\bar{k}}^{-1}(L_k^{-n} + L_{\bar{k}}^{-n}) h_{\tilde{s}}(k,\bar{k},l), \tag{2.15}$$

where $\tilde{s}$ depends on n as well as N. Specifically we are applying $(\nabla+1)^{-n}$ to ψ_k and $(\nabla+1)^n$ to $u_l v_{\bar{k}}^{(\varepsilon\bar{i})}$ to obtain (2.13), $(\nabla+1)^{-n}$ to $v_{\bar{k}}^{(\varepsilon\bar{i})}$ and $(\nabla+1)^n$ to $u_l\psi_k$ to obtain (2.14), and so on.

The estimates on numerical factors that we now have comprise the most basic part of the perturbation theory when combined with the counting estimates, which we now enumerate. For arbitrary $l \in \mathscr{F} \cup \mathscr{B}$,

$$\sum_{L_k = 2^{-\rho}} h_{\tilde{s}}(k,l) \leqslant c, \qquad L_l \leqslant 2^{-\rho}, \tag{2.16}$$

$$\sum_{L_k = 2^{-\rho}} h_{\tilde{s}}(k,l) \leqslant c\left(\frac{L_l}{2^{-\rho}}\right)^3, \qquad L_l \geqslant 2^{-\rho}. \tag{2.17}$$

These estimates are not new [18, 19], and the rough intuition is no more complicated than counting the cubes of a given scale that intersect with a fixed cube of some other scale.

Now the sum over histories of expansion steps is a multiple sum with a tree structure [18, 19], but the perturbation theory is contained in one summation or a few successive ones, with the factors corresponding to all outer summations held fixed. An ondelette diagram corresponds to the restriction of the summation to some case. For example, suppose an expansion step arising from interpolation happens to fall in the case shown in Fig. 6 with k and $\bar{k}$ "old" and k', l, and $\bar{k}'$ "new." Then we must sum over the possibilities for l, k', $\bar{k}'$ while holding k and $\bar{k}$ fixed. This sum is convergent—i.e.,

$$L_k^{1/2} \sum_{l: L_l \leqslant L_{\bar{k}}} \; \sum_{k', \bar{k}': L_{\bar{k}'} \geqslant L_{k'} \geqslant L_l} L_{k'}^{1/2} \left| \int u_l \psi_k v_{\bar{k}}^{(\varepsilon \bar{\imath})} \right| \left| \int u_l \psi_{k'} v_{\bar{k}'}^{(\varepsilon' \bar{\imath}')} \right| \leqslant c \tag{2.18}$$

for $L_{\bar{k}} \leqslant L_k$. We derive this by applying (2.9) to the second factor and (2.15) to the first factor ($n = 1$ will do). The point is that (2.16) is used to control the inner sum while (2.17) is used to control the outer sum.

On the other hand, suppose $\bar{k}$ is "new" as well (with $k' \neq \bar{k}$). Then we must sum over both l and $\bar{k}$, in which case (2.15) becomes useless and we can really do no better than (2.9) for the estimation of the first factor. Thus we have—missing by a full power of the length scale—

$$L_k^{1/2} \sum_{\bar{k}, l: L_l \leqslant L_{\bar{k}} \leqslant L_k} \; \sum_{k', \bar{k}': L_{\bar{k}'} \geqslant L_{k'} \geqslant L_l} L_{k'}^{1/2} \left| \int u_l \psi_k v_{\bar{k}}^{(\varepsilon \bar{\imath})} \right| \left| \int u_l \psi_{k'} v_{\bar{k}'}^{(\varepsilon' \bar{\imath}')} \right| \leqslant c(M), \tag{2.19}$$

where $c(M) \to \infty$ as $M \to \infty$, and so we must integrate by parts with respect to $\beta_{k' \iota'}$ for our next expansion step and try to sum over the resulting two-step possibilities. Suppose we have the composite case shown in Fig. 7, where $\hat{k}$, l', k'', $\bar{k}''$ are all "new." We now have the product

$$\begin{aligned} L_k^{1/2} \left| \int u_l \psi_k v_k^{(\varepsilon \bar{\imath})} \right| L_{k'}^{1/2} \left| \int u_l \psi_{k'} v_{\bar{k}'}^{(\varepsilon' \bar{\imath}')} \right| L_{\hat{k}}^{1/2} \left| \int u_{l'} \psi_{\hat{k}} v_{k'}^{(\hat{\varepsilon} \iota')} \right| \\ \cdot L_{k''}^{1/2} \left| \int u_{l'} \psi_{k''} v_{\bar{k}''}^{(\varepsilon'' \bar{\imath}'')} \right| \end{aligned} \tag{2.20}$$

to sum up, where we first sum over k'' and $\bar{k}''$ for fixed l', then over l' and $\hat{k}$ for fixed k', then over k' and $\bar{k}'$ for fixed l, and finally over $\bar{k}$ and l for fixed k. We apply the estimate (2.9) to the last factor in (2.20), the estimate (2.15) to the $(\hat{k}, k', l')$

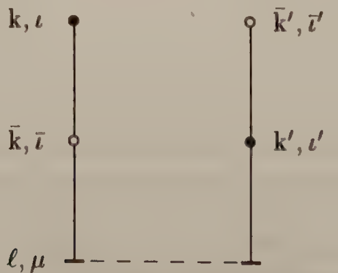

FIGURE 6

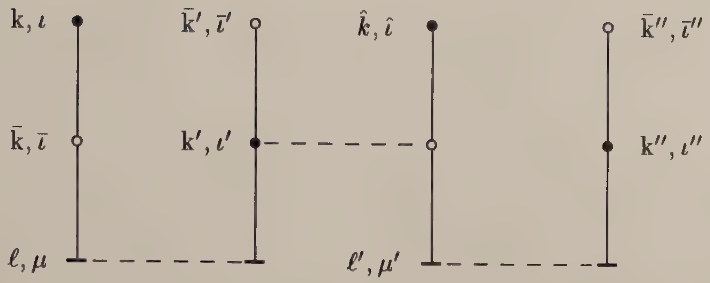

FIGURE 7

factor, and (2.9) to the first two factors. The innermost summation uses (2.16) and we obtain the bound

$$c \sum_{\bar k, l : L_l \leqslant L_{\bar k} \leqslant L_k} \; \sum_{k', \bar k' : L_{\bar k'} \geqslant L_{k'} \geqslant L_l} \; \sum_{l' : L_{l'} \leqslant L_{k'}} \; \sum_{\hat k : L_{\hat k} \geqslant L_{k'}} L_{l'}^{1/2} \log(L_{\bar l'}^{-1}) \cdot (\text{first three numerical factors}). \tag{2.21}$$

Again using (2.16), we sum over $\hat k$ to obtain

$$c \sum_{\bar k, l : L_l \leqslant L_{\bar k} \leqslant L_k} \; \sum_{k', \bar k' : L_{\bar k'} \geqslant L_{k'} \geqslant L_l} \; \sum_{l' : L_{l'} \leqslant L_{k'}} L_{l'}^{3+n} L_{k'}^{-2-n} \cdot \log(L_{\bar k'}^{-1}) \log(L_{\bar l'}^{-1}) h_s(k', l')(\text{first two factors}). \tag{2.22}$$

Set $n = 1$ and apply (2.17) to the sum over l': we get

$$c \sum_{\bar k, l : L_l \leqslant L_{\bar k} \leqslant L_k} \; \sum_{k', \bar k' : L_{\bar k'} \geqslant L_{k'} \geqslant L_l} L_{k'} [\log(L_{\bar k'}^{-1})]^2 \,(\text{first two factors}). \tag{2.23}$$

Once again, (2.16) is applied to the innermost sum, and we finally obtain the bound

$$c \sum_{\bar k, l : L_l \leqslant L_{\bar k} \leqslant L_k} L_l^{3/2} [\log(L_{\bar l}^{-1})]^3 \,(\text{first numerical factor}). \tag{2.24}$$

This sum diverges only marginally as $M \to \infty$. If we integrate by parts with respect to $\beta_{k''\iota''}$ in Fig. 7 and if the composite case shown in Fig. 8 results, then the same successive estimation as above yields a convergent multiple sum. This means that we can stop integrating by parts and resume interpolation.

This completes our description of *one* possible sequence of integration by parts. Obviously there are many others, some of which are terminated by a shortage of "new" variables before obvious convergence is achieved, so the sequence described above is only a happy state of affairs. Suppose, for example, that we get Fig. 6 with $k' = \bar k$, $\iota' = \bar\iota$, as well as with k' "new." Then we have the same divergence problem as before, but when we try to cure it by pushing $\beta_{\bar k, \bar\iota}$ into its "hole" $\bar\beta_{\bar k, \bar\iota}$, it is

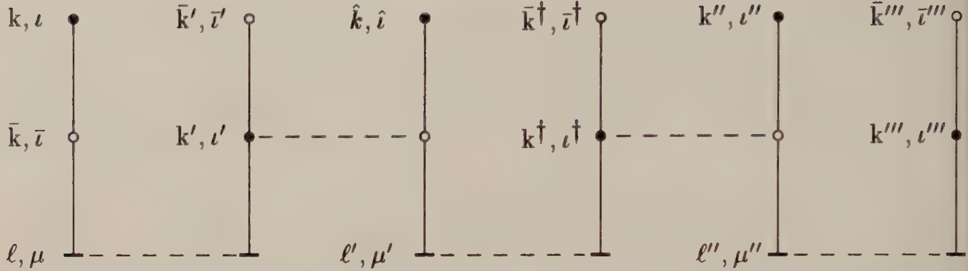

FIGURE 8

possible to have the graph shown in Fig. 9a as well as that shown in Fig. 7. This follows from our use of the integration by parts formula

$$\begin{aligned}
&\Big\langle :\beta_{\bar k\bar\iota}\bar\beta_{\bar k'\bar\iota'}: \, :\beta_{k\iota}\bar\beta_{\bar k\bar\iota}: \mathscr{G} \exp\Big(\sum_{k'',\bar k''}\sum_{\iota'',\bar\iota''} P_{k''\bar k'',\iota''\bar\iota''}(z) :\beta_{k''\iota''}\bar\beta_{\bar k''\bar\iota''}: \\
&\qquad + \sum_{k'',\bar k'',\hat k,\hat{\bar k}}\ \sum_{\iota'',\bar\iota'',\hat\iota,\hat{\bar\iota}} Q_{k''\bar k''\hat k\hat{\bar k},\iota''\bar\iota''\hat\iota\hat{\bar\iota}} :\beta_{\hat k\hat\iota}\bar\beta_{\hat{\bar k}\hat{\bar\iota}}: \, :\beta_{k''\iota''}\bar\beta_{\bar k''\bar\iota''}: \Big)\Big\rangle_f \\
&= -\sum_{k''}\sum_{\iota''} P_{k''\bar k,\iota''\bar\iota}(z)\langle \beta_{k''\iota''}\bar\beta_{\bar k'\bar\iota'} :\beta_{k\iota}\bar\beta_{\bar k\bar\iota}: \mathscr{G} \exp(\text{ditto})\rangle_f \\
&\qquad - \sum_{k'',\bar k'',\hat k}\ \sum_{\iota'',\bar\iota'',\hat\iota} Q_{k''\bar k''\bar k\hat k,\iota''\bar\iota''\bar\iota\hat\iota}\langle \beta_{\hat k\hat\iota}\bar\beta_{\bar k'\bar\iota'} :\beta_{k''\iota''}\bar\beta_{\bar k''\bar\iota''}: \, :\beta_{k\iota}\bar\beta_{\bar k\bar\iota}: \mathscr{G} \exp(\text{ditto})\rangle_f \\
&\qquad - \sum_{k'',\hat k,\hat{\bar k}}\ \sum_{\iota'',\hat\iota,\hat{\bar\iota}} Q_{k''\bar k\hat k\hat{\bar k},\iota''\bar\iota\hat\iota\hat{\bar\iota}}\langle :\beta_{\hat k\hat\iota}\bar\beta_{\hat{\bar k}\hat{\bar\iota}}: \beta_{k''\iota''}\bar\beta_{\bar k'\bar\iota'} :\beta_{k\iota}\bar\beta_{\bar k\bar\iota}: \mathscr{G} \exp(\text{ditto})\rangle_f \\
&\qquad - \langle \bar\beta_{\bar k',\bar\iota'}\beta_{k\iota}\mathscr{G} \exp(\text{ditto})\rangle_f, \qquad (2.25)
\end{aligned}$$

where $\mathscr{G}$ does not include $\bar k, \bar\iota$. Formula (1.35) does not apply to this case because

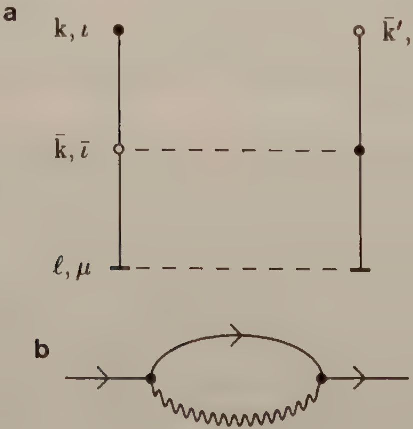

FIGURE 9

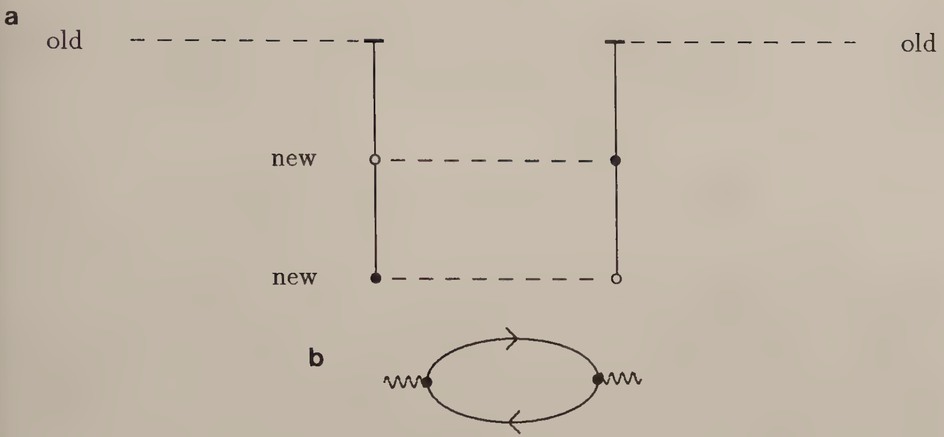

FIGURE 10

$\mathscr{G}$ is replaced by $:\beta_{\bar{k}i}\bar{\beta}_{\bar{k}'i'}:\mathscr{G}$. The additional term in this formula corresponds to Fig. 9, and the point is that the expansion step selecting this term does not introduce a third numerical factor.

Figure 9 is divergent, so we "try again" by integrating by parts with respect to $\bar{\beta}_{\bar{k}'i'}$ because—as in the preceding problem-- we have assumed that $\bar{k}'$ is "new." But suppose $\bar{k}'$ is "old" instead. This slight change in case has two effects.

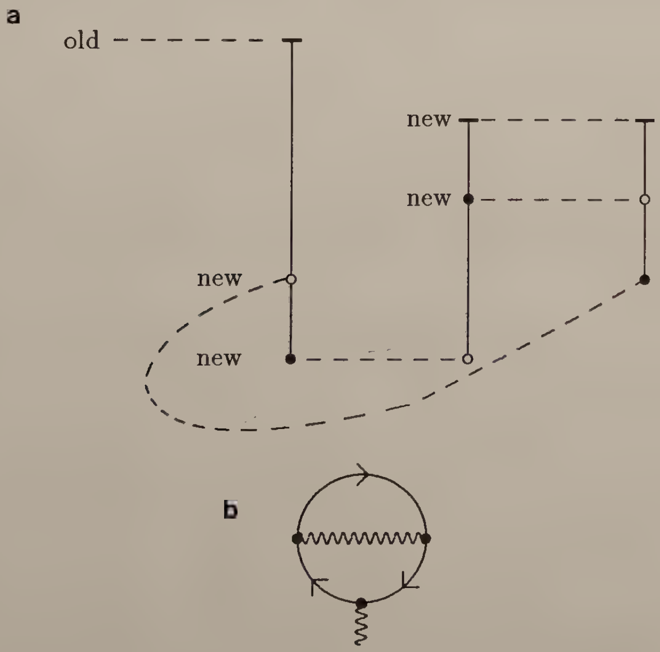

FIGURE 11

First, we cannot integrate by parts anymore, so we are now stuck with Fig. 9. Second, the sum over possibilities has changed because $\bar{k}'$, $\bar{\imath}'$ as well as k, $\imath$ is fixed. Our power-counting for $L_k^{1/2} |\int u_l \psi_k v_{\bar{k}}^{(\varepsilon\imath)}| \, L_{\bar{k}}^{1/2} |\int u_l \psi_{\bar{k}} v_{\bar{k}'}^{(\bar{\varepsilon}\bar{\imath}')}|$ is now organized as follows:

$$(L_l^{5/2} L_k^{-1} L_{\bar{k}}^{-1})(L_l^{5/2} L_{\bar{k}}^{-1} L_{\bar{k}'}^{-1}) = \left(\frac{L_l}{L_{\bar{k}}}\right)^5 \left(\frac{L_{\bar{k}}}{L_k}\right)^3 L_k, \tag{2.26}$$

where we have assumed $L_k \leqslant L_{\bar{k}'}$ without loss. Hence the seeming divergence is only marginal when we sum over $\bar{k}$ and l.

Figure 9a corresponds to the Feyman diagram in Fig. 9b, where vertices replace basic three-mode graphs, momentum lines replace identification lines, and external legs replace modes that are "old." Now it is known [6] that in $2+1$ dimensions the latter diagram is cancelled by a symmetry. In Section 4 we cancel the ondelette diagram in an analogous way, using the same symmetry.

We close this section with an enumeration of the other diagrams that are seemingly divergent but are forced on us by an exhaustion of integration by parts (see Figs. 10–13).

Each open dashed line in Figs. 10–13 may connect to the rest of a 5-mode graph or to a z-parameter. We expect to cancel the diagrams shown in Figs. 11a, 12a, and 13a by using Furry's Theorem and to control Fig. 10a with a Ward identity. Both types of cancellation will be realized as expansion steps of the third kind.

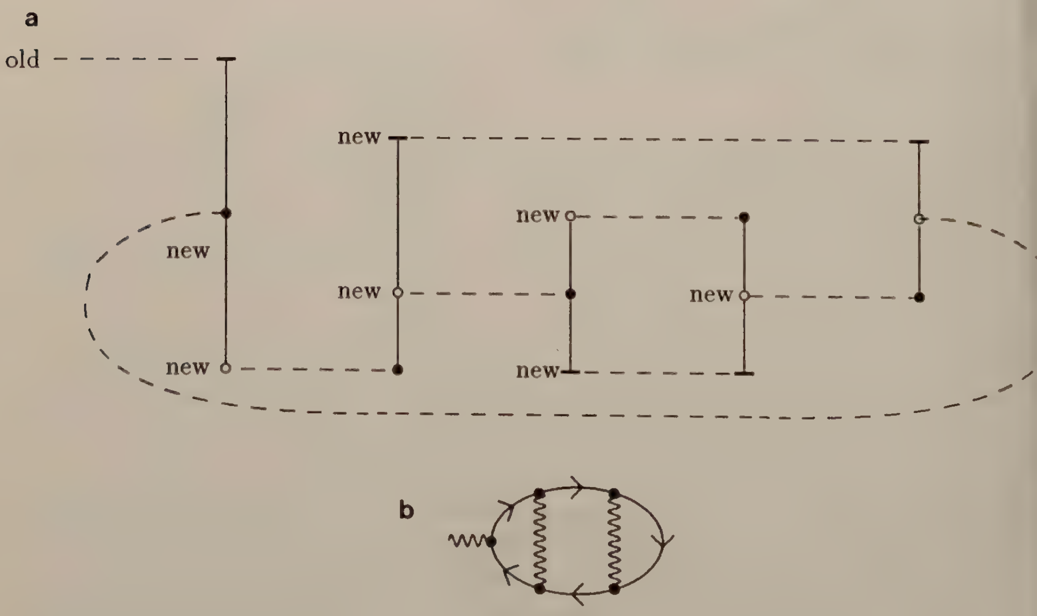

FIGURE 12

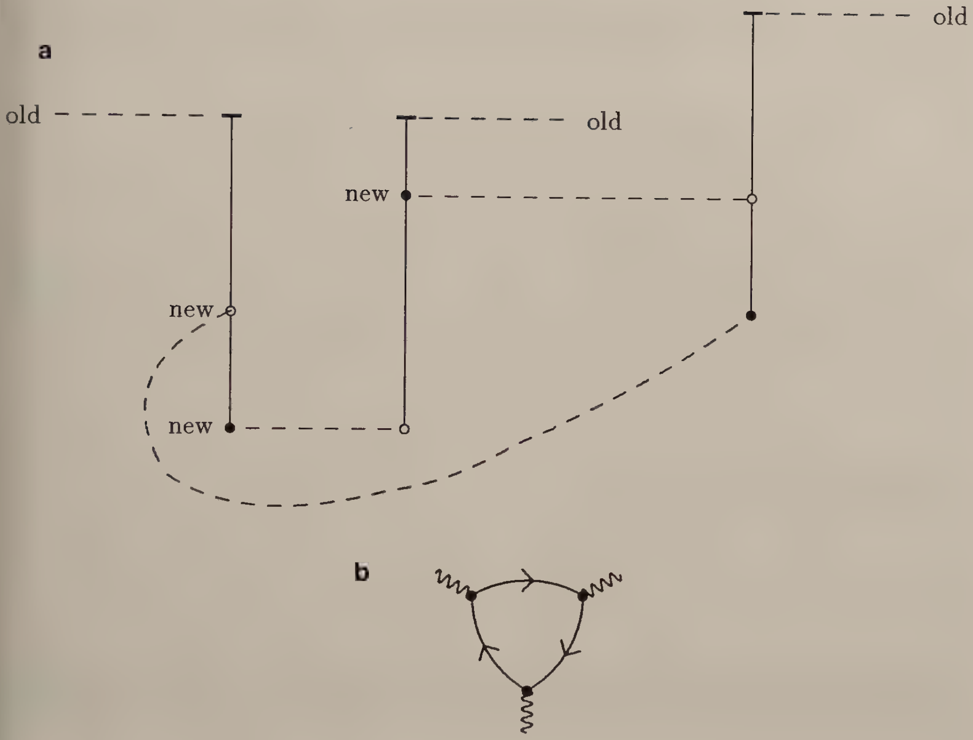

FIGURE 13

3. ELEMENTARY STABILITY

In this section we establish the stability bound needed for the convergence of the cluster expansion. As in [18, 19] the only stability we need is linear in the number of modes.

THEOREM 3.1. *Let A be an arbitrary finite set of modes. Then*

$$\|e^{-J_A(z)}\| \leqslant \exp\left(c \sum_{(l,\mu)\in A} |z_{l\mu}|^2 + c\,|A|\right), \tag{3.1}$$

where $\|\cdot\|$ denotes the operator norm for Euclidean Fermi Fock space and the bound is uniform in M.

Proof. Clearly, it is a matter of showing that

$$\sum_{(l,\mu)\in A} \left\| z_{l\mu} - \lambda \sum_{\varepsilon,\iota} \gamma_\mu^{\varepsilon\iota} \int u_l :\Psi_\iota^A \bar{\Psi}_{\varepsilon,M}^A: \right\|^2 \leqslant c \sum_{(l,\mu)\in A} |z_{l\mu}|^2 + c\,|A|. \tag{3.2}$$

Now if we expand the fermi fields and apply the bounds (1.16) and (1.17), we obtain

$$\sum_{l\in A}\left\| \int u_l :\Psi_l^A \bar{\Psi}_{\varepsilon,M}^A: \right\|^2 \leqslant c \sum_{k,k',\bar{k},\bar{k}',l\in A} L_k^{1/2} L_{k'}^{1/2} \left| \int v_{\bar{k}} u_l \psi_k \right| \left| \int \psi_{k'} u_l v_{\bar{k}'} \right|. \tag{3.3}$$

But if we examine the estimates (2.7)–(2.9) covering the cases for a numerical factor $L_k^{1/2} \int u_l \psi_k v_{\bar{k}}$, we find that the worst case extracts a $\frac{1}{2}$-power of $\min\{L_k, L_{\bar{k}}, L_l\}$. Therefore, we have a $\frac{1}{2}$-power of $\min\{L_k, L_{\bar{k}}, L_{k'}, L_{\bar{k}'}, L_l\}$ extracted from the product of numerical factors in (3.3). Applying the counting extimate (2.16), which covers all cases summed over if we always fix the smallest-scale mode first, we get

$$\sum_{l\in A}\left\| \int u_l :\Psi_l^A \bar{\Psi}_{\varepsilon,M}^A: \right\|^2 \leqslant c \sum_{k\in A} L_k^{1/2-\varepsilon} \leqslant c\,|A|, \tag{3.4}$$

so (3.2) now follows if we apply the Schwarz inequality and $ab \leqslant \frac{1}{2}a^2 + \frac{1}{2}b^2$ to the cross-term. ∎

4. THE FERMI MASS DIAGRAM

In this section we exploit a symmetry to show that the fermi mass diagram in Fig. 9 is really convergent, in spite of initial appearances. By (1.22) the implied counting problem is to control the sum of

$$\sum_{\varepsilon,\varepsilon'} \gamma_\mu^{\varepsilon\imath} \gamma_\mu^{\varepsilon'\bar{\imath}'} \beta_{k\imath} \bar{\beta}_{\bar{k}'\bar{\imath}'} L_k^{1/2} L_{\bar{k}}^{1/2} \int u_l \psi_k v_{\bar{k}}^{(i\varepsilon)} \int u_l \psi_{\bar{k}} v_{\bar{k}'}^{(\bar{\imath}'\varepsilon')} \tag{4.1}$$

over (l, μ), $(\bar{k}, \bar{\imath})$ having smaller scale than the fixed modes $(k, \imath)$, $(\bar{k}', \bar{\imath}')$. The variables $\bar{\beta}_{\bar{k}\imath}$ and $\beta_{\bar{k}\imath}$ have been eliminated by integration by parts, but of course their numerical imprints are left behind to be summed. By (1.8), (1.9), (1.21), and the identity $(-\nabla + m)(\nabla + m) = -\Delta + m^2$, we have

$$v_{\bar{k}} = (\nabla + m) D_m^{-2} M^2 D_M^{-2} \psi_{\bar{k}}, \tag{4.2}$$

so we concentrate on controlling the terms

$$L_k^{1/2} L_{\bar{k}}^{1/2} \int u_l \psi_k \partial_\sigma D_m^{-2} M^2 D_M^{-2} \psi_{\bar{k}} \int u_l \psi_{\bar{k}} \partial_\nu D_m^{-2} M^2 D_M^{-2} \psi_{\bar{k}'}. \tag{4.3}$$

The other terms, such as

$$L_k^{1/2} L_{\bar{k}}^{1/2} m \int u_l \psi_k D_m^{-2} M^2 D_M^{-2} \psi_{\bar{k}} \int u_l \psi_{\bar{k}} \partial_\nu D_m^{-2} M^2 D_M^{-2} \psi_{\bar{k}'}, \tag{4.4}$$

can be summed with no complication.

Our basic strategy is to consider two simple decompositions, where the choice is determined by even and odd cases. One decomposition is to split (4.3) into

$$L_k^{1/2} L_{\bar{k}}^{1/2} \left[\int u_l(x) (\partial_\sigma D_m^{-2} M^2 D_M^{2} \psi_{\bar{k}})(x)\, dx \right] \left[\int u_l(y) \psi_k(y) \psi_{\bar{k}}(y) \right.$$

$$\left. \cdot (\partial_\nu D_m^{-2} M^2 D_M^{-2} \psi_{\bar{k}'})(y)\, dy \right] \tag{4.5}$$

and

$$L_k^{1/2} L_{\bar{k}}^{1/2} \int dx \int dy\, u_l(x) u_l(y) (\partial_\sigma D_m^{-2} M^2 D_m^{-2} \psi_{\bar{k}})(x) \psi_{\bar{k}}(y)$$

$$\cdot (\partial_\nu D_m^{-2} M^2 D_M^{-2} \psi_{\bar{k}'})(y) (\psi_k(x) - \psi_k(y)). \tag{4.6}$$

We are motivated by the observation:

LEMMA 4.1. *Either* $\int u_l \psi_{\bar{k}} = 0$ *or* $\int u_l \partial_\sigma D_m^{-2} M^2 D_M^{-2} \psi_{\bar{k}} = 0$.

This is obvious because the second integral vanishes when the functions are either both odd or both even.

Thus (4.5) vanishes in two of the even and odd cases, leaving only (4.6). The lemma implies that we can carry out the same scheme in the other two cases if we apply the same decomposition with the role interchange

$$\psi_k \leftrightarrow \partial_\nu D_m^{-2} M^2 D_M^{-2} \psi_{\bar{k}'}. \tag{4.5', 4.6'}$$

LEMMA 4.2. *For a sufficiently large value of the ondelette construction parameter* κ, (4.6) *and* (4.6′) *are bounded by*

$$c L_l^{6-\varepsilon_0} L_{\bar{k}}^{-2} L_k^{-2+\varepsilon_0} L_{\bar{k}'}^{-1} h_s(k, l, \bar{k}) h_s(\bar{k}, \bar{k}', l), \tag{4.7}$$

$$(k \leftrightarrow \bar{k}' \text{ interchange}), \tag{4.7'}$$

respectively, where the constant is independent of M.

Remark. This result is analogous to the key result in the ϕ_3^4 case [19] for implementing the mass cancellation.

Proof. By the smoothness and scaling properties of ψ_k [15] we have

$$|\psi_k(x) - \psi_k(y)| \leqslant \int |e^{ip\cdot x} - e^{ip\cdot y}|\, |\hat{\psi}_k(p)|\, dp$$

$$\leqslant |x-y| \int |p|\, |\hat{\psi}_k(p)|\, dp$$

$$\leqslant c L_k^{-5/2} |x-y|, \tag{4.8}$$

so (4.6) is bounded by

$$cL_l^{-\varepsilon}L_{\bar{k}}^{-2}L_k^{-\varepsilon_0}L_{\bar{k}'}^{-1}h_s(k, l, \bar{k})h_s(\bar{k}, \bar{k}', l)$$
$$\cdot L_k^{-2+2\varepsilon_0}\int\int|x-y|^{1-\varepsilon_0}\,|u_l(x)u_l(y)|^{1-\varepsilon}\,dx\,dy, \tag{4.9}$$

uniformly in M, where we have used up $|u_l(x)u_l(y)|^{\varepsilon}$ and

$$|\psi_k(x)-\psi_k(y)|^{\varepsilon_0}\leqslant|\psi_k(x)|^{\varepsilon_0}+|\psi_k(y)|^{\varepsilon_0} \tag{4.10}$$

in applying (2.2), (2.5), and (2.6) (with $\delta=0$) to the extraction of h-factors. (This is where we need a sufficiently large value of the parameter κ—it is related to ε_0.) But by the scaling properties of u_l, we know

$$\int\int|x-y|^{1-\varepsilon_0}\,|u_l(x)u_l(y)|^{1-\varepsilon}\,dx\,dy\leqslant cL_l^{1-\varepsilon_0}L_l^{-1+\varepsilon}L_l^{6}, \tag{4.11}$$

so we have established the bound (4.7) on (4.6). The bound (4.7′) on (4.6′) is obtained in the same way. ∎

Naturally, we apply this lemma to the case $L_l\leqslant L_{\bar{k}}$. The case $L_{\bar{k}}\leqslant L_l$ calls for another estimate.

LEMMA 4.3. *For sufficiently large* κ, (4.6) *and* (4.6′) *are dominated by*

$$cL_{\bar{k}}^{5-\varepsilon_0}L_l^{-1}L_k^{-2+\varepsilon_0}L_{\bar{k}'}^{-1}h_s(k, l, \bar{k})h_s(\bar{k}, \bar{k}', l), \tag{4.12}$$
$$(k\leftrightarrow\bar{k}'\ \textit{interchange}), \tag{4.12′}$$

respectively, where the constant is independent of M.

Proof. Apply (4.8) and sup out products of functions as before, only this time we leave $|(\partial_\sigma D_m{}^2M^2D_M{}^2\psi_{\bar{k}})(x)\psi_{\bar{k}}(y)|^{1\;\varepsilon}$ inside the integral. Thus we dominate (4.6) with

$$cL_{\bar{k}}^{-2\varepsilon}L_l^{-1}L_k^{-\varepsilon_0}L_{\bar{k}'}^{-1}h_s(k, l, \bar{k})h_s(\bar{k}, \bar{k}', l)$$
$$\cdot L_k^{-2+2\varepsilon_0}\iint|x-y|^{1\;\;\varepsilon_0}\,|(\partial_\sigma D_m^2M^2D_M^{-2}\psi_{\bar{k}})(x)\psi_{\bar{k}}(y)|^{1-\varepsilon}\,dx\,dy. \tag{4.13}$$

But the double integral is bounded by $cL_{\bar{k}}^{1-\varepsilon_0}L_{\bar{k}}^{-2+2\varepsilon}L_{\bar{k}}^{6}$. This yields the desired bound on (4.6), and the estimation of (4.6′) is similar.

Given Lemma 4.1, our goal is reached by:

THEOREM 4.4. *Assume without loss that $L_k \leqslant L_{\bar{k}'}$. Then*

$$\sum_{\bar{k} \in \mathscr{F} : L_{\bar{k}} \leqslant L_k} \; \sum_{l \in \mathscr{B} : L_l \leqslant L_k} |\text{Expression (4.6)}| \leqslant c, \tag{4.14}$$

$$\sum_{\bar{k} \in \mathscr{F} : L_{\bar{k}} \leqslant L_k} \; \sum_{l \in \mathscr{B} : L_l \leqslant L_k} |\text{Expression (4.6}')| \leqslant c, \tag{4.14$'$}$$

where c is independent of M.

Proof. We establish only (4.14), since the proof of (4.14′) is similar. First consider the sub-sum

$$\sum_{\bar{k} \in \mathscr{F} : L_{\bar{k}} \leqslant L_k} \; \sum_{l \in \mathscr{B} : L_l \leqslant L_{\bar{k}}} |\text{Expression (4.6)}| \tag{4.15}$$

to which we apply Lemma 4.2: the bound to be summed is

$$cL_l^{6-\varepsilon_0} L_{\bar{k}}^{-2} L_k^{-3+\varepsilon_0} h_s(k, \bar{k}, l) h_s(\bar{k}, \bar{k}', l), \tag{4.16}$$

and the counting (2.17) done by the inner sum burns up the small factor $(L_l/L_{\bar{k}})^{3+\varepsilon}$—indeed we throw away the rest of $(L_l/L_{\bar{k}})^{6-\varepsilon_0}$—leaving us with the outer sum applied to

$$cL_{\bar{k}}^{4-\varepsilon_0} L_k^{-3+\varepsilon_0} h_s(k, \bar{k}) h_s(\bar{k}, \bar{k}'). \tag{4.17}$$

But the latter counting burns up the small factor $(L_{\bar{k}}/L_k)^{3+\varepsilon}$, so we have room to spare.

The remaining sub-sum is

$$\sum_{\bar{k} \in \mathscr{F} : L_{\bar{k}} \leqslant L_k} \; \sum_{l \in \mathscr{B} : L_{\bar{k}} \leqslant L_l \leqslant L_k} |\text{Expression (4.6)}|. \tag{4.18}$$

This time we apply Lemma 4.3 to bound the summand with

$$cL_{\bar{k}}^{5-\varepsilon_0} L_l^{-1} L_k^{-3+\varepsilon_0} h_s(k, \bar{k}, l) h_s(\bar{k}, \bar{k}', l). \tag{4.19}$$

The counting (2.16) done by the inner sum burns up the small factor L_k^{ε}, where we also wash out L_l^{-1} with $L_l^{-1} \leqslant L_{\bar{k}}^{-1}$. This leaves us with the outer sum applied to

$$cL_{\bar{k}}^{5-\varepsilon_0} L_k^{-4+\varepsilon_0-\varepsilon} h_s(k, \bar{k}) h_s(\bar{k}, \bar{k}'). \tag{4.20}$$

With only $(L_{\bar{k}}/L_k)^{3+\varepsilon}$ needed for bounding this last sum, we again have room to spare. ▮

5. EXPANSION STEP OF THE THIRD KIND

In this section we introduce our expansion step of the *third kind*. This involves the application of a Ward identity to Fig. 10, whose modes we label as in Fig. 14.

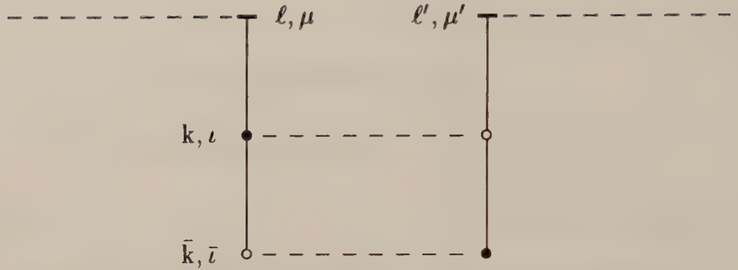

FIGURE 14

Each open dashed line may connect to the rest of a 5-mode graph or to a z-parameter, but the numerical factor associated with this central part of the composite graph are

$$L_k^{1/2}\sum_{\varepsilon}\gamma_\mu^{\iota\varepsilon}\int u_l\psi_k v_{\bar k}^{(\varepsilon\bar\imath)}L_{\bar k}^{1/2}\sum_{\varepsilon'}\gamma_{\mu'}^{\bar\imath\varepsilon'}\int u_{l'}\psi_{\bar k}v_k^{(\varepsilon'\iota)}. \tag{5.1}$$

The problem is to sum over (k, ι), $(\bar k, \bar\imath)$ having smaller scale than the fixed modes (l, μ), (l', μ'). The variables $\beta_{k\iota}$, $\bar\beta_{\bar k\bar\imath}$, $\beta_{\bar k\bar\imath}$, $\bar\beta_{k\iota}$ have been wiped out by the integration by parts that developed this graph.

As in the preceding section, we extract from the product of integrals a product where the functions are partitioned differently between the integrations. In this case the bound on the remainder will involve a new trick, but as we have already seen in the proofs of Lemmas 4.2 and 4.3, the remainder can be controlled only if the function associated with and "old" and larger scale mode is shifted from one integral to the other—in this case u_l or $u_{l'}$.

On the other hand, the symmetry scheme of Lemma 4.1 does not apply here, because the alternatives are

$$L_k^{1/2}\sum_{\varepsilon}\gamma_\mu^{\iota\varepsilon}\int \psi_k v_{\bar k}^{(\varepsilon\bar\imath)}L_{\bar k}^{1/2}\sum_{\varepsilon'}\gamma_{\mu'}^{\bar\imath\varepsilon'}\int u_l u_{l'}\psi_{\bar k}v_k^{(\varepsilon'\iota)}, \tag{5.2}$$

$$L_k^{1/2}\sum_{\varepsilon}\gamma_\mu^{\iota\varepsilon}\int u_{l'}u_l\psi_k v_{\bar k}^{(\varepsilon\bar\imath)}L_{\bar k}^{1/2}\sum_{\varepsilon'}\gamma_{\mu'}^{\bar\imath\varepsilon'}\int \psi_{\bar k}v_k^{(\varepsilon'\iota)}. \tag{5.3}$$

If ψ_k is even and $\psi_{\bar k}$ is odd, then neither $\int\psi_k\partial_\sigma D_m{}^{2}D_M^{-2}\psi_{\bar k}$ nor $\int\psi_{\bar k}\partial_\nu D_m^{-2}D_M^{-2}\psi_k$ are zero. However, if we sum up either (5.2) or (5.3) over the fermi modes, a global cancellation occurs in the form of a regularized Ward identity:

THEOREM 5.1. *For fixed* (l, μ) *and* (l', μ'),

$$\sum_{k,\iota}\sum_{\bar k,\bar\imath}\text{Expression (5.2)} = -4M^4 i\delta_{\mu\mu'}\int u_l u_{l'}\ \mathrm{tr}\int dp(-i\not p+m)\ {}^{1}\gamma_\mu p_\mu(p^2+M^2)\ {}^{3}, \tag{5.4}$$

where the sum is over all k, $\bar k$. *The same identity holds for the summation of* (5.3).

Remark. Clearly, the integral goes to zero as $M \to \infty$.

Proof. Observe that

$$\sum_{k \in \mathscr{F}} L_k^{1/2} \int \psi_k v_{\bar{k}}^{(\varepsilon\bar{\iota})} \int u_l u_{l'} \psi_{\bar{k}} v_k^{(\varepsilon'\iota)}$$

$$= M^2 \sum_{k \in \mathscr{F}} \int \psi_k v_{\bar{k}}^{(\varepsilon\bar{\iota})} \int u_l u_{l'} \psi_{\bar{k}} (\not\nabla + m)_{\varepsilon'\iota} D_m^{-2} D_M^{-2} \psi_k \tag{5.5}$$

by (4.2), so by Parseval's identity this sum is

$$M^2 \int v_{\bar{k}}^{(\varepsilon\bar{\iota})} D_m^{-2} D_M^{-2} (-\not\nabla + m)_{\varepsilon'\iota} (u_l u_{l'} \psi_{\bar{k}})$$

$$= M^2 L_{\bar{k}}^{1/2} \int [D_m^{-4} D_M^{-4} (\not\nabla + m)_{\varepsilon\bar{\iota}} (\not\nabla + m)_{\varepsilon'\iota} \psi_{\bar{k}}] u_l u_{l'} \psi_{\bar{k}}. \tag{5.6}$$

Hence

$$\sum_{\bar{k} \in \mathscr{F}} \sum_{k \in \mathscr{F}} L_k^{1/2} \int \psi_k v_{\bar{k}}^{(\varepsilon\bar{\iota})} L_{\bar{k}}^{1/2} \int u_l u_{l'} \psi_{\bar{k}} v_k^{(\varepsilon'\iota)}$$

$$= M^4 \operatorname{Tr}[u_l u_{l'} D_m^{-4} D_M^{-4} (\not\nabla + m)_{\varepsilon\bar{\iota}} (\not\nabla + m)_{\varepsilon'\iota}], \tag{5.7}$$

and so it follows that

$$\sum_{\bar{k} \in \mathscr{F}} \sum_{k \in \mathscr{F}} \sum_{\iota, \bar{\iota}} \text{Expression (5.2)} = M^4 \operatorname{Tr}[u_l u_{l'} D_m{}^4 D_M^{-4} (\not\nabla + m) \gamma_{\mu'} \cdot (\not\nabla + m) \gamma_\mu], \tag{5.8}$$

which reduces to

$$M^4 \operatorname{Tr}[u_l u_{l'} D_M^{-4} S_m \gamma_{\mu'} S_m \gamma_\mu]$$

$$= M^4 \operatorname{tr} \int dx \int dy \, u_l(x) u_{l'}(x) D_M^{-4}(x-y) [S_m \gamma_{\mu'} S_m \gamma_\mu](y-x)$$

$$= M^4 \int u_l u_{l'} \operatorname{tr} \int dy' \, D_M^{-4}(-y') [S_m \gamma_{\mu'} S_m \gamma_\mu](y')$$

$$= M^4 \int u_l u_{l'} \operatorname{tr} \int dp (p^2 + M^2)^{-2} (-i\not p + m)^{-1} \gamma_{\mu'} (-i\not p + m)^{-1} \gamma_\mu$$

$$= -iM^4 \int u_l u_{l'} \operatorname{tr} \int dp (p^2 + M^2)^{-2} \frac{\partial}{\partial p_{\mu'}} (-i\not p + m)^{-1} \gamma_\mu. \tag{5.9}$$

By the properties of the Dirac matrices, we know this trace vanishes for $\mu' \neq \mu$. Finally, we integrate by parts. ∎

Naturally, we must remember that the double sum to be reckoned with is not the double sum in (5.4). What our theorem actually proves is that if A is the set of "old" modes, then the correct sum decomposes as follows:

$$\begin{aligned}
&\sum_{\substack{k,\bar{k}\in\mathscr{F}\setminus A\\ L_{k\bar{k}}\leqslant\min\{L_l,L_{l'}\}}}\ \sum_{\iota,\bar{\iota}}\text{Expression (5.1)}\\
&\quad=\sum_{\substack{k,\bar{k}\in\mathscr{F}\setminus A\\ L_{k\bar{k}}\leqslant\min\{L_l,L_{l'}\}}}\ \sum_{\iota,\bar{\iota}}[\text{Expression (5.1)}-\text{Expression (5.2)}]\\
&\qquad-4M^4 i\delta_{\mu\mu'}\int u_l u_{l'}\operatorname{tr}\int dp(-i\not{p}+m)^{-1}\gamma_\mu p_\mu(p^2+M^2)^{-3}\\
&\qquad-\sum_{\bar{k}\in\mathscr{F}}\ \sum_{\iota,\bar{\iota}}\left(\sum_{k\in A}\text{Expression (5.2)}+\sum_{\substack{k\in\mathscr{F}\setminus A\\ L_k>\min\{L_l,L_{l'}\}}}\text{Expression (5.2)}\right)\\
&\qquad-\sum_{\substack{k\in\mathscr{F}\setminus A\\ L_k\leqslant\min\{L_l,L_{l'}\}}}\left(\sum_{\bar{k}\in A}\text{Expression (5.2)}+\sum_{\substack{\bar{k}\in\mathscr{F}\setminus A\\ L_{\bar{k}}>\min\{L_l,L_{l'}\}}}\text{Expression (5.2)}\right).
\end{aligned}\tag{5.10}$$

We now apply this identity to carry out the next expansion step. We define our *expansion step of the third kind* in this case to be the replacement of the possibilities on the lhs of (5.12) by the possibilities on the rhs. We claim that every case generated by this step yields a convergent sum uniform in M.

Consider the sum of (5.2) over $k\in A$ and $\bar{k}\in\mathscr{F}$. Given the discussion in Section 2, we see how to deal with such a graph, because k is "old" in this case. True, we have to sum over "old" modes as well, but this is related to the problem of summing over possible $l, l'\in A$, which we have ignored. This summation is part of the tree graph attachment problem [18, 19], which we reserve for the sequel. Section 2 also tells us how to deal with the case $k\in\mathscr{F}\setminus A$, $L_k>\min\{L_l, L_{l'}\}$, $\bar{k}\in\mathscr{F}$. Indeed, the only sum on the rhs of (5.10) that must be estimated with greater care is the sum of the remainder (5.1)–(5.2).

Now (5.1)–(5.2) is similar to the cancellation that was controlled in the preceding section because we can write this difference as

$$\begin{aligned}
&L_k^{1/2}\sum_{\varepsilon}\gamma_\mu^{\iota\varepsilon}L_{\bar{k}}^{1/2}\sum_{\varepsilon'}\gamma_{\mu'}^{\bar{\iota}\varepsilon'}\int dx\int dy(u_l(x)-u_l(y))\psi_k(x)\\
&\quad\cdot v_k^{(\varepsilon'\iota)}(y)v_{\bar{k}}^{(\varepsilon\bar{\iota})}(x)\psi_{\bar{k}}(y)u_{l'}(y).
\end{aligned}\tag{5.11}$$

However, if we estimate as we did before, we cannot extract enough smallness for the counting. In classical perturbative terms, we have cancelled a linear divergence to obtain what appears to be a marginal divergence. If the remaining divergence were really there, a wave function renormalization would be required, but we have an additional, hidden cancellation in the sum over spinor indices:

$$\begin{aligned}
Q&\equiv\sum_{\varepsilon,\varepsilon'}[\text{Expression (5.1)}-\text{Expression (5.2)}]\\
&=L_k^{1/2}L_{\bar{k}}^{1/2}\int dx\int dy(u_l(x)-u_l(y))\psi_k(x)\\
&\quad\times\operatorname{tr}(v_k(y))\gamma_{\mu'}v_{\bar{k}}(x)\gamma_\mu)\psi_{\bar{k}}(y)u_{l'}(y).
\end{aligned}$$

The idea is to compare this double integral to

$$\begin{aligned} &L_k^{1/2} L_{\bar{k}}^{1/2} \int dx \int dy (u_l(y) - u_l(x)) \psi_k(x) \\ &\quad \times \operatorname{tr}(v_k(y) \gamma_{\mu'} v_{\bar{k}}(x) \gamma_\mu) \psi_{\bar{k}}(y) u_{l'}(x) \\ &= L_k^{1/2} L_{\bar{k}}^{1/2} \int dx \int dy (u_l(x) - u_l(y)) \psi_k(y) \\ &\quad \times \operatorname{tr}(v_k(x)) \gamma_{\mu'} v_{\bar{k}}(y) \gamma_\mu) \psi_{\bar{k}}(x) u_{l'}(y), \end{aligned} \tag{5.13}$$

which we denote by Q'. We write

$$Q = \tfrac{1}{2}[Q + Q'] + \tfrac{1}{2}[Q - Q'] \tag{5.14}$$

and control the sum and difference separately. We use the rhs of (5.13) to write the difference:

$$\begin{aligned} Q - Q' = L_k^{1/2} L_{\bar{k}}^{1/2} &\int dx \int dy \\ &\cdot (u_l(x) - u_l(y)) u_{l'}(y) [\psi_k(x) \operatorname{tr}(v_k(y) \gamma_{\mu'} v_{\bar{k}}(x) \gamma_\mu) \psi_{\bar{k}}(y) \\ &- \psi_k(y) \operatorname{tr}(v_k(x) \gamma_{\mu'} v_{\bar{k}}(y) \gamma_\mu) \psi_{\bar{k}}(x)]. \end{aligned} \tag{5.15}$$

On the other hand, we use the lhs of (5.13) to write

$$\begin{aligned} Q + Q' = L_k^{1/2} L_{\bar{k}}^{1/2} &\int dx \int dy (u_l(x) - u_l(y))(u_{l'}(x) - u_{l'}(y)) \psi_k(x) \\ &\cdot \operatorname{tr}(v_k(y) \gamma_{\mu'} v_{\bar{k}}(x) \gamma_\mu) \psi_{\bar{k}}(y). \end{aligned} \tag{5.16}$$

Now the divergent contribution may seem to be $Q - Q'$ when we sum over k and $\bar{k}$, but there is a symmetry to exploit. Combine the graph in Fig. 14 with the graph in Fig. 15 which is certainly differentiated down as well. The advantage gained is that—by a symmetry in the $(k, \imath) \leftrightarrow (\bar{k}, \bar{\imath})$ interchange—the summation of

$$\begin{aligned} &[Q(\mu, \mu') - Q'(\mu, \mu')] + [Q(\mu', \mu) - Q'(\mu', \mu)] \\ &\quad = [Q(\mu, \mu') - Q'(\mu', \mu)] + [Q(\mu', \mu) - Q'(\mu, \mu')] \end{aligned} \tag{5.17}$$

over $k, \bar{k} \in \mathscr{F} \setminus A$, $L_{k\bar{k}} \leqslant \min\{L_l, L_{l'}\}$, $\imath, \bar{\imath} = 0, 1$, *vanishes*. (The roles of l and l' are not symmetric, but they have not been reversed.)

We turn to the problem of controlling $Q + Q'$, which is the more interesting part of the cancellation. We assume for the sake of definiteness that $L_{\bar{k}} \leqslant L_k$. The summation of $Q + Q'$ over $k, \bar{k} \in \mathscr{F} \setminus A$, $L_{\bar{k}} \leqslant L_k \leqslant \min\{L_l, L_{l'}\}$, is controlled by the following estimate.

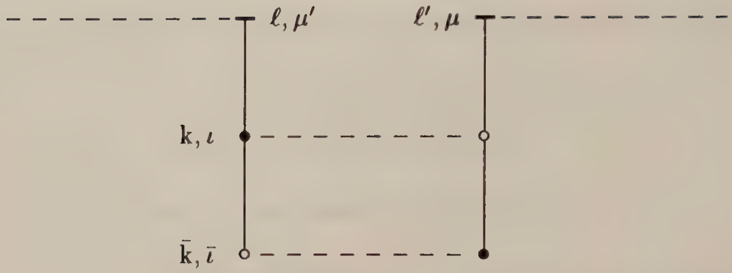

FIGURE 15

THEOREM 5.2. *For a sufficiently large value of the ondelette construction parameter,*

$$|Q+Q'| \leqslant cL_{\bar{k}}^{6-2\varepsilon_0} L_k^{-2} L_l^{-3/2+\varepsilon_0} L_{l'}^{-3/2+\varepsilon_0} h_s(k,\bar{k},l,l'). \tag{5.18}$$

Proof. We estimate as we did in the proof of Lemma 4.2 to obtain

$$|u_{l*}(x) - u_{l\#}(y)| \leqslant cL_{l*}^{-3/2}\,|x-y|, \tag{5.19}$$

so $Q+Q'$ is bounded by

$$\begin{aligned} &cL_{\bar{k}}^{-2\varepsilon} L_k^{-2} L_{l'}^{-3/2+3\varepsilon_0/2} L_{l'}^{-3/2+3\varepsilon_0/2} L_l^{-\varepsilon_0/2} L_{l'}^{-\varepsilon_0/2} h_s(k,\bar{k},l,l') \\ &\quad \cdot L_{\bar{k}}^{1/2-\varepsilon/2} \int dx \int dy\, |x-y|^{2-2\varepsilon_0}\, |v_{\bar{k}}(x)\psi_{\bar{k}}(y)|^{1-\varepsilon}, \end{aligned} \tag{5.20}$$

where we have used up $|v_{\bar{k}}(x)\psi_{\bar{k}}(y)|^{\varepsilon} L_{\bar{k}}^{\varepsilon/2}$ and

$$|u_{l*}(x) - u_{l*}(y)|^{\varepsilon_0} \leqslant |u_{l*}(x)|^{\varepsilon_0} + |u_{l*}(y)|^{\varepsilon_0} \tag{5.21}$$

on basic estimation for the extraction of *h*-factors. But by the approximate scaling properties of $v_{\bar{k}}$ and $\psi_{\bar{k}}$, we know that

$$L_{\bar{k}}^{1/2-\varepsilon/2} \int dx \int dy\, |x-y|^{2-2\varepsilon_0}\, |v_{\bar{k}}(x)\psi_{\bar{k}}(y)|^{1-\varepsilon} \leqslant cL_{\bar{k}}^{2-2\varepsilon_0} L_{\bar{k}}^{-2+2\varepsilon} L_{\bar{k}}^{6}, \tag{5.22}$$

so we have the desired bound. ▮

6. FURRY'S THEOREM AS AN EXPANSION STEP

We now treat the diagrams covered by Figs. 11–13. Since the ondelette diagrams correspond to Feynman diagrams having closed fermion loops with odd numbers of fermion lines, we expect Furry's Theorem [27] to be applicable here. This is indeed the case, but—like the regularized Ward identity—this theorem involves sums over *all* fermi modes, and so its application is an expansion step of the third kind.

Now both Fig. 11 and Fig. 13 have developed the numerical expression

$$\sum_{\varepsilon, \varepsilon', \varepsilon''} L_k^{1/2} L_{\bar{k}}^{1/2} L_{k'}^{1/2} \gamma_{\mu}^{\iota\varepsilon} \gamma_{\mu'}^{\iota'\varepsilon'} \gamma_{\mu''}^{\bar{\iota}\varepsilon''} \int u_l \psi_k v_{\bar{k}}^{(\varepsilon\bar{\iota})} \cdot \int u_{l'} \psi_{k'} v_k^{(\varepsilon'\iota)} \int u_{l''} \psi_{\bar{k}} v_{k'}^{(\varepsilon''\iota')}, \tag{6.1}$$

and our version of Furry's Theorem is embodied in:

THEOREM 6.1. *For given (l, μ), (l', μ'), and (l'', μ''),*

$$\sum_{k,\iota} \sum_{\bar{k},\iota} \sum_{k',\iota'} \text{Expression (6.1)} = 0, \tag{6.2}$$

where the sum is over all k, $\bar{k}$, k'.

Proof. We apply Parseval's identity twice.

$$\sum_{k \in \mathscr{F}} L_k^{1/2} \int u_l \psi_k v_{\bar{k}}^{(\varepsilon\bar{\iota})} \int u_{l'} \psi_{k'} v_k^{(\varepsilon'\iota)}$$

$$= M^2 \int u_l v_{\bar{k}}^{(\varepsilon\bar{\iota})} (-\not\nabla + m)_{\varepsilon'\iota} D_m^{-2} D_M^{-2} (u_{l'} \psi_{k'}), \tag{6.3}$$

$$\sum_{\bar{k} \in \mathscr{F}} L_{\bar{k}}^{1/2} \int u_{l''} \psi_{\bar{k}} v_{k'}^{(e''\iota')} \int u_l v_{\bar{k}}^{(\varepsilon\bar{\iota})} (-\not\nabla + m)_{\varepsilon'\iota} D_m^{-2} D_M^{-2} (u_{l'} \psi_{k'})$$

$$= M^2 \int u_{l''} v_{k'}^{(\varepsilon''\iota')} (-\not\nabla + m)_{\varepsilon\bar{\iota}} D_m^{-2} D_M^{-2}$$

$$\times [u_l (-\not\nabla + m)_{\varepsilon'\iota} D_m^{-2} D_M^{-2} (u_{l'} \psi_{k'})] \tag{6.4}$$

(remember that v_k contains the factor $L_k^{-1/2}$). Observe that

$$\sum_{k' \in \mathscr{F}} L_{k'}^{1/2} \int u_{l''} v_{k'}^{\varepsilon''\iota')} (-\not\nabla + m)_{\varepsilon\bar{\iota}} D_m^{-2} D_M^{-2}$$

$$\times [u_l (-\not\nabla + m)_{\varepsilon'\iota} D_m^{-2} D_M^{-2} (u_{l'} \psi_{k'})]$$

$$= M^2 \operatorname{Tr}[u_{l'} (\not\nabla + m)_{\varepsilon'\iota} D_m^{-2} D_M^{-2} u_l$$

$$\times (\not\nabla + m)_{\varepsilon\bar{\iota}} D_m^{-2} D_M^{-2} u_{l''} (\not\nabla + m)_{\varepsilon''\iota'} D_m^{-2} D_M^{-2}]. \tag{6.5}$$

It follows that

$$\sum_{k,\iota} \sum_{\bar{k},\bar{\iota}} \sum_{k',\iota'} \text{Expression (6.1)}$$

$$= M^6 \operatorname{Tr}[u_{l'} S D_M^{-2} \gamma_m u_l S D_M^{-2} \gamma_{\mu''} u_{l''} S D_M^{-2} \gamma_{\mu'}]$$

$$= M^6 \int dx \int dx' \int dx'' \, u_l(x) u_{l'}(x') u_{l''}(x'')$$

$$\cdot \operatorname{tr}[(S D_M^{-2})(x' - x) \gamma_\mu (S D_M^{-2})(x - x'') \gamma_{\mu''} (S D_M^{-2})(x'' - x') \gamma_{\mu'}], \tag{6.6}$$

but the matrix trace in the integrand is zero by Furry's Theorem [27]. ▌

Thus our expansion step of the third kind in the case of Fig. 13 is given by the identity

$$\begin{aligned}
&\sum_{\iota,\bar{\iota},\iota'} \sum_{\substack{k,\bar{k},k' \in \mathcal{F}\setminus A \\ L_{k\bar{k}k'} \leqslant \min\{L_l, L_{l'}, L_{l''}\}}} \text{Expression (6.1)} \\
&\quad = -\sum_{\iota,\bar{\iota},\iota'} \sum_{k,\bar{k}\in\mathcal{F}} \Bigg(\sum_{k'\in A} \text{Expression (6.1)} + \sum_{\substack{k'\in\mathcal{F}\setminus A \\ L_{k'} > \min\{L_l, L_{l'}, L_{l''}\}}} \text{Expression (6.1)} \Bigg) \\
&\qquad - \sum_{\iota,\bar{\iota},\iota'} \sum_{k\in\mathcal{F}} \sum_{\substack{k'\in\mathcal{F}\setminus A \\ L_{k'} \leqslant \min\{L_l, L_{l'}, L_{l''}\}}} \Bigg(\sum_{\bar{k}\in A} \text{Expression (6.1)} + \sum_{\substack{\bar{k}\in\mathcal{F}\setminus A \\ L_{\bar{k}} > \min\{L_l, L_{l'}, L_{l''}\}}} \text{Expression (6.1)} \Bigg) \\
&\qquad - \sum_{\iota,\bar{\iota},\iota'} \sum_{\substack{\bar{k},k'\in\mathcal{F}\setminus A \\ L_{\bar{k}k'} \leqslant \min\{L_l, L_l', L_{l''}\}}} \Bigg(\sum_{k'\in A} \text{Expression (6.1)} + \sum_{\substack{k'\in\mathcal{F}\setminus A \\ L_{k'} > \min\{L_l, L_{l'}, L_{l''}\}}} \text{Expression (6.1)} \Bigg),
\end{aligned} \tag{6.7}$$

where

$$L_{k\bar{k}k'} = \max\{L_k, L_{\bar{k}}, L_{k'}\}. \tag{6.8}$$

We can control all of these new cases with the estimation and counting described in Section 2. Our expansion step in the case of Fig. 11 is given by (6.7) with $\min\{L_l, L_{l'}, L_{l''}\}$ replaced by L_l and with the sum over (l', μ') and (l'', μ'') included.

Now Fig. 12 has developed the numerical expression

$$\begin{aligned}
&\sum_{\varepsilon_1,\dots,\varepsilon_5} L_{k_1}^{1/2}\cdots L_{k_5}^{1/2}\gamma_{\mu_1}^{\iota_1\varepsilon_1}\cdots\gamma_{\mu_5}^{\iota_5\varepsilon_5} \int u_{l_1}\psi_{k_1}v_{k_2}^{(\varepsilon_1\iota_2)} \\
&\quad \cdot \int u_{l_2}\psi_{k_2}v_{k_3}^{(\varepsilon_2\iota_3)} \int u_{l_3}\psi_{k_3}v_{k_4}^{(\varepsilon_3\iota_4)} \int u_{l_4}\psi_{k_4}v_{k_5}^{(\varepsilon_4\iota_5)} \\
&\quad \cdot \int u_{l_5}\psi_{k_5}v_{k_1}^{(\varepsilon_5\iota_1)},
\end{aligned} \tag{6.9}$$

and Furry's Theorem implies:

THEOREM 6.2. *For given* $(l_1, \mu_1), \dots, (l_5, \mu_5)$,

$$\sum_{\iota_1,\dots,\iota_5} \sum_{k_1,\dots,k_5} \text{Expression (6.9)} = 0, \tag{6.10}$$

where the sum is over all $k_1, \dots, k_5$.

The proof is similar to the proof of the preceding theorem, and this identity replaces

$$\sum_{l_2,\dots,l_5} \sum_{\mu_2,\dots,\mu_5} \sum_{\substack{k_1,\dots,k_5\in\mathcal{F}\setminus A \\ L_{k_1\cdots k_5} \leqslant L_{l_1}}} \sum_{\iota_1,\dots,\iota_5} \text{Expression (6.9)}$$

with sums that we already know how to control.

7. APPENDIX

We give here a brief review of the ondelette cluster expansion, applying it to the ϕ_2^4 model in the interests of simplicity. If Λ is a finite set of modes, the corresponding regularization of the scalar field $\phi(x)$ is defined as

$$\phi_\Lambda(x) = \sum_{k\in\Lambda} \alpha_k u_k(x), \tag{7.1}$$

where in this appendix,

$$\alpha_k = \int \phi D_m \psi_k, \tag{7.2}$$

$$u_k = D_m^{-1} \psi_k, \tag{7.3}$$

and m is the mass of the field. The regularized interaction is given by

$$I_\Lambda = \lambda \int :\phi_\Lambda^4:, \tag{7.4}$$

where : : denotes Wick-ordering with respect to the free boson expectation $\langle\cdot\rangle_0$. Since

$$\langle \alpha_k \alpha_l \rangle_0 = \delta_{kl}, \tag{7.5}$$

it follows that the interacting expectation for an arbitrary product $\prod_{i=1}^N \alpha_{k_i}$ of these phase cell variables is given by

$$\left\langle \prod_{i=1}^N \alpha_{k_i} \right\rangle_\Lambda = Z_\Lambda^{-1} \prod_{k\in\Lambda} \left(\int_{-\infty}^{\infty} d\alpha_k e^{-\alpha_k^2/2} \right) e^{-I_\Lambda(\alpha)} \prod_{i=1}^N \alpha_{k_i}, \tag{7.6}$$

$$Z_\Lambda = \prod_{k\in\Lambda} \left(\int_{-\infty}^{\infty} d\alpha_k e^{-\alpha_k^2/2} \right) e^{-I_\Lambda(\alpha)}. \tag{7.7}$$

Since the free measure is a product measure with respect to these variables, the cluster expansion modifies the quartic interaction only.

The expansion is a sum over histories, where each history is a sequence of choices made in an inductive process—i.e., the expansion constantly develops many branches that must ultimately be summed over. The most basic expansion step is an application of the interpolation formula

$$\langle e^{-P} Q \rangle_0 = \langle e^{-R} Q \rangle_0 - \int_0^1 ds \langle e^{-sP-(1-s)R} (P-R) Q \rangle_0, \tag{7.8}$$

where P, Q, and R depend on the branch (or history) and the stage in that history.

Now for the term $\langle e^{-R} Q \rangle_0$ the inductive process is over. But to each of the terms induced by expressing $P-R$ as a linear combination of interaction terms, we apply the interpolation formula again:

$$\langle e^{-P'}T_nQ\rangle_0=\langle e^{-R_n'}T_nQ\rangle_0-\int_0^1 ds'\langle e^{-s'P'-(1-s')R_n'}\cdot(P'-R_n')T_nQ\rangle_0, \quad (7.9)$$

$$P-R=\sum_n T_n, \quad (7.10)$$

$$P'=sP+(1-s)R. \quad (7.11)$$

The inductive process is over for $\langle e^{-R_n'}T_nQ\rangle_0$, the terms contributed by $P'-R_n'$ are each subject to yet another expansion step, and so on.

The aim of each interpolation is to decouple the interaction between the set of variables already differentiated down (the *interior set*) and its complement in Λ (the *exterior set*). Thus $P=I_\Lambda$, $Q=\prod_{i=1}^N \alpha_{k_i}$, and $R=I_A+I_{\Lambda\setminus A}$ for the first interpolation, where the interior set A is just $\{k_1, ..., k_N\}$ in this case. For the general interpolation, P is the modified interaction $I(\sigma)$ arising from previous interpolation with σ the sequence of parameters, Q is the product of interaction terms differentiated down thus far, and

$$R=I_A(\sigma)+I_{\Lambda\setminus A}, \quad (7.12)$$

where A is now the set of variables included in Q and $I_A(\sigma)$ is simply the restriction of the sum $I(\sigma)$ to those terms $:\alpha_{l_1}\alpha_{l_2}\alpha_{l_3}\alpha_{l_4}:$ for which l_1, l_2, l_3, l_4 all lie in A. In the following step,

$$R_n'=I_{A_n'}(\sigma, s)+I_{\Lambda\setminus A_n'}, \quad (7.13)$$

where A_n' is the set of variables included in T_nQ and $I_{A_n'}(\sigma, s)$ is the restriction of the sum

$$I(\sigma, s)=sI(\sigma)+(1-s)[I_A(\sigma)+I_{\Lambda\setminus A}] \quad (7.14)$$

to those terms $:\alpha_{l_1}\alpha_{l_2}\alpha_{l_3}\alpha_{l_4}:$ for which l_1, l_2, l_3, l_4 all lie in A_n'.

This completes our inductive definition of the interpolation (but not of the whole phase cell cluster expansion). The expansion of (7.6) generates terms of the form

$$Z_\Lambda^{-1}\langle e^{-R}Q\rangle_0=Z_\Lambda^{1}\langle e^{-I_{\Lambda\setminus A}}\rangle_0\langle e^{-I_A(\sigma)}Q\rangle_0=\frac{Z_{\Lambda\setminus A}}{Z_\Lambda}\langle e^{-I_A(\sigma)}Q\rangle_0. \quad (7.15)$$

Since the interior set grows for every history (or branch), the finite set Λ is eventually exhausted even if the history avoids choosing (7.15), so every branch of the expansion eventually terminates anyway. Thus every term in the completed expansion has the form (7.15)—with $A=\Lambda$ for the special histories that choose remainder terms until there are none. Obviously the complete sum is finite, but the estimates must be uniform in Λ.

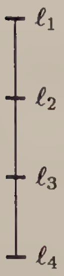

FIGURE 16

Our inductive definition of the cluster expansion does not involve interpolation alone. The process is occasionally interrupted by an integration by parts to implement the Wick-ordering cancellation of an ultraviolet divergence. The integration by parts formula is

$$\langle e^{-P} :\alpha_{l_1}\alpha_{l_2}\alpha_{l_3}\alpha_{l_4}: Q\rangle_0 = -\left\langle \frac{\partial P}{\partial \alpha_{l_4}} e^{-P} :\alpha_{l_1}\alpha_{l_2}\alpha_{l_3}: Q\right\rangle_0, \tag{7.16}$$

where Q does not depend on α_{l_4} and multiplicity of α_{l_4} inside the Wick-ordering is allowed. The next expansion step—whether interpolation or integration by parts—is applied to each term induced on the lhs by expressing P as a linear combination of interaction terms.

The rule for when to apply (7.16) is as simple as can be. If A is the set of modes included in Q and if $L_{l_4} \leqslant L_{l_3} \leqslant L_{l_2} \leqslant L_{l_1}$ with L_{l_3} smaller than the length scale of every mode in $A \cap \{l_1, l_2, l_3, l_4\}$ (automatically implying $l_3, l_4 \notin A$), then apply (7.16). Otherwise apply (7.9) with T_n a numerical multiple of $:\alpha_{l_1}\alpha_{l_2}\alpha_{l_3}\alpha_{l_4}:$. This completes the definition of the Battle–Federbush ondelette cluster expansion for the ϕ_2^4 Euclidean field theory.

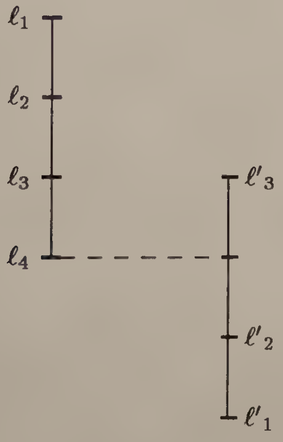

FIGURE 17

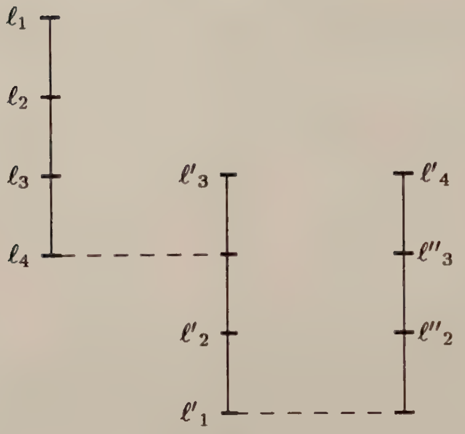

FIGURE 18

To illustrate how a few steps may occur in a given history, we return to ondelette diagrams. The diagram that appears when a product of previous interpolation parameters times a basic interaction term $\lambda \int u_{l_1} u_{l_2} u_{l_3} u_{l_4} :\alpha_{l_1} \alpha_{l_2} \alpha_{l_3} \alpha_{l_4}:$ is differentiated down looks like the diagram shown in Fig. 16 in the case $L_{l_1} > L_{l_2} > L_{l_3} > L_{l_4}$. Now suppose $l_3, l_4 \notin A$—calling for integration by parts with respect to α_{l_4}—and that the next step in the history differentiates down $:\alpha_{l'_2} \alpha_{l'_2} \alpha_{l'_3}:$, which has a numerical factor of $\int u_{l'_1} u_{l'_2} u_{l'_3} u_{l_4}$, and $L_{l'_1} < L_{l'_2} < L_{l_4} < L_{l'_3}$. Then the composite diagram is as shown in Fig. 17. If l'_1, l'_2 do not lie in A either, then the next step is to integrate by parts with respect to $\alpha_{l'_1}$. Suppose this step chooses $:\alpha_{l''_2} \alpha_{l''_3} \alpha_{l'_4}:$, which has a numerical factor of $\int u_{l'_1} u_{l''_2} u_{l''_3} u_{l'_4}$. If $L_{l'_1} < L_{l''_2} < L_{l''_3} < L_{l'_4}$, then we have developed the graph shown in Fig. 18 which converges in two dimensions when "new" modes are summed over for these smaller length scales. With the ultraviolet divergence cancelled, one now resumes interpolation.

We close this section with the remark that the expansion rules have been determined by perturbative problems alone. In the convergence proof the large field problem is solved by the combinatoric estimation of Battle and Federbush [18].

ACKNOWLEDGMENTS

I thank Lon Rosen, Paul Federbush, and Joel Feldman for a number of valuable conversations.

REFERENCES

1. S. DESER, R. JACKIW, AND S. TEMPLETON, *Ann. Phys. (N.Y.)* **140**, No. 2 (1982), 372.
2. S. DESER, R. JACKIW, AND S. TEMPLETON, *Phys. Rev. Lett.* **48** (1982), 975.
3. A. REDLICH, *Phys. Rev. Lett.* **52** (1984), 18.
4. M. GOPFERT AND G. MACK, *Commun. Math. Phys.* **82** (1982), 545.

5. A. Polyakov, *Phys. Lett. B* **59** (1975), 82.
6. R. Jackiw and S. Templeton, *Phys. Rev. D* **23**, No. 10 (1981), 2291.
7. A. Niemi and G. Semenoff, *Phys. Rev. Lett.* **51**, No. 23 (1983), 2077.
8. M. Bernstein and T. Lee, *Phys. Rev.* **23**, No. 4 (1985), 1020.
9. P. Cea, *Phys. Rev.* **32**, No. 10 (1985), 2785.
10. K. Osterwalder and E. Seiler, *Ann. Phys. (N.Y.)* **110** (1978), 440.
11. K. Gawedzki, *Commun. Math. Phys.* **63** (1978), 31.
12. J. Magnen and R. Seneor, *in* "Third International Conference on Collective Phenomena" (J. Lebowitz, J. Langer, and W. Glaberson, Eds.), New York Academy of Sciences, New York, 1980.
13. G. Battle, *Commun. Math. Phys.* **114** (1988), 93.
14. P. Lemarié, Une nouvelle base d'Ondelettes de $L^2(\mathbb{R}^n)$, *J. Math. Pures Appl.*, to appear.
15. G. Battle, *Commun. Math. Phys.* **110** (1987), 601.
16. G. Battle and P. Federbush, *Commun. Math. Phys.* **109** (1987), 417.
17. K. Osterwalder and R. Schrader, *Helv. Phys. Acta* **46** (1973), 277.
18. G. Battle and P. Federbush, *Ann. Phys. (N.Y.)* **142** (1982), 95.
19. G. Battle and P. Federbush, *Commun. Math. Phys.* **88** (1983), 263.
20. E. Seiler, *Commun. Math. Phys.* **42** (1974), 163.
21. E. Seiler and B. Simon, *Commun. Math. Phys.* **45** (1975), 99.
22. E. Seiler and B. Simon, *Ann. Phys. (N.Y.)* **97** (1976), 470.
23. J. Magnen and R. Seneor, *Commun. Math. Phys.* **51** (1976), 297.
24. A. Cooper and L. Rosen, *Trans. Amer. Math. Soc.* **234** (1977), 1.
25. A. Lesniewski, *Commun. Math. Phys.* **108** (1987), 437.
26. E. Seiler, "Constructive Quantum Field Theory: Fermions," IHES preprint, 1981.
27. N. Bogoliubov and D. Shirkov, "Introduction to the Theory of Quantized Fields," Wiley–Interscience, New York, 1980.

ANNALS OF PHYSICS **201**, 152–192 (1990)

Barkas Effect in a Dense Medium: Stopping Power and Wake Field*

HENNING ESBENSEN AND PETER SIGMUND[†]

Physics Division, Argonne National Laboratory, Argonne, Illinois 60439

Received September 22, 1989; revised December 20, 1989

A general expression has been derived for the polarization field set up by a heavy charged particle penetrating through a random medium. This expression includes contributions of first and second order in the projectile charge, and it determines the stopping power up to the third order. For a dilute gas, the stopping-power formula reduces to the one that can be derived directly from perturbation theory, applied to an isolated atom or molecule. The interaction between a charged particle and the medium is shown to be characterized by two functions, the well-known dielectric function $\varepsilon(\mathbf{k}, \omega)$ and a function $Y(\mathbf{k}, \omega; \mathbf{k}', \omega')$ depending on two sets of wave number and frequency variables. Explicit expressions for Y have been derived, (i) for a random medium of harmonic oscillators from the classical equation of motion, (ii) for a classical electron gas from Boltzmann's transport equation, (iii) for a system of Hartree atoms from quantal perturbation theory, and (iv) for the Fermi gas. Considerable care has been taken to ensure that different approaches yield identical results in those limits where such is to be expected. The Barkas (or Z_1^3) effect on the stopping power has been evaluated for a medium of classical oscillators with a resonance frequency ω_0 at an arbitrary density, characterized by a plasma frequency ω_P. The isolated classical oscillator and the classical electron gas emerge from this as simple limiting cases. The results can be described well by *one* effective resonance frequency $\alpha_0 = (\omega_0^2 + \omega_P^2)^{1/2}$, as is suggested by classical dispersion theory. The classical description applies to distant collisions only. Quantitative results have been derived for a quantal electron gas with the zero-point motion disregarded (static electron gas). The results compare well with recent experimental data on silicon. The Barkas correction to the spectrum of momentum transfer is positive for positively charged projectiles up to fairly large momenta, but it becomes negative near the edge. The Barkas correction to the stopping power is also mainly positive for positively charged projectiles, but it turns negative at low speed, in agreement with existing results for the harmonic osicllator. The second-order contribution to the induced field (or wake field) contains a higher harmonic, i.e., a field oscillating at twice the standard wave number. This alters the wake potential dramatically behind the penetrating particle at low velocities. This effect is possibly an explanation for observed anomalies in molecular-ion energy-loss spectra. The relative significance of the Barkas term in the stopping power and the wake field increases with increasing electron density in the medium. © 1990 Academic Press, Inc.

---

* The U.S. Government's right to retain a nonexclusive royalty-free license in and to the copyright covering this paper, for governmental purposes, is acknowledged.

[†] Argonne Fellow 1988–1989; present (permanent) address: Physics Department, Odense University, 5230 Odense M, Denmark.

0003-4916/90 $7.50

Copyright © 1990 by Academic Press, Inc.
All rights of reproduction in any form reserved.

CONTENTS.

1. *Introduction.*
2. *Higher-order polarization field.*
3. *Induced charge density.*
4. *General expressions for wake field and stopping power.* 4.1. Classical charge distribution in uniform motion. 4.2. Symmetry considerations. 4.3. Moving point charge.
5. *Stopping power of dilute matter.* 5.1. Derivation from dielectric theory. 5.2. Quantal harmonic oscillator. 5.3. Classical harmonic oscillator.
6. *Electron Gas.* 6.1. Fermi gas. 6.2. Static electron gas. 6.3. Classical limit.
7. *Dense Medium Containing Bound Electrons.* 7.1. Medium of harmonic oscillators. 7.2. The classical limit. 7.3. Binding frequency versus plasma frequency.
8. *Numerical results for the static electron gas.* 8.1. Stopping power. 8.2. Comparison with experiment. 8.3. Wake potential.
9. *Summary and Conclusions.*
Appendix A: Barkas correction to the stopping cross section of a single bound electron.
Appendix B: Semiclassical description of the electron gas.
Appendix C: Classical harmonic oscillator.

1. INTRODUCTION

A charged particle penetrating through matter generates an electromagnetic field which causes electronic excitations in the penetrated medium. If the medium is dense, the field will be determined in part by the properties of the medium, as is well known from classical electrodynamics of continuous media. In the limit of a weak perturbation, i.e., high projectile speed and/or low charge, induced fields ("wake fields") are of first order in the projectile charge, [1–5]. Observable quantities such as excitation cross sections or mean energy loss (stopping power) become proportional to the square of the projectile charge [6, 7].

Deviations from this simple scaling behavior have been documented in the stopping power. The leading correction is the Barkas effect [8–10] which shows up as a term of third order in the projectile charge [11–19]. It is known to be related to target polarization [10, 11]. A particularly clear demonstration of the Barkas effects has been given recently [19] when it was shown that the stopping power of antiprotons in silicon crystals is significantly smaller than that of protons at the same velocity.

Most existing theoretical treatments of the Barkas effect refer to dilute media where a target atom interacts with the unscreened Coulomb field of the penetrating particle [11–16]. Notable exceptions are an unpublished thesis dealing with an electron gas by one of us [17] and a more recent analysis of a Fermi gas [18].

While the existence of the Barkas effect has been well documented in the stopping power, the associated wake field has not been analysed. This is somewhat surprising in view of a very extensive effort to look for manifestations of wake phenomena in molecule penetration, electron emission, and alike [20]. Most of the pertinent experiments have been performed under conditions where deviations from a linear relation between field and projectile charge must be expected: Projectiles are frequently heavier than protons, and the velocities barely exceed the Bohr velocity in many cases.

In previous work [17], a general scheme was set up to self-consistently determine polarization fields induced in a stopping medium to higher than first order. That formalism was employed to estimate the Barkas correction to the stopping power of an electron gas at rest. One purpose of the present paper is to bring this work into the open literature, and to apply the scheme to other model systems of interest in particle penetration. A second purpose is to investigate the associated wake field. Thirdly, there has come up some uncertainty with regard to the Barkas effect in an electron gas, in that the two existing treatments led to opposite conclusions with regard to the significance of a Barkas correction in close encounters [17, 18]. Our conclusions regarding this matter have been published only briefly, without comprehensive documentation [21]. Finally, it was found desirable to trace observable effects in the wake field that would be sensitive to higher-order field contributions.

2. HIGHER-ORDER POLARIZATION FIELD

The present section serves to generalize the self-consistent linear treatment of the polarization field as presented in [3] to the second order in the projectile charge. We consider longitudinal fields only, and nonrelativistic projectile speeds.

Let the electric field in the medium be described by a scalar potential

$$\Phi(\mathbf{r}, t) = \int d^3k \int d\omega\, \Phi(\mathbf{k}, \omega)\, e^{i(\mathbf{k}\cdot\mathbf{r} - \omega t)}, \tag{2.1}$$

where

$$\Phi^*(\mathbf{k}, \omega) = \Phi(-\mathbf{k}, -\omega), \tag{2.1a}$$

because $\Phi(\mathbf{r}, t)$ must be real. Then, Poisson's law reads (in gaussian units)

$$k^2\Phi(\mathbf{k}, \omega) = 4\pi\rho(\mathbf{k}, \omega), \tag{2.2}$$

where $\rho(\mathbf{k}, \omega)$ is the Fourier transform of the total charge density. The latter can be written in the form

$$\rho = \rho_{\text{ext}} + \rho^{(1)} + \rho^{(2)} + \cdots, \tag{2.3}$$

in either real or Fourier space, where ρ_{ext} is determined by the external disturbance, here, a penetrating projectile, while $\rho^{(1)}$ and $\rho^{(2)}$ are induced charges, linear and quadratic in Φ, respectively. The connection between $\rho^{(1)}$ and $\rho^{(2)}$ and Φ is governed by the dynamical properties of the medium, i.e., the equations of motion. We shall determine the expressions for $\rho^{(1)}(\Phi)$ and $\rho^{(2)}(\Phi)$ in the following section by means of first- and second-order, time-dependent perturbation theory, respectively.

The connection between $\rho^{(1)}$ and Φ is commonly expressed in terms of the dielectric function $\varepsilon(\mathbf{k}, \omega)$,

$$4\pi\rho^{(1)}(\Phi) = \{1 - \varepsilon(\mathbf{k}, \omega)\}\, k^2\Phi. \tag{2.4}$$

The dielectric function is independent of the nature of the external perturbation, i.e., it is a property of the medium alone.

If we terminate the expansion (2.3) after the first-order induced density $\rho^{(1)}(\Phi)$ we obtain the conventional, self-consistent equation for the linear field $\Phi^{(1)}$,

$$k^2\Phi^{(1)} = 4\pi\{\rho_{\text{ext}} + \rho^{(1)}(\Phi^{(1)})\}. \tag{2.5}$$

Applying Eq. (2.4) to eliminate $\rho^{(1)}(\Phi^{(1)})$ we obtain the familiar expression

$$k^2\varepsilon(\mathbf{k}, \omega)\, \Phi^{(1)}(\mathbf{k}, \omega) = 4\pi\rho_{\text{ext}}(\mathbf{k}, \omega). \tag{2.6}$$

The next step is to include $\rho^{(2)}$ in Eq. (2.2) and to solve the self-consistent, quadratic equation for the potential,

$$k^2\Phi = 4\pi\{\rho_{\text{ext}} + \rho^{(1)}(\Phi) + \rho^{(2)}(\Phi)\}. \tag{2.7}$$

Eliminating $\rho^{(1)}$ by means of Eq. (2.4) yields

$$k^2\varepsilon\Phi = 4\pi\{\rho_{\text{ext}} + \rho^{(2)}(\Phi)\}. \tag{2.8}$$

This is a nonlinear integral equation determining Φ. Expansion of Φ in powers of the external perturbation, ρ_{ext},

$$\Phi = \Phi^{(1)} + \Phi^{(2)} \cdots \tag{2.9}$$

leads to Eq. (2.5) in the first order. The second-order terms yield

$$\Phi^{(2)}(\mathbf{k}, \omega) = \frac{4\pi}{k^2\varepsilon(\mathbf{k}, \omega)}\, \rho^{(2)}(\Phi^{(1)}). \tag{2.10}$$

This expression was derived in Ref. [17]. It determines the wake field to second order in the projectile charge and, consequently, the stopping power to third order.

3. INDUCED CHARGE DENSITY

In the present section, the induced charge density will be determined to second order in $\Phi(\mathbf{k}, \omega)$ by time-dependent perturbation theory. This generalizes the procedure of Ref. [3], except that we de not treat the electrons of the medium as a Fermi gas but allow for an arbitrary binding force.

Consider a single electron bound by a force centered at some point $\mathbf{R}$. The electron is characterized by eigenstates $\psi_n(\mathbf{r} - \mathbf{R})$ and energies $E_n = \hbar\omega_n$, with

$n = 0, 1, 2, \ldots$ Let the electron be in the state ψ_0 at time $t = -\infty$, and let it be disturbed by the potential (2.1). Expansion of the wave function in powers of Φ,

$$\Psi(\mathbf{r}, t) = \Psi^{(0)}(\mathbf{r}, t) + \Psi^{(1)}(\mathbf{r}, t) + \Psi^{(2)}(\mathbf{r}, t) + \cdots \tag{3.1}$$

yields

$$\Psi^{(0)} = e^{-i\omega_0 t}\psi_0(\mathbf{r} - \mathbf{R}), \tag{3.2a}$$

$$\Psi^{(1)} = \frac{e}{\hbar}\, e^{-i\omega_0 t} \sum_n \psi_n(\mathbf{r} - \mathbf{R}) \int d^3k \int d\omega\, \frac{f_{n0}(\mathbf{k})}{\omega_{n0} - \omega - i\gamma} \times \Phi(\mathbf{k}, \omega)\, e^{i(\mathbf{k}\cdot\mathbf{R} - \omega t)}, \tag{3.2b}$$

$$\Psi^{(2)} = \frac{e^2}{\hbar^2}\, e^{-i\omega_0 t} \sum_n \sum_j \psi_n(\mathbf{r} - \mathbf{R}) \int d^3k \int d\omega \int d^3k' \int d\omega' \times \Phi(\mathbf{k} - \mathbf{k}', \omega - \omega')\, \Phi(\mathbf{k}', \omega')\, \frac{f_{nj}(\mathbf{k} - \mathbf{k}')\, f_{j0}(\mathbf{k}')}{(\omega_{n0} - \omega - i\gamma)(\omega_{j0} - \omega' - i\gamma)} \times e^{i\mathbf{k}\cdot\mathbf{R} - i\omega t}, \tag{3.2c}$$

where $-e$ is the electron charge,

$$f_{nj}(\mathbf{k}) = \int d^3r\, \psi_n^*(\mathbf{r})\, e^{i\mathbf{k}\cdot\mathbf{r}}\psi_j(\mathbf{r}), \tag{3.3}$$

and

$$\omega_{nj} = \omega_n - \omega_j.$$

A negative imaginary increment $-i\gamma$ has been added to ω_n to ensure that only the initial state ψ_0 is occupied at $t = -\infty$ [3].

Next we obtain induced charge densities due to the perturbed motion of the electron bound to $\mathbf{R}$,

$$\delta\rho^{(1)} = -e\{\Psi^{(0)*}\Psi^{(1)} + \Psi^{(1)*}\Psi^{(0)}\} \tag{3.4a}$$

$$\delta\rho^{(2)} = -e\{\Psi^{(0)*}\Psi^{(2)} + \Psi^{(2)*}\Psi^{(0)} + \Psi^{(1)*}\Psi^{(1)}\}. \tag{3.4b}$$

Insertion of Eqs. (3.2a, b) into (3.4a) and integration over a uniform spatial distribution of bound electrons at a density of n [electrons/volume] yields the induced charge density to first order,

$$\rho^{(1)}(\mathbf{r}, t) = n \int d^3R\, \delta\rho^{(1)}(\mathbf{r}, t) \tag{3.5}$$

or, in Fourier space,

$$\rho^{(1)}(\mathbf{k}, \omega) = -\frac{ne^2}{\hbar}\, \Phi(\mathbf{k}, \omega) \sum_n |f_{n0}(\mathbf{k})|^2 \left\{\frac{1}{\omega_{n0} - \omega - i\gamma} + \frac{1}{\omega_{n0} + \omega + i\gamma}\right\},$$

where use has been made of Eq. (2.1a) and the relation

$$\int d^3R\, \psi_0^*(\mathbf{r}-\mathbf{R})\, e^{i\mathbf{k}\cdot\mathbf{R}}\psi_n(\mathbf{r}-\mathbf{R}) = e^{i\mathbf{k}\cdot\mathbf{r}} f_{0n}(-\mathbf{k})$$

which follows from (3.3).

Insertion of $\rho^{(1)}$ into (2.4) yields the dielectric function

$$\varepsilon(\mathbf{k}, \omega) = 1 + \frac{\omega_{\mathrm{P}}^2}{2\omega_k} \sum_n |f_{n0}(\mathbf{k})|^2 \left\{ \frac{1}{\omega_{n0}-\omega-i\gamma} + \frac{1}{\omega_{n0}+\omega+i\gamma} \right\}, \tag{3.6}$$

where $\omega_k = \hbar k^2/2m$ and $\omega_{\mathrm{P}}^2 = 4\pi n e^2/m$, ω_{P} being the plasma frequency.

Application of the same procedure to Eq. (3.4b) yields

$$\rho^{(2)}(\mathbf{k}, \omega) = -\frac{ne^3}{\hbar^2} \int d^3k' \int d\omega'\, \Phi(\mathbf{k}-\mathbf{k}', \omega-\omega') \times \Phi(\mathbf{k}', \omega')\, Y(\mathbf{k}, \omega, \mathbf{k}', \omega'), \tag{3.7a}$$

where

$$\begin{aligned} Y(\mathbf{k}, \omega, \mathbf{k}', \omega') = \sum_n \sum_j \Bigg\{ & \frac{f_{0n}(-\mathbf{k})\, f_{nj}(\mathbf{k}-\mathbf{k}')\, f_{j0}(\mathbf{k}')}{(\omega_{n0}-\omega-i\gamma)(\omega_{j0}-\omega'-i\gamma)} \\ & + \frac{f_{0j}(\mathbf{k}')\, f_{jn}(\mathbf{k}-\mathbf{k}')\, f_{n0}(-\mathbf{k})}{(\omega_{n0}+\omega+i\gamma)(\omega_{j0}+\omega'+i\gamma)} \\ & + \frac{f_{0n}(\mathbf{k}-\mathbf{k}')\, f_{nj}(-\mathbf{k})\, f_{j0}(\mathbf{k}')}{(\omega_{n0}+\omega-\omega'+i\gamma)(\omega_{j0}-\omega'-i\gamma)} \Bigg\}. \end{aligned} \tag{3.7b}$$

The procedure described in this paragraph does not explicitly take into account the Pauli principle. If the initial states of the electrons in the medium are orthogonal, the Pauli principle is obeyed at all times. This holds true for the case of the Fermi gas considered in Ref. [3]. The present set of initial wave functions, i.e., the ground state wave functions $\psi_0(\mathbf{r}-\mathbf{R})$ for different position vectors $\mathbf{R}$, is not orthogonal. Therefore, the Pauli principle is not obeyed in general. On the other hand, many explicit results for the electron gas have been found by ignoring the zero-point motion, i.e., for a "static electron gas," which was also considered in Ref. [3]. That system corresponds to the choice of $\psi_0(\mathbf{r}) = \text{constant}$, i.e., complete lack of orthogonality. Many reasonable results have been derived for that system over the years, and more examples will be discused later in this paper.

The expressions for the induced charge density have been derived above for an ensemble of one-electron atoms, allowing for mutual polarization via Coulomb's law. However, to the extent that the overlap between the wave functions of different atoms is inappreciable, it is easily verified that they also hold for an ensemble of many-electron atoms, provided that the matrix elements Eq. (3.3) are generalized appropriately [7, 22].

4. GENERAL EXPRESSIONS FOR WAKE FIELD AND STOPPING POWER

4.1. *Classical Charge Distribution in Uniform Motion*

We need to specify the external disturbance in order to determine the induced polarization field. For a classical charge distribution in uniform motion, the external charge density is

$$\rho_{\text{ext}} = \rho_0(\mathbf{r} - \mathbf{v}t), \tag{4.1}$$

i.e., in Fourier space,

$$\rho_{\text{ext}}(\mathbf{k}, \omega) = \rho_0(\mathbf{k})\, \delta(\omega - \mathbf{k} \cdot \mathbf{v}), \tag{4.1$'$}$$

where $\mathbf{v}$ is the velocity and $\rho_0(\mathbf{k})$ some function determined by the shape of the charge distribution. Equations (4.1) and (4.1′) imply that the moving particles are much heavier than electrons. The necessary modifications of the theory in case of electron and positron penetration have been considered separately [23].

From Eq. (2.5), we find

$$\Phi^{(1)}(\mathbf{k}, \omega) = \frac{4\pi\rho_0(\mathbf{k})\, \delta(\omega - \mathbf{k} \cdot \mathbf{v})}{k^2 \varepsilon(\mathbf{k}, \omega)}. \tag{4.2}$$

This yields the potential to first order,

$$\Phi^{(1)}(\mathbf{r}, t) = 4\pi \int \frac{d^3k}{k^2} \frac{\rho_0(\mathbf{k})}{\varepsilon(\mathbf{k}, \omega)}\, e^{i\mathbf{k} \cdot (\mathbf{r} - \mathbf{v}t)}, \tag{4.3}$$

where ω now stands as an abbreviation of $\omega = \mathbf{k} \cdot \mathbf{v}$.

The associated stopping power is found from the total force on ρ_{ext}, generated by the induced potential $\Phi_{\text{ind}} = \Phi(\mathbf{r}, t) - \Phi_{\text{ext}}$, where Φ_{ext} is the Coulomb potential of the bare ion. Hence,

$$\mathbf{F} = \int d^3r\, \rho_0(\mathbf{r} - \mathbf{v}t)\{-\nabla\Phi_{\text{ind}}(\mathbf{r}, t)\}. \tag{4.4}$$

After integration and taking the component along $\mathbf{v}$, we find the stopping power $dE/dx = -\mathbf{v} \cdot \mathbf{F}/v$, where the sign has been chosen so that dE/dx is positive if energy is *lost*. The leading term, which is of second order in the external charge, reads

$$(dE/dx)^{(2)} = \frac{(2\pi)^6}{2\pi^2 v} \int d^3k\, \frac{i\omega}{k^2}\, |\rho_0(\mathbf{k})|^2 \left\{\frac{1}{\varepsilon(\mathbf{k}, \omega)} - 1\right\}, \tag{4.5}$$

which is identical with the result of [3] in case of a moving point charge.

The second-order contribution to the wake field is found from Eqs. (2.10), (3.7a), and (4.2), i.e.,

$$\Phi^{(2)}(\mathbf{r}, t) = -\frac{(2\pi)^6\, ne^3}{\pi^3\hbar^2} \int \frac{d^3k}{k^2\varepsilon(\mathbf{k}, \omega)}\, e^{i\mathbf{k}\cdot(\mathbf{r}-\mathbf{v}t)}$$

$$\times \int d^3k'\, \frac{\rho_0(\mathbf{k}')}{k'^2\varepsilon(\mathbf{k}', \omega')}\, \frac{\rho_0(\mathbf{k}-\mathbf{k}')}{(\mathbf{k}-\mathbf{k}')^2\, \varepsilon(\mathbf{k}-\mathbf{k}', \omega-\omega')}\, Y(\mathbf{k}, \omega, \mathbf{k}', \omega'). \tag{4.6}$$

This yields the Barkas term in the stopping power according to Eq. (4.4),

$$(dE/dx)^{(3)} = -\frac{(2\pi)^9\, ne^3}{\pi^3\hbar^2 v} \int d^3k \int d^3k'\, i\omega\, \frac{\rho_0(-\mathbf{k})}{k^2\varepsilon(\mathbf{k}, \omega)}\, \frac{\rho_0(\mathbf{k}')}{k'^2\varepsilon(\mathbf{k}', \omega')}$$

$$\times \frac{\rho_0(\mathbf{k}-\mathbf{k}')}{(\mathbf{k}-\mathbf{k}')^2\, \varepsilon(\mathbf{k}-\mathbf{k}', \omega-\omega')}\, Y(\mathbf{k}, \omega, \mathbf{k}', \omega'). \tag{4.7}$$

Evidently, the Barkas effect is determined by two functions, $\varepsilon(\mathbf{k}, \omega)$ and $Y(\mathbf{k}, \omega, \mathbf{k}', \omega')$, both of which depend on the material.

4.2. *Symmetry Considerations*

Before going further, we find it useful to identify a number of symmetry relations. First, we note that the integrands in Eqs. (4.6) and (4.7) are symmetric against the substitution

$$\mathbf{k}' \Leftrightarrow \mathbf{k}-\mathbf{k}' \tag{4.8}$$

except for the function Y. We may, therefore, substitute the symmetrized function

$$Y_s(\mathbf{k}, \omega, \mathbf{k}', \omega') = \tfrac{1}{2}[\,Y(\mathbf{k}, \omega, \mathbf{k}', \omega') + Y(\mathbf{k}, \omega, \mathbf{k}-\mathbf{k}', \omega-\omega')] \tag{4.9}$$

in (4.6) and (4.7) without changing the integrals, provided that they converge.

Next, in addition to the symmetry property (2.1a), there are similar relations for $\varepsilon(\mathbf{k}, \omega)$ and for $\rho_0(\mathbf{k})$. Since $f^*_{nj}(\mathbf{k}) = f_{jn}(-\mathbf{k})$, one finds from (3.7b) and (4.9) that

$$Y_s^*(\mathbf{k}, \omega, \mathbf{k}', \omega') = Y_s(-\mathbf{k}, -\omega, -\mathbf{k}', -\omega'). \tag{4.10}$$

This guarantees that (4.6) and (4.7) represent real quantities.

4.3. *Moving Point Charge*

Before discussing material parameters in detail, we wish to specify the penetrating charge distribution. Most often, it represents a point charge e_1, i.e., $\rho_0(\mathbf{k}) = e_1/(2\pi)^3$. It is customary, then, to write the stopping power in the form

$$dE/dx = \frac{4\pi e_1^2 e^2 n}{mv^2}\, \{L_0 + L_1 + L_2 \cdots\}, \tag{4.11}$$

where L_ν is proportional to e_1^ν. From (4.5),

$$L_0 = \frac{v}{2\pi^2\omega_{\mathrm{P}}^2} \int d^3k \, \frac{i\omega}{k^2} \left\{ \frac{1}{\varepsilon(\mathbf{k}, \omega)} - 1 \right\} \tag{4.11a}$$

and, from (4.7) and (4.9),

$$L_1 = -\frac{mve_1e}{4\pi^4\hbar^2} \int d^3k \int d^3k' \, \frac{i\omega}{k^2\varepsilon(\mathbf{k}, \omega)} \, \frac{1}{k'^2\varepsilon(\mathbf{k}', \omega')} \, \frac{Y_{\mathrm{s}}(\mathbf{k}, \omega, \mathbf{k}', \omega')}{(\mathbf{k}-\mathbf{k}')^2 \, \varepsilon(\mathbf{k}-\mathbf{k}', \omega-\omega')}. \tag{4.11b}$$

Another charge distribution of interest is that of two penetrating point charges e_1 and e_2, e.g., the fragments of a bombarding molecule. In this case, we have

$$\rho_0(\mathbf{k}) = \frac{1}{(2\pi)^3} \{e_1 + e_2 e^{-i\mathbf{k}\cdot\mathbf{R}}\}, \tag{4.12}$$

where **R** is the vector pointing from 1 to 2.

The results of this section, as summarized in Eqs. (4.6) and (4.7), leave only the material parameters ε and Y unspecified. Several special cases will be considered in the following sections.

5. STOPPING POWER OF DILUTE MATTER

5.1. *Derivation from Dielectric Theory*

This paragraph serves to test the present formulation, i.e., mainly the central Eq. (2.10), by utilizing it to calculate the stopping power of a point charge in a dilute medium. This is achieved by letting n (or ω_{P}^2) become small so that the individual target electrons are excited by the Coulomb field of the bare projectile charge. We show that the resulting stopping power becomes identical with that calculated directly from the perturbation of an individual electron by a bare Coulomb charge.

In Eq. (4.11a), the density enters into the factor ω_{P}^{-2} and into the dielectric function $\varepsilon(\mathbf{k}, \omega)$ in the denominator. Equation (3.6) allows us to expand ε^{-1} in powers of the density. Keeping only terms up to first order in ω_{P}^2 we obtain a stopping number that is independent of the electron density n since the term going as n^{-1} vanishes. This yields

$$L_0 = \frac{v}{(2\pi)^2} \operatorname{Im} \sum_n \int \frac{d^3k}{k^2} \frac{\omega}{\omega_k} |f_{n0}(\mathbf{k})|^2 \left[\frac{1}{\omega_{n0} - \omega - i\gamma} + \frac{1}{\omega_{n0} + \omega + i\gamma} \right],$$

from which Bethe's formula [7] in the form

$$L_0 = \frac{1}{2} \sum_n \omega_{n0} \int_{\hbar\omega_{n0}^2/2mv^2}^{\infty} d\omega_k/\omega_k^2 \, |f_{n0}(\mathbf{k})|^2 \tag{5.1}$$

is readily found by integration, taking into account the relation

$$(\omega-\omega_{n0}+i\gamma)^{-1}=P(\omega-\omega_{n0})^{-1}-i\pi\delta(\omega-\omega_{n0}), \tag{5.2}$$

where P indicates the Cauchy principal value.

Similarly, we find the Barkas correction to the stopping power of a dilute medium. Note that according to Eq. (3.7b), the electron density does not enter explicitly into the function Y. This implies that to lowest order in n, L_1 is found from (4.11b) by setting all three dielectric functions ε equal to one. It is sufficient here to work with the function Y, Eq. (3.7b), rather than the symmetrized function Y_s, Eq. (4.9). It is convenient to bring $i\omega Y$ on a form where all three terms go as $f_{0n}(-\mathbf{k})\, f_{nj}(\mathbf{k}-\mathbf{k}')\, f_{j0}(\mathbf{k}')$. This is achieved by the symmetry transformations $j\to n$ and $\mathbf{k}\to -\mathbf{k}'$ in the second term, and $\mathbf{k}\to -\mathbf{k}+\mathbf{k}'$ in the third term. Application of (5.2) yields, then,

$$L_1=\frac{mve_1e}{2\pi^3\hbar^2}\int d^3k\int d^3k'\,\frac{1}{k^2k'^2(\mathbf{k}-\mathbf{k}')^2}$$
$$\times\sum_n\sum_j f_{0n}(-k)\,f_{nj}(\mathbf{k}-\mathbf{k}')\,f_{j0}(\mathbf{k}')\left\{\frac{\omega\delta(\omega-\omega_{n0})}{\omega_{j0}-\omega'-i\gamma}+\frac{\omega'\delta(\omega'-\omega_{j0})}{\omega_{n0}-\omega+i\gamma}\right\}.$$

Applying the symmetry transformation $j\to n$, $\mathbf{k}\to\mathbf{k}'$ to the second term we find

$$L_1=\frac{e_1emv}{\pi^3\hbar^2}\sum_n\sum_j\int\frac{d^3k}{k^2}\,\frac{d^3k'}{k'^2}\,\frac{1}{(\mathbf{k}-\mathbf{k}')^2}$$
$$\times f_{0n}(-\mathbf{k})\,f_{nj}(\mathbf{k}-\mathbf{k}')\,f_{j0}(\mathbf{k}')\,P\,\frac{\omega}{\omega_{j0}-\omega'}\,\delta(\omega_{n0}-\omega). \tag{5.3}$$

Equation (5.3) was first derived in Ref. [17]. It can also be found from second-order perturbation theory, applied to the bare-Coulomb interaction between a projectile and a single electron with eigenstates specified in Section 3. This derivation is presented separately in Appendix A. We find it important to have verified that the two approaches yield the same results. This is, of course, required by the underlying physics.

The direction of the projectile velocity occurs only in the last two factors via $\omega=\mathbf{k}\cdot\mathbf{v}$ and $\omega'=\mathbf{k}'\cdot\mathbf{v}$. It is obviously allowed to average (5.3) over all directions of $\mathbf{v}$. This can be accomplished by expanding the Dirac function in terms of Legendre polynomials $P_\nu(\omega/kv)\equiv P_\nu(\mathbf{k}\cdot\mathbf{v}/kv)$, applying the addition theorem of spherical harmonics to the latter, and utilizing the integral representation of the Legendre functions of the second kind, Q_ν [24, (8.8.3)]. This yields the replacement

$$\frac{\omega}{\omega_{j0}-\omega'}\,\delta(\omega_{n0}-\omega)\to\frac{\omega_{n0}}{kk'v^2}\sum_\nu\frac{2\nu+1}{2}$$
$$\times P_\nu\left(\frac{\omega_{n0}}{kv}\right)Q_\nu\left(\frac{\omega_{j0}}{k'v}\right)P_\nu\left(\frac{\mathbf{k}\cdot\mathbf{k}'}{kk'}\right). \tag{5.3a}$$

This expression, while more complex looking than (5.3), has the advantage that the four angular integrations have reduced to one, i.e., the integration over the angle between **k** and **k**′.

5.2. *Quantal Harmonic Oscillator*

Previous evaluations of the Barkas effect for a dilute stopping medium have all been based on simplified models where the target atom has been represented by a harmonic oscillator. In Ref. [11] and most other investigations, the classical limit of the harmonic oscillator was considered (for reviews cf. [14, 15]). The quantal oscillator was analysed in a multipole expansion in Ref. [12], and the full quantal Barkas correction was evaluated for the harmonic oscillator in Ref. [16]. The present paragraph serves to provide the connection with previous treatments without going into a numerical evaluation. In the following paragraph, we make the transition to the classical limit.

In order to evaluate the Barkas correction, Eq. (5.3) for an individual oscillator, we need to know the matrix elements $f_{nj}(\mathbf{k})$ defined by Eq. (3.3). For a spherical oscillator, the wave functions factorize in cartesian coordinates, and hence,

$$f_{nj}(\mathbf{k}) = f_{n_x j_x}(k_x)\, f_{n_y j_y}(k_y)\, f_{n_z j_z}(k_z). \tag{5.4}$$

The one-dimensional matrix elements are given by [16]

$$f_{nj}(k) = e^{-\omega_k/2\omega_0} \sum_{\nu} \frac{(n!\, j!)^{1/2}}{\nu!\,(n-\nu)!\,(j-\nu)!}\,(ik\alpha)^{n+j-2\nu}, \tag{5.5}$$

where $\alpha = (\hbar/2m\omega_0)^{1/2}$, and ω_0 is the resonant frequency of the oscillator. Since the denominator and the Dirac function in (5.3) only depend on the excitation energy $\hbar\omega_{n0}$, where

$$\omega_{n0} = \omega_0(n_x + n_y + n_z) \equiv n\omega_0, \tag{5.6}$$

the sums over the matrix elements can be carried out for fixed n and j. This yields

$$\begin{aligned}
&\sum_{\substack{n_x+n_y+n_z=n \\ j_x+j_y+j_z=j}}\sum\sum\sum\sum\sum f_{0n}(-\mathbf{k})\, f_{nj}(\mathbf{k}-\mathbf{k}')\, f_{j0}(\mathbf{k}') \\
&\quad = \exp\left\{-\frac{\hbar}{2m\omega_0}\,(k^2 + k'^2 - \mathbf{k}\cdot\mathbf{k}')\right\} \sum \frac{1}{\nu!\,(n-\nu)!\,(j-\nu)!} \\
&\qquad \times \left(\frac{\hbar\mathbf{k}\cdot(\mathbf{k}-\mathbf{k}')}{2m\omega_0}\right)^{n-\nu} \left(\frac{\hbar\mathbf{k}'\cdot(\mathbf{k}'-\mathbf{k})}{2m\omega_0}\right)^{j-\nu} \left(\frac{\hbar\mathbf{k}\cdot\mathbf{k}'}{2m\omega_0}\right)^{\nu},
\end{aligned} \tag{5.7}$$

with ν running between the limits posted by the factorials. Then,

$$\begin{aligned}
L_1 = {}& \frac{e_1 e m v}{\pi^3 \hbar^2} \sum_n \sum_j \sum_\nu \frac{(\hbar/2m\omega_0)^{n+j-\nu}}{(n-\nu)!\,(j-\nu)!\,\nu!}\, P \iint \frac{d^3k\, d^3k'}{k^2 k'^2 (\mathbf{k}-\mathbf{k}')^2}\, \frac{\omega\delta(n\omega_0 - \omega)}{j\omega_0 - \omega'} \\
& \cdot [\mathbf{k}\cdot(\mathbf{k}-\mathbf{k}')]^{n-\nu}\, [\mathbf{k}'\cdot(\mathbf{k}'-\mathbf{k})]^{j-\nu}\, [\mathbf{k}\cdot\mathbf{k}']^{\nu}\, e^{-\hbar(k^2+k'^2-\mathbf{k}\cdot\mathbf{k}')/2m\omega_0}.
\end{aligned} \tag{5.8}$$

Equation (5.8) could be the starting point of a numerical evaluation of the Barkas correction to the stopping power of an oscillator. We shall refrain from this since accurate values, found along a different route, have become available recently [16].

5.3. *Classical Harmonic Oscillator*

Equation (5.8) is also a convenient starting point for an evaluation of the Barkas correction in the classical limit, i.e., $\hbar = 0$. We note that apart from the exponential, $\hbar$ enters only as a power, i.e., $\hbar^{n+j-\nu-2}$. All terms with $n=0$ drop out because of the factor $\omega\delta(n\omega_0 - \omega)$ (no excitation). The term with the lowest power in $\hbar$ occurring in (5.8) goes as $\hbar^{-1}$. It consists of the two terms $(n, j, \nu) = (1, 0, 0)$ and $(1, 1, 1)$ and is easily seen to vanish after replacement of $\mathbf{k}' \to \mathbf{k} - \mathbf{k}'$.

Hence, the leading term is of zeroth order in $\hbar$ as it should be, and is made up of the contributions from $(n, j, \nu) = (1, 1, 0)$ and $(1, 2, 1)$, while the contributions from $(2, 0, 0)$, $(2, 1, 1)$, and $(2, 2, 2)$ are seen to cancel by the same symmetry transformation as above. Then, Eq. (5.8) yields

$$L_1 = -\frac{e_1 e v}{2\pi^3 m} P \iint \frac{d^3k\, d^3k'}{k^2 k'^2 (\mathbf{k} - \mathbf{k}')^2} e^{-\hbar(k^2 + k'^2 - \mathbf{k}\cdot\mathbf{k}')/2m\omega_0}$$

$$\times [\mathbf{k}' \cdot (\mathbf{k} - \mathbf{k}')][\mathbf{k} \cdot (\mathbf{k} - \mathbf{k}')] \frac{\delta(\omega_0 - \omega)}{\omega_0^2 - \omega'^2}. \tag{5.9}$$

We have kept the exponential even though it contains a factor of $\hbar$, because it prevents the integral from diverging. Equation (5.9) demonstrates that although both dipole and quadrupole transitions contribute to the Barkas correction in the classical (or long-range) limit, in agreement with Ref. [12], excitations to the final state $n = 2$ do not contribute, in agreement with Ref. [16].

We may bring Eq. (5.9) into a simple analytic form by neglecting the exponential factor. Evidently, this is justified only for small k, i.e., soft collisions. As a first step, we perform the integration over the orientation of $\mathbf{k}$. We note that the function to be integrated over d^3k is a scalar depending on the vectors $\mathbf{k}$ and $\mathbf{v}$. Hence, the integrand can only depend on k, v, and $\mathbf{k} \cdot \mathbf{v} = \omega$. We may then carry out the trivial integral over ω and obtain

$$L_1 = \pi \frac{e_1 e \omega_0}{m v^3} \int_{\omega_0/v}^{\infty} \frac{dk}{k} F(k) \tag{5.10}$$

with

$$F(k) = -\frac{v^3}{2\pi^3 \omega_0} P \int d^3k' \frac{\mathbf{k}' \cdot (\mathbf{k} - \mathbf{k}')}{k'^2 (\mathbf{k} - \mathbf{k}')^2} \left\{ \frac{\mathbf{k} \cdot (\mathbf{k} - \mathbf{k}')}{\omega_0^2 - \omega'^2} + \frac{\mathbf{k} \cdot \mathbf{k}'}{\omega_0^2 - (\omega_0 - \omega')^2} \right\}, \tag{5.11}$$

In Eq. (5.10), the "Barkas factor" $\pi e_1 e \omega_0 / m v^3$ has been split off. The integrand in (5.11) has been symmetrized with respect to $\mathbf{k}'$ and $\mathbf{k} - \mathbf{k}'$ in the following. We can close the integration over $k'_z = \omega'/v$ by a semi-circle in the upper complex k'_z-plane. The pertinent poles are at $k'_z = ik'_\perp$ and at $k'_z = \mathbf{k}_z + i\,|\mathbf{k}_\perp - \mathbf{k}'_\perp|$. In addition, there are also poles on the real axis. The two pairs of poles both have the property that the one is the complex conjugate of the other, as can be seen by means of the transformation

$$\mathbf{k}'_\perp \to \mathbf{k}_\perp - \mathbf{k}'_\perp .$$

This observation implies that the sum of the contributions from the poles on the real axis is zero, while the two other contributions may be combined into one expression where the integration over $k'_\perp$ goes from $-\infty$ to $+\infty$. Then,

$$F(k) = -\frac{v}{\pi\omega_0}\int_0^{2\pi}\frac{d\phi}{2\pi}\int_{-\infty}^{\infty} dk'_\perp\,\frac{\mathbf{k}\cdot(\mathbf{k}-\mathbf{k}')}{|\mathbf{k}-\mathbf{k}'|^2}$$
$$\times\left\{\frac{\mathbf{k}\cdot(\mathbf{k}-\mathbf{k}')}{(\omega_0/v)^2+k'^2_\perp}+\frac{\mathbf{k}\cdot\mathbf{k}'}{(\omega_0/v)^2-(\omega_0/v-ik'_\perp)^2}\right\},$$

where $k'_z = ik'_\perp$, $k_z = \omega_0/v$, and ϕ the angle between $\mathbf{k}_\perp$ and $\mathbf{k}'_\perp$.

After again closing the path of integration by a semicircle in the upper complex $k'_\perp$ halfplane, it is seen that only one pole in $k'_\perp = i\omega_0/v$ contributes. Then,

$$F(k) = -\left(\frac{v}{\omega_0}\right)^2\int_0^{2\pi}\frac{d\phi}{2\pi}\,\frac{\mathbf{k}'\cdot(\mathbf{k}-\mathbf{k}')\,\mathbf{k}\cdot(\mathbf{k}-\mathbf{k}')}{(\mathbf{k}-\mathbf{k}')^2}$$
$$= -\left(\frac{v}{\omega_0}\right)^2\int_0^{2\pi}\frac{d\phi}{2\pi}\left\{\frac{\mathbf{k}\cdot\mathbf{k}'}{2}-\frac{k^2}{4}+\frac{1}{4}\,\frac{k^4}{k^2-2\mathbf{k}\cdot\mathbf{k}'}\right\}$$
$$= \frac{1}{4}\left\{2+\left(\frac{kv}{\omega_0}\right)^2\left[1-(1+8(\omega_0/kv)^2\right]^{-1/2}\right\}. \tag{5.12}$$

This result has been derived previously for the limiting case of distant collisions [17]. A corresponding result will emerge in Section 6.3 for a static electron gas in the classical limit. We note that $F(k) \to \frac{3}{2}$ for $k \gg \omega_0/v$. This appears to be characteristic of the harmonic oscillator.

The expression for L_1 in Eq. (5.10) diverges logarithmically at large k if no upper limit of integration is specified. Equation (5.7) demonstrates that for $\hbar \neq 0$, the integral converges, but the effective upper limit is not evident. Various upper limits $k_{\max}$ have been used in the literature. In [11], $k_{\max}$ was adjusted to experimental results. In [25], the choice $k_{\max} = (2m\omega_0/\hbar)^{1/2}$ was made, which appears feasible in view of the exponential in (5.7). In Ref. [13], the result has been extrapolated into the region of close collisions with a cutoff determined by the maximum momentum transfer in a free collision, $k_{\max} = 2mv/\hbar$.

In Ref. [16], it was shown that the range of validity of the classical Barkas correction is limited to rather large impact parameters, i.e., small momentum transfers. Therefore, caution is indicated in extrapolating the classical expression for $F(k)$ up to large momentum transfers. An effective upper limit could be determined by comparing the integral with the rigorous quantal result given in Ref. [16]. It is easily verified that such an upper limit can be written in the form

$$k_{\max} = \eta 2mv/\hbar \tag{5.13}$$

with η varying slowly with $y = 2mv^2/\hbar\omega_0$ over the range $0.4 \lesssim \eta \lesssim 1.4$. Evidently, this upper limit is outside the range of applicability of the classical estimate.

6. ELECTRON GAS

In this section we consider a free electron gas and extend Lindhard's description [3] to the next order in e_1. The numerical calculations of the stopping power and wake potential become rather involved when the zero-point motion of the Fermi gas in included, partly because of a large variety of singularities, partly because of an additional integration in three dimensions. In the actual evaluation, we therefore consider the limit of a static gas (i.e., without Fermi motion). Numerical results for this limit will be presented in Section 8.

6.1. *Fermi Gas*

The target states for a noninteracting Fermi gas are plane waves,

$$\psi_n(\mathbf{r}) = \frac{1}{\sqrt{\Omega}}\, e^{i\mathbf{k}_n \cdot \mathbf{r}}, \tag{6.1}$$

Ω being a periodicity volume. We can satisfy the Pauli principle by letting the initial electron states Ψ_0, i.e., the wave vectors $\mathbf{k}_0$ be distributed over a Fermi sphere (for zero or nonzero temperature), with a weight function $g(\mathbf{k}_0)$ normalized to 1. Then, Eq. (3.6) yields

$$\varepsilon(\mathbf{k}, \omega) = 1 + \frac{\omega_P^2}{2\omega_k} \sum_{\mathbf{k}_0} g(\mathbf{k}_0) \left(\frac{1}{M_k(\omega)} + \frac{1}{M_k(-\omega)} \right), \tag{6.2}$$

since the matrix elements in Eq. (3.6) reduce to the condition $\mathbf{k}_n = \mathbf{k}_0 + \mathbf{k}$. Here, $\omega_k = \hbar k^2/2m$ and

$$M_k(\omega) = \omega_{\mathbf{k}_0 + \mathbf{k}} - \omega_{\mathbf{k}_0} + \omega + i\gamma, \tag{6.3}$$

with the convention that the sign of $i\gamma$ follows the sign on ω in the argument of the function $M_k(\omega)$.

From (3.7b) we obtain similarly

$$Y(\mathbf{k}, \omega, \mathbf{k}', \omega') = \sum_{\mathbf{k}_0} g(\mathbf{k}_0) \left[\frac{\Gamma}{M_k(-\omega)\, M_{k'}(-\omega')} + \frac{1}{M_{-k}(\omega)\, M_{-k'}(\omega')} + \frac{1}{M_{k'-k}(\omega - \omega')\, M_{k'}(-\omega')} \right]. \tag{6.4}$$

The expression (6.2) for ε is the Lindhard function [3]. Equation (6.4) was first derived in [17] for a static electron gas. More recently, derivations based on a diagrammatic expansion of the induced electron density were given [18], which lead to the same result. For example, our Y function, expressed by Eq. (3.7b) in general and Eq. (6.4) for the electron gas is equivalent with the quadratic response function χ_2, Eq. (A6) of Hu, *et al.* [18] and with the M function, Eq. (2.24) of Sung, *et al.* [18]. Similar statements may be made for the stopping power.

Estimates based on the full dielectric functions (6.2) and (6.4) were made in Ref. [18] of the contributions to the Barkas correction in the stopping power due to close and distant collisions, respectively, but a detailed numerical evaluation was not presented. Although the zero-point motion is important and gives rise to significant shell corrections [16], the static electron gas shows sufficient complexity to warrant studying it first.

6.2. *Static Electron Gas*

For a static electron gas, i.e., when all $\mathbf{k}_0$ become zero, Eqs. (6.2) and (6.4) reduce to

$$\varepsilon(\mathbf{k}, \omega) = 1 + \frac{\omega_{\mathrm{P}}^2}{\omega_k^2 - (\omega + i\gamma)^2} \tag{6.5}$$

and

$$\begin{aligned} Y(\mathbf{k}, \omega, \mathbf{k}', \omega') = {} & \frac{1}{(\omega_k - \omega - i\gamma)(\omega_{k'} - \omega' - i\gamma)} \\ & + \frac{1}{(\omega_k + \omega + i\gamma)(\omega_{k'} + \omega' + i\gamma)} \\ & + \frac{1}{(\omega_{k-k'} + \omega - \omega' + i\gamma)(\omega_{k'} - \omega' - i\gamma)}. \end{aligned} \tag{6.6}$$

We evaluate the wake potential (4.6) for a penetrating point charge with $\rho_0(\mathbf{k}) = e_1/(2\pi)^3$ and note that it is the quantity

$$\frac{1}{\varepsilon(\mathbf{k}, \omega)} = \frac{\omega_k^2 - (\omega + i\gamma)^2}{\alpha_k^2 - (\omega + i\gamma)^2} \tag{6.7}$$

with

$$\alpha_k^2 = \omega_k^2 + \omega_{\mathrm{P}}^2 \tag{6.8}$$

which enters into Eq. (4.6).

The symmetry properties of Eq. (4.6) allow the substitution (4.9) which causes the resulting expression to simplify substantially. In particular, all denominators in Eq. (6.6) cancel against the corresponding numerators arising from Eq. (6.7). This is the major simplification achieved by taking the limit of the static electron gas. As a result, one finds

$$\Phi^{(2)}(\mathbf{r}, t) = -\frac{ne_1^2e^3}{\pi^3\hbar^2}\iint \frac{d^3k\, d^3k'}{k^2k'^2(\mathbf{k}-\mathbf{k}')^2}\,\frac{[Q_0+Q_2]\exp[i\mathbf{k}\cdot(\mathbf{r}-\mathbf{v}t)]}{N(\mathbf{k})\,N(\mathbf{k}')\,N(\mathbf{k}-\mathbf{k}')}, \tag{6.9}$$

where

$$N(\mathbf{k}) = \alpha_k^2 - (\omega + i\gamma)^2, \tag{6.10}$$

$$Q_0 = \omega\omega'\omega_{k-k'}^2 + \omega(\omega-\omega')\omega_{k'}^2 - \omega'(\omega-\omega')\omega_k^2$$
$$- (\omega-\omega')^2\,\omega_k\omega_{k'} - \omega'^2\omega_k\omega_{k-k'} - \omega^2\omega_{k'}\omega_{k-k'} \tag{6.11}$$

and

$$Q_2 = \omega_k\omega_{k'}\omega_{k-k'}[\omega_k + \omega_{k'} + \omega_{k-k'}]. \tag{6.12}$$

The associated Barkas correction to the stopping power (4.11b) reads

$$L_1 = -\frac{mve_1e}{4\pi^4\hbar^2}\iint \frac{d^3k\, d^3k'}{k^2k'^2(\mathbf{k}-\mathbf{k}')^2}\,\frac{i\omega(Q_0+Q_2)}{N(\mathbf{k})\,N(\mathbf{k}')\,N(\mathbf{k}-\mathbf{k}')}. \tag{6.13}$$

L_1 must obviously be a real number. This can be verified by complex conjugating the expression and changing sign on all integration variables. While the integrand in (6.13) is symmetric with respect to the transformation $\mathbf{k}' \to \mathbf{k}-\mathbf{k}'$, it is not symmetric in $\mathbf{k}$ and $\mathbf{k}'$. That symmetry is violated by the factors ω and $N(\mathbf{k}-\mathbf{k}')$.

We shall now transform (6.13) in such a way that the integration over $k_z = \omega/v$ becomes trivial. As a first step, we decompose ω into $\omega' + (\omega - \omega')$. Due to the symmetry between $\mathbf{k}'$ and $\mathbf{k}-\mathbf{k}'$ we can transform the second term $(\omega-\omega')$ into ω'. Thus we see that we can replace the factor ω in Eq. (6.13) by $2\omega'$. The next step is to interchange $\mathbf{k}$ and $\mathbf{k}'$. The resulting expression differs from (6.13) by the replacement

$$\frac{\omega}{N(\mathbf{k}-\mathbf{k}')} \to \frac{2\omega}{N(\mathbf{k}'-\mathbf{k})}, \tag{6.14}$$

and it can be written in a form that will become convenient in the following discussion,

$$L_1 = \frac{-e_1e\omega_P}{2\pi mv^2}\int d^3k\, \frac{i\omega}{k^2N(\mathbf{k})}\, F(\mathbf{k}), \tag{6.15}$$

where

$$F(\mathbf{k}) = \frac{m^2v^3}{\pi^3\hbar^2\omega_P}\int d^3k'\, \frac{Q_0+Q_2}{k'^2(\mathbf{k}-\mathbf{k}')^2\,N(\mathbf{k}')\,N(\mathbf{k}'-\mathbf{k})}, \tag{6.16}$$

The function F has the property $F(\mathbf{k})^* = F(-\mathbf{k})$. Moreover, upon performing the transformation $\mathbf{k}' \Rightarrow \mathbf{k}' + \mathbf{k}/2$ we see that $F(\mathbf{k}) = F(-\mathbf{k})$. Therefore, $F(\mathbf{k})$ must be real. Consequently, only the imaginary part of $N(\mathbf{k})^{-1}$ can contribute to L_1 whereas the contribution from the real part vanishes.

In order to evaluate the contribution from the imaginary part of $N(\mathbf{k})^{-1}$ we note that

$$\operatorname{Im} N(\mathbf{k})^{-1} = \frac{\pi}{2\omega} \left[\delta(\omega - \alpha_k) + \delta(\omega + \alpha_k)\right]. \tag{6.17}$$

We may carry out the $\mathbf{k}$-integration in spherical coordinates and obtain

$$L_1 = \pi \frac{e_1 e \omega_{\mathrm{P}}}{mv^3} \int \frac{dk}{k} F(k), \tag{6.18}$$

where the k-integral is subject to the condition $\alpha_k < kv$, or

$$mv^2/\hbar - \{(mv^2/\hbar)^2 - \omega_{\mathrm{P}}^2\}^{1/2} < \omega_k < mv^2/\hbar + \{(mv^2/\hbar)^2 - \omega_{\mathrm{P}}^2\}^{1/2}. \tag{6.19}$$

We shall give some numerical results for these expressions in Section 8. We note that the manipulations leading from Eq. (6.16) to (6.18) cannot, unfortunately, be used in this form to simplify the calculation of the wake field.

6.3. *Classical Limit*

As in Section 5.3, it is useful to check the quantal result in the limit of $\hbar = 0$ against the classical limit. The latter has been evaluated in Appendix B on the basis of Boltzmann's transport equation, in a straight generalization to the next order in e_1 of the procedure developed in Ref. [3]. This treatment yields Eq. (B10) for the function $Y(\mathbf{k}, \omega, \mathbf{k}', \omega')$. After symmetrization, Eq. (4.9), we find

$$Y_s(\mathbf{k}, \omega; \mathbf{k}', \omega') = -\frac{Q_0}{(\omega + i\gamma)^2 (\omega' + i\gamma)^2 (\omega - \omega' + i\gamma)^2}, \tag{6.20}$$

where Q_0 is identical to the function given in Eq. (6.11) of the previous paragraph. The corresponding dielectric function is the well-known Drude expression

$$\varepsilon(\omega) = 1 - \frac{\omega_{\mathrm{P}}^2}{(\omega + i\gamma)^2}. \tag{6.21}$$

Let us now consider the Barkas correction to the stopping number, L_1, Eq. (4.11b). Inserting Eqs. (6.20, 6.21) we obtain

$$L_1 = -\frac{mve_1 e}{4\pi^4 \hbar^2} \iint \frac{d^3k\, d^3k'}{k^2 k'^2 (\mathbf{k} - \mathbf{k}')^2} \frac{i\omega Q_0}{N(\omega) N(\omega') N(\omega - \omega')}, \tag{6.22}$$

where

$$N(\omega) = \omega_p^2 - (\omega + i\gamma)^2.$$

This result is identical with the quantal result (6.13) in the limit of $\hbar = 0$ since the term Q_2 vanishes and $N(\mathbf{k})$ reduces to $N(\omega)$. We can now repeat the transformations that led to Eqs. (6.16) and (6.18). In this way, we obtain L_1 expressed by (6.18) with

$$F(k) = \frac{m^2 v^3}{\pi^3 \hbar^2 \omega_P} \int \frac{d^3k'}{k'^2 (\mathbf{k} - \mathbf{k}')^2} \frac{Q_0}{N(\omega')\, N(\omega' - \omega)}. \tag{6.24}$$

The simple pole in $N(\omega)^{-1}$ determines the lower limit of the integration since $\omega = k_z v = \omega_P$.

The function $F(k)$, Eq. (6.24), is very similar to the one evaluated for the harmonic oscillator, Eq. (5.11), and can be evaluated by exactly the same procedure. The result is, with $k_z = \omega_P / v$ and $k'_z = ik'_\perp = -\omega_P / v$,

$$\begin{aligned} F(k) &= \frac{1}{12\pi} \left(\frac{v}{\omega_P}\right)^2 \int_0^{2\pi} d\phi \left\{ |\mathbf{k} - \mathbf{k}'|^2 - \frac{k^4}{|\mathbf{k} - \mathbf{k}'|^2} + k^2 \right\} \\ &= \frac{1}{3} \left\{ 1 + \left(\frac{kv}{\omega_P}\right)^2 [1 - (1 + 8(\omega_P / kv)^2)^{-1/2}] \right\}. \end{aligned} \tag{6.25}$$

This result may be compared to Eq. (5.12). It is seen to be very similar in structure, but a slight numerical difference occurs in the numbers. In particular, $F(k) \Rightarrow \frac{5}{3}$ for $k \gg \omega_P / v$, whereas the asymptotic value for the classical harmonic oscillator is $\frac{3}{2}$. We have not found a simple physical rationale for the difference in these numbers. We shall see, however, that both results emerge as limiting cases from a more general expression to be discussed in Section 7.2.

The integration over k shows again a logarithmic divergence as it stands, and similar comments apply as the ones made for the classical harmonic oscillator below Eq. (5.12).

7. DENSE MEDIUM CONTAINING BOUND ELECTRONS

The present section serves to establish the functions ε and Y for a dense stopping medium. The standard model for such a medium is the Fermi gas [3] which contains several important ingredients: Zero-point motion, collective and single-particle excitations, and the exclusion principle. The free electron gas was discussed in Section 6, in particular in the static limit where Fermi motion is neglected. Here we shall look at an example of a medium where electron motion is constrained by local binding forces which will be assumed to be harmonic. The discussion serves first to provide the relation between the free-electron-gas and the single-oscillator treatment of the Barkas effect discussed in the previous sections, and second to analyse the dependence of the Barkas correction on the density of the medium. A detailed investigation of the stopping power and excitation spectrum of such a medium to leading order in e_1 is being prepared separately [26].

7.1 *Medium of Harmonic Oscillators*

Going back to Section 5 we shall make use of the relations (5.4)–(5.7) that are satisfied by the matrix elements of a harmonic oscillator, as well as the simple sum rule

$$\sum_{n_x+n_y+n_z=n}\sum\sum f_{0n}(-\mathbf{k})\, f_{n0}(\mathbf{k}) = e^{-\omega_k/\omega_0}\,\frac{1}{n!}\left(\frac{\hbar k^2}{2m\omega_0}\right)^n \tag{7.1}$$

that is readily derived similarly to (5.7). Then Eq. (3.6) yields [26]

$$\varepsilon(\mathbf{k}, \omega) = 1 + \frac{\omega_{\mathrm{P}}^2}{2\omega_k}\, e^{-\omega_k/\omega_0} \sum_n \frac{1}{n!}\left(\frac{\omega_k}{\omega_0}\right)^n \left\{\frac{1}{M_{n0}(-\omega)} + \frac{1}{M_{n0}(\omega)}\right\}, \tag{7.2}$$

where

$$M_{n0}(\omega) = n\omega_0 + (\omega + i\gamma). \tag{7.3}$$

As in Eq. (6.3) above, it is understood that the sign of $i\gamma$ follows the sign on ω. Moreover, Eq. (3.7b) yields

$$\begin{aligned} Y(\mathbf{k}, \omega, \mathbf{k}', \omega') = e^{-(\omega_k+\omega_{k'}-\omega_{kk'})/\omega_0} \sum_n \sum_j \sum_\nu \frac{\omega_0^{-n-j+\nu}}{\nu!\,(n-\nu)!\,(j-\nu)!} \\ \times \left\{\frac{\omega_{kk'}^{\nu}\,\omega_{kq}^{n-\nu}(-\omega_{k'q})^{j-\nu}}{M_{n0}(-\omega)\,M_{j0}(-\omega')} + \frac{\omega_{kk'}^{\nu}\,\omega_{kq}^{n-\nu}(-\omega_{k'q})^{j-\nu}}{M_{n0}(\omega)\,M_{j0}(\omega')}\right. \\ \left. + \frac{(-\omega_{k'q})^{\nu}\,\omega_{kq}^{n-\nu}\omega_{kk'}^{j-\nu}}{M_{n0}(\omega-\omega')\,M_{j0}(-\omega')}\right\}, \end{aligned} \tag{7.4}$$

with $\omega_{kk'} = \hbar\mathbf{k}\cdot\mathbf{k}'/2m$ and $\mathbf{q} = \mathbf{k} - \mathbf{k}'$.

7.2. *The Classical Limit*

It is of interest to compare Eqs. (7.2) and (7.4) with the corresponding expressions for an ensemble of classical harmonic oscillators. In Appendix C, these expressions have been derived directly from the differential equation governing forced vibrations. As a result, we find

$$\varepsilon(\mathbf{k}, \omega) = 1 + \frac{\omega_{\mathrm{P}}^2}{\omega_0^2 - \omega^2 - i\gamma\omega} \tag{7.5}$$

and, cf. Eqs. (3.7a) and (C10)–(C11),

$$\begin{aligned} Y = -\frac{\hbar^2}{2m^2}\left\{\frac{2\mathbf{k}\cdot(\mathbf{k}-\mathbf{k}')}{\omega_0^2-\omega^2-i\gamma\omega}\,\frac{\mathbf{k}'\cdot(\mathbf{k}-\mathbf{k}')}{\omega_0^2-\omega'^2-i\gamma\omega'}\right. \\ \left. - \frac{\mathbf{k}\cdot(\mathbf{k}-\mathbf{k}')}{\omega_0^2-\omega'^2-i\gamma\omega'}\,\frac{\mathbf{k}\cdot\mathbf{k}'}{\omega_0^2-(\omega-\omega')^2-i\gamma(\omega-\omega')}\right\}. \end{aligned} \tag{7.6}$$

Equation (7.5) represents the well-known dielectric function from classical dispersion theory. It is independent of **k** because the classical perturbation expansion implies the dipole approximation. It is also seen that (7.5) is the classical limit ($\hbar=0$) of (7.2). The factor $\hbar^2$ in the Y function is exclusively caused by our notation. It cancels when insected into (4.6) or (4.7).

It is more cumbersome to show the relation between (7.6) and the classical limit of (7.4), and we shall not do it here. Instead, we evaluate the Barkas correction to the stopping power in the classical limit. We first bring Eq. (7.6) into a form that is similar to Eq. (6.20) that applies to the classical limit of the static electron gas. After symmetrizing Y, in accordance with (4.9), and bringing everything on one common denominator, one finds

$$Y_s = \frac{Q'}{[\omega_0^2-\omega^2][\omega_0^2-\omega'^2][\omega_0^2-(\omega-\omega')^2]}, \tag{7.7}$$

where

$$Q' = Q_0 - \frac{\omega_0^2}{2}\frac{\hbar^2}{m^2}\,[(\mathbf{k}\cdot\mathbf{k}')^2 - k^2k'^2], \tag{7.8}$$

and Q_0 is identical with the expression given in Eq. (6.11). The imaginary terms $i\gamma$ have been suppressed in (7.7) for clarity. It is seen immediately that this expression reduces to the result Eq. (6.20) for the classical electron gas when $\omega_0=0$.

For $\omega_0 \neq 0$, the expression (7.7) and the dielectric function (7.5) can be inserted into Eq. (4.11b) that determines the stopping number. The result is very similar to that for the static electron gas in the classical limit, except that Q_0 is replaced by Q', Eq. (7.8), and that the plasma frequency is replaced by the shifted resonance frequency

$$\alpha_0 = (\omega_0^2 + \omega_P^2)^{1/2} \tag{7.9}$$

in the denominators of the form

$$N(\omega) = \alpha_0^2 - (\omega + i\gamma)^2. \tag{7.10}$$

With these two modifications, the procedure outlined in Section (6.3) reproduces Eq. (6.18), with $F(k)$ given by Eq. (6.24), but with ω_P replaced by α_0 and Q_0 by Q'. The lower limit in the k-integral is given by α_0/v. We note that the shifted resonance frequency Eq. (7.9) is well-known from classical dispersion theory. The function $F(k)$ can be evaluated analytically by the same integration procedure as outlined in Section 5.3. The result is

$$F(k) = \frac{1}{3}\left\{1 + \frac{1}{2}\left(\frac{\omega_0}{\alpha_0}\right)^2 + \left[1 - \left(\frac{\omega_0}{2\alpha_0}\right)^2\right]\left[\frac{kv}{\alpha_0}\right]^2 \cdot \left[1 - \left(1 + 8\left(\frac{\alpha_0}{kv}\right)^2\right)^{-1/2}\right]\right\}. \tag{7.11}$$

This expression reduces to the result found for an isolated classical oscillator, Eq. (5.12), in the limit of $\omega_P = 0$. It also reduces to the result found for the static classical electron gas, Eq. (6.25), in the limit of $\omega_0 = 0$.

We also give the associated expression for the stopping number, found by integrating (7.11) in accordance with Eq. (6.18) from the lower limit $k_{\min} = \alpha_0/v$ to some upper limit $k_{\max}$. Different choices of $k_{\max}$ were discussed below Eq. (5.12) for the harmonic oscillator, but here we shall leave it as an adjustable variable. Expressed in terms of $y = k_{\max} v/\alpha_0$ one obtains

$$L_1 = \pi \frac{e_1 e}{mv^3} \alpha_0 L_B(y), \tag{7.12}$$

where

$$L_B(y) = \frac{1}{3}(5 - \xi^2/2) \log y + \frac{1}{3}(1 - \xi^2/4) \times \left(1 + \frac{y^2}{2}\left[1 - (1 + 8/y^2)^{1/2}\right] + 4 \log \frac{1 + (1 + 8/y^2)^{1/2}}{4}\right), \tag{7.13}$$

with $\xi^2 = \omega_0^2/\alpha_0^2$.

7.3. *Binding Frequency versus Plasma Frequency*

The two frequencies, ω_0 and ω_P, enter into Eqs. (7.11) and (7.13) in several ways. First, they determine the scaling variable α_0/v for k; here, the two frequencies enter symmetrically. Second, there are terms containing the ratio $\xi^2 = \omega_0^2/(\omega_0^2 + \omega_P^2)$ which only contribute when the electrons are bound. Finally, they appear in Eq. (7.12) through the simple factor α_0.

Figure 1 shows $F(k)$, Eq. (7.11), for three different cases, $\xi^2 = 0$, 0.707, and 1, i.e., the free electron gas ($\omega_0 = 0$), an intermediate case ($\omega_0 = \omega_P$), and the isolated oscillator ($\omega_P = 0$), respectively. The quantitative difference between the three curves turns out to be surprisingly small (less than 10 %). The same is true for the stopping number (Fig. 2). Ignoring the 10 % difference we may conclude that for distant collisions, the simultaneous presence of a single-electron binding frequency and a plasma frequency is essentially taken care of by introducing the effective frequency α_0, Eq. (7.10), instead of the plasma frequency (in the free electron gas) or the oscillator frequency (in the isolated oscillator).

We note that replacing either frequency by α_0 needs to be done *both* in the quasi-logarithmic function $L_B(y)$, Eq. (7.13), *and* in the frequency factor in front of L_B, Eq. (7.12).

Figure 3a shows the same results in a different plot. First, the upper integration limit $k_{\max}$ has been chosen to be the maximum momentum transfer, $k_{\max} = 2mv/\hbar$, so that L_1 represents a rough measure of the Barkas correction to the stopping number. More important, the frequency in the abscissa variable has been chosen to be the oscillator frequency ω_0 rather than the effective binding frequency α_0. In

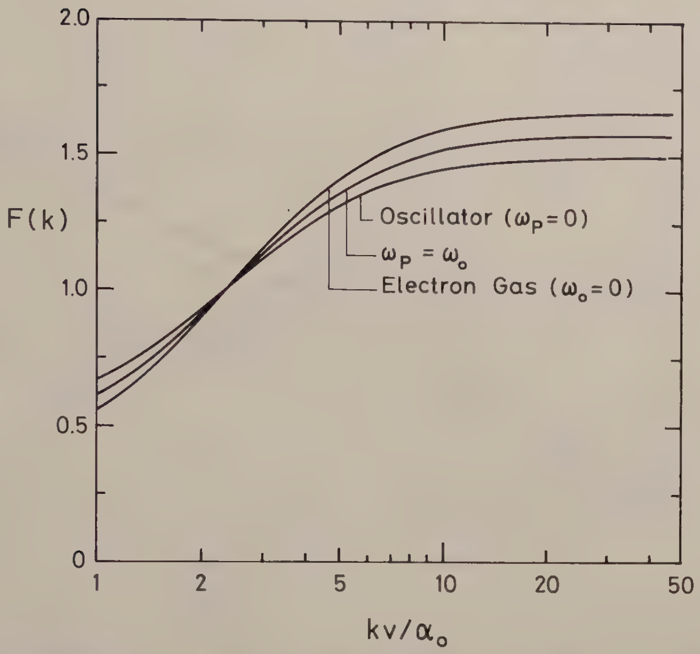

FIG. 1. The function $F(k)$ determining the classical Barkas integral, Eq. (7.11), versus momentum transfer. A constant F would imply a strictly logarithmic dependence of L_B in Eq. (7.12). The three curves represent the harmonic oscillator, the free electron gas, and a medium of harmonic oscillators with $\omega_P = \omega_0$. $\hbar k$ is the momentum transer, and α_0/v the effective adiabatic distance in the stopping medium.

accordance with this, the Barkas factor split off from the ordinate is chosen to be the one containing ω_0. With ω_P^2/ω_0^2 being a parameter, the curves in Fig. 3 show the magnitude of the Barkas correction to the stopping number for a given type of target atom, i.e., fixed oscillator frequency ω_0 at *different target densities.* It is evident that the Barkas correction *increases* with increasing target density. This increase is substantial. Even if ω_P is not allowed to exceed ω_0, the variation is about 50 %. If ω_P is allowed to be twice as large as ω_0, the variation is over more than a factor of two.

This finding is obviously caused by the frequency dependence of the Barkas factor. It needs to be contrasted with the fact that the ordinary Bethe stopping number L_0, evaluated in the same approximation, *decreases* with increasing density because of the sole occurrence of ω_P under the logarithm. The variation in L_0 is, consequently, weaker than in L_B (Fig. 3b).

The normal stopping number L_0 of an atom or of dense matter is often calculated in the local density approximation on the basis of the stopping power of a free Fermi gas. In that case, it has been suggested that one can take into account the effect of binding by replacing the plasma frequency by $\chi\omega_P$ [27]. The value $\chi = \sqrt{2}$, which is commonly used, reflects the choice $\omega_P \simeq \omega_0$, i.e., a comparable strength of

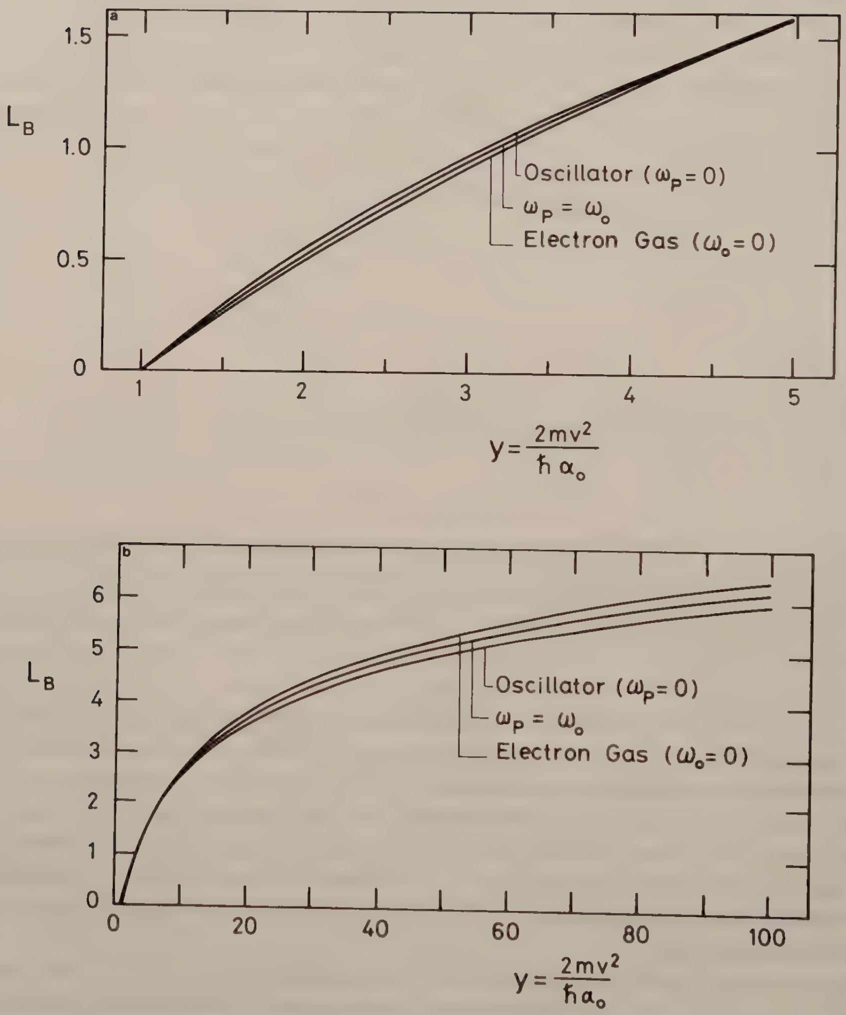

FIG. 2. Classical Barkas function L_B determining the cubic correction to the Bethe stopping power, cf. Eqs. (4.11) and (7.12), versus $2mv^2/\hbar\alpha_0$. α_0, Eq. (7.9), is the effective excitation frequency of the medium. A maximum momentum transfer $\hbar k_{\max} = 2mv$ has been postulated. The three curves represent the same models as those in Fig. 1. They show a crossover at $y \simeq 5$.

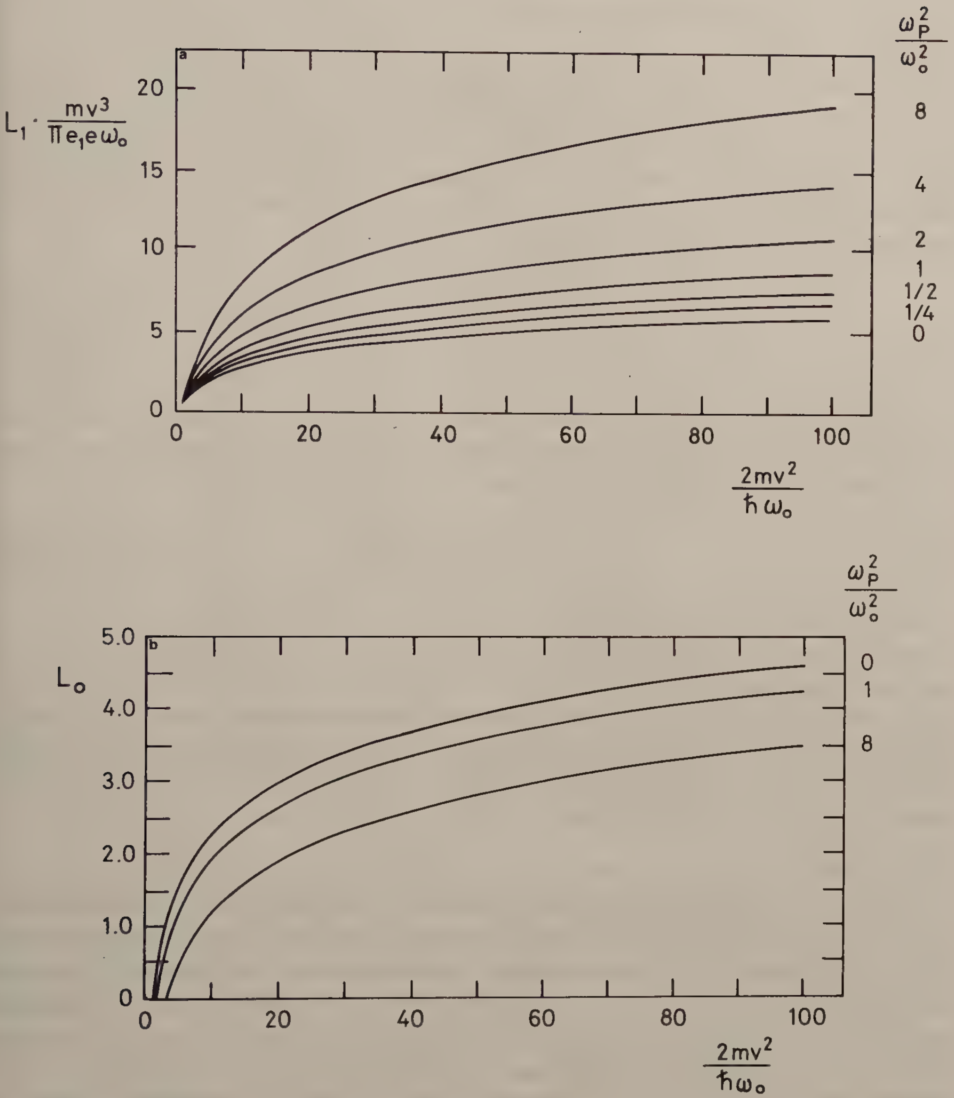

FIG. 3. Stopping number of a medium of harmonic oscillators with a resonance frequency ω_0 for individual oscillators, versus $2m^2/\hbar\omega_0$ for various densities, expressed by the ratio ω_P/ω_0, ω_P being the plasma frequency. (a) Barkas correction L_1; (b) Simplified Bethe stopping number $L_0 = \log(2mv^2/\hbar\alpha_0)$.

collective and individual binding forces. The above discussion of the classical Barkas correction adds nothing to this particular choice of the effective binding frequence. It does, however, make it clear that whatever choice is found justified for the normal stopping number L_0 will also be appropriate for the Barkas term.

8. NUMERICAL RESULTS FOR THE STATIC ELECTRON GAS

In this section we shall report some numerical results obtained from the quantal formulation of the static electron gas given in Section 6.2. Both the stopping power and the wake potential have been evaluated. We shall also make a comparison to recent stopping measurements involving protons and antiprotons in silicon where the Barkas correction was extracted. Some of the results in this section are displayed as a function of the variable y, defined here as

$$y = \frac{2mv^2}{\hbar\omega_P}. \tag{8.1}$$

This quantity depends on the electron density n through the plasma frequency. The dependence can alternatively be expressed in terms of the Wigner–Seitz radius $r_s = (4\pi n a_0^3/3)^{\quad 1/3}$, a_0 being the Bohr radius. Then, (8.1) reads

$$y = (4/3)^{1/2}\,(v/v_0)^2\,r_s^{3/2}, \tag{8.2}$$

where v_0 is the Bohr velocity.

The three-dimensional integrations over $\mathbf{k}'$ discussed in Section 6.2 are difficult to perform numerically due to the poles contained in $N(\mathbf{k}')\,N(\mathbf{k}-\mathbf{k}')$. We have avoided this difficulty to some extent by performing the integrations for a nonvanishing value of the damping constant γ and have chosen $\gamma = \omega_P/10$. Smaller values of γ may change the results slightly, in particular at the largest values of y where the calculations become increasingly time consuming.

8.1. *Stopping Power*

The most detailed information about the Barkas correction for the static electron gas is contained in the function $F(k)$, Eq. (6.16). Figure 4 shows $F(k)$ for different values of y. The dashed curve represents the classical limit, i.e., the analytic expression (6.25). It appears to give a reasonable estimate of $F(k)$ for small momentum transfers and large values of y. It differs drastically, however, from the quantal result at small values of y where $F(k)$ becomes negative. A peculiar feature of the quantal results is that $F(k)$ also becomes negative near the maximum momentum transfer for all the values of y that are shown. In Ref. [16], negative Barkas corrections at small impact parameters were found only at very low projectile velocities.

The Barkas correction to the stopping power depends on $F(k)$ through the integral (6.18). Results are shown in Fig. 5 in terms of the function L_B, defined in analogy to Eq. (7.12),

$$L_1 = \pi\,\frac{e_1 e\omega_P}{mv^3}\,L_B(y). \tag{8.3}$$

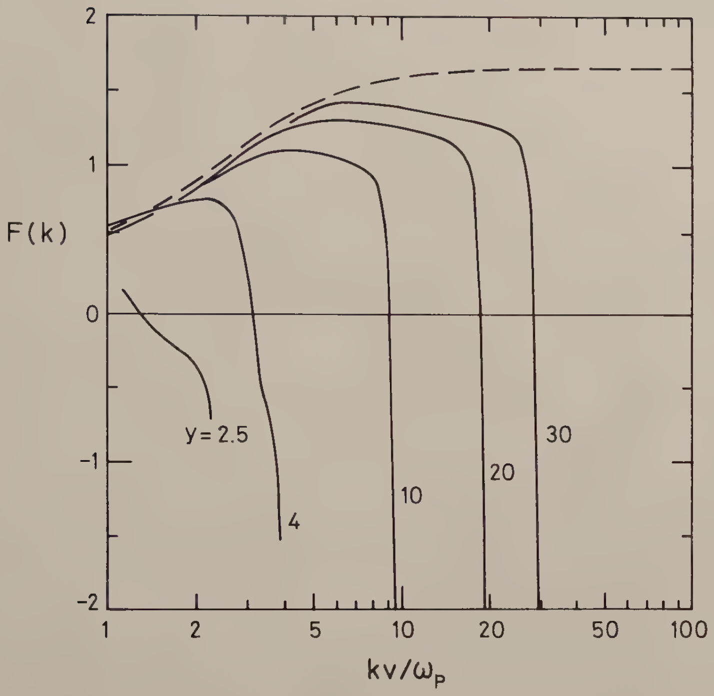

FIG. 4. The function $F(k)$ determining the quantal Barkas integral, Eq. (6.16), for the static electron gas, for different values of $y = 2mv^2/\hbar\omega_P$. The numerical calculations were performed for $\gamma = \omega_P/10$. The dashed curve represents the classical limit, i.e., the curve labelled $\omega_0 = 0$ in Fig. 1. The abscissa is the one in Fig. 1 for $\omega_0 = 0$.

The dot-dashed curve is the simplest version of a classical result, found from Eq. (7.13) for $\omega_0 = 0$ by imposing a cutoff at the maximum momentum transfer, i.e., $k_{\text{max}} = 2mv/\hbar$. The solid curve is the quantal result for the static electron gas. For $y > 30$, this result has been extrapolated (dashed curve) by comparison with the classical curve and by postulating the relation

$$L_B(y) = L_B^{\text{class}}(y/1.438), \quad \text{for} \quad y > 30. \tag{8.4}$$

An approximation for L_B for $y > 30$ was needed in the local density approximation to be applied below.

At small values of y, $2 < y < 2.7$, the quantal result becomes slightly negative, and it vanishes for $y < 2$ as does the ordinary stopping power of the static electron gas [3]. Although a qualitatively similar behavior has been found for the quantal oscillator [16], the quantitative picture is quite different, presumably due to the neglect of the zero-point motion in the electron gas. In case of the oscillator, zero-point motion was fully taken into account; as it turns out, this causes the Barkas correction to turn negative only for $y < 0.4$.

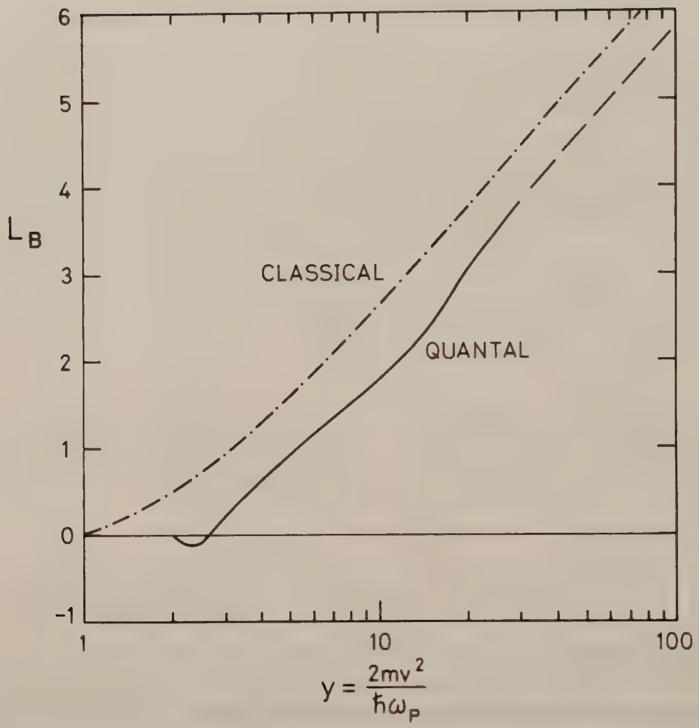

FIG. 5. The Barkas "logarithm" for a static electron gas, Eq. (8.3), as a function of $2mv^2/\hbar\omega_P$. The dot-dashed curve is the classical result, i.e., the curve labeled $\omega_0 = 0$ in Fig. 2. The solid curve is the quantal result found from (6.16) and (6.18) by numerical integration. The dashed part of that curve is based on the extrapolation (8.4).

It is seen that the classical curve lies consistently higher than the quantal one in the range covered by Fig. 5. This means that an effective upper limit in the k-integration that would reproduce the quantal result lies below the maximum momentum transfer $2mv$.

The stopping power for the quantal electron gas is shown in Fig. 6. We have plotted the dimensionless quantity

$$\frac{dE}{dx}\frac{a_0}{\hbar\omega_P} = \left(\frac{e_1}{e}\right)^2 \frac{2}{y}\left\{L_0(y) + 2\pi\left(\frac{2mv_0^2}{\hbar\omega_P}\right)^{1/2}\frac{e_1}{e}\,y^{-3/2}L_B(y)\right\} \tag{8.5}$$

as a function of the variable y, cf. Eqs. (4.11) and (7.12). The dashed curve is the result for the static electron gas without the Barkas correction. As in Fig. 3, the relative magnitude of the Barkas correction becomes density dependent through the parameter

$$2\pi\left(\frac{2mv_0^2}{\hbar\omega_P}\right)^{1/2} = 6.75 r_s^{3/4}. \tag{8.6}$$

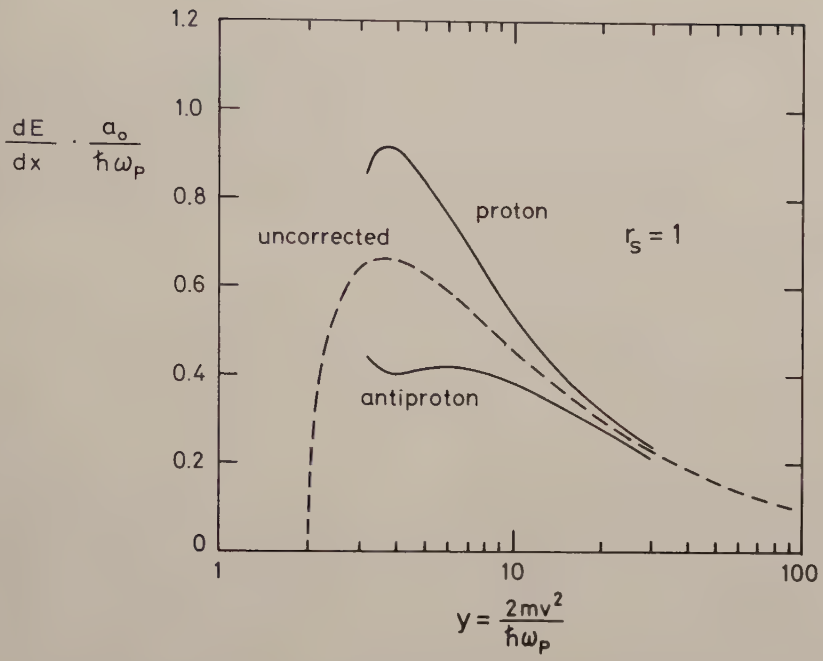

FIG. 6. Reduced stopping power of a static electron gas, Eq. (8.5). The dashed curve is the result obtained without Barkas correction. Solid curves include the Barkas correction for protons and antiprotons, respectively; electron density corresponding to $r_s = 1$.

The results shown in Fig, 6 were obtained for $r_s = 1$. This makes it easy to scale them to a different density. It is seen that for $r_s = 1$, the Barkas correction changes the maximum stopping power by about 40 %.

The limit of the static electron gas must become inadequate to characterize a Fermi gas at velocities approaching the Fermi velocity. A pertinent quantity in this connection is

$$y(v = v_F) \simeq 4.25 r_s^{-1/2} \tag{8.7}$$

Higher-order polarization terms may also become important for the lower range of y-values shown in Fig. 6. The results must therefore be questionable for $y \lesssim 4$. There are also other higher-order corrections in the stopping power that become important at low velocities. The best known one is a purely quantal correction that has been extracted [13] by expansion of Bloch's stopping formula [28],

$$L_2 = -1.2(e_1 e/\hbar v)^2. \tag{8.8}$$

This correction does not depend on the sign of the projectile charge. A detailed discussion of the e_1^4 term in the stopping cross section is in preparation [29].

8.2. *Comparison with Experiment*

In a recent experiment, Andersen *et al.* [19] compared the energy loss of antiprotons in silicon with that of protons. The difference between the two stopping powers must be a measure of the odd terms in the expansion of the stopping power in terms of the projectile charge, and it was identified as the Barkas correction.

In a recent communication [21], results from the present work as well as from Ref. [16] have been utilized to provide three different predictions of the Barkas correction. These predictions were based on

(a) representing a silicon atom as a harmonic oscillator,

(b) representing solid silicon as a homogeneous electron gas, or

(c) representing a silicon atom as a inhomogeneous electron gas in the local density approximation.

Neither model defines the numerical input uniquely. In case (a), the resonance frequency of the oscillator was chosen to be $\omega_0 = I/\hbar$, with I taken to be the recommended value of the mean excitation energy, $I = 165$ eV. Similarly, the plasma frequency in case (b) was chosen to be $\omega_P = I/\hbar$. Finally, the electron distribution in case (c) was chosen to be Lenz–Jensen like, and the local plasma frequency was left uncorrected.

Estimates of Barkas corrections on the basis of an extended oscillator model implying an ensemble of oscillators [30] are being published separately [31]. Presently, we wish to elaborate on the two approaches (b) and (c).

Figure 7 shows three predictions for L_1, all based on the static homogeneous electron gas in the quantal description, with the plasma frequency chosen either as $I/\hbar$ as mentioned above, or in accordance with either 4 or 14 electrons per silicon atom, corresponding to the number of valence electrons or the total number of electrons, respectively. It is seen that the curve employing the empirical mean excitation energy yields a very good agreement with the experimental curve, in particular at the upper end of the considered velocity range where the neglect of shell corrections is immaterial. This good agreement may not be too surprising in view of the discussion in Section 7.3. Indeed, the empirical mean excitation energy I is expected to take into account both the individual electron binding forces and the collective effects. At least for a single-oscillator model, the same effective frequency is to be applied in the Barkas term. Figure 7 also shows that the two curves ignoring single-electron binding lie consistently low.

Figure 8 shows the corresponding results for two versions of the local density approximation. Writing the Barkas correction to the stopping number in the form

$$L_1^{\text{atom}} = \pi \frac{e_1 e}{m v^3} \frac{1}{Z_2} \int d^3 r\, n(\mathbf{r})\, \omega_P(\mathbf{r})\, L_B\left(\frac{2mv^2}{\hbar \omega_P(\mathbf{r})}\right), \tag{8.9}$$

where Z_2 is the atomic number of the target atom and $n(\mathbf{r})$ the electron density, we have the option of inserting the local plasma frequency $\omega_P = [4\pi n(\mathbf{r})\, e^2/m]^{1/2}$, or to

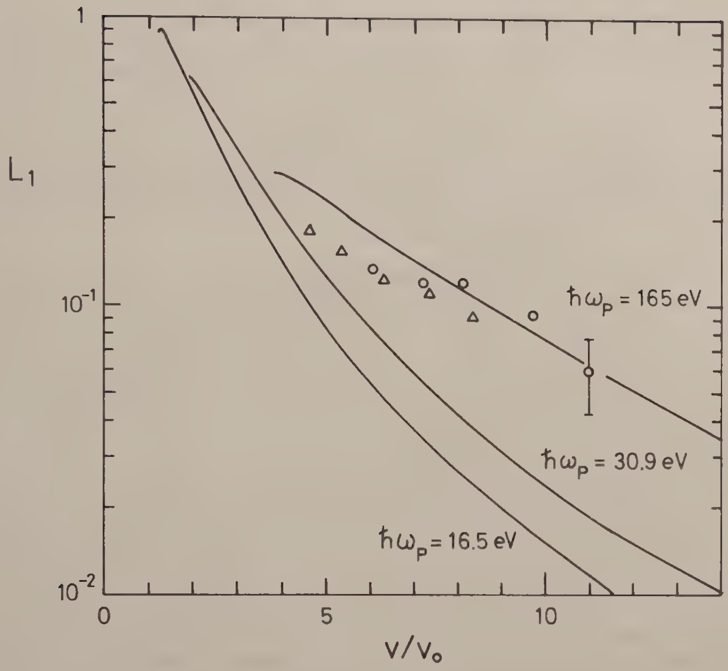

FIG. 7. Barkas correction L_1 to the stopping number (4.11) of solid silicon versus projectile velocity in units of the Bohr velocity v_0. Experimental points extracted from proton and antiproton stopping powers [19]. Theoretical curves from quantal calculation for the static electron gas for three effective plasma frequencies corresponding to 4 or 14 electrons per atom ($\hbar\omega_P = 16.5$ or 30.9 eV, respectively), and for $\hbar\omega_P = 165$ eV, the empirical value of I for solid silicon.

add a factor of $\chi = \sqrt{2}$ in order to account approximately for atomic binding, cf. Section 7.3. Both options have been carried out. For the electron density, we have employed the Lenz–Jensen distribution [32]. This choice provides a simple scaling law so that $Z_2^{1/2}\, L_1^{\text{atom}}$ is the same for all media when plotted versus $Z_2^{-1/2} v$. It is seen that the two theoretical curves lie somewhat below the experimental data. Note also the very small influence of the factor χ. This behavior differs from the one in the first Born approximation.

The experimental data were compared in Ref. [19] to the predictions of Ref. [25] which are based on distant collisions and the classical harmonic oscillator. These results underestimate the data by almost a factor of two. It has been demonstrated already [16] that the prediction of Ref. [25] lies below the quantal result for the harmonic oscillator for $2mv^2/\hbar\omega_0 > 5$. Our calculations add further support to the assertion made in Ref. [13] that close collisions make a significant contribution to the Barkas correction. In accordance with Ref. [16], our results do not support the simple factor-of-two scaling advocated in Ref. [13].

We refer the reader to Ref. [15] for a survey of experimental work on the Barkas effect. Earlier results involved helium and even lithium ions where higher-order

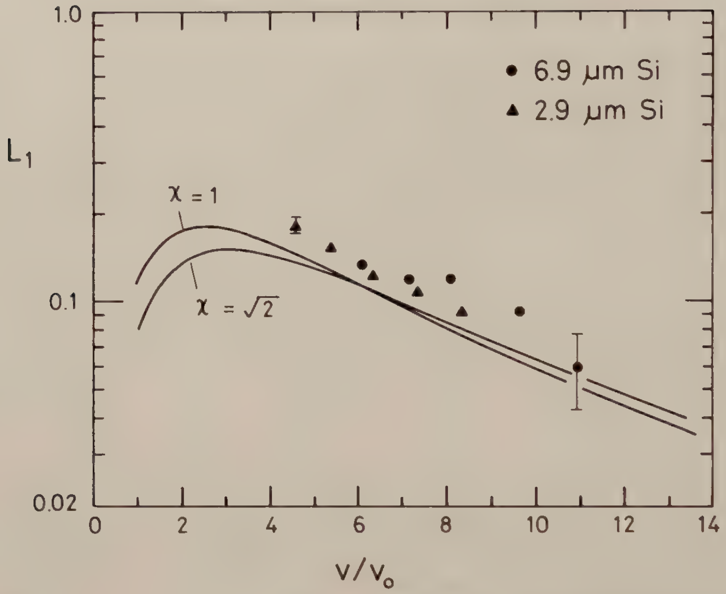

FIG. 8. Same as Fig. 7 except that the curves were obtained in the local density approximation to the quantal electron gas, Eq. (8, 9), for two choices of the Lindhard–Scharff parameter χ accounting for electron binding ($\chi = 1$ and $\sqrt{2}$).

Born terms may become of comparable magnitude as the e_1^3 term. Although these results demonstrated unambioguously the significance of higher-order Born terms in the stopping power, the extracted e_1^3 corrections were not found sufficiently accurate.

The results reported in Ref. [19] allow us to extract the sum $L_1 + L_3 + \cdots$, i.e., the uneven terms in an expansion of the stopping number in powers of the projectile charge. This is a major step forward. Evidently, the present comparison assumes the terms $L_3 + L_5 + \cdots$ to be negligible.

8.3. *Wake Potential*

Our evaluation of the wake potential has been purely numerical because we have not yet found a scheme of reducing the complexity of the general expression by means of suitable symmetry arguments. All calculations refer to the static electron gas in the quantal formulation.

The first-order induced potential can be obtained from Eq. (4.3) by subtracting the bare Coulomb potential

$$\Phi_{\text{ind}}^{(1)}(\mathbf{r}, t) = \frac{e_1}{2\pi^2} \int \frac{d^3k}{k^2} e^{i\mathbf{k}\cdot\mathbf{R}} \left\{ \frac{1}{\varepsilon(\mathbf{k}, \omega)} - 1 \right\}, \tag{8.10}$$

where $\mathbf{R}=\mathbf{r}-\mathbf{v}t$. The first-order and the total induced potential will be shown in units of $e_1\omega_P/v$,

$$\Phi_{\text{ind}}(\mathbf{R})=\frac{e_1\omega_P}{v}\,g(\mathbf{R}). \tag{8.11}$$

For the second-order correction alone, Eq. (6.9), also the Barkas factor will be extracted,

$$\Phi^{(2)}(\mathbf{R})=\frac{e_1\omega_P}{v}\,\frac{\pi e_1 e\omega_P}{mv^3}\,g^{(2)}(\mathbf{R}). \tag{8.12}$$

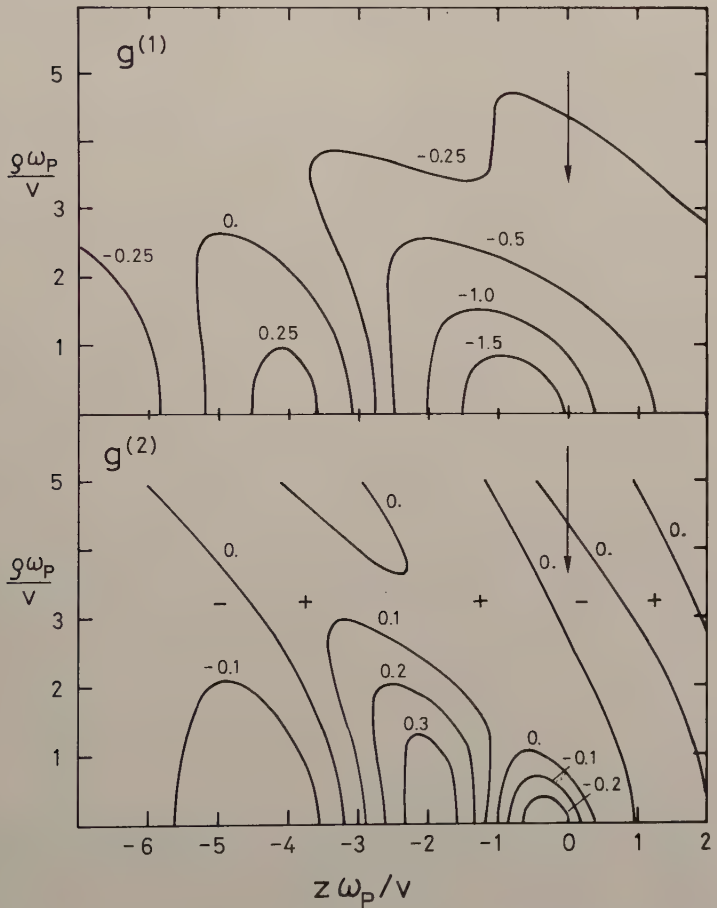

FIG. 9. Contour plots of the reduced first and second order induced potentials, Eqs. (8.10)–(8.12). Static electron gas an $2mv^2/\hbar\omega_P=4$. The z direction points along the projectile velocity, and the ρ direction is perpendicular to it. The projectile is located in $\mathbf{R}=(z,\rho)=(0,0)$. The coordinates are given in units of the adiabatic distance.

This makes it convenient to scale the results to an arbitrary electron density and to a different charge of the particle.

Contour plots are shown in Fig. 9 for $y = 2mv^2/\hbar\omega_P = 4$. This value is low enough to make the Barkas term sizable, but not so low as to cause the neglect of zero-point motion to be detrimental. The induced potential is axially symmetric. The coordinate system is chosen with the z-axis along the beam and the ρ-axis perpendicular to it. The length unit is the adiabatic distance v/ω_P. The particle is located in $\mathbf{R} = (z, \rho) = (0, 0)$.

The most interesting feature in Fig. 9 is the doubling of the wave number of the oscillations behind the particle for the second-order potential, as compared to first order. This is not surprising in view of the quadratic dependence, Eq. (2.10), and must therefore be a general feature for all values of y. This may cause a significant change in the wake potential, in particular for a large effective charge of the penetrating particle.

Another interesting feature is the occurrence of oscillations in front of the charged particle. Such oscillations are also present in the first-order potential, but they are not seen so clearly. They are more pronounced in the first and second-order induced electron densities (not shown). On the axis, i.e., for $\rho = 0$, the period of the oscillations is determined by the wave number for the maximum momentum transfer ($\simeq 2mv/\hbar$), as one would expect for the induced density generated by an electron hitting the projectile in a nearly head-on collision.

The Barkas effect on the induced potential is shown in Fig. 10. All curves refer to potentials on the axis, $\rho = 0$. Solid curves refer to $g^{(1)}$ and $g^{(2)}$, respectively. The dashed curve is for $e_1 = e$, and the dotted curve for $e_1 = 4e$. The electron density chosen corresponds to $r_s = 2$. It is seen that including the second-order potential moves the position of the first minimum closer to the projectile by about $\frac{1}{4}$ of the adiabatic distance, and it makes the minimum noticeably deeper. Clearly, these effects increase with increasing projectile charge.

An analysis of the Coulomb explosion of 11.2 MeV OH^+ in carbon foils [33] indicated that the first-order wake potential could not account for the data. It appeared that a wake field with a narrower minimum closer to the oxygen ion gave a better description. The second-order potential described above contributes an effect in this direction. Its magnitude depends on the assigned value of the plasma frequency. An upper limit is presumably determined by the recommended value of the mean excitation energy, $I = 77.3$ eV for solid carbon. With this, one finds a Barkas factor $\pi e_1 e \alpha_0/mv^3 \simeq 0.5$, i.e., a value large enough to cause noticeable modifications of the first-order potential.

The wake field of an antiproton, which has received interest recently [34], has the opposite sign of that of a proton to first order in e_1. The Barkas correction, on the other hand, does not change sign. Therefore, changes in wavelength are expected to go into the opposite direction as that for protons.

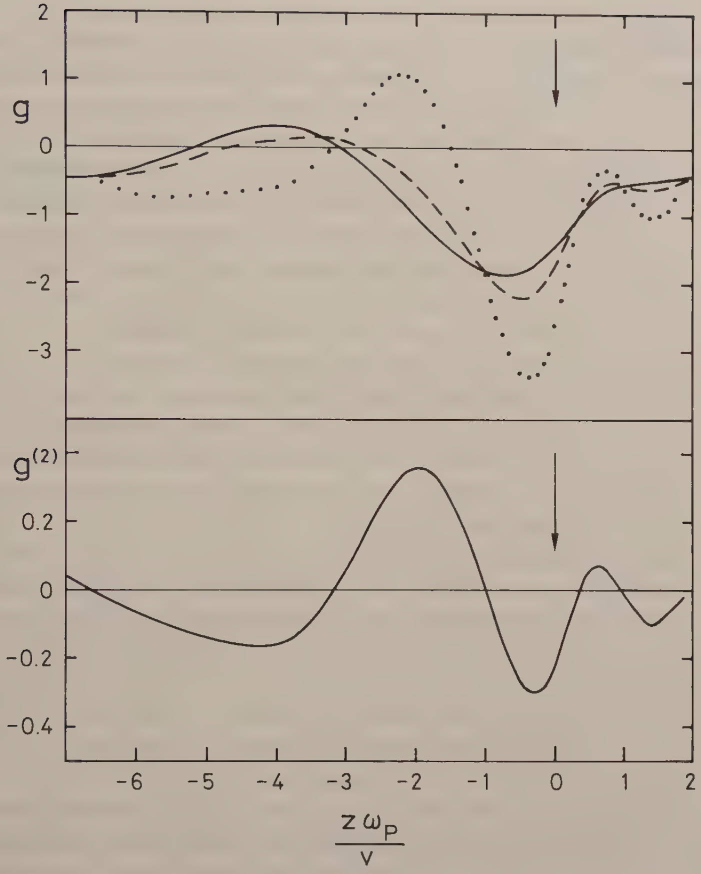

FIG. 10. Variation with longitudinal distance of the induced potential on the axis ($\rho = 0$). Static electron gas with $r_s = 2$ for $y = 2mv^2/\hbar\omega_P = 4$. The solid curves are the reduced first- and second-order potentials, Eqs. (8.10)–(8.12). The dashed curve is the total induced potential for protons (in units of $e_1\omega_P/v$), and the dotted curve is for a particle with the effective charge $e_1 = 4e$.

9. SUMMARY AND CONCLUSIONS

We have developed a formalism for calculating the self-consistent field generated by a penetrating charged particle up to second order in the projectile charge. The projectile has been assumed to be much heavier than an electron. The medium has been assumed to be a random distribution of Hartree atoms. The formalism is an extension of Lindhard's treatment of the self-consistent linear field generated in an electron gas.

The formalism has been applied to the stopping power of a penetrating particle up to third order in the projectile charge. The third-order term is commonly referred to as the Barkas correction. It is related to the polarization of the medium induced by the moving particle. In the limit of a dilute medium, our stopping formula reduces to the result of a conventional perturbation expansion of the excitation amplitude of an individual atom. In the limit of negligible binding forces on the electrons, the formalism describes penetration properties of a Fermi gas.

We have studied in detail the Barkas correction in the classical limit (for $\hbar \to 0$) and have obtained a simple analytic expression for a medium of classical harmonic oscillators. This expression depends both on the plasma frequency and the oscillator frequency. It reduces to the correct limits when either the plasma frequency or the oscillator frequency are set equal to zero. The classical limit provides useful guidance and reference for quantal calculations.

Previously, calculations of the Barkas correction to the stopping power were limited to distant interactions with a harmonic oscillator, and they were therefore effectively based on classical dynamics. A fully quantal evaluation of the Barkas correction for a harmonic oscillator, valid for both close and distant collisions, has become available only very recently [16]. Our results are consistent with this work to the extent that a comparison is feasible.

We have in particular studied the Barkas correction in a quantal electron gas. In order to circumvent the complexity of the numerical calculations caused by the Fermi motion we have concentrated on a static electron gas. This model becomes accurate at sufficiently high velocities where the so-called shell corrections, due to moving target electrons, become unimportant.

In contrast to all classical evaluations of the Barkas effect, the treatment is valid also for close collisions, and the maximum momentum transfer in an individual interaction emerges from the theory, rather than having to be postulated or used as an adjustable parameter. The choice of a cutoff at large momentum transfers (or small impact parameters) in classical calculations has led to much debate and to an uncertainty in the magnitude of the Barkas correction, which was of the order of a factor of two.

Our calculations for the static electron gas confirm the importance of the close-collision contribution to the Barkas effect. At low velocities, the Barkas correction to the stopping power becomes negative. Moreover, for close collisions, near the maximum momentum transfer, the Barkas correction to the energy loss is also negative at higher velocities. However, the region of negative values is narrow and becomes less important at large velocities. These features are in qualitative agreement with those found for an isolated harmonic oscillator [16].

The quantitative agreement of our result with the measured Barkas correction, extracted from the stopping power of protons and antiprotons, is quite satisfactory, considering the fact that we have neglected the zero-point motion in the medium. The best agreement is obtained on the basis of a homogeneous electron gas and by inserting the empirical mean excitation energy for the effective plasma frequency. A local density approximation of the target atoms, approximating the atomic electron density by a Lenz–Jensen distribution, yields likewise reasonable agreement with the experimental data.

We have also studied the induced potential (or wake potential) in the static electron gas. A characteristic feature of the second-order potential is a narrower and deeper minimum behind the particle, compared to the first-order potential. The minimum also tends to move closer to the projectile. The effect becomes quite dramatic at low velocities, in particular for a high effective projectile charge. This may have a significant effect on the Coulomb explosion of molecular beams in foils.

From the classical treatment, one concludes that the relative significance of the Barkas correction, both in the stopping power and the wake field, increases with increasing target density if all other parameters remain unchanged.

APPENDIX A: BARKAS CORRECTION TO THE STOPPING CROSS SECTION OF A SINGLE BOUND ELECTRON

Consider a single electron bound by some force to the origin and perturbed by a potential

$$V(\mathbf{r}, t) = -\frac{e_1 e}{|\mathbf{r} - \mathbf{R}(t)|} = -\frac{e_1 e}{2\pi^2} \int d^3k \, e^{i\mathbf{k}\cdot(\mathbf{r} - \mathbf{R}(t))} \frac{1}{k^2}, \tag{A1}$$

where $\mathbf{R}(t) = \mathbf{p} + \mathbf{v}t$, and $\mathbf{p}$ is the impact parameter.

In the notation of Ref. [16], the third-order (Barkas) correction to the stopping cross section reads

$$S^{(3)} = \int d^2p \, 2 \, \mathrm{Re} \sum_n (E_n - E_0) \, c_n^{(1)*} c_n^{(2)}, \tag{A2}$$

where the $c_n^{(1)}$ and $c_n^{(2)}$ are the transition amplitudes to first and second order in the projectile charge e_1, respectively, i.e.,

$$c_n^{(1)} = \frac{1}{i\hbar} \int_{-\infty}^{\infty} dt \, e^{i\omega_{n0} t} V_{n0}(t), \tag{A3}$$

$$c_n^{(2)} = -\frac{1}{\hbar^2} \sum_j \int_{-\infty}^{\infty} dt' \int_{-\infty}^{t'} dt'' \, e^{i\omega_{nj} t' + i\omega_{j0} t''} V_{nj}(t') \, V_{j0}(t'') \tag{A4}$$

and

$$\begin{aligned} V_{nj}(t) &= \int d^3r \, \psi_n^*(\mathbf{r}) \, V(\mathbf{r}, t) \, \psi_j(\mathbf{r}) \\ &= -\frac{e_1 e}{2\pi^2} \int \frac{d^3k}{k^2} f_{nj}(\mathbf{k}) \, e^{-i\mathbf{k}\cdot(\mathbf{p} + \mathbf{v}t)}. \end{aligned} \tag{A5}$$

Insertion of (A3)–(A5) into (A2) and integration over the impact parameter yields a Dirac function containing the transverse components of the three **k**-vectors entering through the three matrix elements. A Dirac function containing the corresponding longitudinal components (i.e., the components parallel to the velocity), is found by substituting $t' \to t' + t$ and $t'' \to t'' + t$ and integrating over t. This yields

$$S^{(3)} = -\frac{2e_1^3 e^3}{\pi^3 \hbar^2 v} \operatorname{Re} \frac{1}{i} \sum_n \omega_{n0} \sum_j \int \frac{d^3k}{k^2} \int \frac{d^3k'}{k'^2} \frac{1}{(k-k')^2}$$

$$\cdot f_{0n}(-\mathbf{k}) f_{nj}(\mathbf{k}') f_{j0}(\mathbf{k}-\mathbf{k}')$$

$$\times \int_{-\infty}^{\infty} dt' \int_{-\infty}^{t'} dt''\, e^{i(\omega_{nj}-\omega')t'} e^{i(\omega_{j0}-\omega+\omega')t''}, \tag{A6}$$

where $\omega = \mathbf{k} \cdot \mathbf{v}$ and $\omega' = \mathbf{k}' \cdot \mathbf{v}$.

Substitution of $t' \to t' + t''$ and integration over t' and t'' yields Eq. (5.3).

APPENDIX B: SEMICLASSICAL DESCRIPTION OF THE ELECTRON GAS

Here we shall derive semiclassical expressions for the first- and second-order induced charge densities in an electron gas. The derivation is based on Boltzmann's equation for the phase space distribution $f(\mathbf{p}, \mathbf{r}, t)$ of electrons, perturbed by the self-consistent potential $\Phi(\mathbf{r}, t)$ [3], i.e.,

$$\left[\frac{\partial}{\partial t} + e\nabla_r \Phi \cdot \nabla + \frac{1}{m} \mathbf{p} \cdot \nabla\right] f = -\frac{1}{\tau}(f - f_0), \tag{B1}$$

where $f_0 = n g_0(p)$ is the equilibrium distribution with $\int d^3p\, g_0(p) = 1$. The damping term on the right-hand side serves to ensure that we obtain the retarded solution, i.e., $f \to f_0$ for $t \to -\infty$. This implies that ω is replaced by $\omega + i/\tau$ in Fourier space. This will be implicitly assumed in the following.

The solution to (B1) can be written as an expansion in powers of the self-consistent field,

$$f = f_0 + f^{(1)} + f^{(2)} + \cdots, \tag{B2}$$

and the associated induced charge densities are

$$\rho^{(j)}(\mathbf{r}, t) = -e \int d^3p\, f^{(j)}(\mathbf{p}, \mathbf{r}, t). \tag{B3}$$

In Fourier space, the first-order solution is

$$f^{(1)}(\mathbf{p}, \mathbf{k}, \omega) = \frac{e\Phi(\mathbf{k}, \omega)}{\omega - \mathbf{k} \cdot \mathbf{p}/m} \mathbf{k} \cdot \nabla_p f_0. \tag{B4}$$

The first-order induced charge density (B3) can be obtained by partial integration,

$$\rho^{(1)}(\mathbf{k}, \omega) = \frac{ne^2}{m} k^2 \Phi(\mathbf{k}, \omega) \langle (\omega - \mathbf{k} \cdot \mathbf{p}/m)^{-2} \rangle, \tag{B5}$$

where the brackets denote the average over $g_0(p)$.

For the particular case of an electron gas at rest, (B5) and Eq. (2.4) yield

$$\varepsilon(\mathbf{k}, \omega) = 1 - \omega_{\mathrm{P}}^2/\omega^2 \tag{B6}$$

which coincides with Eq. (6.5) in the classical limit where $\omega_k = \hbar k^2/2m$ approaches zero.

The second-order solution reads

$$f^{(2)}(\mathbf{p}, \mathbf{k}, \omega) = \frac{1}{\omega - \mathbf{k} \cdot \mathbf{p}/m} \int d^3k' \int d\omega' \, e\Phi(\mathbf{k} - \mathbf{k}', \omega - \omega')(\mathbf{k} - \mathbf{k}') \cdot \nabla_p f^{(1)}(\mathbf{p}, \mathbf{k}', \omega'), \tag{B7}$$

where $f^{(1)}$ is given by (B4). The associated charge density takes on the form of Eq. (3.7a) with

$$Y(\mathbf{k}, \omega, \mathbf{k}', \omega') = \hbar^2 \int d^3p \, \frac{\mathbf{k} - \mathbf{k}'}{\omega - \mathbf{k} \cdot \mathbf{p}/m} \cdot \nabla_p \frac{\mathbf{k}'}{\omega' - \mathbf{k}' \cdot \mathbf{p}/m} \cdot \nabla_p g_0(p), \tag{B8}$$

or, after partial integration,

$$Y(\mathbf{k}, \omega, \mathbf{k}', \omega') = \hbar^2 \left\langle \mathbf{k}' \cdot \nabla_p \frac{1}{\omega' - \mathbf{k}' \cdot \mathbf{p}/m} (\mathbf{k} - \mathbf{k}') \cdot \nabla_p \frac{1}{\omega - \mathbf{k} \cdot \mathbf{p}/m} \right\rangle. \tag{B9}$$

For the electron gas at rest, this reads

$$Y(\mathbf{k}, \omega, \mathbf{k}', \omega') = \frac{\hbar^2 \mathbf{k} \cdot (\mathbf{k} - \mathbf{k}')}{m^2} \left\{ \frac{k'^2}{\omega'^2 \omega^2} + 2 \frac{\mathbf{k} \cdot \mathbf{k}'}{\omega' \omega^3} \right\}. \tag{B10}$$

This result is used in Section 6.3 to derive an analytical expression for the Barkas term in the classical limit.

APPENDIX C: CLASSICAL HARMONIC OSCILLATOR

In this appendix, the general scheme outlined in Section 2 is applied to an ensemble of spherical harmonic oscillators, but unlike in Section 3, the connection between the induced charge densities and the potential is provided by the classical equation of motion. As in Section 3, the oscillators all have the same resonance frequency, and they are randomly distributed in space at a density n.

Consider a single oscillator, bound to an equilibrium position **R**, and a displacement vector $\boldsymbol{\xi} = \mathbf{r} - \mathbf{R}$. Then, the equation of motion is

$$\frac{\partial^2 \boldsymbol{\xi}}{\partial t^2} + \gamma \frac{\partial \boldsymbol{\xi}}{\partial t} + \omega_0^2 \boldsymbol{\xi} = \frac{e}{m} \int d^3k \int d\omega \, \Phi(\mathbf{k}, \omega) \, i\mathbf{k} e^{i\mathbf{k} \cdot (\mathbf{R} + \boldsymbol{\xi}) - i\omega t}, \tag{C1}$$

with an infinitesimal damping constant γ.

This equation is linearized in powers of the potential Φ,

$$\boldsymbol{\xi} = \boldsymbol{\xi}^{(1)} + \boldsymbol{\xi}^{(2)} + \cdots, \tag{C2}$$

and

$$e^{i\mathbf{k} \cdot \boldsymbol{\xi}} = 1 + i\mathbf{k} \cdot \boldsymbol{\xi}^{(1)} + \cdots. \tag{C3}$$

Note that unlike in the quantal calculation, the perturbation expansion (C2) implies the dipole expansion (C3).

The solutions of (11) can readily be determined by means of the Green function of the harmonic oscillator and read

$$\boldsymbol{\xi}^{(1)}(t) = \frac{ie}{m} \int d^3k \int d\omega \, \frac{\mathbf{k}\Phi(\mathbf{k}, \omega)}{\omega_0^2 - \omega^2 - i\gamma\omega} \, e^{i(\mathbf{k} \cdot \mathbf{R} - \omega t)}, \tag{C4}$$

and

$$\boldsymbol{\xi}^{(2)} = -\frac{ie^2}{m^2} \int d^3k \int d\omega \int d^3k' \int d\omega' \, \Phi(\mathbf{k} - \mathbf{k}', \omega - \omega') \, \Phi(\mathbf{k}', \omega')$$

$$\cdot \frac{(\mathbf{k} - \mathbf{k}')[\mathbf{k}' \cdot (\mathbf{k} - \mathbf{k}')]}{(\omega_0^2 - \omega^2 - i\gamma\omega)(\omega_0^2 - \omega'^2 - i\gamma\omega')} \, e^{i(\mathbf{k} \cdot \mathbf{R} - \omega t)}. \tag{C5}$$

The induced charge density due to one oscillator reads

$$\delta\rho = -e\delta(\mathbf{r} - \mathbf{R} - \boldsymbol{\xi}) + e\delta(\mathbf{r} - \mathbf{R}) \tag{C6}$$

or

$$\delta\rho = e(\boldsymbol{\xi}^{(1)} + \boldsymbol{\xi}^{(2)}) \cdot \nabla_r \delta(\mathbf{r} - \mathbf{R}) - \tfrac{1}{2} e(\boldsymbol{\xi}^{(1)} \cdot \nabla_r)^2 \, \delta(\mathbf{r} - \mathbf{R}) \cdots$$

up to second order. Integration over all oscillator positions, $n \int d^3R$, yields

$$\rho^{(1)} = ne\nabla_R \cdot \boldsymbol{\xi}^{(1)} |_{\mathbf{R} = \mathbf{r}} \tag{C7}$$

and

$$\rho^{(2)} = ne\nabla_R \cdot \boldsymbol{\xi}^{(2)} - \frac{1}{2} ne \sum_\mu \sum_\nu \left. \frac{\partial^2 \xi_\mu^{(1)} \xi_\nu^{(1)}}{\partial X_\mu \, \partial X_\nu} \right|_{\mathbf{R} = \mathbf{r}}. \tag{C8}$$

After insertion of (C4) and (C5), we find

$$\rho^{(1)}(\mathbf{k}, \omega) = -\frac{ne^2}{m} \frac{k^2 \Phi(\mathbf{k}, \omega)}{\omega_0^2 - \omega^2 - i\gamma\omega} \tag{C9}$$

and

$$\rho^{(2)}(\mathbf{k}, \omega) = \frac{ne^3}{2m^2} \int d^3k' \int d\omega' \, \Phi(\mathbf{k}-\mathbf{k}', \omega-\omega') \, \Phi(\mathbf{k}', \omega') \, Z(\mathbf{k}, \omega, \mathbf{k}', \omega'), \tag{C10}$$

where

$$Z(\mathbf{k}, \omega, \mathbf{k}', \omega') = \frac{2\mathbf{k}\cdot(\mathbf{k}-\mathbf{k}')}{M(\omega)} \frac{\mathbf{k}'\cdot(\mathbf{k}-\mathbf{k}')}{M(\omega')} - \frac{\mathbf{k}\cdot(\mathbf{k}-\mathbf{k}')}{M(\omega-\omega')} \frac{\mathbf{k}\cdot\mathbf{k}'}{M(\omega')} \tag{C11}$$

and $M(\omega) = \omega_0^2 - \omega^2 - i\gamma\omega$.

ACKNOWLEDGMENTS

Several aspects of this work were first studied by one of us (H.E.) as a part of his PhD thesis at Aarhus University more than a decade ago. Thanks are due to Jens Lindhard for his stimulation and interest. Various aspects of this work were discussed with D. S. Gemmell, A. Belkacem, E. P. Kanter, Z. Vager, and H. H. Mikkelsen. M. Inokuti provided very valuable suggestions on the manuscript. One of us (P.S.) is very grateful to the management and the staff of the Physics Division at ANL for the hospitality and stimulation he enjoyed during his sabbatical. The present work is supported by the U.S. Department of Energy, Nuclear Physics Division and Office of Basic Energy Sciences, under Contract W-31-109-ENG-38.

REFERENCES

1. E. FERMI, *Phys. Rev.* **57** (1940), 485.
2. A. BOHR, *Mat. Fys. Medd. K. Dan. Vidensk. Selsk.* **24**, No. 19 (1948)
3. J. LINDHARD, *Mat. Fys. Medd. K. Dan. Vidensk. Selsk.* **28**, No. 8 (1954).
4. J. NEUFELD AND R. H. RITCHIE, *Phys. Rev.* **98** (1955), 1632.
5. U. FANO, *Phys. Rev.* **103** (1956), 1202.
6. N. BOHR, *Philos. Mag.* **25** (1913), 10.
7. H. BETHE, *Ann. Phys.* **5** (1930), 325.
8. F. M. SMITH, W. BIRNBAUM, AND W. H. BARKAS, *Phys. Rev.* **91** (1953), 795; W. H. BARKAS, W. BIRNBAUM, AND F. M. SMITH, *Phys. Rev.* **101** (1956), 778.
9. H. H. ANDERSEN, H. SIMONSEN, AND H. SØRENSEN, *Nucl. Phys. A* **125** (1969), 171.
10. H. H. HECKMAN AND P. J. LINDSTRÖM, *Phys. Rev. Lett.* **22** (1969), 871.
11. J. C. ASHLEY, R. H. RITCHIE, AND W. BRANDT, *Phys. Rev. B* **5** (1972), 2393.
12. K. W. HILL AND E. MERZBACHER, *Phys. Rev. A* **9** (1974), 156.
13. J. LINDHARD, *Nucl. Instrum. Methods* **132** (1976), 1.
14. G. BASBAS, *Nucl. Instrum. Methods B* **4** (1984), 227.
15. H. H. ANDERSEN, *in* "Semiclassical Descriptions of Atomic and Nuclear Collisions" (J. Bang *et al.*, Eds.), p. 409, New York, 1985.
16. H. H. MIKKELSEN AND P. SIGMUND, *Phys. Rev. A* **40** (1989), 101.

17. H. Esbensen, Ph.D. thesis, Univ. Aarhus, Denmark, 1976, unpublished.
18. C. C. Sung and R. H. Ritchie, *Phys. Rev. A* **28** (1983), 674; see also C. D. Hu and E. Zaremba, *Phys. Rev. B* **37** (1988), 9268.
19. L. H. Andersen, P. Hvelplund, H. Knudsen, S. P. Møller, J. O. P. Pedersen, E. Uggerhøj, K. Elsener, and E. Morenzoni, *Phys. Rev. Lett.* **62** (1989), 1731.
20. Proceedings of the series of International Conferences on Atomic Collisions in Solids, 1973–1987; latest reference: *Nucl. Instrum. Methods B* **48** (1990).
21. H. H. Mikkelsen, H. Esbensen, and P. Sigmund, *Nucl. Instrum. Methods B* **48** (1990), 8.
22. U. Fano, *Ann. Rev. Nucl. Sci.* **13** (1963), 1.
23. P. Sigmund and H. Esbensen, *Surf. Sci.*, to be submitted.
24. M. Abramowitz and I. A. Stegun, "Handbook of Mathematical Functions," Dover, New York, 1972.
25. J. D. Jackson and R. L. McCarthy, *Phys. Rev. B* **6** (1972), 4131.
26. A. Belkacem and P. Sigmund, *Nucl. Instrum. Methods B* **48** (1990), 29.
27. J. Lindhard and M. Scharff, *Mat. Fys. Medd. K. Dan. Vidensk. Selsk.* **27**, No. 15 (1953).
28. F. Bloch, *Ann. Phys.* **16** (1933), 285.
29. H. H. Mikkelsen, submitted for publication.
30. P. Sigmund and U. Haagerup, *Phys. Rev. A* **34** (1986), 892.
31. H. H. Mikkelsen and E. H. Mortensen, *Nucl. Instrum. Methods B* **48** (1990), 39.
32. H. Jensen, *Z. Phys.* **77** (1932), 722.
33. A. Faibis, R. Kain, I. Plesser, and Z. Vager, *Nucl. Instrum. Methods* **170** (1980), 99; A. Breskin, A. Faibis, G. Goldring, M. Hass, R. Kaim, Z. Vager, and N. Zwang, *Nucl. Instrum. Methods* **170** (1980) 93.
34. Y. Yamazaki, *Nucl. Instrum. Methods B* **48** (1990), 97.

ANNALS OF PHYSICS **201**, 193–220 (1990)

Log Terms for Leading Radiative Corrections in Atoms in the Dirac–Fock Approximation*

G. FELDMAN AND T. FULTON

Department of Physics and Astronomy, The Johns Hopkins University,
Baltimore, Maryland 21218

Received September 21, 1989

Analytical expressions are obtained for the log terms arising from the low photon frequency part of the radiative corrections in the Dirac–Fock (DF) approximation of many-electron atoms. The atoms considered are iso-electronic sequences of non-degenerate electronic cores, plus or minus one electron. The nuclear charge is taken to be small enough that the Lamb shift is still a small correction to the DF energies. If the unshielded nuclear charge is a point charge, the principal effect of the shielding by the electrons in the DF approximation is to replace the absolute square of the hydrogenic wave function at the origin of coordinates by the corresponding expression for the DF wave function. A preliminary numerical test of this result leads to better agreement between theory and experiment for the Li iso-eletronic sequence than has hitherto been the case. © 1990 Academic Press, Inc.

1. INTRODUCTION

In this paper, we continue our discussion of radiative corrections for many-electron atoms which we considered in recent work [1]. In that work, which is devoted solely to analytical, and does not include numerical, considerations, we computed "leading log" (LL) radiative corrections (terms in which logarithms of energies appear) in perturbation theory in the electron–electron interaction. By "leading log," we mean both the "constant log" (CL) terms, which arise from a constant low virtual photon frequency cutoff term in the argument of the log terms in the Lamb shift, and the "Bethe log" (BL) terms, arising from an infinite sum over all energies, which complement them [2; 3; 1, Eqs. (41), (42)]. This is the customary way in which these log terms are presented in analyzing the non-relativistic (NR) contribution to the Lamb shift.

The starting point of the perturbation theory [1] was taken to be relativistic (R) electrons in the presence of a nuclear Coulomb field. Electron–electron interactions were neglected. The structure of the results we obtained had a simple physical interpretation, which, in turn, led to a rather natural conjecture for generalizing these results to the Dirac–Fock (DF) case: For a point nucleus, the dominant influence of electron shielding on the Lamb shift in perturbation theory, and for virtual photons of low frequency, was a correction of the absolute square of the wave

---

* Supported in part by the National Science Foundation.

0003-4916/90 $7.50

Copyright © 1990 by Academic Press, Inc.
All rights of reproduction in any form reserved.

function at the origin of coordinates, due to the effect of the electron–electron interaction. This result was most transparent when only the constant log terms were considered. It led to a replacement of the log coefficient of Z^4 in the unshielded, or hydrogenic, case by ZZ_{eff}^3, where Z_{eff} was given a precise meaning in terms of the perturbation theory. This result is to be contrasted with one particular approach for taking shielding into account [4], in which the coefficient of the hydrogenic log term was replaced by Z_{eff}^4, and Z_{eff} was calculated from an ad hoc (though physically quite reasonable) ansatz.

We will use our experience with perturbation theory in Ref. [1] to attempt to verify the conjecture made in that reference for radiative corrections in the DF case. We begin the next section with a particular definition of the DF approximation which will be convenient for the purposes of the present work. As in the previous work, in which the DF (or HF) approximation is defined in terms of approximations to one-body propagators, we restrict our discussion to atoms consisting of a non-degenerate core plus (or minus) one electron (e.g., Li, B, and Ne and their isoelectronic sequences). We next consider a reformulation of the radiative correction problem, to make it applicable to the DF case. We treat a single virtual transverse photon first. Our approach is similar in spirit to the point of view espoused in our previous papers [5–7], but different in detail. The final result of this section is an integral equation for the Lamb shift. It is gauge invariant (GI) and formally correct in leading order in the effect of transverse photons.

In order to proceed further toward actual numerical results, in Section 3 we make successive approximations to the formal result of Section 2. We are led to consider the expansion of the integral equation of Section 2 in powers of the electron–electron Coulomb potential, V_{ee}, through first order in V_{ee}. The matrix elements of V_{ee} (i.e., integrals of the Coulomb potential with four single-particle wave functions) which appear in this expansion, differ from those which are used to set up the DF approximation. The latter always involve expectation values of V_{ee} (in direct or exchange terms) with one of the core electrons. Accordingly, our perturbation theory is based on the DF energies and wave functions in zeroth order and is carried out in the same spirit as perturbative corrections for correlation [8], Breit and retardation effects [9] to DF energies. The results up to any finite order of this expansion will not be strictly GI, but one can carry out the expansion in V_{ee} to whatever degree of accuracy is required. The structure of this approximation is very similar to that of the perturbation theory based on hydrogenic wave functions as a starting point, which we previously explored [1].

Having made this approximation, we can write the result (to order α^5) for these corrections to the DF energy (for a state labeled n) in terms of two-particle expectation values of operators, where the two particles are labeled by n and a (the latter is a label for core electrons). A sum over a is always implied.

The diagrams associated with the various terms can be divided into two classes: one in which the transverse photon is exchanged between two electron lines in a diagram, and one in which it is emitted and absorbed on the same line. In this way, our present result resembles that for He, discussed by Kabir and Salpeter [10].

In order to obtain the radiative corrections (of order α^5), one must take care to extract first the "Breit interaction" contribution (including retardation corrections to it), i.e., terms of leading order α^4. We proceed further (in analogy to the He case) by breaking the integral over the transverse photon momentum into a low and a high frequency part.

In this work, we focus on the leading log terms coming from the low frequency part of the radiative corrections. We shall leave for subsequent consideration the non-log terms (including the Uehling effect), the log terms arising from high frequency photons, and the contribution from the exchange of two transverse photons [10] (both log and non-log terms). Using the results for He, we shall argue that all of the latter terms will not contribute, given the accuracy of present experiment. We shall test these arguments in our subsequent, more detailed, numerical work.

We conclude Section 3 with a detailed evaluation of the constant log terms for these low frequency contributions. Our principal result parallels that of Ref. [1]: the terms we have dubbed "contact terms" in this reference, which involve derivatives of V_{ee}, cancel out, and, in the leading $Z\alpha$ expansion, only terms containing the Laplacian of the nuclear potential remain. (This cancellation of contact terms does not persist when the relativistic contributions due to high photon frequencies are added.) The CL terms we obtain here are precisely the two leading terms of the V_{ee} expansion of the DF integral equation we conjectured in Ref. [1], if the kernel in that equation is taken to be just the constant log part of the Lamb shift. The BL terms are considered in detail in Appendix A. In addition to an expression analogous to the BL terms in the hydrogenic case, there are many additional similar energy-dependent log terms, which we also label BL terms.

Our exposition is rigorous up to this point, in the sense that we have clearly specified the terms we have not evaluated. In principle, they can be evaluated, both analytically and numerically. Indeed, the analytic calculations of a majority of these terms have been completed. We will present both analytical and numerical results in the future. However, using the analogy of the He results, we are in a position to obtain some preliminary numerical results which may be considered of some interest. In Section 4 we find that the principal effect of shielding appears in the term of the Lamb shift containing the absolute square of the DF wave function at the origin. (We remind the reader that, for the hydrogenic case in leading order, the BL and the non-log terms are independent of nuclear charge [11] and the CL term depends only logarithmically on this charge.)

Section 5 contains a summary and discussion of our work, as well as indications of future lines of research.

Appendix A is devoted to the presentation of our new BL results. By definition, these are the terms in which the argument of the logarithm depends on an average of DF energies.

In Appendix B, we address a peripheral issue. The energy shifts represent the real part of self-energy contributions calculated from virtual photon emission and absorption. The imaginary parts of these terms give inverse lifetimes for transitions between states. Consistency requires that, if the DF picture we have described is a correct one, transitions from excited states to core states which are occupied should be forbidden. We demonstrate this property in Appendix B.

2. Integral Equation for Leading Radiative Correction in the DF Approximation

In order to generate a GI expression for radiative corrections in the DF approximation which involve a single virtual transverse photon, we shall follow our previous strategy for generating GI expressions for transition amplitudes [5]. We consider first the one-lepton propagator, the equation of which has a kernel involving a single Coulomb interaction between leptons. This propagator, which we label G^N_{Coul}, contains the DF propagator but also includes the effects of the Coulomb part of the Lamb shift, which will be considered explicitly later. We write G^N_{Coul} (see below and Figs. 1, 2, and 3) as an infinite subset of Feynman diagrams, representing the emission and absorption of an infinite number of "nested" and "iterated" Coulomb "photons" (interactions). We then attach the two vertices of the single additional transverse photon to the electron line in all possible ways and resum the resulting diagrams.

The one-electron Coulomb propagator for an atom with a non-degenerate core of N electrons, plus or minus one electron, satisfies the equation [5–7]

$$G^N_{\text{Coul}} = g^N + g^N(\Sigma^N_{\text{Coul}} - \delta m_{\text{c}})G^N_{\text{Coul}}, \tag{2.1}$$

or the equation

$$[G^N_{\text{Coul}}]^{-1} = g^{-1} - \Sigma^N_{\text{Coul}} + \delta m_{\text{c}}. \tag{2.2}$$

g^{-1} is the inverse of the one-lepton propagator in the absence of the electron–electron interaction,

$$g_\omega^{-1} = \omega - (\boldsymbol{\alpha}\cdot\mathbf{p} + \beta m + V_{\text{nuc}}). \tag{2.3}$$

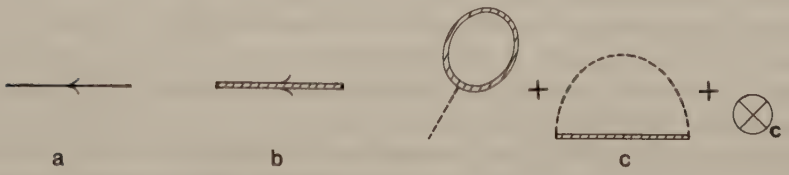

Fig. 1. (a) Designation of the propagator in the absence of V_{ee}, ig^N. (b) Designation of the propagator in the presence of V_{ee}, iG^N_{Coul}. (c) The self-energy, $\Sigma^N_{\text{Coul}} - \delta m_{\text{c}}$. The dashed lines represent Coulomb "photons" (interactions) only. $\otimes_{\text{c}}$ is the negative of the mass counterterm, δm_{c}, due to the Coulomb interaction. Σ^N_{Coul} contains the Coulomb contribution to the lowest order Lamb shift (including vacuum polarization).

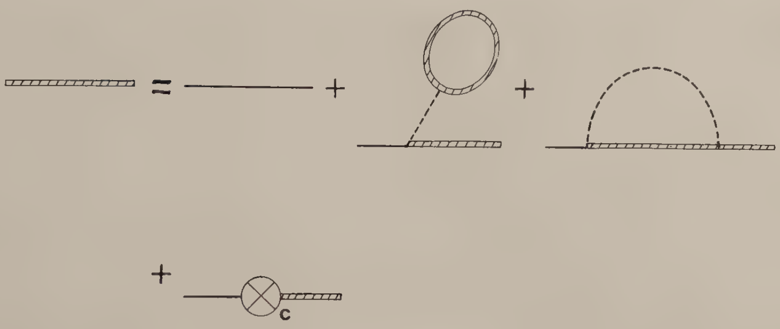

FIG. 2. Graphical representation of Eq. (2.1).

g^N and G^N_{Coul} are represented by the diagrams of Figs. 1a and 1b, respectively. Σ^N_{Coul} is the self-energy in this "Coulomb kernel" approximation. The physical lepton mass, m, appears in all expressions above, and the Coulomb part of the mass renormalization is accounted for by the (operator) counterterm, δm_c. Later, when we consider the transverse photons, we shall introduce an additional counterterm, δm_t, to give a total mass counterterm

$$\delta m = \delta m_c + \delta m_t. \tag{2.4}$$

As usual, the counterterms δm_c and δm_t are chosen so that expectation values of the self-energy operator minus δm in free particle states vanish [3, 11] in the limit as all potentials, V_{nuc} and V_{ee}, approach zero.

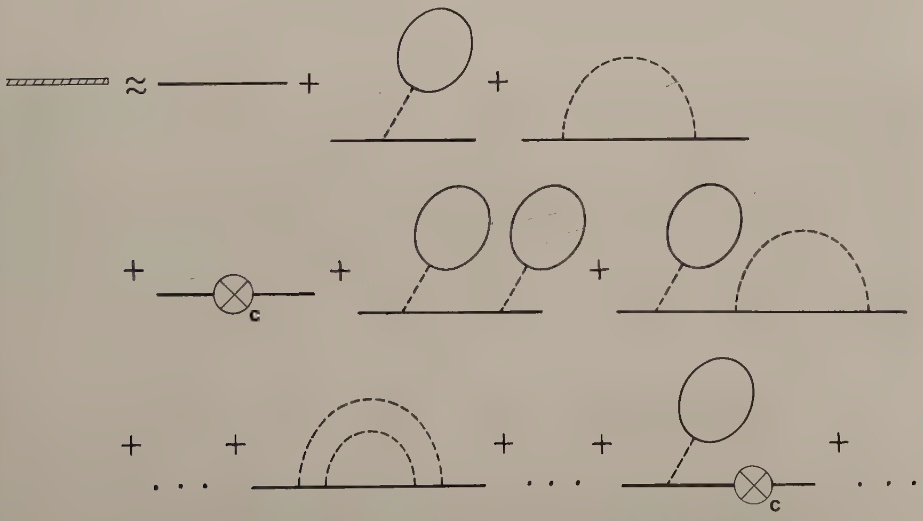

FIG. 3. Partial expansion of the graphical representation, Fig. 2.

$\Sigma^{N}_{\text{Coul}} - \delta m_{c}$ is defined in Fig. 1(c). Equation (2.1) is represented diagrammatically by Fig. 2. A few terms in the expansion of Eq. (2.1) in powers of V_{ee} are given in Fig. 3.

In the above equations, we have suppressed energy indices (wherever possible) and coordinate indices, since these Green's functions have been defined and discussed a number of times in our previous work.[1]

The propagator G^{N}_{Coul} is an approximation to the exact one-electron propagator,[2] G^{N}, which is defined as an expectation value between lepton states of total lepton charge Ne of a time ordered product of lepton field operators ψ and $\psi^{\dagger}$, in the presence of a nuclear potential of charge $-Ze$ (due to a point or distributed nuclear source), and of V_{ee}. One goes from the exact G^{N} to G^{N}_{Coul} by replacing the exact self-energy, Σ^{N}, by the Coulomb self-energy, Σ^{N}_{Coul}.

The DF propagator, $G^{N}_{\omega,\text{DF}}$, is an approximation to $G^{N}_{\omega,\text{Coul}}$. It is defined in Eq. (2.5) below. The DF energies and states are written as e_n and $|n\rangle$, respectively. They satisfy the equation

$$(G^{N}_{e_n,\text{DF}})^{-1}\,|n\rangle = 0. \tag{2.5}$$

The energies associated with $G^{N}_{\omega,\text{Coul}}$ are $e_n + \delta e_n$. The additional energy, δe_n, of order α^5, is given by

$$\delta e_n = \langle n|\,(\Sigma^{\text{“0”}}_{\text{c}} - \delta m_{\text{c}})\,|n\rangle, \tag{2.6}$$

where $\Sigma^{\text{“0”}}_{\text{c}}$ is defined below. Equation (2.6) gives the Coulomb contribution to the Lamb shift in the DF approximation.

The DF propagator is [12, (3.12)]

$$G^{N}_{\omega,\text{DF}} = \sum_{j=N+1}^{\infty} \frac{Q_j}{\omega - e_j + i\eta} + \sum_{a=1}^{N} \frac{P_a}{\omega - e_a - i\eta} + \sum_{j} \frac{\bar{Q}_j}{\omega - \bar{e}_j - i\eta}, \qquad \eta \to 0^{+}, \tag{2.7}$$

where the subscript DF and the superscript N in Q_j, P_a, $\bar{Q}_j$ and in the energies e_j, etc., on the right side of (2.7) are suppressed. We will continue to suppress these from here on. (Note that the e_j are negative numbers.) The Σ's in the equation denote sums over discrete states and integrals over continuous ones.

Q_j, P_a, and $\bar{Q}_j$ are projection operators in the form of Dirac ket-bra's for valence (discrete and continuous) and core electron states, and for positron states, respectively [12, (3.11)]. Both the states and the energies which appear in Eq. (2.7) are solutions of the DF equation [12, (3.36)], Eq. (2.5). We further define H^{-} and Σ^{N}_{DF} as

$$G^{N}_{\omega,\text{DF}} \equiv \frac{1}{\omega - H^{-}_{\text{DF}}} \qquad \text{and} \qquad (G^{N}_{\omega,\text{DF}})^{-1} = g^{-1}_{\omega} - \Sigma^{N}_{\text{DF}}. \tag{2.8}$$

---

[1] See, for example, Ref. [6, Eq. (2.56)]. This equation is formally the same for the NR and the R case.

[2] See Ref. [6, Eq. (2.27)]. The definition is formally the same in the NR and R case.

The negative superscript on $H_{\rm DF}$ is introduced to indicate the negative imaginary part in the denominator associated with the hole state projection operator, P_a.

We give $\Sigma^N_{\rm DF}$ explicitly, partly to define new notation which will be convenient to use below. We have, with $V_{\rm ee}\equiv V$,

$$\langle m|\,\Sigma^N_{\rm DF}\,|n\rangle = \alpha\int\frac{d^3\mathbf{x}\,d^3\mathbf{y}}{|\mathbf{x}-\mathbf{y}|}\sum_{a=1}^{N}\langle m|\mathbf{x}\rangle\langle a|\mathbf{y}\rangle[\langle\mathbf{x}|n\rangle\langle\mathbf{y}|a\rangle-\langle\mathbf{x}|a\rangle\langle\mathbf{y}|n\rangle]$$

$$\equiv\left\{\left(\begin{matrix}m\\a\end{matrix}\middle|V\middle|\begin{matrix}n\\a\end{matrix}\right)-\left(\begin{matrix}m\\a\end{matrix}\middle|V\middle|\begin{matrix}a\\n\end{matrix}\right)\right\}\equiv\left[\begin{matrix}m\\a\end{matrix}\middle|V\middle|\begin{matrix}n\\a\end{matrix}\right], \tag{2.9}$$

where, in the last two expressions, a summation over the core labels, a, is understood.

We note that

$$\left(\begin{matrix}m\\p\end{matrix}\middle|V\middle|\begin{matrix}n\\q\end{matrix}\right)=\left(\begin{matrix}p\\m\end{matrix}\middle|V\middle|\begin{matrix}q\\n\end{matrix}\right)\quad\text{and}\quad\left[\begin{matrix}m\\p\end{matrix}\middle|V\middle|\begin{matrix}n\\q\end{matrix}\right]=\left[\begin{matrix}p\\m\end{matrix}\middle|V\middle|\begin{matrix}q\\n\end{matrix}\right]. \tag{2.10}$$

From here on, we will generally suppress the subscript DF in $G^N_{\omega,\rm DF}$ (where such suppression does not lead to confusion), but not the superscript N, in order to distinguish G^N_ω from a new Green's function, $G^{``0"}_\omega$,

$$G^{``0"}_\omega\equiv\frac{1}{\omega-H^+}, \tag{2.11}$$

diagrammed as in Fig. 4a. $G^{``0"}$ has the same form as Eq. (2.7), except that $-i\eta\to+i\eta$ in the middle term on its right side, containing P_a. The positive superscript in H^+ is meant to indicate this change of sign.

It should be emphasized that $G^{``0"}$ is not the vacuum expectation value of a time ordered product of two lepton field operators. It would be so only if $V_{\rm ee}$ were neglected and hydrogenic states instead of DF states were used in the projection operators of Eq. (2.7). The superscript zero in quotation marks is used in $G^{``0"}$ to indicate that it is not a vacuum expectation value but is closely related to one. In particular, neither $G^{``0"}$ nor $G^N_{\rm DF}$ can be expanded in a series of Feynman diagrams, unlike $G^N_{\rm Coul}$, which is so expanded in Fig. 3.

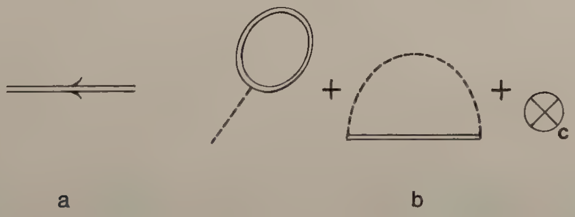

FIG. 4. (a) Designation of the propagator $G^{``0"}$. (b) The Coulomb Lamb shift, $\Sigma^{``0"}_{\rm c}-\delta m_{\rm c}$.

G^N_{DF} and $G^{\text{``0''}}$ are related to each other by the equation [7, Eq. (2.10)]

$$G^N_{\omega,\mathrm{DF}} = 2\pi i \sum_a P_a\, \delta(\omega - e_a) + G^{\text{``0''}}_{\omega}. \tag{2.12}$$

$G^{\text{``0''}}$ will have an important role to play below in the evaluation of radiative corrections. We can immediately express the Coulomb contribution to the Lamb shift in terms of it, as is indicated in Fig. 4b.

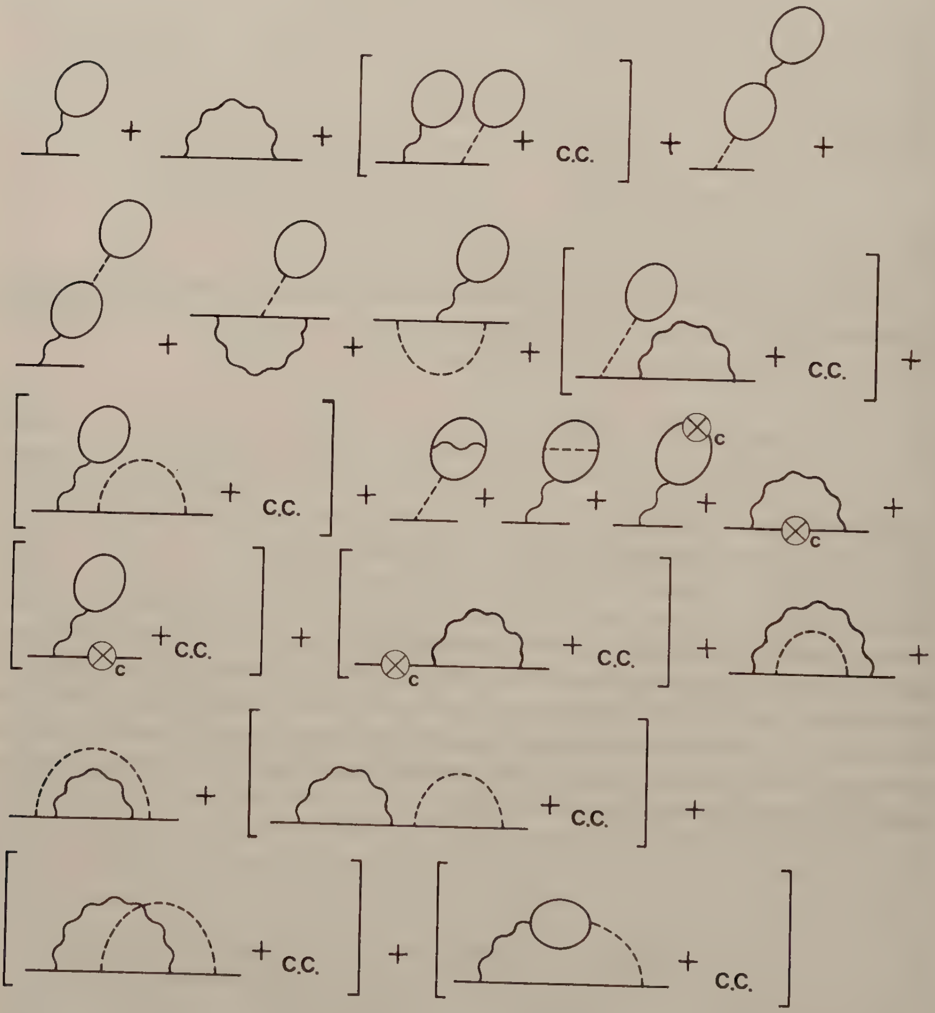

FIG. 5. Insertion of a single virtual transverse photon in the graphical representation of Fig. 3, to leading order in the radiative correction. The transverse photon propagator is represented by a wavy line.

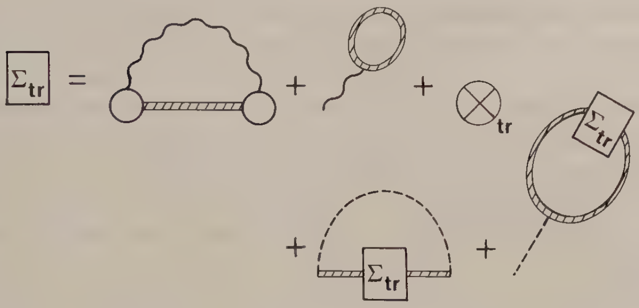

FIG. 6. Graphical representation of the integral equation for the leading order radiative correction due to one transverse photon. The mass counterterm, $-\delta m_t$, is represented by $\otimes_{tr}$.

In order to generate the integral equation for the leading radiative correction operator due to transverse photons, we use the expanded form of $G^N_{\omega,\mathrm{Coul}}$, as illustrated in Fig. 3. To generate a GI form of the radiative corrections involving a single transverse photon, we insert a virtual transverse photon in all possible ways into the graphical representation of Fig. 3. We illustrate in Fig. 5 the diagrams which arise after such a transverse photon insertion in those diagrams in Fig. 3 which contain no more than a single V_{ee}.

Resummation of the infinite sets of diagrams which are generated in the transverse photon insertion process just discussed, and introduction of a mass counterterm, δm_t, for the transverse photon interaction lead to the inomogeneous integral equation of Fig. 6. The source term, represented by the first three figures on the right, is itself quite complicated, since vertex functions also appear in it. They, in turn, satisfy an integral equation [5, 6, 12], which is diagrammatically represented in Fig. 7. Observe that these vertex terms are present in the "self-energy" type of source term (the first term on the right of Fig. 6) but are absent in the "vacuum polarization" or tadpole term (the second term on the right). This, incidentally, also ensures the correct counting of "overlapping divergences."

We will not give the algebraic expressions corresponding to Figs. 6 and 7, since we shall not make explicit use of them in what follows. In the next section, we will make an expansion of the integral equation, represented by Fig. 6, as a power series

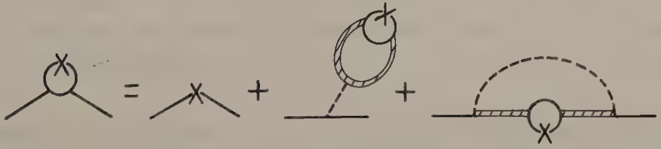

FIG. 7. Graphical representation of the integral equation for the vertex function, contained in sections of the diagrams of Fig. 6. This figure is the same as Fig. 9 of Ref. [6]. The ×'s in the figure mark the points of attachment of the transverse photon propagator, and the short lines the points of attachment of the electron propagators.

in the V_{ee} which appear explicitly in the kernels of Figs. 6 and 7. We will deal with the expressions which will result from this expansion, both diagrammatically and algebraically.

We would like to emphasize that our results for the radiative corrections in Fig. 6 are GI. The gauge dependence of the photon propagator can be incorporated into the definition of the transverse propagator alone [13], with the Coulomb part (V_{ee}), which appears in G^N_{Coul} and elsewhere, fixed. Inserting this propagator in all possible ways in the expanded form of G^N_{Coul} ensures that matrix elements of the operator Σ_t are GI.

3. Leading Contributions to the Lamb Shift in DF Perturbation Theory

In this section, we first set up an approximation procedure for the lowest order contribution to the radiative correction, an expansion in α, (already implicit in the previous section), Z and/or Z_{eff} ($-eZ_{\mathrm{eff}}$ is the effective—shielded— nuclear charge). It is a functional of the number of protons in the nucleus, Z, with $Z > Z_{\mathrm{eff}}$, so that the magnitude of Z alone can serve as a criterion of the validity of our perturbation theory.

The DF approximation serves as our zeroth order problem. The corrections to it which we shall study involve the effect of one additional transverse photon (taken into account to order α^5 or $\alpha^5 \ln \alpha$). Breit interaction terms (and retardation corrections to them), which also arise from one transverse photon exchange[3] and are of leading order α^4, must first be extracted. Other corrections to the DF energies arise from two or three Coulomb interaction correlation effects. These have been discussed and evaluated elsewhere [9]. In addition, there are contributions arising from the exchange of two transverse photons. These, along with other contributions mentioned below, will be the subject of a future publication. We shall consider initially, and continue to retain in this paper, only such terms which give log contributions.

The Lamb shift itself is indeed a small correction to the DF energies for Z not very large. The actual restriction on the values of Z allowed is given by the limit of the validity of the Z expansion for the hydrogenic Lamb shift [11, 14].

The relevant DF perturbation theory diagrams are obtained from Figs. 6 and 7, by considering at most one virtual Coulomb "photon," in addition to the virtual transverse photon. They are given in Fig. 8. Since the "tadpole" term in the inhomogeneous part of Fig. 6 does not lead to a log contribution, it is left out in Fig. 8a.

The next approximation is to set $G^N_{\mathrm{Coul}} \approx G^N_{\mathrm{DF}}$, wherever G^N_{Coul} appears in Fig. 8, since Coulomb Lamb shift contributions are clearly negligible in the leading transverse radiative corrections.

---

[3] See Ref. [7] and the argument leading from Figs. 2.2–2.4 to Figs. 2.5–2.10 in that reference.

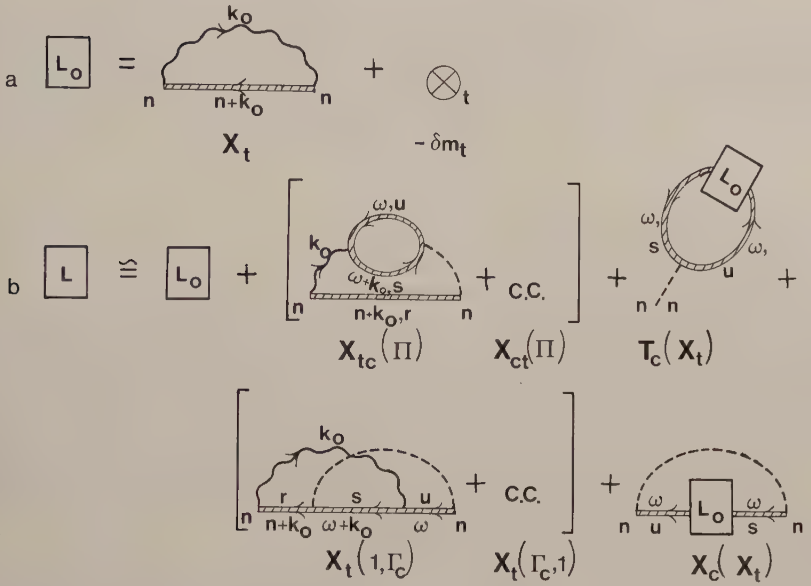

FIG. 8. DF perturbation theory expansion of Σ_t to first order in V_{ee}, which contains the log contributions. For convenience, the fourth components of momentum four-vectors and the states are labeled, corresponding to the algebraic expressions used in the text.

The labeling of the individual diagrams in Figs. 8a and 8b is essentially self-explanatory. The notation used is based on that of Ref. [7]. Thus, T and X refer to "tadpole" (vacuum polarization) and "exchange" (self-energy) contributions. An insertion of X and T, as well as vacuum polarization (Π) and a vertex (Γ) in a larger diagram, is denoted by the corresponding label in parentheses. The subscripts t and c indicate whether a transverse or a Coulomb photon appears in the corresponding part of the diagram. As an example, consider the symbol $X_t(1, \Gamma_c)$, labeling one of the diagrams of Fig. 8b. The diagram is that for a transverse photon self-energy, with the left vertex a local one, and the right vertex a non-local one, containing a single Coulomb interaction. It is easy to generate terms of higher order in V_{ee}. A single representative of terms involving two V_{ee} is given in Fig. 9.

The first step is to examine separately each of the terms corresponding to the diagrams of Fig. 8, and to extract the Breit interaction part. The remaining calculation carried out in the present work is in the photon momentum region for which $0 \leqslant k \leqslant \lambda$, $\lambda \ll m$, for which the NR approximation [2] may be used. For values of

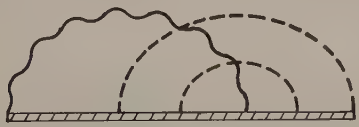

FIG. 9. A representative term in the perturbation expansion of Σ_t in V_{ee} which would have to be present in Fig. 8 to make the radiative correction GI.

k such that $\lambda \leqslant k \leqslant \infty$, an R approximation has to be used [3], but the compensating gain in this region is that G^N_{DF} may be expanded in powers of the full potential operator, $V_{\mathrm{nuc}} + V_{\mathrm{DF}}$, where

$$\langle m| V_{\mathrm{DF}} |n\rangle \equiv \left[\begin{array}{c|c|c} m & V & n \\ a & & a \end{array}\right], \tag{3.1}$$

which is Eq. (2.9), where we have replaced the symbol Σ_{DF} by V_{DF}. Summation over the core states, labeled a, is understood.

The cutoff parameter, λ, disappears when the high and low photon momentum results are joined [3] as will be demonstrated in subsequent work. However, careful consideration of these terms shows that the parts of the subsequent analysis in the present paper which contain exchanged transverse photons (terms in which the operators ${}^{\mathbf{p}\cdot}_{\mathbf{p}}V$, ${}^{\mathbf{p}\cdot}V_{\mathbf{p}}$, and their complex conjugates, all defined below, appear) contain a natural cutoff, when the hight photon momenta are taken into account. As a consequence, the cancellation of "contact terms," demonstrated below, does not persist when the full analysis, including R as well as NR parts, is carried out. (See the analogous result for He in Ref. [10].)

We shall not be concerned further with high photon momenta in the present work.

We begin our detailed calculation of the leading log terms with the evaluation of the low photon momentum contributions of $X_{\mathrm{t}} - \delta m_{\mathrm{t}}$, diagrammatically represented in Fig. 8a. The Breit interaction (with retardation) involves the exchange of one transverse photon (and no Coulomb "photon") and is obtained by replacing the propagator $G^N_{n+k_0,\mathrm{DF}}$ in X_t by $[\sum_a 2\pi i\, \delta(k_0 + n - a) P_a]$, namely, the first term on the right side of Eq. (2.12). The remaining term, $G^{\text{"0"}}_{n+k_0}$, in the low virtual transverse photon momentum region leads to essentially the same expression for the radiative correction as that originally considered by Bethe [2] for hydrogen. The only difference is that the hydrogenic energies and wave functions which appear in Ref. [2] are here replaced by DF (or, more correctly, Hartree–Fock (HF), since we take the NR limit) energies and wave functions. Thus, we can immediately write the low k contribution to the radiative correction (noting that the dipole approximation can also be made) as

$$\langle n|\, (X_{\mathrm{t}} - \delta m_{\mathrm{t}})\, |n\rangle_{\mathrm{LL}} = \frac{2\alpha}{3\pi m^2} \int_0^{\lambda} dk \sum_s \frac{\langle n|\, \mathbf{p}\, |s\rangle \cdot \langle s|\, (n-s)\mathbf{p}\, |n\rangle}{n-s-k}. \tag{3.2}$$

This gives a leading log contribution (hence the subscript LL). We have taken $e_n \rightarrow n$, etc., and e_n, $|n\rangle$, etc., are solutions of the HF equation (the non-relativistic limit of the DF equation, (2.5)),

$$H\,|n\rangle = e_n\,|n\rangle, \tag{3.3}$$

with

$$H = h + V_{\mathrm{HF}}, \qquad h = (1/2m)\mathbf{p}^2 + V_{\mathrm{nuc}}. \tag{3.4}$$

Note that the sum over s in Eq. (3.2) $\sum_s$ runs over all HF states (discrete and continuous), and, since only the NR approximation is relevant, there are no positron states. Again, after suitable replacements of hydrogenic by DF energies and states, the $k > \lambda$ contribution can be obtained as in Ref. [3].

Integration over k in Eq. (3.2) leads to

$$\langle n|\,(X_t - \delta m_t)\,|n\rangle_{\mathrm{LL}} = \frac{\alpha}{3\pi m^2}\langle n|\left\{[\mathbf{p}\cdot, H]\ln\frac{\lambda}{|e_n - H|}\,\mathbf{p} - \mathbf{p}\cdot\ln\frac{\lambda}{|e_n - H|}\,[\mathbf{p}, H]\right\}|n\rangle. \tag{3.5}$$

We next make a small change in the standard approach [1–3] followed in Lamb shift calculations, by adding and subtracting log terms with constant arguments $(\tilde{Z}\alpha)^2 m$. $\tilde{Z}$ is to be chosen so as to minimize the $\tilde{Z}$ dependence of the BL term on $\tilde{Z}$. It is convenient to define the BL terms for the hydrogenic case so that they contain log terms of the form $\ln[(Z\alpha)^2 m/(2\,|e_n - h|)]$, which are completely independent of Z [11, 15]. Following the above argument, we set

$$\begin{aligned} \ln\frac{\lambda}{|e_n - H|} &= \mathscr{L}_B(n) + \ln\frac{1}{(\tilde{Z}\alpha)^2} + \ln\frac{2\lambda}{m}, \\ \mathscr{L}_B(n) &= \ln\frac{(\tilde{Z}\alpha)^2\, m}{2\,|e_n - H|}. \end{aligned} \tag{3.6}$$

The first of the terms in Eq. (3.6) is contained in the BL terms and is dealt with in Appendix A. The third contains the photon momentum cutoff, which is eliminated by the high photon momentum contributions. We shall deal with it in subsequent work. For the moment, we focus on expressions containing the second term, which we call [1] "constant log" (CL). Using Eq. (3.4), we obtain

$$\langle n|\,(X_t - \delta m_t)\,|n\rangle_{\mathrm{CL}} = \langle n|\, l\,|n\rangle - \beta\left[\begin{matrix} n \\ a \end{matrix}\middle|\,(V^{\mathbf{p}^2} + {}^{\mathbf{p}^2}V - 2^{\mathbf{p}\cdot}V^{\mathbf{p}})\,\middle|\begin{matrix} n \\ a \end{matrix}\right], \tag{3.7}$$

where[4]

$$l = \frac{\alpha}{3\pi m^2}\nabla^2 V_{\mathrm{nuc}}\ln\frac{1}{(\tilde{Z}\alpha)^2}, \qquad \beta = \frac{1}{3\pi}\frac{\alpha}{m^2}\ln\frac{1}{(\tilde{Z}\alpha)^2}. \tag{3.8}$$

The second term of Eq. (3.7) contains expressions which are generalizations of the notation defined in Eq. (2.9). Two examples of this generalized notation are

$$\begin{aligned} \left(\begin{matrix} m \\ s \end{matrix}\middle|\, {}_{\mathbf{p}^2}V\,\middle|\begin{matrix} n \\ u \end{matrix}\right) \equiv {} & -\alpha\int d^3\mathbf{x}\, d^3\mathbf{y}\langle m|\mathbf{x}\rangle\langle \mathbf{x}|n\rangle\langle s|\mathbf{y}\rangle \\ & \times\nabla_y^2\left\{\frac{1}{|\mathbf{x} - \mathbf{y}|}\langle \mathbf{y}|u\rangle\right\}, \end{aligned} \tag{3.9}$$

---

[4] See Ref. [1, Eqs. (43), (47), (50), (51)]. The change from these equations to the present Eqs. (3.7) and (3.8) is that $Z \to \tilde{Z}$, and the hydrogenic states of Ref. [1] now become HF states.

and

$$\left(\begin{matrix} m \\ s \end{matrix}\right| {}_{\mathbf{p}\cdot} V^{\mathbf{p}} \left| \begin{matrix} n \\ u \end{matrix}\right) \equiv -\alpha \int d^3\mathbf{x}\, d^3\mathbf{y} \langle m | \mathbf{x} \rangle \langle s | \mathbf{y} \rangle$$

$$\times \nabla_y \cdot \left\{ \frac{1}{|\mathbf{x}-\mathbf{y}|} (\nabla_x \langle \mathbf{x} | n \rangle \langle \mathbf{y} | u \rangle) \right\}, \tag{3.10}$$

with

$$\left[\begin{matrix} m \\ s \end{matrix}\right| {}^{\mathbf{p}\cdot} V^{\mathbf{p}} \left| \begin{matrix} n \\ u \end{matrix}\right] = \left(\begin{matrix} m \\ s \end{matrix}\right| {}^{\mathbf{p}\cdot} V^{\mathbf{p}} \left| \begin{matrix} n \\ u \end{matrix}\right) - \left(\begin{matrix} m \\ s \end{matrix}\right| {}^{\mathbf{p}\cdot} V_{\mathbf{p}} \left| \begin{matrix} u \\ n \end{matrix}\right), \text{ etc.} \tag{3.11}$$

Note the simple rule (illustrated in (3.11)) for antisymmetrization of expressions in which an operator such as **p** "hangs" on V: the operator always "sticks" to its state upon antisymmetrization. One must be careful to note how this compact operator formalism translates into actual matrix elements, as indicated in Eqs. (3.9) and (3.10).

Another simple interpretation which our notation makes apparent is that, when the operators "hang" on V at a single level in a nonexchange matrix element (upper or lower), we are dealing with "self-energy" terms. When operators "hang" on V at both upper and lower levels in such matrix elements, we are dealing with the exchange of a transverse photon. It is just this difference between self-energy (also vertex) and exchange which will be important when the high-k integrations are performed. The transverse photon exchange diagrams lead to a "natural" cutoff ($k \simeq \alpha m$), which is absent in the self-energy terms. A consequence of this result is that the high k integration of the self-energy terms exactly cancels the entire $\ln(2\lambda/m)$ term which appears when Eq. (3.6) is inserted in (3.5), whereas, in the exchange terms, a $\ln \alpha$ term remains. (See Kabir and Salpeter [10] and Salpeter [16].)

We turn next to the evaluation of $X_{\text{tc}}(\Pi)$. We may read off the algebraic result from the diagram, Fig. 8(b), which also contains the labeling of the intermediate energies and states. We obtain

$$\langle n | X_{\text{tc}}(\Pi) | n \rangle = \frac{e^2}{m^2} \sum_{r,s,u} \int \frac{d^4k}{(2\pi)^4} \frac{d\omega}{2\pi} \frac{\delta'_{ij}}{k^2} \langle n | p_i G^N_{n+k_0} | r \rangle$$

$$\times \langle s | G^N_{\omega+k_0} p_j G^N_{\omega} | u \rangle \left(\begin{matrix} r \\ u \end{matrix}\right| V \left| \begin{matrix} n \\ s \end{matrix}\right). \tag{3.12}$$

The function δ'_{ij} is

$$\delta'_{ij} = \delta_{ij} - (\mathbf{k}_i \mathbf{k}_j / \mathbf{k}^2). \tag{3.13}$$

Since we are interested here only in the region of the $|\mathbf{k}|$ integration from 0 to λ, we have already gone to the NR approximation: the current operators have become

$\mathbf{p}/m$ and the G^N are HF, rather than DF, propagators. Next, we perform the k_0 integration. There are poles in the k_0 plane which arise from $1/k^2$, $G^N_{n+k_0}$, and $G^N_{\omega+k_0}$. Contributions to what we have referred to as the "Breit terms" (and which have been dealt with elsewhere [9]) arise from the k_0 poles of $G^N_{n+k_0}$ and $G^N_{\omega+k_0}$. Accordingly, we need only consider the contribution from the poles in the photon propagator, $1/k^2$. The addition of $X_t(1, \Gamma_c)$ to $X_{tc}(\Pi)$ just leads to the antisymmetrization of the electron states labeled r, u. That is,

$$\left(\begin{matrix} r \\ u \end{matrix}\right| V \left|\begin{matrix} n \\ s \end{matrix}\right) \to -\left(\begin{matrix} u \\ r \end{matrix}\right| V \left|\begin{matrix} n \\ s \end{matrix}\right). \tag{3.14}$$

For the CL terms corresponding to $X_{tc}(\Pi)+X_t(1, \Gamma_c)$, we obtain after k_0 integration, followed by ω integration

$$\langle n|\ \{X_{tc}(\Pi)+X_t(1, \Gamma_c)\}\ |n\rangle_{CL} = -2\beta \left[\begin{matrix} n \\ a \end{matrix}\right| ({}^{\mathbf{p}\cdot}_{\mathbf{p}}V - {}^{\mathbf{p}\cdot}V_{\mathbf{p}}) \left|\begin{matrix} n \\ a \end{matrix}\right]. \tag{3.15}$$

The evaluation of this type of term is concluded by the consideration of the complex conjugate of (3.15), which is

$$\begin{aligned} \langle n|\ \{X_{tc}(\Pi)+X_t(1, \Gamma_c)\}\ |n\rangle^*{}_{CL} &= \langle n|\ \{X_{ct}(\Pi)+X_t(\Gamma_c, 1)\}\ |n\rangle \\ &= -2\beta v \left[\begin{matrix} n \\ a \end{matrix}\right| (V^{\mathbf{p}\cdot}_{\mathbf{p}} - {}_{\mathbf{p}\cdot}V^{\mathbf{p}}) \left|\begin{matrix} n \\ a \end{matrix}\right]. \end{aligned} \tag{3.16}$$

We have used the identity

$$\left(\begin{matrix} a \\ n \end{matrix}\right| {}^{\mathbf{p}\cdot}V^{\mathbf{p}} \left|\begin{matrix} n \\ a \end{matrix}\right) = \left(\begin{matrix} n \\ a \end{matrix}\right| {}_{\mathbf{p}\cdot}V_{\mathbf{p}} \left|\begin{matrix} a \\ n \end{matrix}\right), \tag{3.17}$$

which is a generalization of Eq. (2.10), to obtain the final form of Eq. (3.16). Note again that the second term in both Eq. (3.15) and Eq. (3.16), when taken between states $\left(\begin{smallmatrix} n \\ a \end{smallmatrix}\right|$ and $\left|\begin{smallmatrix} a \\ n \end{smallmatrix}\right)$, is a "self-energy," rather than an "exchange," term.

Finally, we turn to the evaluation of the expressions corresponding to the last two diagrams of Fig. 8b. It is important to note that the mass counterterm, δm_t, is included in the insertion of L_0. The evaluation procedures are similar to those which have been carried out for the previous terms. We make the same approximations as before and obtain, after k_0 integration and spherical averaging,

$$\langle n|\ \{T_c(X_t)+X_c(X_t)\}\ |n\rangle_{LL} = \frac{2\alpha}{3\pi m^2} \sum_{s,u} \left[\begin{matrix} n \\ s \end{matrix}\right| V \left|\begin{matrix} n \\ u \end{matrix}\right] \int \frac{d\omega}{2\pi i} \mathcal{Q}_{us}(\omega), \tag{3.18}$$

where

$$\mathcal{Q}_{us}(\omega) = \langle u|\ G^N_\omega \mathbf{p} \cdot \int_0^\lambda dk(\omega - H)\, G^N_{\omega-k}\, \mathbf{p} G^N_\omega\ |s\rangle. \tag{3.19}$$

The log term arises from the integral of the operator $D(\omega)$, where

$$D(\omega)=\int_0^\lambda dk G^N_{\omega-k}. \tag{3.20}$$

We note the identity [1, Eq. (39)]

$$-2\mathbf{p}\cdot(\omega-H)\,D\mathbf{p}=[\mathbf{p}\cdot,H)\,D\mathbf{p}-\mathbf{p}\cdot D[\mathbf{p},H]-(\omega-H)\mathbf{p}\cdot D\mathbf{p}-\mathbf{p}\cdot D\mathbf{p}(\omega-H). \tag{3.21}$$

Next, we carry out the ω integration, keeping in mind the fact that the G^N_ω are HF propagators, with poles corresponding to holes in the upper half, and to particles in the lower half ω plane. Replacing the energy-dependent logarithms by constants, we finally obtain for the CL terms contributed by the last two diagrams of Fig. 8b,

$$\langle n|\,\{T_c(X_t)+X_c(X_t)\}\,|n\rangle_{\mathrm{CL}}=\langle n|\,\{\cdots\}\,|n\rangle^{\mathrm{nuc}}_{\mathrm{CL}}+\langle n|\,\{\cdots\}\,|n\rangle^{\mathrm{ee}}_{\mathrm{CL}}, \tag{3.22}$$

where

$$\begin{aligned}&\langle n|\,\{T_c(X_t)+X_c(X_t)\}\,|n\rangle^{\mathrm{nuc}}_{\mathrm{CL}}\\&\quad=\beta\sum_{a=1}^{N}\sum_{j=N+1}^{\infty}\left\{\frac{\langle a|\,\nabla^2 V_{\mathrm{nuc}}\,|j\rangle}{j-a}\left[\begin{matrix}n\\j\end{matrix}\right|V\left|\begin{matrix}n\\a\end{matrix}\right]+\text{c.c.}\right\},\end{aligned} \tag{3.23}$$

and

$$\langle n|\,\{T_c(X_t)+X_c(X_t)\}\,|n\rangle^{ee}_{\mathrm{CL}}=-\beta\left\{\left[\begin{matrix}n\\a\end{matrix}\right|({}_{\mathbf{p}^2}V+V_{\mathbf{p}^2}-2\,{}_{\mathbf{p}\cdot}V_{\mathbf{p}})\left|\begin{matrix}n\\a\end{matrix}\right]\right\}, \tag{3.24}$$

and where we neglected $1/Z^2$ corrections, i.e., terms in which two V_{ee} appear.

We are now ready to collect the various terms we have calculated. We refer to the terms appearing in Eq. (3.7) in which V_{nuc} is not explicitly present, (3.24) and the sum of the terms in Eqs. (3.15), (3.16) as contact terms, since making use of the identities

$$\nabla_x^2\frac{1}{|\mathbf{x}-\mathbf{y}|}=\nabla_y^2\frac{1}{|\mathbf{x}-\mathbf{y}|}=-\nabla_x\cdot\nabla_y\frac{1}{|\mathbf{x}-\mathbf{y}|}=-4\pi\,\delta^3(\mathbf{x}-\mathbf{y}) \tag{3.25}$$

leads to

$$\begin{aligned}{}^{-\nabla^2}V&={}^{\mathbf{p}^2}V+V^{\mathbf{p}^2}-2^{\mathbf{p}\cdot}V^{\mathbf{p}}={}_{\mathbf{p}^2}V+V_{\mathbf{p}^2}-2\,{}_{\mathbf{p}\cdot}V_{\mathbf{p}}\\&=-\{{}^{\mathbf{p}\cdot}_{\mathbf{p}}V+V^{\mathbf{p}\cdot}_{\mathbf{p}}-{}_{\mathbf{p}\cdot}V^{\mathbf{p}}-{}^{\mathbf{p}\cdot}V_{\mathbf{p}}\},\end{aligned} \tag{3.26}$$

and thus, e.g., yields

$$\begin{aligned}\left(\begin{matrix}r\\ s\end{matrix}\right|\,(V^{\mathbf{p}^2}+{}^{\mathbf{p}^2}V-2^{\mathbf{p}\cdot}V^{\mathbf{p}})\,\left|\begin{matrix}t\\ u\end{matrix}\right)&\\ &=\int d^3\mathbf{x}\,d^3\mathbf{y}\langle r\,|\,\mathbf{x}\rangle\langle s\,|\,\mathbf{y}\rangle\,4\pi\alpha\,\delta^3(\mathbf{x}-\mathbf{y})\langle\mathbf{x}\,|\,t\rangle\langle\mathbf{y}\,|\,u\rangle\\ &=4\pi\alpha\int d^3\mathbf{x}\langle r\,|\,\mathbf{x}\rangle\langle s\,|\,\mathbf{x}\rangle\langle\mathbf{x}\,|\,t\rangle\langle\mathbf{x}\,|\,u\rangle.\end{aligned}\tag{3.27}$$

The total coefficient of these contact terms is zero. We found the same result in our analysis of perturbation theory based on hydrogenic states [1]. A similar result occurs for He, as discussed by Kabir and Salpeter [10]. They also find that the constant log contribution to the Lamb shift for low frequency photons ($0<|\mathbf{k}|<\lambda$) contains no contact term, i.e., no term proportional to $\delta^3(\mathbf{r}_{12})$ in their notation.

The only surviving terms are those which explicitly contain V_{nuc} (Eq. (3.23) and part of Eq. (3.7)). These are an expansion through first order in the e–e Coulomb interaction of the integral equation conjectured in Ref. [1] for the CL terms in the HF case,[5] i.e.,

$$\langle n|\,L_{\mathrm{CL}}\,|n\rangle=\langle n|\,l\,|n\rangle+\int\frac{d\omega}{2\pi i}\sum_{u,s}\left[\begin{matrix}n\\ u\end{matrix}\right|V\left|\begin{matrix}n\\ s\end{matrix}\right]\langle s|\,G_\omega L_{\mathrm{CL}}G_\omega\,|u\rangle.\tag{3.28}$$

If we use Eq. (3.8) for a point nucleus, we obtain

$$\langle n|\,l\,|n\rangle_{\text{point}}=\frac{4}{3}\frac{Z\alpha^2}{m^2}\ln{(\tilde{Z}\alpha)^{-2}}\,|\langle n\,|\,\mathbf{0}\rangle|^2,\tag{3.29}$$

where $\langle n\,|\,\mathbf{0}\rangle$ is the HF wave function at the origin of coordinates.

4. PRELIMINARY NUMERICAL RESULTS

We are now ready to make a preliminary numerical test of the results of our preceding sections. We will focus on the particular case of the Lamb shift contribution to the $2p_{1/2}$–$2s_{1/2}$ energy difference for atoms with a small to moderate number of protons and three electrons (the Li isoelectronic sequence). Specifically, we will take $3\leqslant Z\leqslant 20$. These $2p_{1/2}$–$2s_{1/2}$ energy differences are among those treated in Ref. [9] and thus can provide us with a test of our results. Second and third order correlation corrections, as well as contributions of the Breit interaction through second order correlation corrections to it, and the lowest order effect of transverse photon retardation were calculated in this reference. The difference between experiment and the DF energies plus all these corrections to them serves as an "experimental" measure of the Lamb shift to be expected. It can therefore provide a convenient test of our formalism for the case of these three-electron atoms.

---

[5] See Ref. [1, Eq. (65)]. We shall rewrite this equation more compactly below in the HF basis, rather than in the coordinate basis, in which it is written in Ref. [1].

In this preliminary analysis, we will focus initially on the CL contributions obtained in the previous section. Further, we will take the nucleus to be point-like, and so the $2p_{1/2}$ CL contribution to the $2p_{1/2}$–$2s_{1/2}$ Lamb shift will vanish. In essence, we will be testing the effect of replacing the absolute square of the hydrogenic wave function at the origin by that of the HF wave function. This is a specific consequence of our discussion in the previous section and implies that the coefficient $\alpha^5 Z^4$ for the hydrogenic Lamb shift is to be replaced by $\alpha^5 Z(Z_{n,\mathrm{eff}})^3$, where $Z_{n,\mathrm{eff}}$ is defined by

$$|\langle n|\mathbf{0}\rangle|^2 \equiv |\psi_{ns}^{\mathrm{HF}}(\mathbf{0})|^2 \equiv \frac{(\alpha Z_{n,\mathrm{eff}})^3}{\pi n^3}. \tag{4.1}$$

This dependence of the Lamb shift on Z and $Z_{n,\mathrm{eff}}$ is to be contrasted with a number of other ways of taking electron screening into account. For example, in Ref. [4], a different shielded nuclear charge, $Z'_{n,\mathrm{eff}}$, is defined by setting the ratio $Z'_{n,\mathrm{eff}}/Z$ equal to the ratio of the expectation value of the radius of the (n, κ) orbital of a hydrogen-like atom of nuclear charge $-eZ$ to that of the corresponding DF atom. Moreover, the prescription for taking screening into account is to replace the coefficient, $\alpha(\alpha Z)^4$, of the Lamb shift by $\alpha(\alpha Z'_{n,\mathrm{eff}})^4$, but to leave the argument Z in Mohr's point-Coulomb self-energy function [14], $F(Z\alpha)$, the same, i.e., to choose it to be that for the unshielded nucleus [4, Eq. (5)].

We would like even our preliminary numerical results to be accurate to within a few percent. With this in mind, we must calculate or estimate the contributions not determined in Section 3. The terms which may contribute are those coming from the high-frequency part of the $|\mathbf{k}|$ integral containing V_{nuc} and V_{ee}. There is also the contribution from the exchange of two transverse photons. Further, there are those terms which arise from higher powers of $Z\alpha$ in the $Z\alpha$ expansion, in particular those proportional to $\alpha(Z\alpha)^5$.

The large $|\mathbf{k}|$ contribution proportional to V_{nuc} can be incorporated easily, since, following the technique of Ref. [3], it will come from a perturbation expansion (in powers of $V_{\mathrm{nuc}} + V_{\mathrm{ee}}$) of the expression corresponding to the diagram of Fig. 8a, for L_0. One simply takes the result for H and replaces the hydrogenic wave function at the origin by the HF wave function at the origin. This procedure includes all the non-log terms (including the Uehling term) which involve V_{nuc}, as well as a reasonable approximation to the BL term associated with V_{nuc}.

The most sensitive dependence on the nuclear charge, Z, in the leading order Lamb shift appears in the second term on the right side of Eq. (3.6), $\ln[1/(\tilde{Z}\alpha)^2]$. $\tilde{Z}$ is a function of Z. We shall determine this dependence in subsequent work, when we explicitly evaluate all the BL terms which our analysis has generated. However, in this preliminary numerical evaluation, we will take

$$\tilde{Z} = Z_{n,\mathrm{eff}}, \tag{4.2}$$

where $Z_{n,\mathrm{eff}}$ was defined in Eq. (4.1). Since the dependence on $\tilde{Z}$ is only logarithmic, the numerical results are not very sensitive to the exact choice of $\tilde{Z}$.

The large $|\mathbf{k}|$ contributions proportional to V_{ee} (some of which also contain a $\ln \alpha$) and the two-transverse-photon exchange terms will be contact terms. That is, they will depend on $\int d^3\mathbf{x} |\langle n|\mathbf{x}\rangle\langle a|\mathbf{x}\rangle|^2$. We can estimate their magnitude by making use of the He results of Ref. [10]. We see from Section V of this reference that the ratio of the contact term to the square of the wave function at the origin is typically about 1/16. Further, the V_{nuc} part contains an extra factor of Z relative to the V_{ee} part. Thus, we estimate our error in neglecting these V_{ee} terms in the Lamb shift (and also those coming from the second term in Eq. (3.28)) to be less than 10% of the leading Lamb shift term.

By making use of the results of Erickson and Yennie [17], we may obtain the next term in the expansion in $Z\alpha$, i.e., the term containing the coefficient C_5. For hydrogen (except for the Uehling contribution), this coefficient is again multiplied by the square of the wave function at the origin. The Uehling contribution (which, as we will demonstrate in subsequent work, leads to an effective potential yielding the radial derivative of the square of the wave function, evaluated at the origin), is negligible, relative to the main C_5 contribution. However, the coefficient C_5 is large, approximately 7, and constitutes the main correction to the leading Lamb shift term for Z up to 20. Accordingly, we state the approximate result for the energy shift ΔE_{ns} for the ns state to be

$$\Delta E_{ns} = \alpha^2 Z\, L(Z, \tilde{Z}_n)\, |\langle n|\mathbf{0}\rangle|^2, \tag{4.3}$$

with

$$L(Z, \tilde{Z}_n) \approx \frac{4}{3}\left\{\ln\frac{1}{(\tilde{Z}_n\alpha)^2} + \ln\frac{(\tilde{Z}_n\alpha)^2 m}{2\Delta e_n} + \frac{19}{30} + (Z\alpha) C_5\right\}, \tag{4.4}$$

where [10, 11, 18, 19]

$$C_5 \approx 6.97, \qquad \Delta e_n \equiv k_0(n, 0), \tag{4.5}$$

and

$$\tfrac{19}{30} = \tfrac{11}{24} + \tfrac{3}{8} - \tfrac{1}{5}, \tag{4. 6}$$

so that the leading Uehling term is included in (4.4). For hydrogen, $L(Z, \tilde{Z}_n) \to L(Z, Z)$, and $L(Z, Z) \cong F(Z\alpha)$, where $F(Z\alpha)$ is defined[6] in Table II of Ref. [18].

We continue to ignore the contribution of the $2p_{1/2}$ state to the Lamb shift in the course of these further approximations, since the BL term, the only contribution through this order for p states, is negligible. Thus, ΔE_{ns} is, in fact, approximately equal to the negative of the $2p_{1/2}$–$2s_{1/2}$ Lamb shift.

---

[6] In contrast, $F(Z\alpha)$ of Ref. [18, Eq. (4)] includes only self energy terms, and thus specifically excludes Uehling terms, as does Mohr's [14] $F(Z\alpha)$. We emphasize that we use the $F(Z\alpha)$ of [18, Table II] and not the other definitions of $F(Z\alpha)$, to make our comparisons.

Our numerical results are summarized in Tables I and II for the $2p_{1/2}$–$2s_{1/2}$ Lamb shift. The effective shielded nuclear charge number, $\tilde{Z}_2 \equiv Z_{2,\text{eff}}$, in the third column of Table I is calculated from the data in the second column, using Eq. (4.1). The ratio $L(Z, \tilde{Z}_2)/F(Z\alpha)$ in column four of Table I is presented to indicate how the new approximate $F(Z\alpha)$, i.e., $L(Z, \tilde{Z}_2)$, differs from the hydrogenic form, as calculated by Mohr [14]. The "experimental" Lamb shift in column five (in reality, the negative of this shift, as conventionally defined) is actually a difference of the sum of all the theoretical contributions [9][7] other than the Lamb shift, and the experimental results [20]. Column six is from Refs. [9, Table IV, column five; 18]. The final column of Table I gives our new results.

Table II provides a quick overview of our initial numerical results, in comparison with related results. The range of Z is now restricted to $7 \leqslant Z \leqslant 20$, since correlation effects are not calculated to sufficient accuracy [21] for $3 \leqslant Z \leqslant 6$ for one to be able to derive an accurate "experimental" Lamb shift value for comparison purposes. (Hence, these entries are left blank for $3 \leqslant Z \leqslant 6$ in column five of Table I.)

The second column of Table II, gives the percentage "experimental" error, calculated by taking the ratio of the quoted experimental error to the "experimental" value of the Lamb shift. Columns three and five give the differences between "experiment" and the particular model for the theory (hydrogenic or DF), divided by "experiment." Column four, labeled "empirical," gives the percentage deviation for a theoretical model [4, Eq. (5) and immediately above] where Z^4, appearing in

TABLE I

DF Lamb Shift ($2p_{1/2} - 2s_{1/2}$) for the Li Isoelectronic Sequence (Energies in AU × 10^3)

				$-E$ (Lamb)		
Z	$\left\lvert\dfrac{\psi_{2s}^{\text{HF}}(\mathbf{0})}{\psi_{2s}^{\text{hydr}}(\mathbf{0})}\right\rvert$	$\tilde{Z}_2$	$\dfrac{L(Z, \tilde{Z}_2)}{F(Z\alpha)}$	"Expt"[a]	hydr	DF
3	0.390	1.60	1.22		0.010	0.002
4	0.558	2.71	1.16		0.027	0.010
5	0.652	3.76	1.13		0.062	0.029
6	0.713	4.79	1.11		0.119	0.066
7	0.755	5.81	1.10	0.14(1)	0.207	0.127
8	0.787	6.82	1.10	0.22(1)	0.334	0.221
9	0.811	7.83	1.09	0.36(2)	0.508	0.356
10	0.830	8.84	1.09	0.52(1)	0.739	0.542
11	0.846	9.84	1.09	0.76(2)	1.04	0.788
13	0.870	11.85	1.10	1.42(2)	1.86	1.51
15	0.887	13.85	1.10	2.52(6)	3.06	2.59
17	0.901	15.85	1.11	3.89(6)	4.73	4.16
20	0.915	18.86	1.14	7.06(4)	8.31	7.69

[a] "Expt" = DF + correlation + transverse γ's − Experiment.

---

[7] This column is from [9, Table IV, column four].

TABLE II

$2p_{1/2}-2s_{1/2}$ Lamb Shift Experimental Errors and Deviation between Theory and Experiment (in Percent)

Z	"Expt"[a]	hydr	emp.[b]	DF
7	(7.1)	+48	−30	−9.2
8	(4.6)	+52	−20	+0.5
9	(5.6)	+41	−19	−1.0
10	(1.9)	+42	−14	+4.2
11	(2.6)	+36	−13	+3.6
13	(1.4)	+31	−9.5	+6.0
15	(2.4)	+21	−11.7	+2.7
17	(1.5)	+22	−8.0	+6.9
20	(0.6)	+18	−7.0	+9.0

[a] For definition of "Expt," see Table I.

[b] emp. = empirical; $E_{\text{emp}}(\text{Lamb}) \sim \tilde{Z}_2^4 F(Z\alpha)$.

the Lamb shift formula, is replaced by $\tilde{Z}_2^4$, as given in column three of Table I. Observe that, even for this preliminary computation, our DF results appear to fit the "experimental" Lamb shift results to within a few percent, as hoped. Indeed, the scatter of error values in the lower Z range which we consider in Table II is probably due to the experimental uncertainties. In the higher Z range, use of $L(Z, \tilde{Z}_2)$ is no longer fully satisfactory. An analogy with the case of hydrogen serves to clarify this point. In that case, the leading Lamb shift can be calculated to all orders [14] in $Z\alpha$, using the exact Coulomb propagator. The approximation corresponding to $L(Z, \tilde{Z}_2)$ in the case of H is to replace $F(Z\alpha)$ by $L(Z, Z)$ for the $2s$ state. At $Z=3$, the deviation of $L(Z, Z)$ from $F(Z\alpha)$ is only 0.03%, while it rises to 8.8% at $Z=20$. This fact provides a motivation for extending the DF analysis to the $(Z\alpha)^2$ corrections to the leading Lamb shift terms.

We note that the hydrogenic Lamb shift overestimates the experimental Lamb shift by tens of percents, while the "empirical" Lamb shift consistently underestimates it.

5. SUMMARY AND DISCUSSION

In this paper, we have continued our consideration of atomic energy levels of many-electron atoms, using the Green's function approach. Our present focus is on radiative corrections in the Dirac–Fock (DF) approximation. The relativistic (R) approach we discussed in Ref. [7], and applied to radiative corrections in perturbation theory in the electron–electron Coulomb interaction, V_{ee}, in Ref. [1], has now been considered in the DF case for many-electron atoms, consisting of a non-degenerate core of electrons, plus or minus one electron (as exemplified by alkali atoms). We have dealt only with leading order radiative corrections in α, the fine structure constant, i.e., corrections which involved only one virtual transverse photon. We derived an integral equation satisfied by these radiative corrections in Section 2. It was obtained by formally expanding the propagator generated by the Coulomb kernel, V_{ee}, to all orders in V_{ee}, inserting the transverse photon in all possible ways, and then resumming the resulting expression. This procedure guarantees that the integral equation so generated is gauge invariant (GI).

The integral equation of Section 2 is too difficult to deal with in its entirety. However, it does provide the framework for systematically considering approximations to it and for estimating the numerical significance of various terms.

Since our starting point for the generation of the integral equation for radiative corrections in the DF approximation was the equation for the one-electron DF Green's function, we necessarily must have radiative correction energy contributions which are small relative to the DF energies. We can, therefore, also develop a perturbation theory for the energy, with the DF energies as the zeroth order approximation. We thus consider the expansion of the integral equation of Section 3 in powers of those matrix elements of V_{ee} not present in the determination of the DF states and energies. This expansion is developed in the same sense as is that for correlation effects and can be treated perturbatively, starting with the DF energies and states. Once we carry out such an expansion in V_{ee}, we lose GI in any given finite order in V_{ee}. However, for a given order in V_{ee}, the violation of GI is of higher order in α.

At this point in our approximation, we included effects of the exchange of transverse photons (Breit interactions and retardation corrections to them) with our radiative corrections. These have to be separated from Lamb shift type terms, on which we would like to focus our interest further.

It is convenient to consider the remaining Lamb shift terms (which include both self-energy and vacuum polarization effects) by separating the integration over the virtual transverse photon wave vector into a low and a high energy part [3, 10, 16]. The low energy part can be treated non-relativistically [2].

We also restrict ourselves to the leading log contributions to the Lamb shift from the low virtual photon energy part. While the dominant part of the Lamb shift is due to these leading log contributions, and the dominant part of the leading log terms is contributed in this non-relativistic (NR) region, it is important to note that leading log terms also arise from the R region of high virtual momentum photons [10, 16]. We will leave the evaluation of the high energy log and non-log contributions (for which even G_{DF} can be expanded in powers of $V_{nuc} + V_{ee}$) to subsequent work. The usual cancellation of the parameter separating the low from the high virtual photon momenta (well known in the cases of the hydrogen [2, 3] and the helium [10] Lamb shift) will also be demonstrated in this later work, as well as the contribution due to the exchange of two transverse photons. We estimate the total effect of all of these terms to be less than 10% of the leading terms.

By following the approach of Refs. [2, 3], we have limited ourselves to the consideration of moderate nuclear charge, Z, as far as a rigorous analysis goes. A significantly new departure in the analysis, which could not be based on these references, is required to extend it to higher Z. At this time we do not as yet possess the analogs of the Coulomb propagator [14] for G_{DF} to be able to accomplish this extension. We do, however, carry out an expansion in $1/Z$ and consider terms through order $1/Z$.

We next divided the logarithmic parts of the non-relativistic Lamb shift, in analogy with the hydrogenic case, into a constant (i.e., energy independent) and a Bethe (energy dependent) log part. We did this by introducing a parameter, $\tilde{Z}$, so that the dependence of the Bethe log part on $\tilde{Z}$ is minimized. (For the hydrogenic case, $\tilde{Z} \rightarrow Z$, the number of protons in the nucleus, and the Bethe log (BL) term is strictly independent [11] of Z.) The BL terms are dealt with analytically in Appendix A. The constant log (CL) terms in the NR part of the Lamb shift were treated in the second part of Section 3. An interesting analytic result of the present paper is that explicit dependence on V_{ee} disappears for these terms. Only implicit dependence remains, through the term $\langle n|\, \nabla^2 V_{\mathrm{nuc}}\, |n\rangle$, where the bra and ket denote HF states. Indeed, for the case of a point nucleus, this term becomes $4\pi\alpha Z\, |\langle n|\mathbf{0}\rangle|^2$, where $-Ze$ is the bare nuclear charge, and where the electron shielding appears only through the presence of the HF wave function at the origin of coordinates. It must be pointed out, however, that this cancellation of CL terms involving V_{ee} no longer occurs when log terms from the R radiative corrections are taken into account. The parts of these corrections arising from exchanged transverse and Coulomb photons contain a natural cutoff which reintroduces a CL term. Log terms also arise from the exchange of two transverse photons.

We had previously obtained the result in perturbation theory [1] that the V_{ee} parts of the CL terms cancel and had conjectured it for the DF case, and we have now confirmed it. We have also confirmed the previously conjectured integral equation [1] for the CL contribution to the Lamb shift. This integral equation provides non-local contributions to the leading local term in the CL NR Lamb shift, in analogy with similar non-local contributions to the photon vertex term, needed to describe radiative transitions in a GI manner [5, 6] in the DF approximation. Just as for the latter case, these contributions are expected to be small for compact cores [22] (closed shell cores, such as those for Li and Na), but they could be significant for more diffuse cores [23] (for example, for the $(1s)^2\,(2s)^2$ closed subshell core of B).

We wish to gain a preliminary indication of the numerical usefulness of our present approach by a semi-empirical application of our results of Section 3. To this end, we note that the numerical evaluation of the energy-dependent log terms which are given in Appendix A would lead to a determination of $\tilde{Z}_n$. However, the dependence of the dominant leading Lamb shift contribution on $\tilde{Z}_n$ (indeed, of the entire numerically unevaluated energy dependence of the leading order Lamb shift) is only logarithmic. In order to proceed with specific numerical work, we therefore took $\tilde{Z}_n \equiv Z_{n,\mathrm{eff}}$, where the effective charge is determined from the DF wave function at the origin of coordinates (see Eq. (4.1)). Using the results of Ref. [17], we were able to evaluate the next term in the $Z\alpha$ expansion. This term is proportional to $\alpha(Z\alpha)^2\, |\psi_{ns}^{\mathrm{HF}}(\mathbf{0})|^2$. The proportionality constant [17] is approximately that which is the coefficient of the corresponding expression for hydrogen. We could follow Ref. [17] further and extend the results to even higher powers of $Z\alpha$, but we will leave this, as well as a detailed presentation of the $\alpha(Z\alpha)^2\,|\psi_{ns}^{\mathrm{HF}}(\mathbf{0})|^2$ coefficient, to a later publication.

We carried out a preliminary numerical test of our predictions for the Li isoelectronic sequence. Accurate experimental data exist for these cases [20]. The theoretical contributions due to the DF energies and the added contributions of correlation, the Breit interaction and retarded photon effects have also been recently calculated [9] to sufficient accuracy for a test of our DF Lamb shift predictions to be feasible. We carried out this test in Section 4 for the Lamb shift contribution to the $2s_{1/2}$–$2p_{1/2}$ energy difference for the Li isoelectronic sequence in the proton number range $3 \leqslant Z \leqslant 20$. In the part of this range ($7 \leqslant Z \leqslant 20$) in which the correlation calculations have been evaluated with sufficient accuracy to provide a useful test [21], we find satisfactory values for the Lamb shift. They are superior to the Lamb shift contribution for these cases obtained by using an unshielded nucleus [18], or the predictions made by a typical empirical method [4] for taking shielding into account. We were encouraged by these results to pursue our analytical work further. We also intend, in the future, to carry out detailed and more precise numerical computations of our numerous analytical terms and to present both these computational—as well as our analytic—results in a future publication.

APPENDIX A. EVALUATION OF BETHE-LOG TERMS

In this appendix, we evaluate all of the energy-dependent log terms, i.e., those which contain expressions of the form of the first expression on the right side of Eq. (3.6). We collectively call these BL. Actually, it is only the term of this type associated with $(X_{\mathrm{t}} - \delta m_{\mathrm{t}})$ which is completely analogous to the usual BL. It is given by

$$\langle n|\,(X_{\mathrm{t}} - \delta m_{t})\,|n\rangle_{\mathrm{BL}} = \frac{-\alpha}{3\pi m^2}\,\langle n|\,\{[H, \mathbf{p}]\,\mathscr{L}_B(n)\cdot\mathbf{p} + \mathrm{c.c.}\}\,|n\rangle. \tag{A.1}$$

Equation (A.1) is exactly of the form of the usual BL term [11, 15]. The only generalization in the present case is that the states and energies in the sums implied in Eq. (A.1) are given in the HF approximation, and that we take $Z \to \tilde{Z}_n$. This equation may well provide the largest numerical contribution of all the BLs appearing in this appendix, since the others go as $N_{n,\mathrm{eff}}/Z$. ($N_{n,\mathrm{eff}}$ is the effective number of shielding electrons and is obtained, e.g., from $\tilde{Z}_2$ in Table I, by use of the relation $N_{2,\mathrm{eff}} = Z - \tilde{Z}_2$. It is a number of the order one in the case of the Li isoelectronic sequence.) The magnitude of the other BL contributions may be reduced further due to lack of overlap of the states in the evaluation of expectation values of V_{ee} which appears in all of these remaining terms.

Results, corresponding to those we list here, are also given by us for many-electron atoms in hydrogenic perturbation theory in Ref. [1, (A.5)]. Here, we provide expressions that are more specific than those in Ref. [1]. Our main concern in Ref. [1] is with the structure of the theory. Our current concern is to provide expressions which are directly amenable to numerical evaluation. We also wish to present the results here in such a way that their relationship to the corresponding CL case will be apparent. The notation of having operators at two levels, an upper and a lower one, is redundant in the present context, except to show this correspondence, since matrix elements of these operators are now always taken before they act on V, or V acts on them.

The remining BL contributions are given by the following equations (the sum and/or integral over all indices, with the exception of the index n, is implied in all the equations below):

$$\begin{aligned}
&\langle n|\,\{X_{\mathrm{tc}}(\Pi)+X_{\mathrm{t}}(1,\Gamma_{\mathrm{c}})\}\,|n\rangle_{\mathrm{BL}}+\mathrm{c.c.}\\
&\quad=\frac{2\alpha}{3\pi m^2}\left(\frac{1}{n+a-t-j}\left\{{}^{\langle n|[\mathbf{p},H]\,\mathscr{L}_B(n)|t\rangle}_{\cdot\langle a|\mathbf{p}|j\rangle}\left[\begin{array}{c|c|c} t & & n\\ & V & \\ j & & a\end{array}\right]\right.\right.\\
&\quad\quad\left.+\,{}^{\langle n|\mathbf{p}|t\rangle}_{\cdot\langle a|[\mathbf{p},H]\,\mathscr{L}_B(a)|j\rangle}\left[\begin{array}{c|c|c} t & & n\\ & V & \\ j & & a\end{array}\right]\right\}+\frac{1}{t+a-n-j}\\
&\quad\quad\times\left\{{}^{\langle n|[\mathbf{p},H]\,\mathscr{L}_B(n)|t\rangle}\left[\begin{array}{c|c|c} t & & n\\ & V & \\ a & & j\end{array}\right]_{\cdot\langle j|\mathbf{p}|a\rangle}\right.\\
&\quad\quad\left.\left.+\,{}^{\langle n|\mathbf{p}|t\rangle}\left[\begin{array}{c|c|c} t & & n\\ & V & \\ a & & j\end{array}\right]_{\cdot\langle j|[\mathbf{p},H]\,\mathscr{L}_B(j)|a\rangle}\right\}+\mathrm{c.c.}\right),
\end{aligned}\tag{A.2}$$

$$\begin{aligned}
&\langle n|\,\{T_{\mathrm{c}}(X_{\mathrm{t}})+X_{\mathrm{c}}(X_{\mathrm{t}})\}\,|n\rangle^{\mathrm{nuc}}_{\mathrm{BL}}\\
&\quad=\frac{\alpha}{3\pi m^2}\left(\left\{\left[\ln\frac{m(\alpha\tilde{Z})^2}{2\,|j-a|}\langle a|\,\mathbf{p}\cdot Q_j\mathbf{p}\,|l\rangle\frac{i+a-2j}{i-a}\right.\right.\right.\\
&\quad\quad\left.\left.+\ln\frac{m(\tilde{Z}\alpha)^2}{2\,|b-j|}\langle a|\,\mathbf{p}\cdot P_b\mathbf{p}\,|j\rangle\frac{j+a-2b}{j-a}\right]\left[\begin{array}{c|c|c} n & & n\\ & V & \\ j & & a\end{array}\right]+\mathrm{c.c.}\right\}\\
&\quad\quad+\ln\left|\frac{j-c}{j-a}\right|\langle a|\,\mathbf{p}\cdot Q_j\mathbf{p}\,|c\rangle\frac{a+c-2j}{c-a}\left[\begin{array}{c|c|c} n & & n\\ & V & \\ c & & a\end{array}\right]\\
&\quad\quad\left.-\ln\left|\frac{b-j}{b-i}\right|\langle i|\,\mathbf{p}\cdot P_b\mathbf{p}\,|j\rangle\frac{i+j-2b}{j-i}\left[\begin{array}{c|c|c} n & & n\\ & V & \\ j & & i\end{array}\right]\right),
\end{aligned}\tag{A.3}$$

and

$$\langle n|\,T_{\mathrm{c}}(X_{\mathrm{t}})\,|n\rangle^{\mathrm{ee}}_{\mathrm{BL}}=\frac{\alpha}{3\pi m^2}\left(\begin{array}{c|}n\\a\end{array}\;\{[{}_{\mathbf{p}\cdot\mathscr{L}_B(a)},V]_{\mathbf{p}}-{}_{\mathbf{p}\cdot}[{}_{\mathscr{L}_B(a)\mathbf{p}},V]\}\;\begin{array}{|c}n\\a\end{array}\right),\tag{A.4a}$$

$$\langle n|\,X_{\mathrm{c}}(X_{\mathrm{t}})\,|n\rangle^{\mathrm{ee}}_{\mathrm{BL}}=-\frac{\alpha}{3\pi m^2}\left(\begin{array}{c|}n\\a\end{array}\;\{{}_{\mathbf{p}\cdot\mathscr{L}_B(a)}(V^{\mathbf{p}}-{}_{\mathbf{p}}V)-(V^{\mathbf{p}}-{}_{\mathbf{p}}V)^{\cdot\mathscr{L}_B(a)\mathbf{p}}\}\;\begin{array}{|c}a\\n\end{array}\right).\tag{A.4b}$$

Corrections of order $1/Z^2$, i.e., terms with two V_{ee} in them, have again been neglected.

The sum of Eqs. (A.1)–(A.4) is the total energy contribution of the BL terms. We note the similarity in the structures of Eqs. (A.2) and (3.15) and that in the structures of Eqs. (A.4) and (3.24).

APPENDIX B. RADIATIVE TRANSITIONS AND THE IMAGINARY PART OF THE SELF-ENERGY

The present work provides us with another opportunity to test the consistency of the Green's function formalism. We have been concerned so far with the real contributions to the self-energy. It is well known from elementary quantum field theory [19, pp. 354, 408–410] that the self-energy can also have imaginary parts, leading to a finite natural line width, and a corresponding finite lifetime for the decay of excited states. We will be concerned with this aspect of the Green's function formalism in the present appendix.

Consider a many-electron atom, in which the valence electron makes a radiative transition. We wish to address the question: How does the formalism take into account the fact that the core states are occupied, and thus that these states are not allowed as final states in a radiative transition? Colloquially put, do the electrons "know" that they have to obey Fermi statistics?

The crucial element in the analysis which follows is the existence of a core (i.e., a Fermi level which is set just above the energy of the N particles in the core). In other words, the one-particle Green's function has to be of the form of Eq. (2.7), with the essential feature the difference in the sign in front of $i\eta$ in the particle (Q_j) and hole (P_a) terms. The specific model is not important. It can be any particle or quasi-particle model, hydrogenic, HF, or other.

We can address this problem by considering the zeroth order self-energy and can ignore the mass counterterm. We will be studying the structure of energy denominators (in particular, the possibility of their vanishing). We may write

$$\langle n|\, X_{\text{t}}\, |n\rangle = ie^2 \int \frac{d^4k}{(2\pi)^4} \frac{\delta^{t}_{lm}}{k_0^2 - \mathbf{k}^2 + i\eta} \langle n|\, \mathscr{P}_l \times \left[\sum_j \frac{Q_j}{n-j+k_0+i\eta} + \sum_a \frac{P_a}{n-a+k_0-i\eta} + \sum_{\bar{j}} \frac{\bar{Q}_{\bar{j}}}{n-\bar{j}+k_0-i\eta} \right] \mathscr{P}^{\dagger}_m\, |n\rangle, \tag{B.1}$$

where the operator $\mathscr{P}_m$ is given by

$$\mathscr{P}_m = e^{-i\mathbf{k}\cdot\mathbf{X}} \boldsymbol{\alpha}_m, \tag{B.2}$$

where $\mathbf{X}$ is the position operator, and the $\boldsymbol{\alpha}_m$ are the Dirac $\boldsymbol{\alpha}$'s.

The k_0 integration is performed easily, by suitably closing the contour in the k_0 plane for each term, resulting in

$$\langle n|\, X_t \,|n\rangle = e^2 \int \frac{d^3\mathbf{k}}{(2\pi)^3} \frac{\delta^t_{lm}}{2\,|\mathbf{k}|} \langle n|\, \mathscr{P}_l \left\{ \sum_j \frac{Q_j}{n-j-|\mathbf{k}|+i\eta} + \sum_a \frac{P_a}{n-a+|\mathbf{k}|-i\eta} + \sum_j \frac{\bar{Q}_j}{n-\bar{j}+|\mathbf{k}|-i\eta} \right\} \mathscr{P}^\dagger_m \,|n\rangle. \tag{B.3}$$

A real decay process can occur whenever any of the denominators in (B.3) vanishes, since

$$\frac{1}{x \pm i\eta} = \text{P.V.}\,\frac{1}{x} \mp i\pi\,\delta(x), \tag{B.4}$$

For n one of the particle (valence or hole) states, the denominators in the antiparticle term never vanish since the energy $e_{\bar{j}}$ $(\bar{j})$ is a negative quantity. For the other two sets of denominators, consider first, as an example, transitions in Li where the core (label a) is $(1s)^2$. There can be no real valence–core transition, since for all valence states, n, $n-a+|\mathbf{k}|$ cannot vanish. Of course, real valence–valence transitions can occur, since, e.g., for n the $3s$ and j the $2p$ state, $n-j-|\mathbf{k}|$ can vanish. The translation operators in $\mathscr{P}_l$, $\mathscr{P}^\dagger_m$ ensure that both energy and momentum must be conserved in a real process.

Let us contrast these results for a many-electron atom with the corresponding result for H. Aside from the obvious change of the states and energies from HF to hydrogenic, the crucial change is in the sign of the imaginary part in the denominator associated with P_a. This change, after k_0 integration, causes the sign in front of $|\mathbf{k}|$ to change. That is, as we go from, e.g., Li to H, we have

$$\frac{1}{n-a+|\mathbf{k}|-i\eta} \rightarrow \frac{1}{n-a-|\mathbf{k}|-i\eta}. \tag{B.5}$$

In this case, the $2p \rightarrow 1s$ transition is a real process, since $n-a-|\mathbf{k}|$ can vanish.

We thus conclude that the imaginary parts of the self-energy contributions behave as we want them to, and that the Green's function formalism has met this additional test.

ACKNOWLEDGMENT

We thank Dr. S.-S. Liaw for providing us with numerical values of $|\langle 2s|\mathbf{0}\rangle^{\text{HF}}/\langle 2s|\mathbf{0}\rangle^{\text{hydr}}|$, needed for our preliminary evaluation of the DF Lamb shift shown in Table I.

REFERENCES

1. G. FELDMAN AND T. FULTON, *Ann. Phys.* (*N.Y.*) **184** (1988), 231.
2. H. A. BETHE, *Phys. Rev.* **72** (1947), 339.
3. J. B. FRENCH AND V. F. WEISSKOPF, *Phys. Rev.* **75** (1949), 1240.

4. M. H. Chen, B. Crasemann, M. Aoyagi, K.-N. Huang, and H. Mark, *At. Data Nucl. Data Tables* **26** (1981), 561.
5. G. Feldman and T. Fulton, *Nucl. Phys. A* **362** (1981), 361.
6. G. Feldman and T. Fulton, *Ann. Phys.* (*N.Y.*) **152** (1984), 376.
7. G. Feldman and T. Fulton, *Ann. Phys.* (*N.Y.*) **179** (1987), 20.
8. W. R. Johnson, M. Idrees, and J. Sapirstein, *Phys. Rev. A* **35** (1987), 3218.
9. W. R. Johnson, S. A. Blundell, and J. Sapirstein, *Phys. Rev. A* **37** (1988), 307.
10. P. K. Kabir and E. E. Salpeter, *Phys. Rev.* **108** (1949), 1256.
11. G. W. Erickson and D. R. Yennie, *Ann. Phys.* (*N.Y.*) **35** (1965), 271.
12. G. Feldman and T. Fulton, *Ann. Phys.* (*N.Y.*) **172** (1986), 40.
13. D. L. Heckathorn, *Nucl. Phys. B* **156** (1979), 328.
14. P. J. Mohr, *Ann. Phys.* (*N.Y.*) **88**, No. 26 (1974), 52.
15. H. A. Bethe, L. M. Brown, and J. R. Stehn, *Phys. Rev.* **77** (1950), 370.
16. E. E. Salpeter, *Phys. Rev.* **87** (1952), 328.
17. G. W. Erickson and D. R. Yennie, *Ann. Phys.* (*N.Y.*) **35** (1965), 447.
18. W. R. Johnson and G. Soff, *At. Data Nucl. Data Tables* **33** (1985), 405.
19. J. M. Jauch and F. Rohrlich, "The Theory of Photons and Electrons," 2nd ed., Springer-Verlag, New York, 1976.
20. B. Edlen, *Physica Scripta* **28** (1983), 51; B. Denne and E. Hinnov, *Physica Scripta* **35** (1987), 811.
21. W. R. Johnson, private communication.
22. T. Fulton and W. R. Johnson, *Phys. Rev. A* **34** (1986), 1686.
23. S.-S. Liaw, Ph. D. dissertation, The Johns Hopkins University, 1988, unpublished.

ANNALS OF PHYSICS **201**, 221–222 (1990)

Abstracts of Papers to Appear in Future Issues

Simulation of Multiparticle Scattering. E. A. REMLER. Department of Physics, The College of William and Mary, Williamsburg, Virginia 23185.

This paper shows how to simulate a multiparticle system whose dynamics is defined by its multiple scattering series. The simulation takes the form of a covariant stochastic process in 8 dimensional phase space. Probabilities are absolute values of covariant Wigner transforms of field theoretic n-point functions. Although partially resembling a classical stochastic process, solutions differ topologically because of the existence of off-mass-shell particles. Formation times imply that unscattered particles undergo proper time dependent renormalization. An interesting consequence is that a particle entering a system of scatterers has a higher than classical probability to scatter near the surface. Only the "skeleton" of the problem is discussed; the system is described by straight path segments connecting short range collisions. Long range forces, medium effects, and production are not treated.

Field Transformations, Collective Coordinates, and BRST Invariance. J. ALFARO. Facultad de Fisica, Universidad Catolica de Chile, Casilla 6177, Santiago 22, Chile; AND P. H. DAMGAARD. The Niels Bohr Institute, University of Copenhagen, Blegdamsvej 17, DK-2100 Copenhagen, Denmark.

A very large class of general field transformations can be viewed as a field theory generalization of the method of collective coordinates. The introduction of new variables induces a gauge invariance in the transformed theory, and the freedom left in gauge fixing this new invariance can be used to find equivalent formulations of the same theory. First the Batalin–Fradkin–Vilkovisky formalism is applied to the Hamiltonian formulation of physical systems that can be described in terms of collective coordinates. We then show how this type of collective coordinate scheme can be generalized to field transformations, and discuss the Ward Identities of the associated BRST invariance. For Yang–Mills theory a connection to topological field theory and the background field method is explained in detail. In general the resulting BRST invariance we find hidden in any quantum field theory can be viewed as a consequence of our freedom in choosing a basis of coordinates $\phi(x)$ in the action $S[\phi]$.

Dissipative Thermal Field Theory and Renormalization. I. HARDMAN AND H. UMEZAWA. Department of Physics, University of Alberta, Edmonton, Alberta, Canada T6G 2J1.

Using methods of thermo field dynamics we develop a perturbation and renormalization procedure for thermally dissipative quantum fields. We emphasize the need to construct dissipative asymptotic fields and to treat the dissipation self consistently. From a stationarity condition we find the Bose–Einstein distribution for the number density in the zero dissipation limit. Considering a simple model with symmetry breaking we find that Goldstone's theorem is satisfied and at zero energy the Goldstone boson does not interact or dissipate, even though at finite momentum and energy the particles are dissipating. The theory should find uses in any physical process involving thermal effects.

Abelian Chern–Simons Theories in $2+1$ Dimensions. ALEXIOS P. POLYCHRONAKOS. Department of Physics, University of Florida, Gainesville, Florida 32611.

Abelian topological Chern–Simons theories in $2+1$ dimensions are examined. The Hilbert space is constructed explicitly for all two-dimensional space manifolds and is shown to be finite-dimensional, in

0003-4916/90 $7.50

Copyright © 1990 by Academic Press, Inc.
All rights of reproduction in any form reserved.

the case of compact $U(1)$. It is determined by the genus of the spatial surface, the coefficient of the action k, and a set of vacuum angles, and it corresponds to the space of conformal blocks of a free scalar in two dimensions compactified on a circle of radius squared k. The expectation of an arbitrary knot is then evaluated by relating the theory in the presence of the knot to a theory in a background gauge field. In this framework, the dependence of the result on the regularization and the framing of the knot becomes explicit. Finally, possible extensions of the methods used in this work to nonabelian theories are discussed.

Aharonov–Bohm Effect and Vacuum Polarization. PAWEŁ GÓRNICKI. Institute for Theoretical Physics, Polish Academy of Sciences, Al. Lotników 32/46, PL-02-668 Warsaw, Poland.

The problem of motion of a Dirac electron in the vicinity of the thin tube of magnetic flux is explicitly solved. Summation over the electrons from the "sea" allows us to calculate the polarization current that flows around the flux tube introduced into the physical vacuum. The formula for the energy density is also given.

Dynamical Correlations in Low-Energy Pion Double Charge Exchange. E. R. SICILIANO AND MIKKEL B. JOHNSON. Los Alamos National Laboratory, Los Alamos, New Mexico 87545; AND H. SARAFIAN. Department of Physics, Pennsylvania State University, York, Pennsylvania 17403.

We consider various processes that contribute to low-energy pion double charge exchange (DCX), and we study their sensitivity to short-range correlations. Within the framework of the fixed-nucleon field theory, we derive a general expression for the following two-nucleon DCX processes: two sequential single charge exchanges via intermediate π (SEQ-π) plus ρ (SEQ-ρ) exchange and the lowest-order Δ_{33}–nucleon (Δ–N) interactions via explicit $\pi + \rho$ exchange. We retain the full spin dependence of the various contributions, and we present the results in a form that can be used for any transition whose corresponding two-body density matrix elements are known. Detailed evaluations are made for ^{14}C to illustrate the importance of short-range correlations. We show the effects on the calculated DCX cross sections that result from three different wave functions: two defined entirely within the p-shell and the other involving configuration mixing with the sd-shell. Our results indicate that SEQ-π is the dominant mechanism for low-energies and that the inclusion of the short-range correlation function decreases the cross section by nearly 50% for standard choices of the pion–nucleon interaction. The largest contribution to the cross section from configuration mixing occurs in off-diagonal transitions [e.g., $(0p)^2$ to $(0d)^2$]. Pairs of nucleons coupled to spin $S=0$ are substantially more sensitive to the short-range correlations than pairs coupled to $S=1$. The size of the ρ-meson contribution to the SEQ mechanism is somewhat model-dependent, but the size of the Δ–N interaction is fixed from other sources. The SEQ-ρ contribution and the Δ–N interaction are about 5–20% effects, and they may increase or decrease the cross section, depending upon details such as the energy and the amount of configuration mixing.

Printed in Belgium

INFORMATION FOR AUTHORS

Annals of Physics is devoted to the publication of papers describing original work in all areas of basic physics research. Original papers only will be considered. Manuscripts are accepted for review with the understanding that the same work has not been published, that it is not under consideration for publication elsewhere, and that its submission for publication has been approved by all of the authors and by the institution where the work was carried out; further, that any person cited as a source of personal communications has approved such citation. Written authorization may be required at the Editor's discretion. Articles and any other material published in *Annals of Physics* represent the opinions of the author(s) and should not be construed to reflect the opinions of the Editor(s) and the Publisher.

Authors submitting a manuscript do so on the understanding that if it is accepted for publication, copyright in the article, including the right to reproduce the article in all forms and media, shall be assigned exclusively to the Publisher. The Publisher will not refuse any reasonable request by the author for permission to reproduce any of his or her contributions to the journal.

Manuscripts should be submitted to the Editor, Dr. Herman Feshbach, *Annals of Physics*, Room 6-318A, Massachusetts Institute of Technology, Cambridge, Massachusetts 02139.

Form of Manuscript: Submit manuscripts in duplicate—*either the original (typewritten or printed) manuscript and one copy or two clear, even-density photocopies*, preferably triple-spaced but at least double-spaced—on one side of 8.5 × 11-inch white paper, and leave wide margins. Number each page. *Page 1* should contain the article title, author and coauthor names, complete affiliation(s) (name of institution, city, state, and zip code), *and a short abstract*. Also place on page 1 any footnotes to the title (indicated by superscript *, †, ‡). At the bottom of page 1 note the number of manuscript pages, figures, and tables. *Page 2* should contain a proposed running head (abbreviated form of the title) of less than 35 characters. It should also contain the name and mailing address of the author to whom proofs should be sent. *A copy of the title page with the abstract and a copy of the reference page(s) should be submitted in addition to the two complete manuscripts.*

The journal can accept only typed or wordprocessed manuscripts at the present time.

List of Symbols. If the text or equations contain any unusual or handwritten symbols, please attach to the manuscript a complete list of these symbols, handwritten or typed to agree with their appearance in the manuscript. Identify the symbols typographically, not mathematically. For manuscripts with typed mathematics, and where standard symbols are used, a symbols list is not required. This list will not appear in print but is essential in order to avoid costly author's corrections in proof. Distinguish between "oh," "zero"; "ell," "one"; "kappa," "kay"; upper- and lowercase "kay"; etc. Indicate also when special type is required (German, Greek, vector, scalar, script, etc.); all other letters will be set in *italic*.

Figures should be numbered consecutively with Arabic numerals in order of mention in the text; each figure should have a descriptive legend. Legends should be typed together on a separate sheet, double-spaced. All figures and illustrations are to be submitted in such form as to permit photographic reproduction without retouching or redrawing. Lettering on drawings should be of professional quality or generated by *high-resolution* computer graphics and should be large enough (10–12 points) to take a reduction of 50–60%. Drawings should be made with black India ink on tracing linen, smooth-surface white paper, or Bristol board, no larger than 8.5 × 11.5-inches overall (21 × 27.5 cm). Alternatively, *high-quality* computer graphics may be acceptable. Graph paper, if used, should be ruled in blue. High-quality glossy prints are acceptable. **Photocopy prints are not acceptable;** however, copies of figures must be included in each copy of the manuscript.

Tables. Number tables consecutively with Roman numerals. Extensive tables will be reproduced photographically and so should be typed carefully and in the *exact* format desired. Authors will be charged for any new photoreproductions necessitated by changes in proof. Use superscript lowercase italic letters (a, b, c) for table footnotes, which should be typed immediately below the table. Type tables at least double-spaced, including titles and footnotes. Do *not* underline table titles; reserve underlining for text that is to be *italicized*.

Equations should be typewritten and with the number placed in parentheses at the right margin. Reference to equations should use the form "Eq. (3)" or simply (3). Superscripts and subscripts should be typed or handwritten clearly above and below the line, respectively. Use the exponent $^{1/2}$ wherever possible.

"Style." In general, authors should be guided by the *Style Manual*, 1978, of the American Institute of Physics, 335 East 45 Street, New York, N.Y. 10017 (price $7.50), **but**

References should be styled and punctuated according to the following examples:

1. H. D. Sivak, *Ann. Phys. (N.Y.)* **159** (1985), 351.
2. G. B. Arfken, "Mathematical Methods for Physicists," 3rd ed., p. 20, Academic Press, New York, 1985.
3. J. M. Aitken and E. A. Irene, *in* "Treatise on Materials Science and Technology" (H. Herman, Ed.), Vol. 24, p. 50, Academic Press, New York, 1985.

For unpublished lectures or symposia, include title of the paper, name of the sponsoring society in full, and date. For journal names, follow the style of *Chemical Abstracts Service Source Index*, 1985, which has also been adopted by the American Institute of Physics. Abbreviation of AEC Laboratory Report names should follow the style of *Nuclear Science Abstracts*. Cite references in the text by an Arabic numeral between square brackets, as [1], [1, 2], [1, Theorem 1.5], etc. Type references consecutively on a separate page, double- or triple-spaced throughout.

Footnotes in text should be avoided if at all possible. If they must be used, identify by superscript numbers and type together on a separate page, double- or triple-spaced.

Proofs. Proofs will be sent to the author, with a reprint order form. Authors will be charged for alterations in excess of 10% of the cost of composition.

Reprints. Fifty reprints without covers will be provided free of charge. Additional reprints may be purchased; an order form will be included with the proofs.

An International Forum in Computer Science . . .

Journal of Parallel and Distributed Computing

Editors-in-Chief: **Kai Hwang**
University of Southern California, Los Angeles
Howard J. Siegel
Purdue University, West Lafayette, Indiana

This international journal is directed to researchers, engineers, educators, managers, programmers, and users of computers who have particular interests in parallel processing and/or distributed computing. The ***Journal of Parallel and Distributed Computing*** publishes original research papers and timely review articles on the theory, design, evaluation, and practices of parallel and/or distributed computing systems.

Research Areas Include

- Theory of parallel/distributed computing
- Innovative computer architectures
- Supercomputers and numerical methods
- Software tools and environments
- Parallel algorithms and implementations
- Languages, compilers, and operating systems
- Shared-memory multiprocessors
- Multicomputers and distributed processing
- Fault-tolerant computing
- Artificial intelligence machines
- Applications and performance analysis
- Optical computing
- Neural networks

Volumes 8–10 (1990), 12 issues
ISSN 0743-7315

In the U.S.A. and Canada: $261.00
All other countries: $324.00

Sample copies and privileged personal subscription rates are available.
For more information or to enter your subscription, please write or call:

ACADEMIC PRESS, INC., Journal Promotion Dept.
1250 Sixth Avenue, San Diego, CA 92101, U.S.A. (619) 699-6742

All prices are in U.S. dollars and are subject to change without notice

S0086